THE EXPRESSION AND FUNCTION OF TWEAK AND FN14 IN LIVER FIBROSIS

by

ANNIKA WILHELM

A thesis submitted to the
University of Birmingham
for the degree of
DOCTOR OF PHILOSOPHY

Centre for Liver Research
School of Immunity and Infection
College of Medical and Dental Sciences
The University of Birmingham
December 2014

Abstract

Liver disease is the fifth largest cause of mortality and is the only major cause of death still increasing in the UK every year. Liver disease is often associated with increased deposition of extracellular matrix, which leads to fibrosis and in many cases progresses to end stage cirrhosis. Hepatic stellate cells (HSC) are considered to be one of the main contributors to liver fibrosis.

Tumour necrosis factor-like weak inducer of apoptosis (TWEAK) is a multifunctional TNF superfamily cytokine that signals through fibroblast growth factor-inducible 14 (Fn14). TWEAK/Fn14 signalling has been primarily associated with liver progenitor cell proliferation. In this thesis I demonstrate that expression of both Fn14 and TWEAK were elevated in acute and chronic human liver injury, and co-localised with markers of activated HSCs. Fn14 expression was low in quiescent HSCs but was significantly induced in HSCs activated *in vitro*, which could be further enhanced with TGF-β. Stimulation with recombinant TWEAK induced proliferation, but not activation of HSCs. Fn14 gene expression was also significantly upregulated in CCl_4 models of hepatic injury while TWEAK KO, but not Fn14 KO, mice showed significantly reduced levels of liver fibrosis following acute and chronic CCl_4 injury *in vivo*. Furthermore, low soluble TWEAK levels in serum levels of PSC patients were an independent risk factor for death or transplantation. Overall these studies demonstrate a previously undescribed role of TWEAK in directly mediating liver fibrosis making it a potential therapeutic target in fibrotic liver disease.

Dedication

I dedicate this thesis to my parents Brigitte and Klaus, who have been a constant source of support and encouragement during my life.

Ich widme diese Doktorarbeit meinen Eltern Brigitte und Klaus, die mich jederzeit von ganzem Herzen unterstützt haben.

Acknowledgements

First I would like to thank my supervisors Dr Simon Afford and Dr Chris Weston for their guidance and support throughout this PhD project.

Furthermore, I would like to thank all members of the Centre for Liver Research, both past and present, for their advice, technical support and for making my time here so enjoyable over the past three years. In particular, I would like to say thanks to Dr Victoria Aldridge who helped me on a day-to-day basis when I first started as a PhD student. In addition, I would like to thank Dr Patricia Lalor who supported me during the write up phase of my thesis. I would also like to extent my gratitude to Prof Stefan Hübscher who aided me in the analysis of my immunohistochemistry staining.

The animal work during my PhD would have not been possible without the team from Biogen Idec. Especially the continuous support from Dr Linda Burkly and Aldo Amatucci in carrying out all my *in vivo* experiments has been invaluable.

I am also very grateful to patients and clinical staff at the Queen Elizabeth Hospital, Birmingham for tissue/blood donation and collection. Furthermore, I would like to acknowledge the support I have received from the BBSRC who funded this project.

Finally, I would like to thank my family and friends especially my parents who kindly accepted my decision to study abroad. I am also very grateful to my housemates Claire, Kate, Aliesha and Amy who have been so much fun to be around. In addition I would like to thank Mandy, Jeannette and Palak who have been very encouraging during the last year of my PhD.

Last but not least I am extremely grateful to my beloved Serif Sasmaz who has been incredibly supportive during all the ups and downs of my PhD. He always believed in me and helped me through moments of despair.

Table of Contents

List of figures

Chapter 5

Chapter 6

Chapter 7

List of tables

Chapter 2

Chapter 6

Abbreviations

AEC	3-amino-9-ethylcarbazole
AIH	Autoimmune hepatitis
ALD	Alcoholic liver disease
ALF	Acute liver failure
ALP	Alkaline phosphatase
ALT	Alanine aminotransferase
AP-1	Activator protein-1
α-SMA	α-smooth muscle actin
AST	Aspartate transaminase
AUROC	Area under the receiver operator characteristic
bFGF	Basic fibroblast growth factor
β-ME	β-mercaptoethanol
BSA	Bovine serum albumin
CCL	Chemokine (C-C motif) ligand
CCl_4	Carbon tetrachloride
CDE diet	Choline-deficient, ethionine-supplemented diet
CRD	Cysteine rich domain
DAB	3,3′-diaminobenzidine
DAPI	4',6-diamidino-2-phenylindole
DDC diet	3,5-diethoxycarbonyl-1,4-dihydrocollidine diet
dH_2O	distilled H_2O
ddH_2O	deionised distilled H_2O
DMEM	Dulbecco's Modified Eagle's Medium
DMSO	Dimethyl sulfoxide
DRC	ductular reactive cell
ECL	Enhanced chemiluminescence
ECM	Extracellular matrix
EMT	Epithelial to mesenchymal transition
FasL	Fas ligand
FCS	Foetal calf serum
FGF	Fibroblast growth factor
Fn14	Fibroblast growth factor inducible 14
Gapdh	Glyceraldehyde 3-phosphate dehydrogenase
geNorm M	geNorm stability measurement
GFAP	Glial fibrillary acidic protein
GS	goat serum
GUSB	β-glucuronidase
HC	Healthy control
HCC	Hepatocellular carcinoma
H&E	Haematoxylin and eosin
HET	Heterozygous
HGF	Hepatocyte growth factor

HR	Hazard ratio
HRP	Horseradish peroxidase
HSC	Hepatic stellate cell
IACUC	Institutional Animal Care and Use Committee
IBD	Inflammatory bowel disease
IFN-γ	Interferon-γ
IHEC	Intrahepatic sinusoidal endothelial cell
IκB	Inhibitors of κB
IKK	IκB kinase
INR	International normalised ratio
IQR	Interquartile range
JNK1	C-jun-N-terminal kinase 1
KO	Knock-out
LMF	Liver myofibroblast
LPC	Liver progenitor cells
LPS	Lipopolysaccharide
MAPK	Mitogen activated protein kinases
MCD diet	Methionine- and choline-deficient diet
MELD	Model for End-Stage Liver Disease
MFI	Median fluorescent intensity
MMP	Matrix metalloproteinase
NASH	Non-alcoholic steatohepatitis
N-CAM	Neural-cell adhesion molecule
NF-κB	Nuclear factor κ-light-chain-enhancer of activated B cells
NK cell	Natural killer cell
NKG2D	Natural killer group 2 member D
NL	Normal liver
PBC	Primary biliary cirrhosis
PBS	Phosphate buffered saline
PDGF	Platelet derived growth factor
PH	Partial hepatectomy
PMA	Phosphomolybdic acid
PSC	Primary sclerosing cholangitis
PSR	Picrosirius red staining
qPCR	Quantitative polymerase chain reaction
SMC	Smooth muscle cell
sTWEAK	Soluble TWEAK
TAK1	Transforming growth factor beta activated kinase-1
TBS	Tris buffered saline
TGF	Transforming growth factor
THD	TNF homology domain
TIMP	Tissue inhibitors of metalloproteinase
TLR	Toll-like receptor
TNF	Tumour necrosis factor

TNFR1	TNF receptor 1
TRAF	TNF receptor-associated factor
TRAIL	TNF-related apoptosis-inducing ligand
TWEAK	TNF-like weak inducer of apoptosis
UKELD	United Kingdom model for End-stage Liver Disease
ULN	Upper limit of normal
WT	Wild type

Chapter 1

Introduction

1.1 Overview of the liver anatomy and its function

The liver is, after the skin the second largest organ of the body. It is located below the diaphragm mostly on the right side of the upper abdomen and has a unique dual blood supply from the hepatic artery and the portal vein (Figure 1.1 A). The liver consists of two lobes that are made up of small units, called lobules (Figure 1.1 B). In the centre of each lobule is a central vein. At the periphery of the lobule are portal triads. A portal triad consists of a branch of the hepatic portal vein, hepatic artery and a bile duct. The arterial and venous blood flows through the sinusoids from the portal triad to the central vein. The liver lobules can be divided into three zones, based on oxygen levels (Figure 1.1 C). Zone 1 encircles the portal triad where the highly oxygenated blood from hepatic arteries enters. The blood flow through zone 2 to zone 3 that is located around the central vein where oxygenation is poor.

The anatomical location of the liver allows it to perform many vital functions as it directly receives and metabolises nutrients from the digestive system through the portal vein. Some of the metabolic functions include maintenance of normal blood glucose levels and metabolism of fatty acids for energy production (Taub, 2004). The liver also serves as storage place for many essential nutrients (glycogen, fatty acids), vitamins (Vitamin A, E, D, K and B_{12}) and minerals (iron and copper). Another important function of the liver is the production of plasma proteins including prothrombin, fibrinogen, and albumin. It also synthesizes bile, which is essential for absorption of fat and lipophilic nutrients. Furthermore, the liver is the main detoxifying organ of the body as it cleans the blood of many potentially harmful substances prior to release into the circulation. Those substances are then excreted either into bile that then enters the intestine or by blood for elimination by the

kidneys. In addition, it is involved in phagocytosis of foreign particles and infecting organisms. During the process of blood detoxification and removal of infection some of the liver cells can become damaged and die. However, the liver has a unique regenerative potential after injury. It is able to completely reconstruct its functional liver mass after 70% partial hepatectomy (PH) within days in rodents and weeks in humans. It is also able to regenerate but to a slower extent after ischemic, toxic, and infectious types of acute liver injury (Diehl and Chute, 2013).

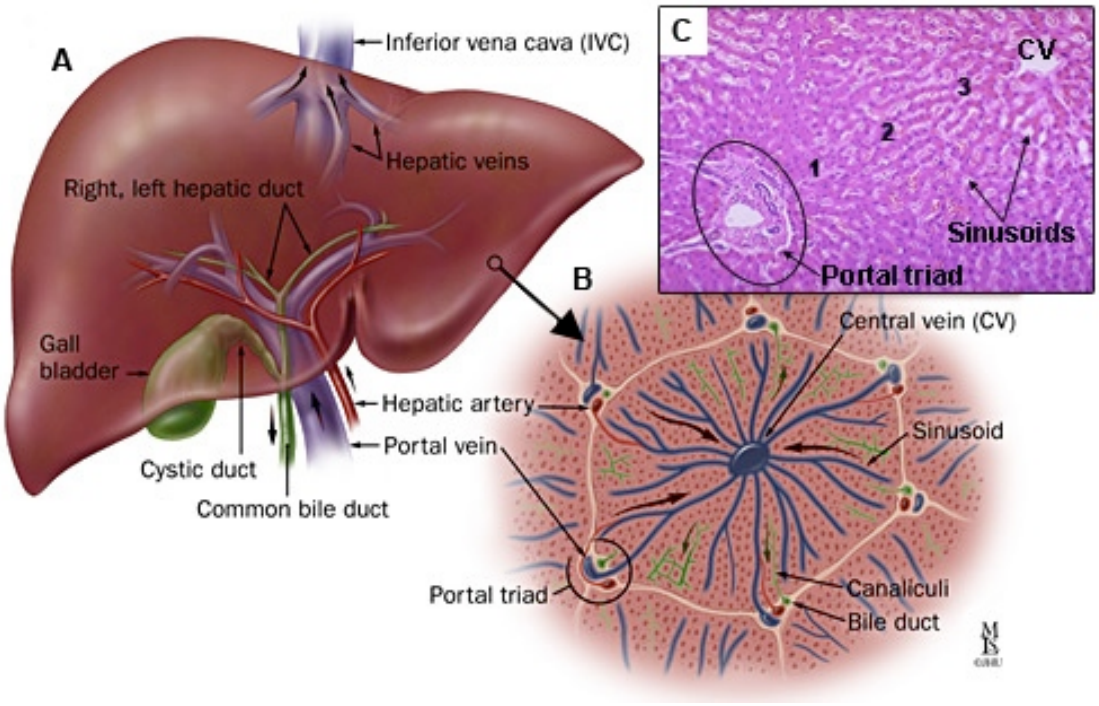

Figure 1.1 Structure of the liver and the liver lobules
The liver is made up of two main lobes. It has a dual blood supply arising from the hepatic artery and portal vein **(A)**. The lobes of the liver are further subdivided into lobules that have portal triads at the periphery containing of a branch of the hepatic artery, portal vein and bile duct. The blood flows from the portal triad to the central vein **(B)**. Tissue in zone 1 receives more oxygenated blood than tissue in zone 3 **(C)**. Image adapted from: https://gi.jhsps.org/Upload/200710290953_38845_000.jpg

1.1.1 Liver cell populations

The main cell type that carries out many of the liver's vital functions are the parenchymal cells called hepatocytes. Up to 80% of the liver is made up of hepatocytes and the remaining 20% of hepatic cells are non-parenchymal cells, including hepatic stellate cells (HSCs), endothelial cells, cholangiocytes, Kupffer cells and lymphocytes (Taub, 2004). Hepatocytes are polarised epithelial cells and are arranged in single cell thick chords in the liver lobules separated by blood filled sinusoids (Figure 1.2). In addition, tight junctions between hepatocytes form bile canaliculi, which are not ducts but rather dilated intercellular spaces between adjacent hepatocytes. Hepatocytes secrete bile into the canaliculi that then flows into the opposite direction of the blood flow draining into bile ducts (Müsch, 2014). Bile ducts are lined with another type of liver epithelial cell called cholangiocyte.

Sinusoids correspond to capillary beds and are the segments of the liver where supply of nutrients and removal of metabolic products takes place. Fenestrated intrahepatic sinusoidal endothelial cells (IHECs) line the sinusoids. They are highly permeable and act as a selective barrier controlling the extensive exchange of materials between liver cells and blood (Vollmar and Menger, 2009). Within the sinusoids are Kupffer cells, which are anchored to the endothelium and exposed to the bloodstream. They are resident macrophages and responsible for phagocytosis of foreign particles and infecting organisms.

The space between the hepatocytes and the endothelial lining is called the space of Disse. Within this space reside quiescent HSCs that are considered to be the pericytes of the liver (Pellicoro et al., 2014). The most characteristic feature of quiescent HSCs

is the presence of cytoplasmic lipid droplets that store vitamin A. They store over 80% of the total body vitamin A and maintain vitamin A blood homeostasis (Sato et al., 2003). Other important functions of HSCs include remodelling of extracellular matrix (ECM), contraction and dilation of sinusoids and secretion of growth factors and cytokines.

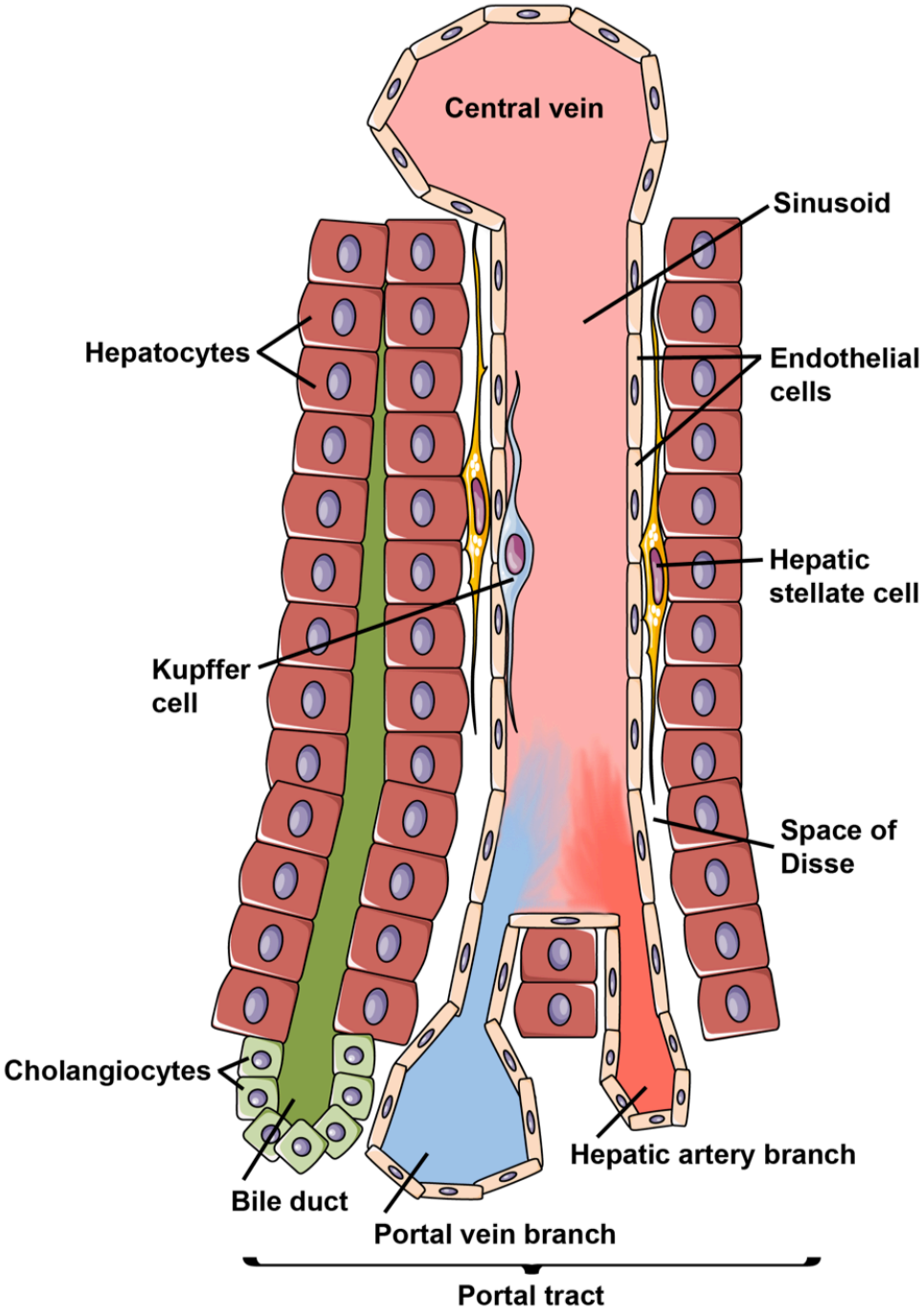

Figure 1.2 The hepatic sinusoid

In the liver lobule, hepatocytes are arranged as single cell chords. They are separated by blood filled sinusoids that are lined with fenestrated endothelial cells. Kupffer cells, the liver resident macrophages, are anchored to the endothelium. Between hepatocytes and endothelial cells is the space of Disse where hepatic stellate cells reside. Bile from hepatocytes drains into canaliculi that empty into bile ducts.

1.2 The burden of liver disease

Despite the liver's remarkable ability to regenerate itself following injury, there are several types of liver diseases that cause chronic injury and therefore attenuate regeneration. Chronic liver disease can develop in response to a number of factors including chronic infections with hepatitis B or C virus, chronic alcohol abuse, non-alcoholic fatty liver disease and immune-mediated liver diseases. It is an increasing problem worldwide which is reflected in the United Kingdom where levels of chronic liver disease have been sharply increasing since the 1990s and are now amongst the highest in Europe (Leon and McCambridge, 2006). Chronic liver disease can lead to the progressive replacement of functional hepatic parenchyma with excessive ECM causing the deformation of normal tissue and vascular architecture, which is then termed cirrhosis. Cirrhosis can interfere with vital liver functions and cause organ dysfunction that is ultimately fatal (Friedman et al., 2013). Patients with cirrhosis are also at highest risk of developing primary neoplasms that can derive from hepatocytes (Hepatocellular carcinoma; HCC) and cholangiocytes (Cholangiocarcinoma) (Forner et al., 2012). As chronic liver diseases are rising, cirrhosis and liver cancer are major causes of death worldwide (Lozano et al., 2012). In Europe, cirrhosis and HCC together represent the third cause of death in adults over 50 years old (Fernández et al., 2009). Despite this global burden of chronic liver disease, treatment options are limited and currently involve either removing the underlying trigger for the liver disease, which is unfortunately not always possible or liver transplantation. Although liver transplantation can be a highly effective therapy it has also major drawbacks. One of the biggest issues is the increasing imbalance between demand and supply of donor livers (Callaghan et al., 2013). Furthermore, liver transplantation is a major operation and factors such as other co-existing medical issues can prevent patients

from being considered for transplantation. Patients that have been transplanted have to take life-long immunosuppressive medications to protect allografts from acute rejection. However, immunosuppressive medications can cause toxic effects that can lead to an increased risk of patient morbidity and mortality (Lechler et al., 2005). In addition, problems with chronic rejection can also occur, which is a major cause of graft loss (Neumann et al., 2002). Although the use of new immunosuppressive medications has generally enhanced patient's survival rates, the recurrence of primary liver disease after transplantation is also a growing concern (El-Masry et al., 2011). This highlights the need of new preventative therapies for chronic liver disease. Most types of chronic liver disease follow a common pathway independent of aetiology leading to liver fibrosis (Schuppan and Kim, 2013). Gaining a greater understanding of one of the root problems such as fibrosis could therefore aid in the development of new treatment options.

1.3 Pathogenesis of liver fibrosis

1.3.1 Liver injury

Hepatic fibrosis is caused by a dysregulated physiological wound-healing response to liver injury. The pathogenesis of liver injury is not fully understood but most types of liver injury damage epithelial cells (hepatocytes or cholangiocytes) that then causes the release of inflammatory and fibrogenic mediators (Pellicoro et al., 2014). Acute liver failure (ALF) for example is caused when hepatocyte death exceeds regeneration and is the most severe damage the liver can undergo (Chung et al., 2012). In addition, hepatocytes are also thought to be primarily affected in alcoholic liver disease (ALD) (Gao and Bataller, 2011) and non-alcoholic steatohepatitis (NASH) that is associated with excess free saturated fatty acids and insulin resistance (Peverill et al., 2014).

Autoimmune hepatitis (AIH) presents with autoreactive immune cells and also primarily leads to hepatocyte damage. It is likely to be caused by an environmental trigger in a genetically susceptible patient (Lapierre et al., 2007). In contrast, cholangiocytes are mainly affected in cholestatic liver diseases including primary biliary cirrhosis (PBC) in which the autoreactive immune response seems to be the most likely pathogenic mechanism (Hirschfield and Gershwin, 2013) and primary sclerosing cholangitis (PSC) where the trigger is unknown but thought to be immune-mediated in individuals with a genetic predisposition (Hirschfield et al., 2013).

Liver injury can then lead to fibrosis that involves transformation of HSCs into collagen producing liver myofibroblasts (LMFs) and accumulation of ECM. After acute injury, LMFs and ECM transiently appear but are gone once the injury is resolved. However, the sustained signals during chronic liver disease lead to a several-fold increase in the production and deposition of ECM, mostly collagen type I, resulting in liver fibrosis (Bataller and Brenner, 2005). Excessive accumulation of liver fibrosis in combination with damaged epithelial cells contributes to the ongoing architectural distortion and the loss of organ function. The discussion that follows describes cellular and non-cellular mediators of liver fibrosis with an emphasis on the role of HSCs and LMFs during fibrogenesis. Ultimately however, liver fibrosis is a complex process that involves the interaction between many factors and cell types including epithelial cells, endothelial cells and various types of immune cells.

1.3.2 Cellular mediators

1.3.2.1 Epithelial cells –Hepatocytes and cholangiocytes

Damaged hepatocytes or cholangiocytes release pro-fibrogenic and pro-inflammatory cytokines that activate Kupffer cells and HSCs and stimulate the recruitment of leukocytes creating an inflammatory environment. Recruited leukocytes and Kupffer cells will then phagocytose dead cells and further amplify the inflammatory response (Bataller and Brenner, 2005). Excessive inflammation can then lead to further hepatocyte apoptosis or necrosis. This can partly be regulated by members of the tumour necrosis factor (TNF) superfamily including TNF-α, Fas ligand (FasL) and TNF-related apoptosis-inducing ligand (TRAIL), which are death ligands and therefore can directly induce hepatocyte death (Brenner et al., 2013). One source of those ligands are Kupffer cells that induce expression of TNF-α, TRAIL and FasL after phagocytosis of apoptotic hepatocytes (Canbay et al., 2003). Another TNF ligand that can modulate hepatocyte apoptosis is CD40 ligand (also known as CD154) (Afford et al., 1999). It is expressed by lymphocytes and macrophages/Kupffer cells in the chronically inflamed liver (Alabraba et al., 2008) and activation of the receptor, CD40 can induce Fas-mediated apoptosis in hepatocytes (Afford et al., 1999). Apoptotic hepatocytes can also be phagocytosed by HSCs during chronic liver injury (Zhan et al., 2006). Upon phagocytosis, HSCs increase expression of procollagen 1α (I) and transforming growth factor-β1 (TGF-β1) (Zhan et al., 2006) enhancing the pro-fibrogenic response.

In early stages of cholangiopathies and during severe liver injury, proliferation of activated cholangiocytes may also occur. They usually form small clusters or non-functional bile ductular structures that are associated with inflammation. These are frequently referred to as ductular reactions (Schuppan and Kim, 2013). Ductular

reactions also contain a population of liver progenitor cells (LPCs) that are bipotential adult stem-like cells and have the capacity to differentiate into hepatocytes or cholangiocytes (Duncan et al., 2009). Evidence has shown that ductular reactions are directly proportional to levels of fibrosis (Williams et al., 2014). Activated cholangiocytes acquire the ability to release pro-inflammatory cytokines and chemokines such as TNF-α, IL-6 and chemokine (C-C motif) ligand 2 (CCL2). In addition they also produce growth factors such as hepatocyte growth factor (HGF), platelet derived growth factor-BB (PDGF-BB) and TGF-β2 that can influence HSC and portal fibroblast behaviours (Lazaridis et al., 2004). Therefore activated cholangiocytes are considered to be potential mediators of biliary fibrosis.

1.3.2.2 Intrahepatic sinusoidal endothelial cells

In a healthy liver, normal IHECs inhibit activation of quiescent HSCs and promote reversion from an activated to a quiescent HSC phenotype. Disruption of the endothelium causes fenestrated IHECs to alter their phenotype towards capillarisation consequently losing the ability to inhibit HSC activation (DeLeve et al., 2008; Xie et al., 2012). Capillarisation of IHECs is tightly associated with perisinusoidal fibrosis. During perisinusoidal fibrosis, IHECs contribute in small amounts to production of the ECM with fibronectin and collagen type I and produce pro-fibrogenic factors such as TGF-β1 and PDGF-BB (Schuppan and Kim, 2013). In addition, activated IHECs also release mediators of angiogenesis including angiopoietins and members of the fibroblast growth factor (FGF) family (Cong et al., 2012). Furthermore, they secrete endothelin-1 that is involved in vasoconstriction that can exacerbate portal hypertension in liver cirrhosis (Schuppan and Kim, 2013).

1.3.2.3 Macrophages

Liver-resident Kupffer cells are the largest population of resident macrophages in the body (Pellicoro et al., 2014). As Kupffer cells reside within hepatic sinusoids they are in close proximity to circulating immune cells and bacterial antigens derived from the intestinal flora entering via the portal vein. Liver injury causes bacterial translocation from the intestine leading to increased levels of lipopolysaccharide (LPS) in the blood circulation that causes activation of Kupffer cells (Seki et al., 2007). Furthermore, damaged epithelial cells also lead to Kupffer cell activation (Bataller and Brenner, 2005). In the early phases after injury, Kupffer cells secrete pro-inflammatory cytokines and chemokines including CCL5 and IL-1β causing activation of cytoprotective or apoptotic pathways in hepatocytes and amplification of the inflammatory response (Tacke and Zimmermann, 2014). In addition, not only immediate injury but also an overload of lipids can lead to secretion of pro-inflammatory cytokines and chemokines in Kupffer cells (Leroux et al., 2012).

The number of Kupffer cells is reduced during active inflammation and fibrogenesis and replenished again during resolution (Ramachandran et al., 2012). In contrast, the number of bone marrow-derived macrophages, originating from circulating monocytes, markedly increase in response to hepatic injury (Ramachandran et al., 2012). Macrophages are a heterogeneous population and several subsets with distinct functions have been described. A simple way to classify them is by dividing the macrophage population into "pro-inflammatory" M1 macrophages and "immunoregulatory" M2 macrophages. M1 macrophages release pro-inflammatory factors (including TNF-α, IL-1β, IL-12, reactive oxygen species) and mediate the defence against pathogens and tumour cells. M2 macrophages are involved in

regulating tissue remodelling and secrete immune-modulatory mediators (including IL-10, TGF-β, IL-4, IL-13) (Tacke and Zimmermann, 2014). However, macrophages can adopt context-dependent phenotypes that can carry out different functions and it is difficult to classify them into categories as they represent a spectrum of activated phenotypes (Murray and Wynn, 2011).

During liver fibrosis macrophages are located in close proximity to activated LMFs in the scar tissue (Duffield et al., 2005). They can produce a variety of different cytokines, chemokines and other factors that can influence HSCs and LMFs including TGF-β and PDGF (Wynn and Barron, 2010). Other factors that macrophages produce are CCL7 and CCL8 that are involved in the recruitment and activation of LMFs and IL-4 and IL-13 that are potent pro-fibrogenic cytokines (Wynn and Barron, 2010).

Using macrophage depletion in experimental models of liver fibrosis provided further evidence that macrophages play an important role during fibrogenesis. The depletion of hepatic macrophages in rats with gadolinium chloride led to a decrease in liver fibrosis in response to thioacetamide-induced injury (Ide et al., 2005). Another model that also demonstrated the pro-fibrogenic effect of macrophages was the CD11b-DTR transgenic mouse model that induced selective depletion of macrophages. This model in combination with the hepatotoxin carbon tetrachloride (CCl_4) resulted in fewer LMFs and less collagen (Duffield et al., 2005).

It is now recognized that liver fibrosis is not an unidirectional, irreversible process and in accordance with that macrophages exhibit a dual role in liver fibrosis, as they can also be involved in resolution (Duffield et al., 2005). Next to promoting fibrosis pro-

resolution macrophages can lead to ECM degradation by expression of fibrolytic matrix metalloproteinases (MMPs) such as MMP-12 and MMP-13 (Pellicoro et al., 2012; Fallowfield et al., 2007). Furthermore, macrophages cause phagocytosis of apoptotic cells that leads to increased MMP production and resolution of ECM in models of hepatocellular and biliary fibrosis (Ramachandran et al., 2012; Popov et al., 2010)

1.3.2.4 Natural killer cells

Natural killer (NK) cells are enriched in the liver and belong to the innate immune system. Between 30 to 50% of the human liver lymphocyte population are NK cells whereas only about 10% are present in mouse livers. They recognise and kill infected, injured and transformed cells and are normally present in the hepatic sinusoids in close proximity to non-parenchymal cells (Gao and Radaeva, 2013). NK cells can have a negative regulatory effect on fibrosis in two different ways. They mediate the direct killing of HSCs that are in the process of activation and senescent activated HSCs. In order to do so they release interferon-γ (IFN-γ) that induces HSC apoptosis and cell cycle arrest (Gao and Radaeva, 2013). However, despite the anti-fibrotic abilities of NK cells, chronic liver injury still leads to fibrosis. One possibility is that chronic alcohol consumption supresses NK cell activity, which possibly contributes to the progression of ALD. Indeed, patients with ALD have fewer NK cells and those that were present exhibited reduced cytotoxicity (Cook, 1998). In addition, alcohol intake also seemed to influence NK cell function in mice as a chronic ethanol diet caused reduced NK cytotoxicity towards HSCs, possibly caused by the reduction of natural killer group 2 member D (NKG2D), TRAIL, FasL and IFN-γ expression by NK cells (Jeong et al., 2008). Furthermore, HSCs and LMFs may use mechanisms to

avoid NK cell-mediated killing, as NK cells do not seem to lyse fully activated HSCs/LMFs as they express high levels of TGF-β, which is an inhibitor of NK cell cytotoxicity towards HSCs (Jeong et al., 2011).

1.3.2.5 T cells

The heterogeneity of fibrotic diseases rules out that only one subtype of T cells is responsible for pro or antifibrotic effects of the immune system. However, extensive evidence shows that CD4-positive T helper cells with a Th2 polarisation can promote fibrosis (Barron and Wynn, 2011). Th2 cells can produce IL-4 and IL-13 and experimental models of schistosomiasis have demonstrated that Th2 cells can be strongly pro-fibrotic. Furthermore, CD4-positive Th17 cells express IL-17 and are considered to be pro-fibrogenic cells. The IL-17 receptor is expressed by HSCs and stimulation with IL-17 leads to collagen type I production in HSCs (Meng et al., 2012). Regulatory T cells are a subset of CD4-positive cells and seem to be pro or antifibrotic in a context dependent manner. Subsets can express the immunosuppressive cytokine IL-10 and the profibrotic mediator TGF-β (Schuppan and Kim, 2013). Furthermore, CD8-positive T cells have been implicated in promoting liver fibrogenesis (Safadi et al., 2004). However, studies with depletion of CD4 and CD8-positive T cells in mice have demonstrated no effect on liver fibrogenesis in mice treated with CCl_4 (Novobrantseva et al., 2005).

Natural killer T cells are a subset of T cells that express both T cell and NK cell markers. The percentages of NKT cells in human liver ranges between 3-15% of the liver lymphocyte population whereas the liver lymphocyte population in mice contain 30-40% (Gao and Radaeva, 2013). Evidence suggests that NKT cell play complex

and even opposing roles during liver fibrosis in patients with different disease stages and different aetiologies (Gao and Radaeva, 2013). Similar to NK cells, NKT cells can produce IFN-γ and kill HSCs (Park et al., 2009) but they can also produce the pro-fibrotic cytokines such as IL-4 and IL-13 (Gao and Radaeva, 2013). Therefore, the precise functions of T cell populations remains unclear and data so far suggests that their role depends on disease aetiology.

1.3.2.6 Liver myofibroblasts

Accumulation of LMFs is a key feature of liver fibrosis. They are considered to be the master regulator of liver fibrosis due to their ability to produce ECM, proliferate, migrate, contract and modulate the immune system and phagocytose damaged cells (Pellicoro et al., 2014). LMFs are not found in normal liver tissue but accumulate after liver injury.

There are three potential sources of LMFs consisting of resident mesenchymal cells (quiescent HSCs and portal fibroblasts), epithelial to mesenchymal transition (EMT) that involves hepatocytes or cholangiocytes, which transform into myofibroblasts or bone marrow derived cells (fibrocytes and mesenchymal progenitor cells). HSCs and portal fibroblasts are considered to be the most relevant source of LMFs in the liver (Brenner et al., 2012; Schuppan and Kim, 2013). In hepatocellular injury, HSCs are the main contributors to the LMF population. This has been demonstrated by Kisseleva *et al.* who has shown that more than 92% of LMFs derived from activated HSCs in response to toxic liver injury using CCl_4 and fate tracing (Kisseleva et al., 2012). Furthermore, Schwabe and colleagues confirmed that 82-96% of LMFs were derived from HSCs using fate tracing in chemical induced liver injury and fatty liver disease (Mederacke et al., 2013). In chronic cholangiopathies, where periductular

fibrosis is prominent, portal fibroblasts are thought to be an important myofibroblast source. They are considered to be the first responders to biliary injury that are then later supplemented by HSC-derived myofibroblasts (Xu et al., 2014). Conversely, recent research by Schwabe and colleagues have also demonstrated that HSCs were a far more dominant source of LMFs than portal fibroblasts even during early periductular fibrosis using three well establish models of cholestasis-induced liver fibrosis (Mederacke et al., 2013). Despite that they suggested that due to their location portal fibroblasts probably perform specialised functions in cholangiopathies (Mederacke et al., 2013; Wells, 2014). Other sources such as bone marrow-derived mesenchymal cells or fibrocytes have been suggested to have a minimal contribution to the LMF population. However, they might still contribute to liver fibrosis in other ways such as modulation of the immune system (Brenner et al., 2012). Epithelial cells have also been proposed as progenitors of LMFs through EMT. Although EMT of hepatocytes has been documented *in vitro* (Kaimori et al., 2007), fate-mapping studies have failed to identify hepatocytes as a source of LMFs (Taura et al., 2010). Similarly, genetic labelling of CK19, a marker of cholangiocytes also demonstrated that cholangiocytes do not contribute to LMFs in experimental model of cholestasis-induced liver fibrosis (Scholten et al., 2010).

1.3.2.7 Hepatic stellate cells

In a healthy adult liver, HSCs comprise approximately 15% of the total liver cell population and have a spindle-shaped morphology (Friedman, 2008). Their multiple processes extend across the space of Disse, which allows them to be in close contact with several hepatocytes and IHECs at once. When HSCs are quiescent their most prominent characteristic is their cytoplasmic storage of retinoids (lipid-soluble vitamin

A metabolites). HSCs not only express mesenchymal cell marker such as vimentin but also neural cell markers such as glial fibrillary acidic protein (GFAP), neural-cell adhesion molecule (N-CAM) and synaptophysin (Cassiman and Roskams, 2002).

HSC activation Liver injury triggers HSC activation and the structure of quiescent HSCs changes considerably. They lose their characteristic vitamin droplets, downregulate their neural markers and transform into collagen type I and α-smooth muscle actin (α-SMA) expressing myofibroblastic cells (Xu et al., 2014). Induction of α-SMA is the most reliable marker of HSC activation *in vitro* and *in vivo* (Friedman, 2008). HSCs develop increased proliferative, contractile and migratory potential and secrete large amounts of ECM. In addition they release pro-inflammatory and pro-fibrogenic factors including TGF-β (Bataller and Brenner, 2005). HSC activation is caused by pro-inflammatory mediators as well as growth factors particularly TGF-β and cytokines that are released by cellular damage and stimulated immune cells (Pellicoro et al., 2014). In addition, phagocytosis of apoptotic hepatocytes and lymphocytes can induce HSC activation (Muhanna et al., 2008; Jiang et al., 2009). Furthermore, the increased density of ECM as fibrosis accumulates leads to increasing tissue stiffness, which is an important stimulus for HSC activation (Olsen et al., 2011). In accordance with that, HSC activation can be modelled *in vitro* by plating freshly isolated HSCs on uncoated plastic that resembles a stiff environment (Olsen et al., 2011). They transform within 7 days into early activated HSCs that gradually loose their retinoid storage and continue to develop over a longer period into activated HSCs with myofibroblastic-like functionalities (Gao and Radaeva, 2013). Importantly, HSC activation is considered to be a continuous process, in which early changes in the HSC phenotype are probably distinct to changes that occur with progressive

disease in terms of growth characteristics, their response to soluble factors and apoptotic potential (Friedman, 2008).

Perpetuating pathways In order to perpetuate fibrosis HSCs utilise a variety of positive feedback loops. During activation, HSCs induce expression of PDGF receptors and release PDGF to stimulate autocrine proliferation and chemotaxis (Friedman, 2008). Similarly, they also secrete latent TGF-β1 that, once activated, also further stimulates HSC activation and matrix production through autocrine mechanisms (Friedman, 2008). Furthermore, activated HSCs are able to respond to a host of cytokines, chemokines and growth factors from other cells to perpetuate fibrosis. HSC survival for example is promoted by the macrophage-derived cytokines TNF and IL-1 through activation of the nuclear factor κ-light-chain-enhancer of activated B cells (NF-κB) pathway (Pradere et al., 2013). Notably, not all factors that promote fibrosis are necessarily activated at the same time. PDGF for example drives HSC proliferation in some instances in parallel with fibrogenic stimulation but this is not always the case as DNA from apoptotic hepatocytes induces differentiation of HSCs but blocks PDGF-induced chemotaxis via toll-like receptor (TLR) 9 (Watanabe et al., 2007). Activation of TLR9 in HSCs possibly provides a stop signal that allows activated cells to accumulate at the site of damaged hepatocytes where they can deposit scar tissue. Furthermore, in order to maintain ECM deposition activated HSCs also secrete tissue inhibitors of metalloproteinases (TIMPs), in particular TIMP-1 that blocks a variety of MMPs that would normally degrade ECM (Iredale et al., 2013). The importance of HSCs in driving fibrosis was emphasised in a study using a mouse model in which HSCs were specifically depleted (Puche et al., 2013). Depletion of HSCs caused a significant reduction in fibrosis but also led to decreased expression

of cytoprotective cytokines IL-10 and IFN-γ and an altered intrahepatic leukocyte population.

HSC immunomodulation The immune response plays a critical role in the progression of liver fibrosis. HSCs can mediate a range of inflammatory effects by secreting chemokines and other factors including CCL2, CCL3, CCL5, CXCL1, CXCL8, CXCL9 and CXCL10 (Lee and Friedman, 2011). Interestingly, HSCs also express CCR5 and respond to CCL5 stimulation with proliferation and migration identifying the cells as a source as well as a target for CCL5 (Schwabe et al., 2003). CCL5 seems to be an important mediator of liver fibrosis as CCL5 knock-out (KO) mice had decreased levels of fibrosis induced by CCl_4 or methionine- and choline-deficient (MCD) diet (Berres et al., 2010). Furthermore, HSCs express other chemokine receptor including CXCR3 and CXCR4 (Bonacchi et al., 2001; Hong et al., 2009) and can function as antigen presenting cells in liver injury to stimulate lymphocytes (Winau et al., 2007; Bomble et al., 2010).

1.3.2.8 Loss of LMFs during fibrosis regression

Liver fibrosis has not evolved to cause disease but is rather a protective response to liver injury. Under optimal circumstances, especially after acute injury, the excess ECM that accumulated is degraded and removed and normal liver architecture and function can be restored. It has been questioned in the past whether liver fibrosis that develops progressively during chronic injury is also reversible. Studies have now shown that if the underlying source of the injury can be controlled, liver fibrosis can regress (Ellis and Mann, 2012).

Regression of liver fibrosis is characterised by the removal of LMFs (Iredale et al., 1998). Two recent independent studies using genetic tracking in experimental models have revealed the fate of HSCs after liver fibrosis (Troeger et al., 2012; Kisseleva et al., 2012). The studies demonstrated that approximately 50% of activated HSCs/LMFs underwent apoptosis during fibrosis regression. The rest of HSCs on the other hand were shown to downregulate fibrogenic genes and adopted a more quiescent phenotype. However, those cells were not identical to the quiescent HSCs that had never been activated before as they had an increased capacity to reactivate when treated with TGF-β. Whether these cells stay in this intermediate state or whether they eventually revert to fully quiescent HSCs is not known. Nevertheless, it supports the data that HSCs are a heterogeneous population with different functional plasticity (Geerts, 2001; D'Ambrosio et al., 2011).

1.3.3 Non-cellular mediators

1.3.3.1 Extracellular matrix

The ECM is one of the most important regulators of cellular function in the body. ECM proteins can function as signalling molecules but are also architectural components and are involved in maintaining hepatocytes and non-parenchymal cells differentiated (Schuppan et al., 2001). Under homeostatic conditions sinusoids contain a basement membrane matrix, which is mainly made up of collagen type IV and fibronectin (Hahn et al., 1980). During liver fibrosis this matrix is slowly replaced by a denser and continuous matrix rich in collagen type I and III, with an accompanying loss of the fenestrated endothelium (Iredale et al., 2013). The changes in ECM composition during liver fibrosis elicit several positive feedback pathways that then lead to more accumulation of ECM. For example membrane receptors on HSCs, in

particular integrins, sense the changes in ECM and induce HSC activation and migration (Yang et al., 2003; Zhang et al., 2006). In addition, the increased density of the ECM leads to a stiffer environment that is also involved in HSC activation (Olsen et al., 2011). Furthermore, degradation of the ECM by MMPs leads to the release of matrix-bound reservoirs of growth factors and chemokines that can potentially stimulate fibrogenesis (Schuppan et al., 1998; Bauvois, 2012). As fibrosis progresses the ECM becomes progressively denser and stabilised due to thickening of fibrotic septae and increased crosslinking making it less susceptible to MMP degradation, thus interfering with normal remodelling (Xu et al., 2012). The denser matrix can also act as a barrier for infiltrating immune cells and there is evidence that aberrant expression of ECM molecules can influence activation, differentiation and survival of immune cells (Sorokin, 2010).

1.3.3.2 Tissue proteases

The turnover of ECM is controlled by MMPs and their inhibitors TIMPs. MMPs are a family of zinc and calcium dependent proteases that are involved in matrix degradation. In addition, they are involved in a variety of other processes including leukocyte activation, cell migration, antimicrobial defence and chemokine processing. Due to their variety of functions, some MMPs are not only involved in inhibiting fibrosis but also in stimulating it (Giannandrea and Parks, 2014). Even during liver fibrogenesis increased expression of MMPs can be detected and there is evidence of matrix degradation. MMP expression has been detected in HSCs, hepatocytes, Kupffer cells and infiltrating macrophages (Iredale et al., 2013).

They have been grouped into categories including collagenases, gelatinases, stromelysins and others according to their enzymatic substrate. Collagenases play a

key role in remodelling fibrotic tissue. They include MMP-1, -8 and -13 that are able to cleave the native helix of collagens I and III, rendering the product (gelatine) susceptible to degradation by other MMPs. MMP-1 and MMP-8 have been described to be expressed by inflammatory cells in human liver whereas MMP-13, the counterpart of MMP-1 in rodents, has been described in HSCs and macrophages (Iredale et al., 2013). The gelatinases, MMP-2 and -9 are also important as they degrade collagen type IV, fibronectin and elastin in addition to denatured collagens (gelatine). Furthermore, they can also increase the biological activity of pro-inflammatory cytokines such as IL-1β and TNF-α (Kurzepa et al., 2014). The key source of MMP-2 are activated HSCs (Arthur et al., 1992) whereas MMP-9 has been shown to be expressed by HSCs, Kupffer cells and infiltrating macrophages (Han et al., 2007; Winwood et al., 1995). In experimental models of liver fibrosis induced by either CCl_4 or bile duct ligation, MMP-2 and MMP-9 expression significantly increases compared to healthy controls (Kurzepa et al., 2014). Experimental liver injury in MMP-2 KO mice using CCl_4 or bile duct ligation suggested that MMP-2 is antifibrotic as more collagen deposition was detected in MMP-2 KO mice compared to wild type (WT) controls (Onozuka et al., 2011). This was possibly through the ability of MMP-2 to suppress collagen type I expression rather than a possible collagenolytic ability (Radbill et al., 2011). In contrast, other data has demonstrated that MMP-2 can also induce HSC proliferation and migration (Hemmann et al., 2007). Overall, the findings so far indicate that MMP-2 can have pro and antifibrotic functions and that these functions might be separate in time. Similarly, MMP-9 seems to be involved in HSC activation but also HSC apoptosis. IL-1-induced activation was prevented in HSCs from MMP-9 KO mice when cultured in a three-dimensional ECM model compared to HSCs from WT mice (Han et al., 2007). Furthermore,

MMP-9 was also able to activate latent TGF-β (Yu and Stamenkovic, 2000) the main growth factor for HSC activation and collagen deposition. Conversely, a mouse model with CCl_4-induced injury with overexpression of MMP-9 demonstrated reduced fibrogenesis caused by apoptosis of activated HSCs (Roderfeld et al., 2006).

Importantly, TIMPs are able to inhibit the activity of MMPs as they can bind in a reversible manner to the active sites of MMPs. During fibrosis, ECM continues to accumulate because high levels of TIMPs block MMP activity (Iredale et al., 1996). There are four TIMPs, TIMP-1, -2, -3 and -4 (Kurzepa et al., 2014). TIMP-1 and -2 are both expressed by activated HSCs and the expression levels of TIMP-1 are closely associated with the numbers of activated HSCs (Iredale et al., 1996). The different expression levels of TIMP-2 between quiescent and activated HSCs are less pronounced than TIMP-1 levels as quiescent HSCs already express TIMP-2 (Iredale et al., 2013). The importance of TIMP-1 has been demonstrated in a mouse model overexpressing TIMP-1 in the liver that had significantly more ECM accumulation than their WT controls after treatment with CCl_4 (Yoshiji et al., 2000). In addition, blocking TIMP-1 in a mouse model of fibrosis induced fibrolysis (Nie et al., 2001).

1.3.3.3 Growth factors

TGF-β1 The key cytokine involved in fibrogenesis is TGF-β1. During liver injury, TGF-β1 is highly upregulated and is released primarily by Kupffer cells and infiltrating macrophages but also apoptotic hepatocytes (Cong et al., 2012). It is a potent pro-fibrogenic cytokine that induces HSC transformation from a quiescent into an α-SMA-positive active phenotype that expresses collagen type I. Once HSCs are active they also contribute to TGF-β1 production. To mediate the activity of TGF-β1

it undergoes several post-translational changes. Large amounts of the non-active form are stored outside of cells through cross-links in the ECM. Some of the factors that can change TGF-β1 into its active form include MMP-2, and -9 (Cong et al., 2012). The importance of TGF-β1 has been demonstrated in genetically altered mice. TGF-β1 KO mice had significantly less collagen deposition compared to their WT controls after treatment with CCl_4 whereas overexpression of TGF-β1 alone in normal mice caused a 15-fold increase in collagen type I compared to controls (Hellerbrand et al., 1999). Theoretically TGF-β1 would make an attractive target for antifibrotic therapy. However, general and untargeted inhibition of TGF-β1 poses a risk as it has important anti-inflammatory effects (dampening excessive T cell activation) and roles in cellular differentiation and growth regulation within the liver (Yang et al., 2010; Baek et al., 2010).

PDGF. PDGF is the most potent mitogen for HSCs described so far that is secreted by platelets, macrophages and HSCs causing proliferation and migration of HSCs to the site of injury (Bonner, 2004). It is known to work synergistically with TGF-β1 to enhance migration and expression of MMPs (Fibbi et al., 2001; Yang et al., 2003). There are four isoforms of PDGF (PDGF A, B, C and D) that signal through the PDGF receptor composed of α- and β-subunits (PDGFR-α and PDGFR-β). PDGF-B and -D act as potent mitogen in activated HSCs *in vitro* (Pinzani et al., 1991; Borkham-Kamphorst et al., 2007). Induction of PDGF-B and PDGFR-β has been well documented in liver injury induced by CCl_4 administration or bile duct ligation (Pinzani et al., 1994; Wong et al., 1994; Borkham-Kamphorst et al., 2008). Upregulation of PDGFR-β is a hallmark of early HSC activation that is followed by the transformation into myofibroblast-like cells (Bonner, 2004). Downstream

consequences of PDGF signalling in HSCs lead to activation of the PI3K-Akt and ERK signalling pathways and other pathways (Cong et al., 2012).

FGF The fibroblasts growth factors comprise a family of 23 reported members that bind to four FGF receptor kinases (FGFR1 to FGFR4). FGF1 and basic (b)FGF (also known as FGF2) are the most widely studied members of the FGF family that have been implicated in liver fibrogenesis. Basic FGF has been implicated in HSC activation, proliferation and migration *in vitro* (Pinzani et al., 1989; Fibbi et al., 1999). In contrast, FGF1/bFGF-deficient mice did not demonstrate an apparent difference in the number, activation and recruitment of HSCs following CCl_4-induced liver injury *in vivo* (Yu et al., 2003). However, FGF1/bFGF deletion caused a decrease in *Col1a1* (Collagen type I) induction during HSC activation after acute CCl_4 injury and significantly decreased fibrosis that resulted from chronic CCl_4 injury (Yu et al., 2003).

1.4 TNF superfamily

The TNF superfamily consists of cytokines that interact with a corresponding superfamily of receptors, the TNFR superfamily. There are 29 receptors and 19 ligands that can modulate numerous cellular functions including cell survival, differentiation, growth and production of inflammatory cytokines and chemokines (Croft et al., 2013) (Figure 1.3). The specific response depends on the receptor, the type of cell and other signals received by the cell from their surrounding. Most of the TNF superfamily receptors and ligands are expressed by or primarily target cells of the immune system but they are also detected on other cell types including epithelial cells, endothelial cells and mesenchymal cells (Croft et al., 2012). TNF receptors are typically type I transmembrane proteins with one to six cysteine rich domains (CRDs)

in their extracellular domain (Bremer, 2013). All of the TNF ligands have a characteristic TNF homology domain (THD) that initiates formation of homotrimers. They are normally expressed as type II transmembrane proteins that can be cleaved to form a soluble ligand. Certain members of the TNF family elicit different responses depending on whether they are membrane-bound or soluble. Only the membrane-bound form of FasL for example is efficient in inducing cytotoxicity (Reilly et al., 2009). As soluble FasL can compete with the membrane-bound FasL it can even act as an antagonist by preventing apoptosis induction by the membrane-bound form (Suda et al., 1997). In a similar way, membrane-bound CD40L is more potent in inducing cytotoxicity than the soluble form of the ligand (T Georgopoulos et al., 2006; Elmetwali et al., 2010). However, the difference in bioactivity of the soluble compared to the membrane-bound form is not necessarily attributable to all TNF members. For example TNF receptor 1 (TNFR1) is comparably well activated by both the soluble and membrane-bound forms of TNF- α (Grell et al., 1995).

The members of the TNF superfamily have mainly been associated with inflammatory and autoimmune diseases (Croft et al., 2012). However selected members also have an involvement in fibrosis. TNF-α is probably the most widely studied cytokine of this family and next to its pro-inflammatory roles it has been demonstrated to be involved in fibrogenesis (Distler et al., 2008).

In the liver, TNF-α has been demonstrated as a direct mediator of liver injury and subsequent fibrosis as demonstrated by TNF-α KO mice and TNFR1 KO mice that had reduced liver injury and less fibrosis after bile duct ligation compared to controls (Gäbele et al., 2009; Tarrats et al., 2011). Liver injury was assessed by serum levels of alanine aminotransferase (ALT) or aspartate transaminase (AST). Other studies have

shown, using different experimental models of injury, that TNF-α can also influence fibrosis directly without affecting levels of injury. For example, liver fibrosis was reduced in TNFR1 KO mice after CCl_4 treatment with no changes in liver injury as indicated by similar ALT levels compared to control mice (Sudo et al., 2005). Furthermore, TNF-α KO mice had similar levels of injury and inflammation but less fibrosis compared to their WT controls after a combination of bile duct ligation with cystic duct ligation (Osawa et al., 2013). Indeed, TNF-α seems to play a key role in HSC homeostasis by regulating both pro- (via caspase activation) and anti-apoptotic (via NF-κB pathways) signals (Cong et al., 2012). Although knocking out TNF-α reduces liver injury and fibrosis, clinical trials with TNF-α antibodies in patients with PSC or alcoholic hepatitis have not shown consistent results (Spahr et al., 2002; Naveau et al., 2004; Boetticher et al., 2008; Hommes et al., 2008; Sharma et al., 2009). PSC patients that received the TNF-α inhibitor infliximab did not demonstrate any treatment benefits (Hommes et al., 2008). In addition, some studies showed that inhibiting TNF-α with antibodies caused patients to be more susceptible to infections (Naveau et al., 2004; Boetticher et al., 2008). Indeed, patients with alcoholic hepatitis that were treated with etanercept, an antibody that inhibits the TNF receptor, had a higher 6-month mortality rate than the placebo group (Boetticher et al., 2008).

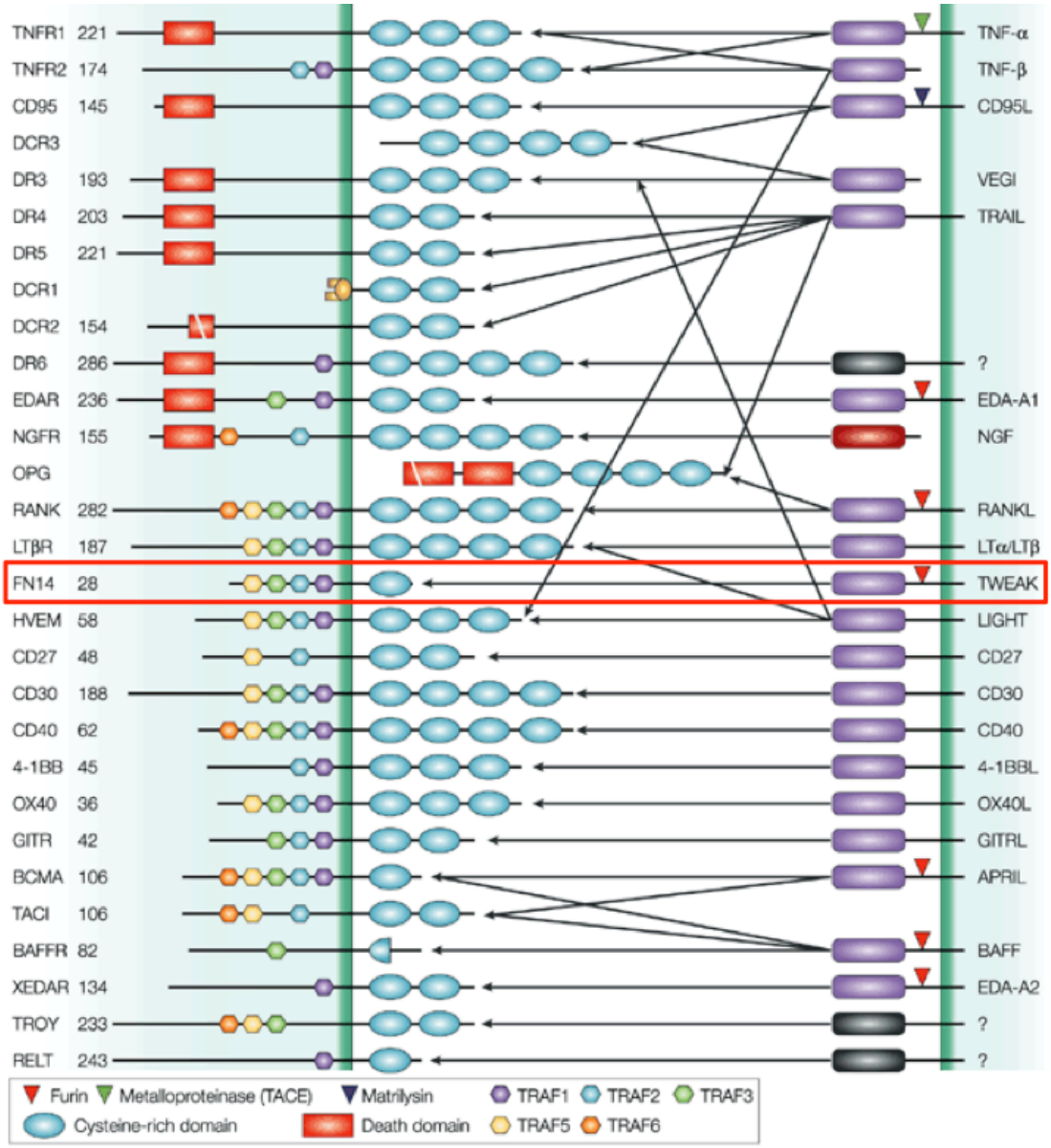

Figure 1.3 Ligands and receptors of the TNF superfamily
The TNF superfamily is a group of structurally related proteins. The receptors contain a characteristic cysteine rich domain (CRD) that can bind the TNF homology domain (THD) of the ligands. Some receptors have death domain that can induce apoptosis and other receptors have TRAF binding motifs.
Image adapted from: (Aggarwal, 2003)

1.5 TWEAK and Fn14

Two members of the TNF/TNFR superfamily that have been more recently discovered are the ligand TNF-like weak inducer of apoptosis (TWEAK) and its cognate receptor fibroblast growth factor inducible 14 (Fn14). TWEAK was discovered in 1997 by Chicheportiche *et al.* who demonstrated that it was pro-apoptotic on IFN-γ-treated human HT-29 colon carcinoma cells and therefore named it TWEAK (Chicheportiche et al., 1997). Fn14 was discovered in 1999 in murine NIH3T3 fibroblasts (Meighan-Mantha et al., 1999) and was later cloned from a HUVEC cDNA expression library and shown to be a receptor for TWEAK (Wiley et al., 2001). It was named Fn14 as its expression was upregulated when quiescent cells were exposed to FGF1 or bFGF and because its predicted molecular mass was about 14 kDa before peptide cleavage (Meighan-Mantha et al., 1999; Feng et al., 2000).

1.5.1 TWEAK structure and expression

Like other ligands of the TNF superfamily, TWEAK is expressed as a type II-transmembrane protein (Figure 1.4). The membrane-bound form of TWEAK consists of 249 amino acids. Extracellularly it comprises of a C-terminal region that contains a stalk region and a characteristic THD domain that is highly conserved between human and mice (Chicheportiche et al., 1997). Intracellularly it has a N-terminal domain that is connected to the C-terminal domain with a transmembrane domain (Chicheportiche et al., 1997; Marsters et al., 1998). As in other ligands of the TNF family, the THD of TWEAK mediates trimerisation and binding to the receptor. TWEAK is proteolytically released on the stalk region by a furin endoprotease to function primarily as a soluble homotrimeric cytokine. However, expression of

TWEAK has also been found on the cell surface of some cells. (Wajant, 2013) and it has recently been reported that membrane-bound TWEAK can bind to Fn14 on neighboring cells in a juxtacrine manner and activate the NF-κB signaling pathway (Brown et al., 2010).

Leukocytes are the main source of TWEAK including human resting and activated monocytes, dendritic cells and NK cells (Maecker et al., 2005). Other cell types that can express TWEAK include endothelial cells, astrocytes and renal tubular epithelial cells (Dohi and Burkly, 2012). Upregulated TWEAK expression has been detected in tissues from patients with inflammatory disease and experimental models of such diseases. These include rheumatoid arthritis, multiple sclerosis, ulcerative colitis and systemic lupus erythematosus (Burkly et al., 2011).

1.5.2 Fn14 structure and expression

Fn14 is the smallest receptor of the TNF receptor superfamily and the only known signalling receptor for TWEAK. It is a type-I transmembrane protein that is initially synthesised as a 129 amino acid protein and then proteolytically processed by signal peptidase into a 102 amino acid cell surface receptor (Winkles, 2008) (Figure 1.4). There is a 90% homology between the human and mouse mature Fn14 protein (Wiley and Winkles, 2003). The extracellular ligand binding region contains only one CRD (Wiley et al., 2001) and TWEAK is the only known ligand of the TNF family that can bind to Fn14 (Bossen et al., 2006). The cytoplasmic domain of Fn14 is 28 amino acids in length and is lacking a classical death domain. Like many other TNFR superfamily members that are lacking a death domain, Fn14 has a TNF receptor-associated factor (TRAF) binding motif. Several members of the TRAF family have been shown to be able to bind to this site including TRAF1, TRAF2, TRAF3, and

TRAF5 (Winkles, 2008). In normal tissue, Fn14 expression is low but becomes quickly upregulated locally during injury and disease. In acute injury, Fn14 is transiently expressed whereas expression of Fn14 is maintained in chronic tissue injury (Burkly, 2014). Parenchymal cells, stromal cells, vascular cells and progenitor cells have been described to express Fn14. Furthermore, expression has also been detected in many tumour cells (Burkly, 2014) and in some instances even in macrophages (Kim et al., 2004; Schapira et al., 2009). Fn14 gene expression can be induced in endothelial and mesenchymal cells by several growth factors and cytokines including FGF-1 and -2, PDGF-BB, TGF-β1, TNF-α, IL-1β and IFN-γ (Winkles, 2008).

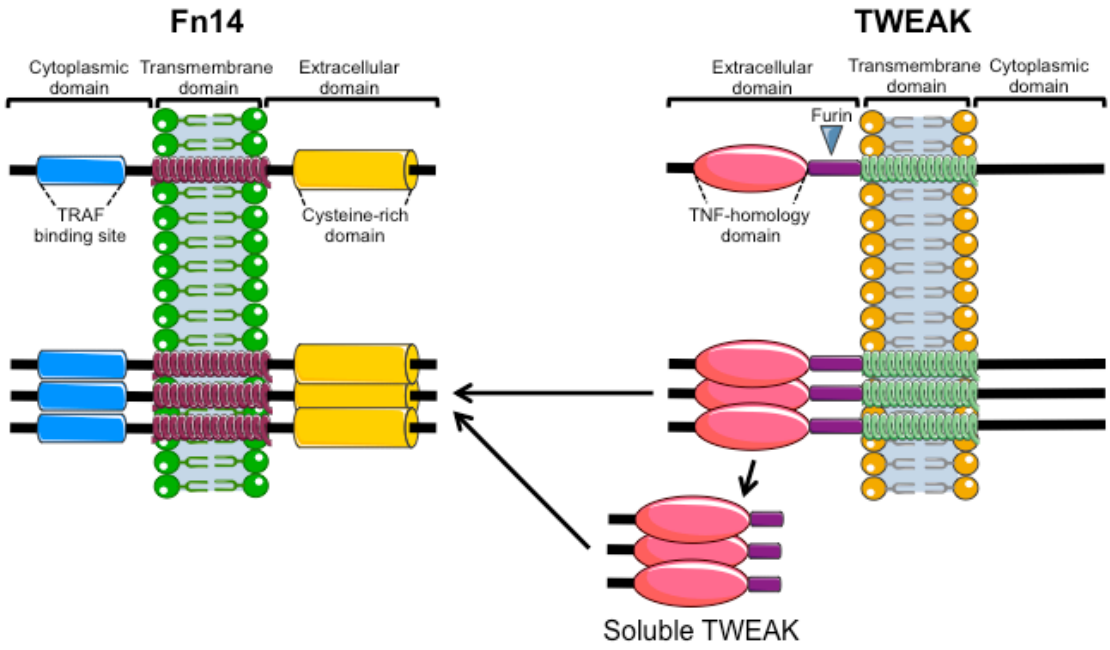

Figure 1.4 Structure of TWEAK and Fn14
TWEAK is a type II transmembrane protein with a TNF homology domain that mediates trimerisation. Furin can cleave TWEAK to release it from the membrane and make it a soluble cytokine. Fn14 is expressed as a type I transmembrane protein that is thought to trimerise upon TWEAK binding.

1.5.3 Function of TWEAK and Fn14

TWEAK signalling has been shown to regulate several biological processes including proliferation, differentiation, migration, fibrosis and inflammation. After acute injury Fn14 is transiently upregulated and involved in inflammation, angiogenesis and fibrogenesis (Burkly, 2014). It has a beneficial effects in acute skeletal muscle and pancreatic injury as demonstrated by Fn14 KO mice having delayed inflammatory and regenerative responses (Girgenrath et al., 2006; Wu et al., 2013). In contrast, the TWEAK and Fn14 pathway in chronic injury has been described to promote pathological tissue changes including chronic inflammation, fibrosis and angiogenesis. The pathological role of TWEAK and Fn14 has been described in experimental models of rheumatoid arthritis, atherosclerosis, ischemic stroke and systemic lupus erythematosus and other diseases associated with inflammation (Burkly et al., 2011).

One important aspect in many chronic diseases is accumulation of fibrosis. TWEAK and Fn14 are elevated in several different experimental models that feature fibrosis including renal ischemia reperfusion injury, skeletal muscle atrophy and chronic kidney disease (Hotta et al., 2011; Mittal et al., 2010; Novoyatleva et al., 2010; Son et al., 2013; Ucero et al., 2013). Studies have shown that overexpression of TWEAK in mouse models led to cardiac and kidney fibrosis (Jain et al., 2009; Hotta et al., 2011; Ucero et al., 2013), and that deletion of Fn14 protected against cardiac fibrosis (Novoyatleva et al., 2013). Evidence that TWEAK can directly affect fibroblasts has been given in several studies. TWEAK induced proliferation in cardiac and renal fibroblasts *in vitro* (Novoyatleva et al., 2010; Ucero et al., 2013). In addition, studies have also demonstrated that TWEAK induced collagen expression in cardiac fibroblasts via Fn14 (Chen et al., 2012; Novoyatleva et al., 2013) and

transdifferentiation of cardiac fibroblasts into myofibroblasts (Novoyatleva et al., 2013). In contrast, TWEAK inhibited transformation of keratocytes into myofibroblasts (Ebihara et al., 2009) and decreased expression of collagen type I and fibronectin in renal fibroblasts *in vitro* (Ucero et al., 2013) suggesting that TWEAK can induce different responses in cell type of the same lineage.

1.5.4 Hepatic expression of TWEAK and Fn14

TWEAK In the liver, expression of TWEAK mRNA has been primarily detected in macrophages and NK cells. In addition, low levels of TWEAK mRNA are also present in CD4-positive and CD8-positive T cells and NKT cells (Tirnitz-Parker et al., 2010) and TWEAK was also expressed and released by HCC cell lines (Kawakita et al., 2004).

Experimental liver injury caused by the choline-deficient, ethionine-supplemented (CDE) diet or by acute ethanol exposure did not change levels of TWEAK mRNA in the liver (Tirnitz-Parker et al., 2010; Affò et al., 2012). Furthermore, TWEAK transcription levels did not change significantly in patients with NASH, HCV infection or alcoholic hepatitis (Affò et al., 2012). In contrast, TWEAK mRNA levels dropped significantly after 12 hours of PH and then levelled out again after 96 hours (Karaca et al., 2014). Apart from these observations, little else is known about the expression of TWEAK in the liver. In addition, nearly all of those studies have looked at the transcriptional levels of TWEAK and not further investigated the protein expression and localisation of TWEAK in the liver.

Fn14 Expression of Fn14 in the liver has mainly been associated with liver epithelial cells and LPCs. Fn14 expression has been detected in cholangiocytes and LPCs in mouse livers and livers from patients with ALD and NASH (Jakubowski et al., 2005; Bird et al., 2013). In addition, Fn14 expression in primary mouse LPCs and an immature cholangiocyte cell line (603B cells) has also been described *in vitro* (Tirnitz-Parker et al., 2010; Karaca et al., 2014). Furthermore, Fn14 was shown to be expressed by immature hepatocytes (Affò et al., 2012; Karaca et al., 2014) but not by primary mature hepatocytes (Karaca et al., 2014) suggesting that it is involved in progenitor cell function but not directly in maintenance of mature hepatocytes. Although research has focused on epithelial cells and their progenitor cells other cell types have also been mentioned in the literature. Smooth muscle cells in normal human liver were Fn14-positive (Jakubowski et al., 2005) and a sub-population of α-SMA-positive cells has been described as Fn14-positive (Tirnitz-Parker et al., 2010). In contrast, CD68 and CD45-positive inflammatory cells isolated from injured mouse livers did not seem to express Fn14 (Tirnitz-Parker et al., 2010). Lastly, Fn14 was present in HCC cell lines and human HCC tissue (Feng et al., 2000; Kawakita et al., 2004; Wang et al., 2012; Li et al., 2013).

In accordance with research in other injuries and diseases, Fn14 becomes quickly upregulated in several different experimental liver injury models including PH (Feng et al., 2000; Ochoa et al., 2010; Karaca et al., 2014), acute CCl_4 injury, acute acetaminophen (also called paracetamol) and acute ethanol exposure (Affò et al., 2012). Also, liver injury caused by the 3,5-diethoxycarbonyl-1,4-dihydrocollidine (DDC) or CDE diets that are associated with LPC expansion induced an upregulation of Fn14 mRNA expression (Jakubowski et al., 2005; Tirnitz-Parker et al., 2010).

Enhanced Fn14 gene expression was also present in high-precision cut livers from healthy mice after treatment with TGF-β1. However, this was not detected when high-precision cut livers were treated with TWEAK or TNF-α (Affò et al., 2012) suggesting that Fn14 can be induced by pro-fibrogenic rather then pro-inflammatory cytokines. Furthermore, patients with alcoholic hepatitis but not NASH or HCV infection had significantly more Fn14 gene expression compared to normal livers (Affò et al., 2012).

1.5.5 Role of TWEAK and Fn14 in the liver

TWEAK has been demonstrated to be a direct mitogen for LPCs and cholangiocytes *in vitro* (Jakubowski et al., 2005; Tirnitz-Parker et al., 2010; Karaca et al., 2014). TWEAK-induced LPC proliferation was regulated through NF-κB pathway as it was reduced by siRNA against the p50 NF-κB subunit (Tirnitz-Parker et al., 2010). In contrast, TWEAK did not induce proliferation of mature hepatocyte *in vitro* (Jakubowski et al., 2005; Karaca et al., 2014), which is in accordance with mature hepatocytes not expressing the receptor.

In vivo studies have demonstrated that genetic overexpression of TWEAK or administration of exogenous TWEAK into healthy mice induced LPC expansion (Jakubowski et al., 2005; Bird et al., 2013). Also, TWEAK further induced LPC proliferation and infiltration of CD45-positive cells in mice on the CDE diet (Tirnitz-Parker et al., 2010) and proliferation of LPCs was inhibited by Fn14 deletion or by administration of TWEAK blocking antibodies in mice on the DDC diet (Jakubowski et al., 2005). Furthermore, administration of TWEAK-expressing bone marrow-derived cells into Fn14 KO mice or administration of bone marrow-derived cells from

TWEAK KO mice into WT mice showed both times a reduction in LPC expansion (Bird et al., 2013) demonstrating that TWEAK-induced LPC proliferation is indeed Fn14 dependent.

Tirnitz-Parker *et al.* also demonstrated reduced LPC expansion in Fn14 KO mice after 14 days on the CDE diet (Tirnitz-Parker et al., 2010). A co-regulation of the inflammatory response and fibrogenesis with LPC proliferation has been demonstrated in other models using the CDE diet (Knight et al., 2007; Van Hul et al., 2009). Therefore, they investigated whether this was also the case during TWEAK-regulated LPC expansion. Indeed, Fn14 KO mice on the CDE diet had reduced collagen deposition, fewer CD45-positive and F4/80-positive inflammatory cells and lower transcript levels of tissue inhibitor of *Timp1* and *2* and other inflammatory cytokines (Tirnitz-Parker et al., 2010). However, a reduced response could only be demonstrated after 14 days but not 21 days on the diet suggesting that other mechanisms can influence LPC proliferation and the associated fibrotic and inflammatory response. Expanding on potential therapeutic roles of TWEAK signalling, Kuramitsu *et al.* performed a PH in CCl_4-treated fibrotic mice with administration of exogenous recombinant TWEAK or TWEAK-blocking antibodies (Kuramitsu et al., 2013). Liver regeneration is generally considered to be impaired in fibrotic livers and indeed mice with fibrotic livers compared to non-fibrotic control mice had increased liver weight loss and worse survival rates after PH (Kuramitsu et al., 2013). The authors then demonstrated that administration of TWEAK to fibrotic mice after PH induced LPC proliferation but did not affect liver weight compared to control mice. In contrast, TWEAK-blocking antibodies inhibited LPC proliferation but enhanced hepatocyte proliferation and liver regeneration (Kuramitsu et al., 2013).

In addition, a downregulation of transcript levels of several pro-fibrogenic markers including *Tgfb1* and *2*, *Col1a1*, *Acta2* and *Timp1* were detected in mice treated with TWEAK-blocking antibodies whereas exogenous TWEAK caused an upregulation of those genes (Kuramitsu et al., 2013). This not only emphasised on the link between LPC proliferation and fibrosis but also indicated that blocking TWEAK improved liver regeneration. Conversely, Karaca *et al.* demonstrated that deficiency of TWEAK and Fn14 led to a decline in hepatocyte proliferation after PH (Karaca et al., 2014). However, in contrast to Kuramitsu *et al.*, they used healthy mice instead of fibrotic mice and investigated earlier time points. As mature hepatocytes do not express Fn14, they investigated how the TWEAK and Fn14 pathway might affect hepatocytes through indirect mechanisms. They demonstrated that mice deficient in TWEAK or Fn14 had reduced levels of the pro-regenerative cytokines TNF-α and IL-6 and the hepatocyte mitogen HGF (Karaca et al., 2014). Furthermore, Fn14 KO mice seemed to have liver failure after PH as indicated by a significant increase in infarcted areas of the liver and three fold higher serum bilirubin levels and most Fn14 KO mice died after PH (60% of Fn14 KO mice compared to 5% of WT mice) (Karaca et al., 2014). The data indicates that TWEAK and Fn14 signalling is beneficial after PH but it might be dysregulated in fibrotic mice undergoing PH.

1.5.6 Signalling pathways for Fn14

TWEAK treatment of Fn14-positive cells have been shown to activate several different signalling pathways but the NF-κB pathway seems to be the most commonly reported pathway (Winkles, 2008). The NF-κB family of transcription factors bind to DNA and induce gene transcription. They control the transcription of many genes encoding proteins that regulate immune and inflammatory processes (Napetschnig

and Wu, 2013). In unstimulated cells, NF-κB dimers are present in the cytoplasm as latent transcription factors as a consequence of their association with members of a family of proteins called inhibitors of κB (IκB). Upon stimulation with an extracellular stimulus a series of event occurs that involves the recruitment and activation of the IκB kinases (IKKs) that phosphorylate IκB leading to the subsequent degradation of IκB and the release of NF-κB. In the canonical NF-κB pathway, IκBα is degraded resulting in the translocation of mainly p65-containing heterodimers into the nucleus. In the non-canonical pathway on the other hand, IKKα phosphorylates p100 that is associated with RelB, which in turn promotes nuclear translocation of p52/RelB (Oeckinghaus et al., 2011). Both, the canonical and non-canonical pathway can be activated by TWEAK (Brown et al., 2003; Saitoh et al., 2003; Roos et al., 2010). Furthermore, the NF-κB pathway is also involved the pathogenesis of several liver diseases and prevents HSC apoptosis (Robinson and Mann, 2010). In addition, TWEAK treatment of several cell types has been shown to activate other signalling pathways including MAPK/ERK, PI3K/Akt, Wnt/GSK3β, Rho GTPases and JAK/STAT pathways (Burkly, 2014). TWEAK-independent Fn14 signalling has also been reported when Fn14 is ectopically overexpressed *in vitro* (Winkles, 2008). However, the importance for this interaction *in vivo* remains unclear.

1.5.7 Potential TWEAK signalling independent of Fn14

A number of reports suggest that TWEAK and Fn14 interaction is not exclusive. A study in 2003 showed that TWEAK was able to induce differentiation of the murine macrophage cell line RAW264.7 independent of Fn14 (Polek et al., 2003). Besides Fn14 another receptor called CD163 has been reported to interact with TWEAK. CD163 is a scavenger receptor with expression restricted to the

monocyte/macrophage lineage and has been demonstrated to bind and internalise TWEAK (Bover et al., 2007; Moreno et al., 2009). However, no evidence of signal transduction to my knowledge has been reported. Furthermore, it has been demonstrated that the intracellular N-terminal domain of TWEAK contains several nuclear localisation sequences and that TWEAK may enter the nucleus (De Ketelaere et al., 2004; Baxter et al., 2006; Al-Sawaf et al., 2014). In addition, the intracellular domain of the membrane bound form of TWEAK also contains a furin recognition site indicating that TWEAK can be cleaved intracellularly (Brown et al., 2010). However, the biological significance of any of these findings is not yet known.

1.5.8 Clinical relevance of TWEAK

A disease-driving role of the TWEAK and Fn14 pathway has been described in several different diseases. Research is now occurring to identify and develop treatment options to either inhibit or activate this receptor/ligand pathway dependent on the type of disease (Wajant, 2013). The first clinical study for the efficacy and tolerability of the monoclonal antibody BIIB023 that is used to block TWEAK in patients with rheumatoid arthritis (phase I) has previously been published (Wisniacki et al., 2013). Furthermore, the efficacy of BIIB023 is currently further explored in a phase II clinical trial in patients with systemic lupus erythematosus (Bertin et al., 2013).

Next to the possibilities of direct modulation of the TWEAK/Fn14 pathway with therapeutics, other research is investigating the potential role of soluble TWEAK (sTWEAK) as a marker for diagnosis and prognosis of various diseases (Bertin et al., 2013). For example, sTWEAK levels served as a predictor of disease progression in patients with systemic lupus erythematosus and advanced non-ischemic heart failure

(Schwartz et al., 2009; Richter et al., 2010). Due to its potential interaction with CD163, other research has focused on the correlation of soluble CD163 and sTWEAK levels in disease outcome. Indeed, high soluble CD163 and low sTWEAK concentrations have been correlated to type 1 diabetes mellitus diagnosis and cardiovascular mortality in peripheral arterial disease (Llaurado et al., 2012; Urbonaviciene et al., 2011). The role of sTWEAK in association with acute or chronic liver disease has not been investigated so far. However, research by Li *et al.* has demonstrated that hepatic expression levels of Fn14 served as a predictor of poorer surgical outcome in patients with HCC (Li et al., 2013). In addition, a study by Affò *et al.* demonstrated that alcoholic hepatitis patients with higher hepatic Fn14 mRNA expression had a worse 90-day survival rate than patients with lower Fn14 mRNA levels (Affò et al., 2012).

1.6 Thesis hypothesis and aims

Chronic liver disease is an increasing problem worldwide. Excess accumulation of fibrosis is a key driver in the progression of liver disease. TWEAK and Fn14 have been implicated in the involvement of fibrosis in several diseases but an immediate role for TWEAK and Fn14 during liver fibrosis has not been investigated in depth. Therefore, we hypothesised that TWEAK and Fn14 expression may be increased in several human liver diseases and that the pathway directly affects HSC behaviour and progression of fibrosis. Furthermore, we also hypothesised that TWEAK can be a predictor of disease outcome in patients with chronic liver disease.

Aims

I. To characterise the expression of TWEAK and Fn14 in human liver disease

II. To examine Fn14 and TWEAK expression in HSCs and to assess the effect of TWEAK on HSC function *in vitro*

III. To investigate the role of TWEAK and Fn14 in CCl_4-induced acute and chronic liver injury *in vivo*

IV. To determine the expression levels of TWEAK in a chronic liver disease and to evaluate whether it can be used as a marker for disease outcome

Chapter 2

Materials and Methods

2.1 Methods for Chapter 3,4 and 6: Human studies

2.1.1 Human tissue and serum samples

Explanted human liver tissue and normal donor liver surplus to surgical requirements, or generated as by-product of surgical resection for secondary liver malignancy were obtained from patients as part of the liver transplant programme based at the Queen Elizabeth Hospital, Birmingham, UK. All patients gave informed, written consent and studies were approved by the Local Research Ethics Committee (reference number 06/Q2702/61). Liver tissue and/or serum samples were obtained from healthy individuals and patients with NASH, ALD, PBC, PSC, AIH, ALF and inflammatory bowel disease (IBD).

2.1.2 Antibodies and cytokines used for human studies

Primary, isotype control and secondary antibodies for the human studies are outlined in Table 2.1, Table 2.2 and Table 2.3. Cytokines used for various experiments are detailed in Table 2.4.

Specificity	Isotype	Clone	Supplier	Working con.
Fn14	mouse IgG_1	mP4A8	Biogen Idec	3.7 µg/mL
TWEAK	mouse IgG_{2a}	mP2D10	Biogen Idec	3.24 µg/mL
α-SMA	mouse IgG_{2a}	1A4	Dako	0.7 µg/mL
Vimentin	mouse IgG_1	V9	Vector Labs	0.6 µg/mL
CD90	mouse IgG_1	eBio5E10	eBioscience	5 µg/mL
CD31	mouse IgG_1	JC70A	Dako	5.15 µg/mL
CK19	mouse IgG_{2a}	Ks19.1	Progen	5 µg/mL
Hepatocyte	mouse IgG_1	OCH1E5	Dako	1.65 µg/mL
CD68	mouse IgG_{2b}	Y1/82A	BioLegend	2.5 µg/mL

Table 2.1 Primary antibodies used for immunostaining

Isotype	Supplier	Working con.
Mouse IgG1	Life Tech.	Appropriate to primary antibody
Mouse IgG2a	Life Tech.	Appropriate to primary antibody
Mouse IgG2b	R&D Systems	Appropriate to primary antibody

Table 2.2 Isotype controls used for immunostaining

Antibody	Conjugate	Host	Supplier	Working con.
ImmPRESS Anti-mouse Ig	HRP	/	Vector Labs	/
Anti-mouse IgG1	Alexa Fluor 546	Goat	Life Tech.	4 µg/mL
Anti-mouse IgG2a	Alexa Fluor 488	Goat	Life Tech.	4 µg/mL

Table 2.3 Secondary antibodies used for immunostaining

Cytokines	Final conc.	Supplier	Application
bFGF	10 ng/mL	Peprotech	qPCR, IF, FC
TGF-β1	10 ng/mL	Peprotech	qPCR, IF, FC, ELISA
TNF-α	10 ng/mL	Peprotech	qPCR, FC, ELISA, Luminex
IFN-γ	100 ng/mL	Peprotech	qPCR, FC
IFN-γ	10 ng/mL	Peprotech	ELISA
PDGF	10 ng/mL	Miltenyi	ELISA, Proliferation
IL-1β	10 ng/mL	Peprotech	ELISA
IL-13	10 ng/mL	Peprotech	ELISA
TWEAK	1 - 500 ng/mL	Biogen Idec	qPCR, WB, Luminex, Proliferation

Table 2.4 Cytokines used to stimulate HSCs

Hepatic stellate cells were treated with cytokines for various different applications including quantitative polymerase chain reaction (qPCR), immunofluorescent staining (IF), flow cytometry (FC), enzyme linked immunosorbent assay (ELISA) and western blot (WB)

2.1.3 Isolation of human hepatic stellate cells

Primary human HSCs were isolated as described previously (Holt et al., 2009). A wedge of approximately 150 g from normal donor liver or from resected uninvolved liver tissue was used for HSC isolation. The perfusion circuit was set up using a peristaltic pump set to 40 RPM (Model IP 505Du, Watson-Marlow Ltd, Falmouth, UK) (Figure 2.1). All buffers were pre-heated to 42°C in a water bath. The wedge was perfused with Buffer I (Table 2.5) in order to remove any residual blood. This was followed by perfusion with Buffer II (Table 2.5), supplemented with 0.235 mg/mL pronase (Roche, Hertford, UK). After perfusion with approximately 300 mL of supplemented Buffer II, 5 mL of 3 mg/mL collagenase A was added (Roche). Perfusion continued with the enzyme solution for approximately 15 min until the liver became flaccid. The tissue was then transferred to a sterile beaker and manually dissociated in 100 mL of enzyme solution supplemented with 10 mL of 3.5 mg/mL pronase and 1 mL of 1 mg/mL DNase I (Sigma, Dorset, UK). The homogenate was then passed through a sterile nylon mesh of 60 µm (John Staniar Ltd, Manchester, UK) and washed four times with Buffer II supplemented with DNase I with centrifugation at 1400 x *g* for 7 min. To enrich the HSC population, the cell pellet was resuspended with 16.6% (v/v) Optiprep (Sigma) diluted in Dulbecco's Modified Eagle's Medium (DMEM, Gibco, Paisley, UK) and buffer II was then gently overlaid. The cells were separated via centrifugation at 1400 x *g* for 20 min. After centrifugation a white band of cells was visible just below the buffer II layer. This band was aspirated and washed with buffer II at 1400 x *g* for 7 min. The HSC suspension was further purified via negative magnetic selection. Specifically, the cell suspension was incubated with mouse anti-human CD31 antibody directly conjugated to Dynabeads (Life Technologies, Paisley, UK) for 15 min at room temperature in

order to select and remove endothelial cells and phagocytic macrophages. The remaining cells were then cultured with complete HSC medium comprising DMEM, 16% (v/v) heat inactivated foetal calf serum (FCS), 2 mM L-glutamine, 100 units/mL penicillin and 100 µg/mL streptomycin (all Sigma) and incubated overnight at 37°C. The following day cultures were washed with sterile phosphate buffered saline (PBS, Oxoid Limited, Hampshire, UK) to remove dead cells.

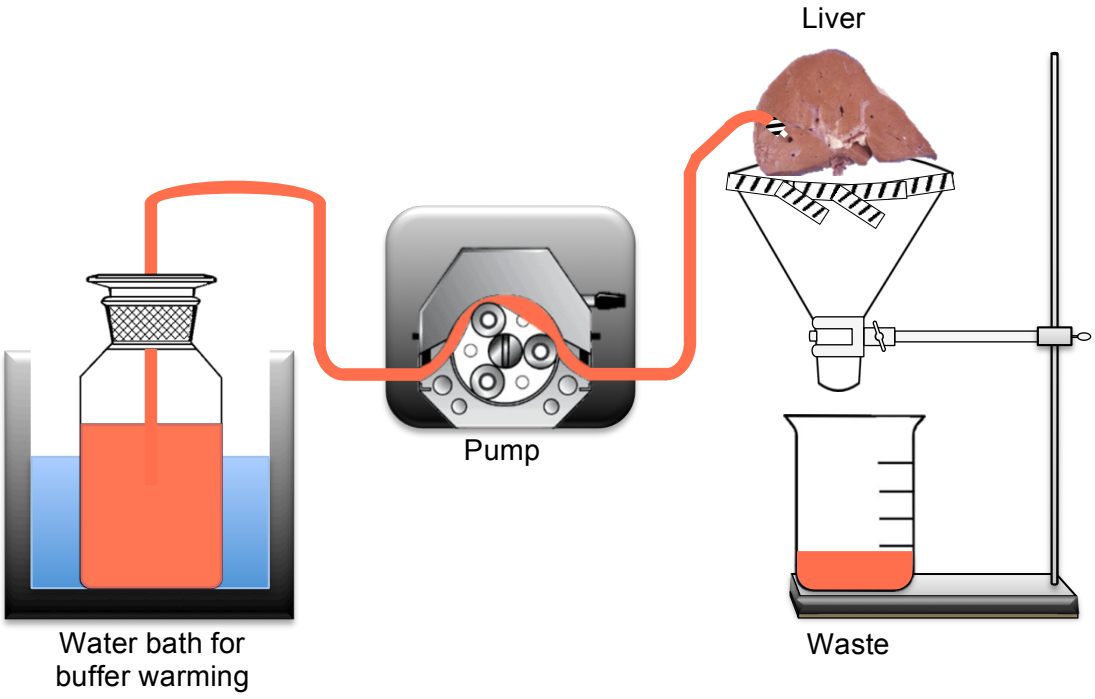

Figure 2.1 Schematic diagram illustrating the set-up for liver perfusion
This is the typical set-up for perfusion of liver wedges in order to isolate hepatic stellate cells. The relevant perfusion buffer was passed through a peristaltic pump and connected to the liver wedge. The liver wedge and buffer were kept sterile in a class II microflow safety cabinet. The liver was placed on a funnel covered with fine nylon mesh to allow the waste to be removed. Once the liver was adequately perfused with the enzymatic buffer, it was placed into a sterile beaker and further processed.

Buffer I		
Reagent	**Volume**	**Supplier**
1x HBSS	1000 mL	Gibco
1 M HEPES	6 mL	Sigma
7.5% (w/v) $NaHCO_3$	4.6 mL	Sigma
Buffer II		
Reagent	**Volume**	**Supplier**
Buffer I (as above)	1000 mL	/
1 M $CaCl_2$	1 mL	Sigma

Table 2.5 Buffers for liver perfusion

2.1.4 Isolation of human liver myofibroblasts

Isolation of LMFs was performed using explanted end-stage diseased liver tissue. Liver tissue was finely chopped with two scalpels and further digested with 0.4 mg/mL collagenase 1A (Sigma). The homogenate was passed through a sterile 60 µm nylon mesh (John Staniar Ltd), washed several times in PBS and then purified on a 33/77% Percoll gradient (GE Healthcare, Buckinghamshire, UK) at 550 x *g* for 30 min. The layer of cells at the interface was removed and washed in PBS several times. LMFs were extracted from the cell suspension after negative selection of IHECs and cholangiocytes. Here, the cell suspension was incubated with mouse anti-human EpCAM antibody (clone HEA125, Progen Biotechnic, Germany) bound to magnetic goat anti-mouse Dynabeads (Life Technologies) for 30 min at 37°C with agitation to eliminate cholangiocytes. The captured cells were removed with a magnet and the remainder of cells were incubated with mouse anti-human CD31 antibody directly conjugated to Dynabeads (Life Technologies) for 30 min at 37°C with agitation to remove IHECs. After removal of CD31-positive cells with a magnet, the remainder of the cells were washed and cultured in complete LMF medium (DMEM, 16% (v/v) FCS, 2 mM L-glutamine, 100 units/mL penicillin and 100 µg/mL streptomycin).

2.1.5 Cell culture and maintenance

2.1.5.1 General cell culture work

Tissue culture was carried out in a class II microflow safety cabinet. Sterile pipettes, 25 and 75 cm^2 culture flasks, 6-well and 24-well plates and 15 and 50 mL tubes were obtained from Corning Costar, Bucks, UK. Twenty mL plastic tubes and 5 mL bijoux were obtained from Greiner Bio One, Stonehouse, UK.

2.1.5.2 Cell culture and passage

HSCs and LMFs were grown in standard uncoated tissue culture flasks at 37°C in a humidified atmosphere of 5% CO_2. Cell growth and morphology was monitored with an inverted phase contrast microscope (IX50, Olympus, Southend-on-Sea, UK).

Cells were passaged at a confluence of about 80%. The medium in the flask was removed and the cells were washed with sterile PBS. After the cells had been washed an appropriate amount of TrypLE Express (1X; Life Technologies) was added to the flask to cover the cell layer. The cells were then incubated for approximately 5 min and gently agitated in order to detach them from the plastic. They were washed in sterile PBS at 550 x *g* for 5 min. The pelleted cells were resuspended in complete culture medium and transferred to a new culture flask.

2.1.5.3 Freezing cells for long-term storage

TrypLE was used to remove the cells from the flask as described above. The cells were pelleted and resuspended in 10% (v/v) dimethyl sulfoxide (DMSO; Sigma) diluted in FCS. The cell suspension was aliquoted into cryovials and stored in a Mr Frosty™ freezing container (Wessington Cryogenics, Houghton le Spring, UK) at -80°C overnight to allow gradual controlled freezing of the cells. The next day, cells were transferred to liquid nitrogen for long-term storage.

2.1.6 Characterisation of HSCs and LMFs

HSCs and LMFs were characterised using phase contrast microscopy to assess morphology and immunohistochemistry or immunofluorescence to confirm expression of phenotypic markers. To assess morphology of HSCs, cells were seeded into a 6-well plate after isolation and were allowed to adhere to the plastic for 24 hours. HSCs activated spontaneously in culture over 10 days with loss of lipid vacuoles and phenotypic changes, which could be visualised using an IX50 inverted microscope (Olympus). Phase contrast images were captured using a Canon EOS 40D digital camera at various time points in culture.

In order to determine the purity of the HSC and LMF cultures, cells were immunostained for various phenotypic markers for activated HSCs and myofibroblasts including α-SMA, Vimentin and CD90. CD31, CK19, Hepatocyte marker (staining a mitochondrial-associated antigen in hepatocytes (Wennerberg et al., 1993)) and CD68 were used to detect potential contamination with IHECs, cholangiocytes, hepatocytes and macrophages, respectively. A list of antibodies can be found in Table 2.1, Table 2.2 and Table 2.3 and an outline of the staining process can be found in section 2.1.9.

2.1.6.1 Oil Red O staining

Following isolation lipid droplets containing retinoic acid are present in the HSC cytoplasm. The lipid droplets were visualised with Oil Red O (Sigma) according to a standard protocol. Briefly, Oil Red O stock solution (0.5% (w/v) Oil Red O in 100% 2-propanol) was diluted to 60% (v/v) in distilled (d)H_2O (ORO working solution). Cells were fixed with 4% formalin solution and incubated with 60% 2-propanol for 5 min. The 2-propanol was aspirated and cells were incubated at room temperature for 30 min with freshly prepared ORO working solution. This was followed by 60% 2-propanol for 5 min and two washes with dH_2O. Images were captured at x20 magnification using an IX50 inverted microscope (Olympus) and a Canon EOS 40D.

2.1.7 Quantitative polymerase chain reaction

To quantify transcript levels in human livers, fresh normal or diseased liver tissue was cut into 1 cm^3 blocks, snap frozen in liquid nitrogen and stored at -80°C. Total RNA was isolated from 30 mg of snap frozen liver tissue using the RNeasy mini kit (Qiagen, Crawley, UK) according to manufacturer's instructions. GentleMACS M-tubes (Miltenyi Biotec, Surrey, UK) were used to homogenise tissue. As part of the isolation protocol all RNA was treated with RNase-free DNase (Qiagen) as an on-column digestion step. RNA was also extracted from HSCs, which were stimulated with cytokines detailed in Table 2.4 for 24 hours using the same kit. Cells treated with media alone were used as a control. RNA quantity and quality were assessed with a Nanophotometer (Implen Geneflow). An OD260/280 value between 1.8-2 was deemed acceptable. All human RNA samples were transcribed into cDNA with 1 µg of total RNA using the iScript cDNA synthesis kit including a blend of oligo(dT) and

random primers (BioRad, Hemel Hempstead, UK) according to manufacturer's instructions.

Quantitative polymerase chain reaction (qPCR) analysis of relative mRNA expression was performed with Roche gene expression assays using cDNA and target specific primers (Alta Biosciences, Birmingham, UK) and FAM/VIC labelled probes (Roche) (Table 2.6). Assays were run in 96-well white plates in a LightCycler 480 II (Roche) with the settings outlined in Table 2.7. Expression levels of the target genes were normalised to *GUSB* (β-glucuronidase, Roche). A study by Yamaguchi *et al.* has demonstrated that *GUSB*, out of 12 investigated housekeeping genes, was the most suitable housekeeping gene for qPCR studies on normal and diseased livers (Yamaguchi et al., 2013). Gene expression values are stated as $2^{-\Delta Ct}$ (Livak and Schmittgen, 2001). Negative controls contained RNase/DNase-free water or non-reverse transcribed RNA instead of cDNA.

Target	Forward primer (5'→3')	Reverse primer (5'→3')	Probe# (Roche)
TNFRSF12A **(Fn14)**	GACCGCACAGCGACTTCT	CACGAAGGTCAGGCTCAGA	26
TNFSF12 **(TWEAK)**	ATCGCAGCCCATTATGAAGT	CTCACTGTCCCGTCCACAC	85
ACTA2	CTGTTCCAGCCATCCTTCAT	TCATGATGCTGTTGTAGGTGGT	58
COL1A1	GGGATTCCCTGGACCTAAAG	GGAACACCTCGCTCTCCA	67
Housekeeping gene			
GUSB	Roche Cat# 05190525001		

Table 2.6 Human primers and probes used for qPCR

Reagents	Volume (µL)	Source
2x Probes Master	10	Roche
Nuclease-free H_2O	7.2	Roche
Forward primer	0.2	Alta Bioscience
Reverse primer	0.2	Alta Bioscience
Probe	0.4	Roche
DNA	2	Tissue/Cells
Total for one reaction	20	

Cycle	Temp. (°C)	Time (min:sec)	
Pre-incubation	95	10:00	
Amplification	95	00:10	Cycling x45
	60	00:30	
	72	00:01	
Cooling	40	00:10	

Table 2.7 qPCR mix and thermal profile for human samples

2.1.8 Western blot

2.1.8.1 Protein lysates from liver tissue

To investigate Fn14 expression, protein lysates were prepared from 30 mg of snap-frozen human liver samples. Liver tissue was homogenised in CelLytic™ MT lysis buffer (Sigma) containing proteinase inhibitor (Roche) and DNaseI (Sigma) according to the manufacturer's instructions. M tubes (Miltenyi Biotec) were used for mechanical homogenisation of the tissue in a gentleMACS system. Protein concentrations were calculated using the Biorad-DC protein assay (Biorad) according to manufacturer's instructions using bovine serum albumin (BSA; Sigma) as protein standard. Samples were stored at -80°C prior to use.

2.1.8.2 Extraction of cellular fractions from HSCs

In order to determine activation of NF-κB in HSCs, cells were stimulated with 100 ng/mL recombinant TWEAK (Biogen Idec, Cambridge, MA, USA) for 5, 30 min, 1, 2, 4, 8, 16 and 24 hours and prepared according to the NE-PER Nuclear and Cytoplasmic Extraction Reagents kit (Thermo Fisher Scientific, Cramlington, UK). Briefly, to purify the cytoplasmic fraction cells were detached from plastic and diluted in 50 µL CER I containing protease/phosphatase inhibitor and EDTA. Cells were vortexed and incubated on ice for 10 min before adding 2.75 µL CER II. After centrifugation at 16,000 x *g* for 5 min, the supernatant containing the cytoplasmic proteins was removed and kept at -80°C. To purify the nuclear fraction the remaining pellet was resuspended in 25 µL NER containing protease/phosphatase inhibitor and EDTA and vortexed four times with 10 min incubation times on ice in between. After centrifugation at 16,000 x *g* for 5 min, the supernatant containing the nuclear proteins

was removed and kept at -80°C for further analysis by western blotting as outlined in section 2.1.8.3 using antibodies detailed in Table 2.10.

2.1.8.3 SDS-PAGE and Western Blot

Protein samples were separated by a SDS-PAGE gel using a standard protocol. All buffers used for the western blot are described in Table 2.8 and stacking and resolving gels were prepared as described in Table 2.9. A maximum of 50 µg per protein sample was diluted in 5x sample buffer with β-mercaptoethanol (β-ME) and incubated for 10 min at 100°C. The samples were run on a 5% stacking/10 or 15% resolving SDS-PAGE gel and the separated proteins were electrotransferred onto nitrocellulose membrane (VWR International, Leighton Buzzard, UK) for 1 hour at 100 V. A molecular weight marker (size range 12-225 kDa; GE Healthcare) was run along with the samples. To check for successful protein transfer, the nitrocellulose membrane was stained with Ponceau Red solution (Sigma). The membrane was then blocked with blocking buffer for 1 hour at room temperature followed by incubation with primary antibodies (Table 2.10) diluted in antibody dilution buffer at 4°C overnight with constant agitation. After several washes in Tris buffered saline (TBS)/0.1% Tween20 the blots were incubated for 1 hour at room temperature with a peroxidase-conjugated secondary antibody diluted in antibody dilution buffer. The blots were washed several times with TBS/0.1% Tween20 and developed with enhanced chemiluminescence (ECL) western blotting substrate (Thermo Fisher Scientific) according to manufacturer's instructions. Enhanced chemiluminescence detection film (GE Healthcare) was exposed to the membrane and developed using a Kodak X-Omat 1000 processor. For re-probing, bound antibodies were removed from the membrane with stripping buffer for 45 min at 50°C. After washing the membrane

under running dH_2O for 1 hour it was blocked and re-probed with new antibodies. ImageJ software v.1.64 was used to analyse western blot images. The data are expressed as density of Fn14 relative to β-actin as a loading control. To investigate NF-κB activation, data are expressed as density of phosphorylated NF-κB relative to total NF-κB. β-tubulin was used a loading control.

Solution	Reagent	Quantity	Source
1.5 M Tris-base (*p*H to 8.8 with HCl)	Tris-base	181.71 g	Sigma
	dH_2O	Make up to 1 L	/
0.5 M Tris-base (*p*H to 6.8 with HCl)	Tris-base	60.57 g	Sigma
	dH_2O	Make up to 1 L	/
10x Running buffer	Glycine	144 g	Sigma
	Tris-base	30.3 g	Sigma
	SDS	10 g	Sigma
	dH_2O	Make up to 1 L	/
Transfer buffer	Glycine	28.8 g	Sigma
	Tris-base	6 g	Sigma
	Methanol	400 mL	Fisher Scientific
	dH_2O	Make up to 2 L	/
5x Sample buffer	200 mM Tris	242 mg	Sigma
	20% Glycerol	2 mL	Sigma
	SDS	1 g	Sigma
	Bromphenol blue	5 mg	Sigma
	dH_2O	Make up to 10 mL	/
10x TBS (*p*H to 7.4 with pure HCl)	Tris HCl	24 g	Sigma
	Tris-base	5.6 g	Sigma
	NaCl	88 g	Sigma
	dH_2O	Make up to 1 L	/
Blocking buffer	5% Non-fat milk	5 g	Marvel
	0.1% Tween20	0.1 mL	Sigma
	1x TBS	Make up to 100 mL	/
Antibody dilution buffer	5% BSA	5 g	Sigma
	0.1% Tween20	0.1 mL	Sigma
	1x TBS	Make up to 100 mL	/
Stripping buffer	10% SDS	20 mL	Sigma
	0.5 M Tris-base (*p*H 6.8)	12.5 mL	/
	β-ME	0.8 mL	Sigma
	dH_2O	67.5 mL	/

Table 2.8 Solutions for western blotting

	Stack	Resolving gel	
	5%	**10%**	**15%**
30%:0.8% degassed Acrylamide:Bis-acrylamide (BioRad)	0.83 mL	3.3 mL	5 mL
0.5M Tris-base *p*H 6.8	0.63 mL	/	/
1.5M Tris-base *p*H 8.8	/	2.5 mL	2.5 mL
10% SDS	40 µL	0.1 mL	0.1 mL
dH_2O	3.4 mL	4 mL	2.3 mL
10% APS	0.1 mL	0.1 mL	0.1 mL
TEMED	20 µL	20 µL	20 µL

Table 2.9 Components of SDS-PAGE gel

Specificity	Isotype	Supplier	Dilution
Fn14	rabbit Ig	New England Biolabs	1 in 1000
phospho-NF-κB p65 (Ser536)	rabbit Ig	New England Biolabs	1 in 1000
total NF-κB	rabbit Ig	New England Biolabs	1 in 1000
β-actin	mouse IgG1	Sigma	1 in 15000
β-tubulin	rabbit Ig	New England Biolabs	1 in 2000
Anti-mouse HRP	/	Dako	1 in 2000
Anti-rabbit HRP	/	Dako	1 in 1000

Table 2.10 Antibodies used for western blotting

2.1.9 Immunostaining and histochemistry

Liver tissues for immunostaining were obtained from the same patients as those used for qPCR and western blot. Snap-frozen liver samples were embedded in Tissue-Tek™ OCT (Fisher-Scientific, Loughborough, UK) and 5-7 µm thick sections were cut on a cryostat (Bright OTF). Freshly cut sections were fixed in acetone (Fisher-Scientific) for 5 min before storing them at -20°C. For immunostaining, sections were placed in a Shandon Sequenza unit (Thermo Shandon Limited, Runcorn, UK). This standardised system uses capillary action to reproducibly apply, incubate and sequentially remove reagents from microscope slides.

Immunostaining was also performed on cultured cells. Here, HSCs and LMFs were grown in 24-well plates on glass coverslips or on 12-well Ibidi chamber slides (Thistle Scientific, Glasgow, UK). In some instances HSCs were stimulated with bFGF and TGF-β1 as outlined in Table 2.4 for 24 hours. Prior to immunostaining cells were washed with PBS and fixed in 100% methanol for 5 min. After washing the cells twice with PBS they were stored in PBS at 4°C until required.

2.1.9.1 Immunohistochemistry

Immediately after removal of sections from -20°C, they were briefly incubated with acetone (5 min) and then placed in a Shandon Sequenza unit. Sections were washed with TBS and then incubated with 0.03% H_2O_2 in methanol for 10 min to quench endogenous peroxidase. They were then washed with TBS and blocked with 2x Casein (Vector Laboratories, Peterborough, UK) diluted in dH_2O for 10 min. Primary antibodies or isotype matched control antibodies (Table 2.1 and Table 2.2) diluted in TBS were added for 1 hour followed by two wash steps for 5 min with TBS/0.1% Tween20. The specimens were then incubated with species-specific horseradish peroxidase (HRP) conjugated-secondary antibody (ImmPRESS kit, Table 2.3) for 30 min followed by three wash steps for 10 min with TBS/0.1% Tween20. This was followed by incubation with 3,3′-diaminobenzidine (DAB; Vector Laboratories) for 5 min, rinsed with tap water and the sections were then counterstained with 25% (v/v) Mayer's Haematoxylin (VWR International) diluted in tap water for 2 min. Sections were then dehydrated and subsequently mounted in DPX (Leica Biosystems, Peterborough, UK).

Cells were stained in a similar way, except that they were stained within their culture vessel and not treated with 0.03% H_2O_2. Following incubation with the secondary

antibodies and the washing step they were incubated with 3-amino-9-ethylcarbazole (AEC; Vector Laboratories) for 20 min, rinsed with tap water and counterstained with 25% Mayer's Haematoxylin. The cells were mounted with aqueous immunomount (Thermo Fisher Scientific).

Staining was viewed with a light microscope and Axiovision 4.4 software was used to capture images (both Carl Zeiss Ltd, Cambridge, UK).

2.1.9.2 Immunofluorescent staining for confocal microscopy

Prior to staining, sections were washed with acetone. This was followed by washing with TBS/0.3% Triton-X100 (Sigma) for 5 min and blocking with 10% goat serum (GS; Vector Laboratories) diluted in TBS/0.1% Triton-X100. Primary antibodies or isotype matched control antibodies (Table 2.1 and Table 2.2) diluted in 10% GS/TBS/0.1% Triton-X100 were added for 1 hour and then washed off with TBS/0.1% Triton-X100. This was followed by incubation with a fluorescent species-specific secondary antibody (Table 2.3) diluted in TBS/0.1% Triton-X100 for 1 hour protected from the light. After three washing steps with TBS/0.1% Triton-X100 for 10 min, 4',6-diamidino-2-phenylindole (DAPI, Life Technologies) was added as a nuclear counterstain and specimens were mounted in fluorescent mounting medium (Dako, Ely, UK). The same protocol was used for cells except for the initial wash with acetone. The staining was viewed with a LSM 510 confocal microscope and images were acquired and analysed by LSM software (both Carl Zeiss Ltd).

2.1.9.3 Picrosirius red staining for quantification of fibrosis

Liver fibrosis was visualised and quantified using picrosirius red staining (PSR) of liver tissue sections. Snap-frozen sections were hydrated with dH_2O and then incubated with 5% (v/v) phosphomolybdic acid (PMA; Sigma) diluted in dH_2O for 5 min. This was followed by incubation in 0.1% (w/v) PSR (Direct red 80 in saturated picric acid) for 30 min. The slides were then dipped in 0.1 M HCl (Sigma) and dH_2O before dehydrating them with 100% ethanol. Sections were mounted in DPX. To quantify PSR staining, five non-overlapping images of each section were taken using a light microscope (Carl Zeiss Ltd) with identical illumination and exposure. Axiovision 4.4 software was used to capture images. Digital image analysis was performed using ImageJ 1.46r software. All images were analysed with equivalent threshold settings. The threshold pixels were expressed as percentage of the total pixel count. This was then used to represent the percentage positive area for collagen.

2.1.10 Flow Cytometry

Cell surface and intracellular expression of Fn14 and in some instances cell viability were assessed using flow cytometry. Baseline expression of Fn14 was determined in HSCs, LMFs and IHECs. To study the regulation of Fn14, HSCs were cultured to 80% confluence and treated with various cytokines (Table 2.4) for 24 hours. Cells were detached from the plastic with TrypLE Express and washed in PBS at 550 x *g* for 5 min. For cell surface expression, cells were resuspended in flow buffer (PBS/2% FCS/1mM EDTA) and filtered to remove cell clumps. Surface marker staining was preformed using unconjugated mouse anti-human Fn14 antibody (3.7 µg/mL; mP4A8, Biogen Idec) diluted in flow buffer. Control samples were treated with isotype-matched IgG1 (Life Technologies) diluted in flow buffer to the same

concentration as mouse anti-human Fn14 antibody. Following incubation with primary antibodies for 30 min at 4°C with constant agitation, samples were washed twice in flow buffer and then labelled with the secondary antibody rat anti-mouse PE (1:100, BD Biosciences, Oxford, UK) for 30 min with constant agitation at 4°C in the dark. Cells were washed twice and then resuspended in flow buffer. Labelled cells were analysed on a Cyan ADP analyser (Dako) using FlowJo software v. 8.7. About 10,000 events were recorded within the gated region of the scatter plot for each cell preparation in all experimental conditions. The pulse width scatter plot was then used to gate individual cells. Only the cells within the gated region were then used to calculate percentage positive cells and Median fluorescent intensity (MFI).

For intracellular staining the BD Cytofix/Cytoperm kit (BD Biosciences) was used according to manufacturer's instructions. Briefly, cells were resuspended in BD Cytofix and fixed for 20 min at 4°C. This was followed by cell permeabilization with BD Cytoperm. From then on cells were treated the same as for the cell surface stain except that permeabilization buffer was used throughout until cells were resuspended in flow buffer prior to analysis.

In some instances a Live/Dead violet dye (Life Technologies) was used to differentiate between live and dead cells. After the cells were detached from the culture flask and resuspended in 1 mL PBS, 1µL Live/Dead dye (stock 50 µg/mL) reconstituted in DMSO was added and cells were incubated for 30 min at room temperature in the dark. The cells were then washed twice in flow buffer and fixed for 20 min at 4°C with BD Cytofix. The intracellular staining protocol was then followed as described above. Dead cells were identified by their uptake of the viability dye represented by increased fluorescence intensity in the violet channel.

2.1.11 Detection of soluble TWEAK using ELISA

2.1.11.1 Samples

Serum samples were collected from 64 newly diagnosed PSC patients attending the Liver Clinic (Queen Elizabeth hospital, Birmingham, UK) between January 2010 and November 2013. Clinical and laboratory data were collected at time of diagnosis and each subsequent clinic visit (3-12 monthly). Severity of liver disease was classified as pre-cirrhotic and cirrhotic. Given that liver biopsy is no longer standard practice of care in PSC, in the absence of histological data the presence of cirrhosis was identified according to a combination of clinical characteristics (ascites, varices, hepatic encephalopathy), laboratory parameters (hypoalbuminaemia, thrombocytopenia, prolonged prothrombin time/international normalised ratio (INR)), radiological features (coarse, irregular liver ± reversed portal vein flow, splenomegaly, intra-abdominal varices, ascites) and/or transient elastography (≥14.4kPa) (Corpechot et al., 2014). Patients with active ascending cholangitis, evident cholangiocarcinoma or colonic cancer were excluded from sampling.

Serum samples from patients with IBD alone (n=24) and healthy individuals (HC) without evidence of liver or gastrointestinal disease (n=22) served as controls. The distribution of intestinal inflammatory activity in IBD patients was classified as predominantly large bowel (colitis), small bowel or peri-anal disease.

To measure endogenous sTWEAK in culture supernatant, HSCs were seeded at 30,000 cells per well of a 24-well plate then serum starved in DMEM containing 0.5% BSA (Sigma) for 24 hours. Cells were stimulated with various cytokines (Table 2.4) diluted in complete HSC medium for 24 hours. Unstimulated macrophages were used as a positive control. Macrophages were isolated as described previously (Fletcher et al., 2014). The supernatant was filtered after collection to remove cell debris and subsequently stored at -80°C.

2.1.11.2 ELISA

Soluble TWEAK levels were quantified using human TWEAK instant ELISA (eBioscience, Hatfield, UK) according to manufacturer's instructions. Briefly, pre-coated standard and sample wells of the provided 96-well plate were hydrated with dH_2O. Then, 50 µL of human serum diluted 1 in 2 with sample diluent or undiluted cell supernatant were added. After a 3 hour incubation on a microplate shaker at 400 RPM the plate was washed six times with wash buffer. Any residual wash buffer was removed by inverting the plate and gently tapping it on a paper towel after the last wash. Upon addition of TMB substrate solution, a blue colour developed which was monitored with a Synergy HT microplate reader (BioTek Instruments, Potton, UK) set at 620nm until the highest standard had reached an optical density of about 0.9. Stop solution was added once colour development had occurred (typically 8 min) and absorbance was measured with the microplate reader set at 450 nm with a reference wavelength set to 620 nm. Each sample was run in duplicate and the sTWEAK concentration was determined by comparison to the standard concentration curve.

2.1.12 Luminex measurement of CCL5 in HSC supernatant

Secretion of the chemokine CCL5 by HSCs into the culture media was measured using a custom-made multiplex array kit (R&D Systems, Abingdon, UK). HSCs were seeded at 30,000 cells per well into a 24-well plate and serum starved with DMEM/0.5% BSA before stimulation with 100 ng/mL TWEAK diluted in complete HSC medium (Table 2.4). The experiment was performed according to manufacturer's instructions by Dr Elizabeth Humphreys (University of Birmingham, UK) on a Luminex 100 plate reader (Luminex Corporation, USA).

2.1.13 Proliferation of HSCs in response to TWEAK

In order to investigate HSC proliferation upon TWEAK stimulation, HSCs were seeded at subconfluence (10,000 cells per well) into 24-well plates and serum-starved for 24 hours in DMEM/0.5% BSA. The medium was replaced by complete medium with or without TWEAK (1-500 ng/mL) or PDGF-BB (10 ng/mL; Table 2.4). Repeated phase contrast images of pre-determined representative fields were taken over 36 hours with the Cell-IQ imaging system (CM Technologies, Finland). Cell count per field was determined by counting nuclei at the beginning and the end of the incubation period. The baseline cell count was subtracted from the final value and data were expressed as percentage increase above the number of untreated cells.

HSC proliferation was also determined with a commercially available CyQUANT NF Cell Proliferation Assay Kit (Life Technologies). A range of HSC cell counts was tested before the optimal density of 4000 cells per well of a 48-well plate was determined. HSCs were stimulated in duplicate with recombinant TWEAK (100ng/mL) or PDGF-BB (10ng/mL; Table 2.4). This quantification method relies on a fluorescent dye, which exhibits strong fluorescence when bound to DNA as a marker of changes in cell number. Proliferation was determined after 48 hours when medium was removed and the detection reagent added to each well. Plates were then incubated at 37°C for 40 min, and fluorescence was measured at 480/520 nm on a Synergy HT plate reader. Background fluorescence was subtracted and data was expressed as fold change compared to an unstimulated control.

2.1.14 Migration assays

HSCs were seeded into a 24-well plate (10,000 cells per well) and serum-starved for 24 hours in DMEM/0.5% BSA. To inhibit endogenous TWEAK, HSCs were treated with 0.125 to 2 μg/mL blocking anti-TWEAK mAb (mP2D10, Biogen Idec) (Sanz et al., 2008). Matched concentrations of mouse IgG2a were used as an isotype control. Both antibodies were diluted in complete HSC medium. Cells were then monitored with the Cell-IQ imaging system for 48 hours. Analysis was carried out with Cell-IQ analyser 4 Pro-Write software v. AN4.3.0.HW and data were expressed as area occupied by cells.

2.2 Methods for Chapter 5: Murine studies

2.2.1 Mouse models (TWEAK KO and Fn14 KO)

Male 6-8 week old homozygous Fn14 KO mice (Jakubowski et al., 2005) and TWEAK KO mice (Campbell et al., 2006) were used for acute and chronic liver injury experiments which were performed in the Biogen Idec Laboratory in Cambridge, MA, USA. Age and sex matched WT littermates for each KO strain (Fn14 WT and TWEAK WT) were used as controls. To ensure that the KO mice had the same microbiome as their matched WT controls, KO mice were backcrossed to Balb/c mice for 10 generations. The heterozygous (HET) mice were then intercrossed and homozygous KO and WT mice selected. The KO mice were then intercrossed to maintain a homozygous KO line and likewise for the WT line. All animal procedures were conducted in accordance with Cambridge, MA laws and the ethic committee of the Institutional Animal Care and Use Committee (IACUC). All mice were on a Balb/c background and maintained in 12 hour light/12 hour dark cycle with free access to food and water.

2.2.2 Genotyping of Fn14 KO mice

Genomic DNA was isolated from the tail or the liver of the mouse using a REDExtract-N-Amp Tissue PCR Kit (Sigma) according to manufacturer's instructions. All mice were genotyped using primers (Table 2.11) designed to distinguish Fn14 WT, Fn14 KO and HET genotypes. Details of the reagents and the thermal PCR profile are described in Table 2.12. Amplified products were run on a 2% agarose gel containing SYBR safe (Life Technologies) at 100 V and visualised under UV light. The PCR products were identified by their sizes; the Fn14 WT gene was a 600bp fragment, the disrupted Fn14 gene (KO gene) was a 400bp fragment and HET animals displayed both bands (600bp and 400bp) (Figure 2.2). The HyperLadder 100bp (Bioline, London, UK) was used as an amplicon length marker.

Target	Primer (5'→3')
Forward	CTCTCCACCAGTCTCCTCTATG
Reverse	ACCTCGACAAGTGCATGGACTG
Neomycin	TGCTAAAGCGCATGCTCCAGACTG

Table 2.11 Fn14 KO and WT primers

Reagents	Volume (µL)	Source
2x REDExtract-N-Amp PCR mix	10	Sigma
Nuclease-free H_2O	5	Promega
Forward primer	1	Biogen Idec
Reverse primer	1	Biogen Idec
Neomycin primer	1	Biogen Idec
DNA	2	Mouse tail
Total for one reaction	20	

Cycle	Temp. (°C)	Time (min:sec)	
Pre-incubation	95	15:00	
Denaturation	94	01:00	Cycling x29
Annealing	60	00:30	
Extension	72	01:00	
Final extension	72	10:00	

Table 2.12 PCR mix and programme cycle for Fn14 genotyping

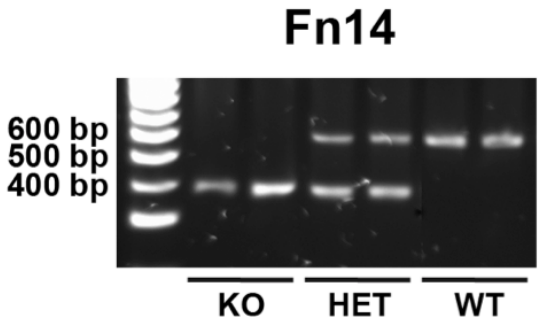

Figure 2.2 Genotyping of Fn14 WT, KO and HET mice
The 400 bp Fn14 knock-out (KO) gene, the 600 bp Fn14 wild type (WT) gene was detected with PCR. When both the KO and WT gene were detected mice were considered heterozygous (HET).

2.2.3 Genotyping of TWEAK KO mice

Genomic DNA was extracted from the tail of the mouse with 0.4 mg/mL proteinase K (Bioline) diluted in lysis buffer (Table 2.13) using an 18 hour incubation step at 60°C followed by a 10 min incubation step at 94°C. The extracted DNA was then amplified with primers to distinguish TWEAK WT, TWEAK KO and HET genotypes (Table 2.14). Details of the qPCR are outlined in Table 2.15. Amplified products were run on a 2% agarose gel containing SYBR safe (Life Technologies) at 100 V and visualised under UV light. The PCR products were identified by their sizes; the TWEAK WT gene was 400 bp, the disrupted TWEAK gene (KO) was 250 bp and HET animals displayed both bands (400 bp and 250 bp) (Figure 2.3).

Reagent	**Quantity (g)**	**Final concentration**	**Source**
Tris-HCl *p*H 8.5	12.11	100 mM	Sigma
NaCl	11.69	200 mM	Sigma
SDS	2	0.2 %	Sigma
EDTA	1.46	5 mM	Sigma
ddH_2O	Make up to 1 L		

Table 2.13 Lysis buffer for DNA extraction

Target	**Primer (5'→3')**
TWEAK KO primer	GGAGACTGCACCTTTGGAAG
Common primer	CGGGGAGGTTGGAGTTTAAT
TWEAK WT primer	TGCTTCTCTGCACTTTCTGC

Table 2.14 TWEAK KO and WT primer

Reagents	Volume (µL)	Source
Nuclease-free H_2O	11	Promega
10X HiFi PCR buffer	2	Life Tech.
10 mM dNTP	1	Life Tech.
DMSO (molecular grade)	1	Sigma
50 mM $MgSO_4$	0.8	Life Tech.
10 µM TWEAK KO primer	1	Biogen Idec
10 µM Common primer	1	Biogen Idec
10 µM TWEAK WT primer	1	Biogen Idec
Platinum HiFi Taq polymerase	0.2	Life Tech.
DNA	1	Mouse tail
Total for one reaction	20	

Cycle	Temp. (°C)	Time (min:sec)	
Pre-incubation	95	02:00	
Denaturation	95	00:30	Cycling x39
Annealing	56	01:00	
Extension	69	01:00	
Final extension	69	05:00	

Table 2.15 PCR mix and programme cycle for TWEAK genotyping

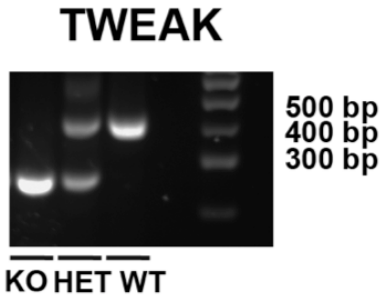

Figure 2.3 Genotyping of TWEAK WT, KO and HET mice
The 250 bp TWEAK knock-out (KO) gene, the 400 bp TWEAK wild type (WT) gene was detected with PCR. When both the KO and WT gene were detected mice were considered heterozygous (HET).

2.2.4 Harvesting of mouse tissue and serum samples

After animals were sacrificed by CO_2 overdose, blood was collected by cardiac puncture and serum was prepared for analysis of ALT activity. The liver lobes were excised and either fixed in 10% Neutral Buffered Formalin for paraffin sections, snap frozen in Tissue-Tek™ OCT for frozen sections or snap frozen only for RNA or protein extraction.

2.2.5 Liver injury model (CCl_4)

To determine expression and function of TWEAK and Fn14 during liver injury, mice were treated with CCl_4. CCl_4 is a toxic chemical that induces hepatocyte necrosis between 24 and 48 hours after administration (Karlmark et al., 2010). Liver regeneration becomes evident between 48 and 72 hours during which time activated HSCs significantly increase and infiltration of inflammatory cells occurs (Ikejima et al., 2001; Karlmark et al., 2010). Therefore, CCl_4 (Sigma; 1 in 4 dilution in mineral oil) or vehicle (mineral oil) was administered orally at a dose of 1 mL/kg body weight. Each mouse was weighed before administration of each dose and given the correct concentration of CCl_4 for their weight. In acute study 1, Fn14 WT mice were dosed once and sacrificed 24, 48, 72, or 96 hours after gavage. Naïve mice were used as a baseline control (Figure 2.4 A). In acute study 2, TWEAK KO and Fn14 KO mice along with their WT controls received one dose of CCl_4 or vehicle and were sacrificed after 72 hours of injury (Figure 2.4 B). For the chronic model, mice were administered CCl_4 or vehicle once a week for four weeks (total of four doses) and were sacrificed three days after the last dose (Figure 2.4 C).

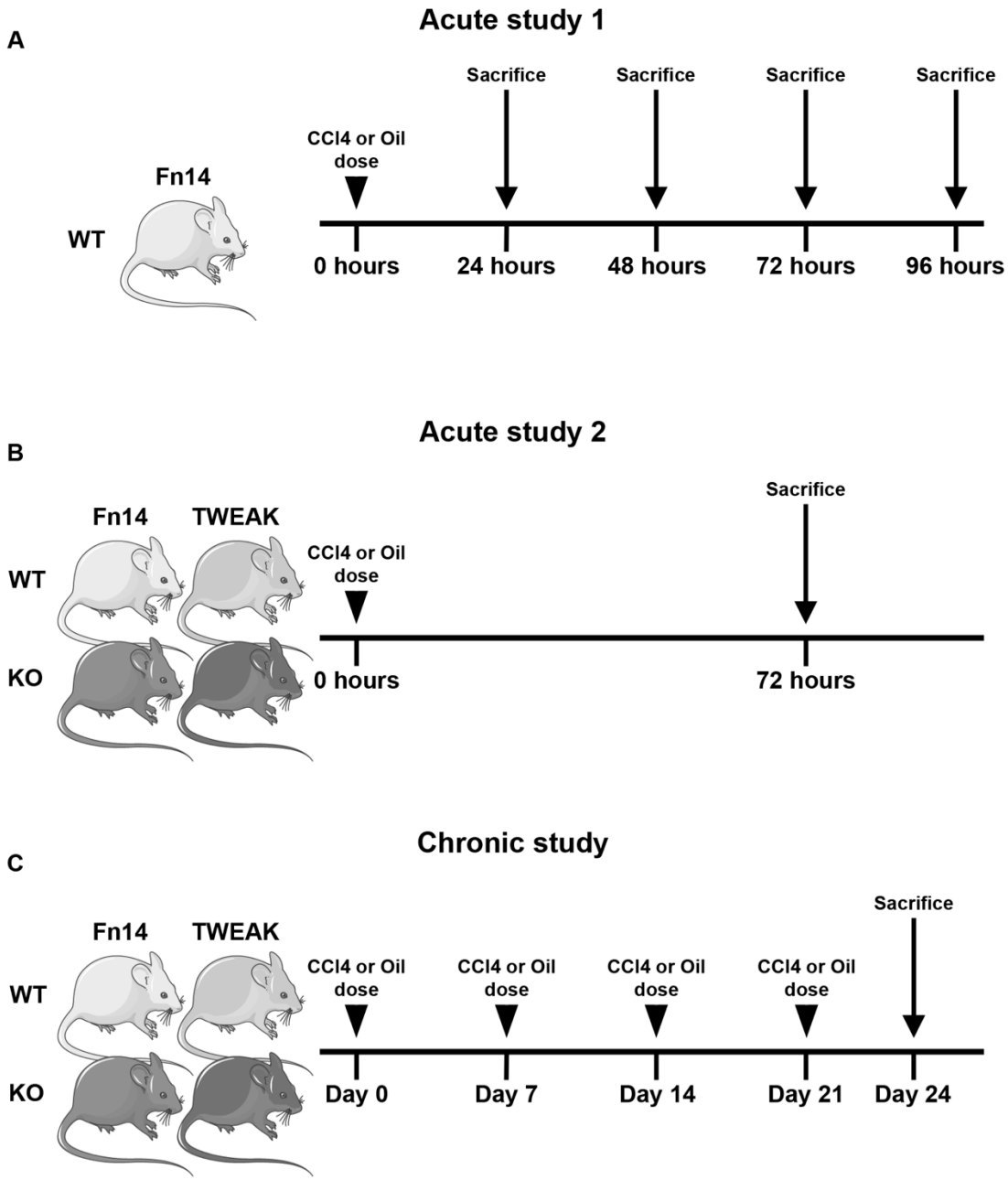

Figure 2.4 Outline of acute and chronic liver fibrosis models
Liver injury was induced with oral doses of 1 mL/kg CCl_4. One dose was administered and Fn14 wild type mice (WT) were sacrificed at the indicated time points (acute study 1) **(A)**. Fn14 and TWEAK knock-out (KO) and corresponding WT mice were scarified after 72 hours of one CCl_4 dose (acute study 2) **(B)**. For the chronic study, Fn14 and TWEAK KO and corresponding WT mice were dosed 4 times over a period of three weeks and sacrificed three days after last CCl_4 dose **(C)**. Serum and tissue was collected after the sacrifice.

2.2.6 Liver function test (ALT)

To determine liver function, ALT activity was measured in serum samples. ALT is an enzyme that is released after hepatocellular injury. It catalyses the transfer of an amino group from alanine to α-ketoglutarate and thereby generates pyruvate and glutamate. ALT was measured using an ALT activity assay (Sigma) as per manufacturer's instructions. Pyruvate standards and samples were diluted in ALT assay buffer and the master mix containing ALT assay buffer, peroxidase substrate, ALT enzyme mix and ALT substrate were added and mixed with a microplate shaker for 2 min. The colorimetric change was then measured every 5 min for 1 hour at 570 nm with a Synergy HT microplate reader (BioTek Instruments) set at 37°C. The ALT activity was determined by the colorimetric change between the first reading and the final reading once the most active sample was greater than the highest standard. Background levels were subtracted and the levels of pyruvate between the two measurements were calculated by comparison to the standard concentration curve. The ALT activity of the samples was then expressed as mU/mL.

2.2.7 RNA isolation and cDNA synthesis for murine studies

RNA from snap-frozen mouse tissue was isolated as described in section 2.1.7. All RNA samples were transcribed into cDNA with 2 µg of total RNA using the Precision-RT-premix (Primerdesign, Southampton, UK) according to manufacturer's instructions.

2.2.7.1 GeNorm housekeeping genes

To identify a stable housekeeping gene for use in the qPCR experiments, the geNorm Reference gene selection kit (Primerdesign) was used to evaluate 6 commonly used reference genes with representative samples in each study (acute 1, acute 2 and chronic study). The cDNA of the samples was measured by qPCR in duplicate wells using PrecisionPLUS master mix premixed with SYBRgreen (Primerdesign) in a LightCycler 480 II (Roche) with the settings described in Table 2.16. The housekeeping genes tested were *Gapdh* (Glyceraldehyde 3-phosphate dehydrogenase), *Rn18s* (18S ribosomal RNA subunit), *Actb* (β-actin), *B2m* (β-2 microglobulin), *Cyc1* (Cytochrome c1) and *Ywhaz* (tyrosine 3-monooxygenase/tryptophan 5-monooxygenase activation protein, zeta polypeptide). The amplification specificity for each qPCR analysis was confirmed by melting curve analysis (Figure 2.5). The stability of the housekeeping genes were analysed with the Biogazelle qbase+ software v.2.6.1 and the geNorm algorithm that has been designed to analyse the expression stability of a list of selected housekeeping genes in all samples. The genes were ranked according to geNorm stability measurements (geNorm M) with a low geNorm M value indicative of a more stable housekeeping gene. Based on geNorm analysis (see data in Figure 2.6), *Rn18s* was used as a housekeeping gene for acute study 1 and the chronic study and *Gapdh* was used for acute study 2.

Reagents	Volume (µL)	Source
2x PrecisionPLUS mix (SYBRgreen)	5	Primerdesign
Primer mix	0.5	Primerdesign
Nuclease-free H_2O	2	Promega
cDNA (25 ng)	2.5	Mouse liver
Total for one reaction	10	

Cycle	Temp. (°C)	Time (min:sec)	
Pre-incubation	95	02:00	
Amplification	95	00:15	Cycling x50
	60	01:00	
Melt curve	95	01:00	
	65	02:00	
	95	Continuous	
Cooling	40	00:10	

Table 2.16 SYBRgreen qPCR mix and thermal profile

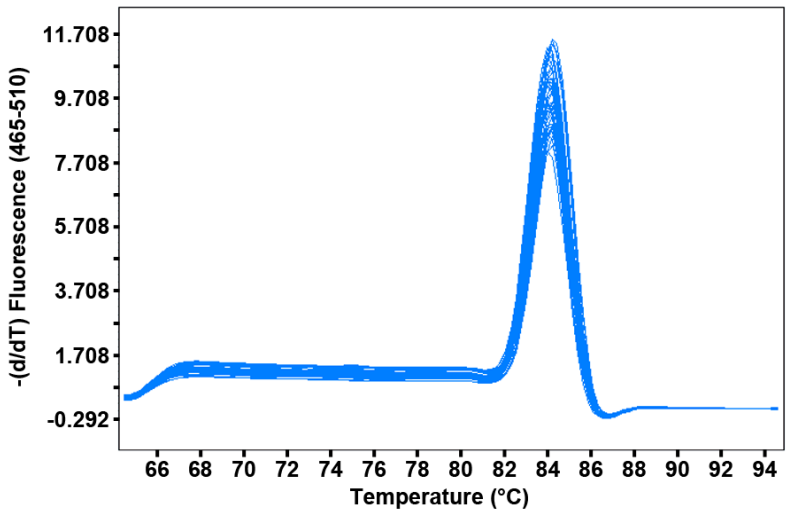

Figure 2.5 Representative example of a SYBRgreen melt curve

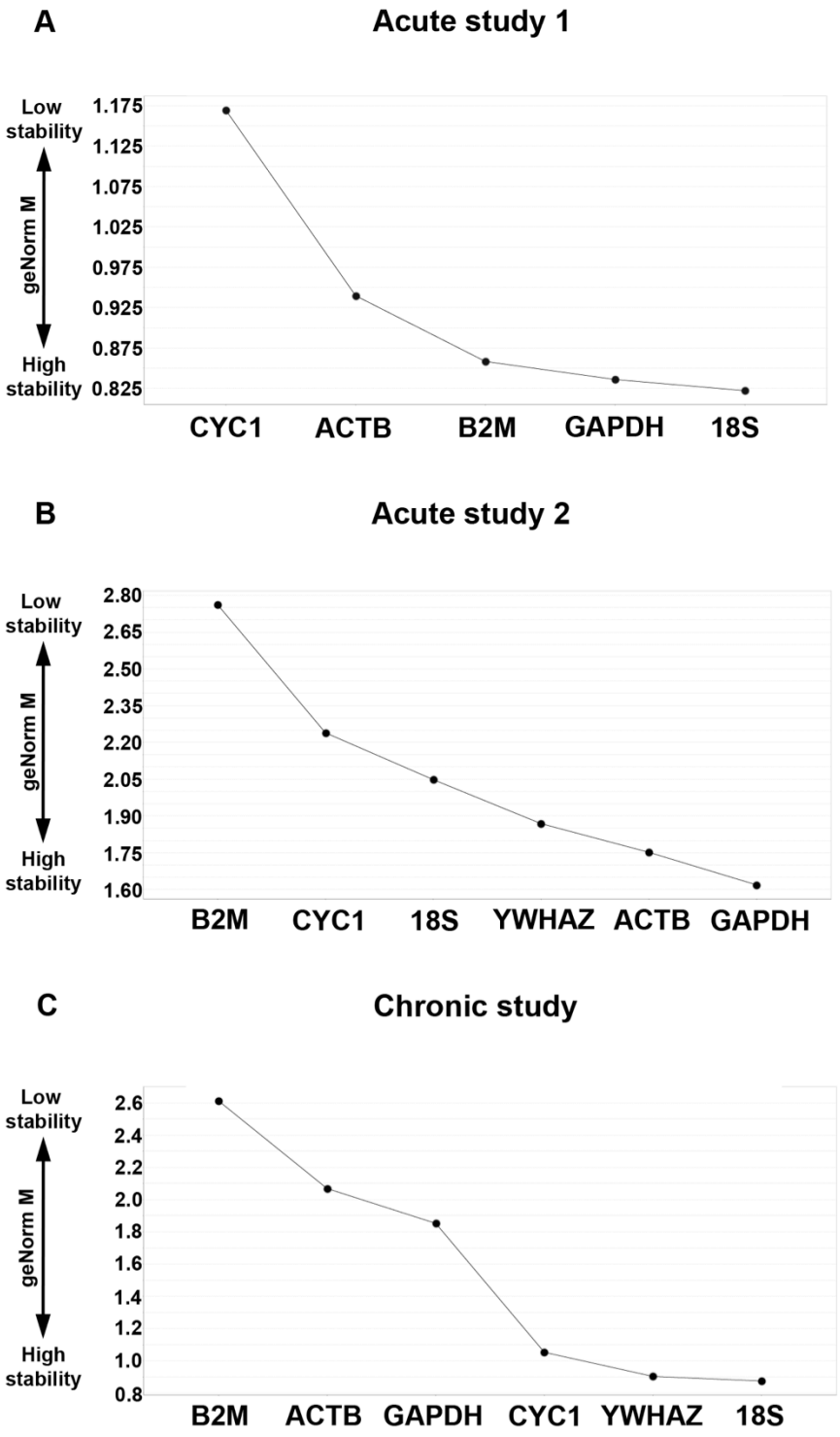

Figure 2.6 Expression stability of housekeeping genes
Candidate reference genes for normalization in liver samples from acute study 1 (n=9) **(A)** acute study 2 (n=16) **(B)** and chronic study (n=8) **(C)** Experimental designs are described in Figure 2.4. Data are expressed as geNorm stability measurements (geNorm M) and reference genes are ranked according to their expression stability by geNorm.

2.2.7.2 Quantitative PCR for murine studies

Quantitative analysis was performed using cDNA prediluted with PCR-grade water to 20-40 ng/µL. Quantitative PCR was carried out using Taqman gene expression assays; Fn14 gene (*Tnfrsf12a*, Mm01302476_g1), TWEAK gene (*Tnfsf12*, Mm02583406_s1), *Acta2* (Mm00808218_g1), *Col1a1* (Mm00801666_g1), *Timp1* (Mm00441818_m1), *Mmp2* (Mm00439498_m1), *Mmp9* (Mm00442991_m1), *Tgfb1* (Mm01178820_m1), and *Rn18s* (Mm03928990_g1) or *Gapdh* (Mm99999915_g1). Assays were run on a LightCycler 480 II (Roche) in duplicate on 384-well plates using the settings outlined in Table 2.17. Expression levels of the target genes were normalised to a housekeeping gene as determined in section 2.2.7.1 using $2^{-\Delta Ct}$. Negative controls contained RNase/DNase-free water or non-reverse transcribed RNA instead of cDNA.

Reagents	**Volume (µL)**	**Source**
2x PrecisionPLUS mix	5	Primerdesign
Primer/Probe mix	0.5	Applied Biosystems
cDNA (50-100 ng)	2.5	Mouse liver
Nuclease-free H_2O	2	Promega
Total for one reaction	10	

Cycle	**Temp. (°C)**	**Time (min:sec)**	
Pre-incubation	95	02:00	
Amplification	95	00:15	Cycling x50
	60	01:00	
Cooling	40	00:10	

Table 2.17 qPCR mix and programme cycle for mouse studies

2.2.8 Histology

Fixed mouse livers were dehydrated, embedded in paraffin and sectioned on a microtome to 3 μm thickness. After dewaxing, sections were stained with haematoxylin and eosin (H&E; Pioneer Research Chemical, Essex, UK) to identify general morphological changes. Briefly, sections were washed in water and then nuclei were stained with haematoxylin for 4 min, rinsed with water and incubated with 0.3% acid alcohol for 30 seconds. Following a further wash in water, sections were incubated in Scott's water, then washed in water and incubated in eosin for 2 min. Following washing the sections in water, they were dehydrated and mounted in DPX. Mouse livers from acute study 2 and the chronic study were stained with H&E by Premier Laboratory, LCC (Colorado, USA).

2.2.8.1 Myofibroblast quantification

Myofibroblasts were detected in paraffin tissue sections from Fn14 and TWEAK KO mice and their corresponding WT mice from the chronic study. Immunohistochemical staining was performed by Dr Gary Reynolds (University of Birmingham, UK) on an automated immunostainer (Dako) using a mouse-on-mouse ImmPRESS HRP kit (Vector Laboratories) according to manufacturer's instruction and an antibody against α-SMA (1:200 dilution, ASM-1, Vector Laboratories) or an isotype matched control antibody (Life Technologies).

Ten non-overlapping fields at x20 magnification from each section were captured using a light microscope (Carl Zeiss Ltd) with identical illumination and exposure. Digital image analysis was performed using ImageJ 1.46r software. Positive staining was identified with the threshold tool and all images were analysed with equivalent

settings. The pixels in the threshold were expressed as percentage of the total pixels. This was taken to represent the percentage area staining positively for α-SMA.

2.2.8.2 Picrosirius red staining on mouse liver tissue

Snap frozen OCT-embedded liver tissue from both acute studies was cut to 7 µm thick sections on a cryostat (Bright OTF) and fixed in acetone. To visualise collagen deposition livers were stained with the PSR protocol outlined in sections 2.1.9.3. For the chronic study paraffin embedded sections were stained with PSR and quantified by Bob Dunstan and Stefan Hamann (Biogen Idec, USA).

2.2.8.3 Von Kossa staining to detect mineralisation

The Queen Elizabeth hospital pathology department (Birmingham, UK) stained paraffin-embedded sections using von Kossa stain with a standard staining protocol. Slides were visualised at x10 magnification and images from each section were captured using a light microscope (Carl Zeiss Ltd) with identical illumination and exposure.

2.2.9 Hydroxyproline assay

Snap-frozen liver samples were weighed (about 80 mg), homogenised in 1 mL dH_2O and incubated with 125 µL of 50% trichloroacetic acid (Sigma) on ice for 30 min. After centrifugation at 16,000 x *g* for 5 min, the pellet was hydrolysed in 500 µL of 6 M HCl (Sigma) at 120°C in sealed borosilicate glass tubes overnight and then up to 48 hours in total in unsealed tubes at 75°C until the samples were dry. The precipitate was resuspended in 500 µL deionised (d)dH_2O and filtered in 0.45 µm centrifuge tube

filters (Sigma) at 2,000 x *g* for 2 min. Fifty µL of each sample were diluted in 950 µL ddH_2O. Hydroxyproline standards were prepared by serial dilutions of trans-4-hydroxy-L-proline (Sigma) starting from 2 µg/mL. One mL of sample or standard solution was then added to 500 µL of 1.75% (w/v) chloramine-T (Sigma, diluted in a solution containing 10% water, 10% n-propanol and 80% dilution buffer, see Table 2.18). The samples or standards were vortexed and incubated for 20 min at room temperature. Next, 500 µL of Ehrlich's solution (Table 2.18) was added, vortexed and incubated at 65°C for 15 min. Once the samples had returned to room temperature, the optical density was measured at 561 nm in triplicate in a 96-well plate using a BioTek plate reader. The hydroxyproline concentrations were calculated against a standard curve and expressed as µg/g wet liver.

Solution	**Reagent**	**Quantity**
Diluion buffer (*p*H to 6.8 with HCl or NaOH)	Citric acid monohydrate	25 g
	Sodium acetate trihydrate	60 g
	Sodium chloride	17 g
	Glacial acetic acid	6 mL
	dH_2O	Make up to 500 mL
Ehrlich's solution	4-(Dimethylamino)benzaldehyde	7.5 g
	60% Perchloric acid	13 mL
	N-propanol	Make up to 50 mL

Table 2.18 Solutions for hydroxyproline assay
All reagents were supplied by Sigma

2.3 Statistical analysis

Results are presented as medians unless otherwise stated. The statistical significance between medians was assessed using Kruskall-Wallis test or non-parametric Mann-Whitney U-test. Correlations between continuous variables were assessed with the Spearman's rho. The Chi-squared test was used to study significance between categorical variables. This analysis was carried out using Prism v6.0a software (GraphPad, CA, USA).

The optimal sTWEAK cut-off levels to predict short-term transplant free survival were calculated by an Area under the receiver operator characteristic (AUROC) curve analysis. Transplant-free survival was assessed using the Kaplan-Meier method and the log-rank test was performed to compare the survival curves of individual groups. Univariate and multivariate Cox proportional hazard models were used to determine impact of clinical parameters on short-term transplant free survival. The reported results included hazard ratios (HR) and 95% confidence intervals. This statistical analysis was carried out by Dr Palak Trivedi (University of Birmingham, UK) using SPSS v21 software (SPSS, Chicago, IL, USA). A p value of <0.05 was considered statistically significant.

Power calculations were performed to determine the number of animals in each treatment group. Based on PSR stain in earlier studies we determined significant differences between KO and WT mice in terms of 50% alteration in total collagen at 8 weeks CCl_4 with 7 mice per arm, 90% power and alpha of 0.05 (G*Power v3.1).

Chapter 3

The expression of TWEAK and Fn14 in normal and diseased human liver tissue

3.1 Introduction

Fn14 is highly regulated *in vivo* with low levels in healthy tissue and increased expression during injury and inflammation. It is a cell surface receptor present on a broad variety of different cell types including endothelial cells, epithelial cells and fibroblasts (Burkly et al., 2011). In the liver, Fn14 becomes quickly upregulated in experimental models of liver injury (Feng et al., 2000; Tirnitz-Parker et al., 2010). So far expression has been mainly associated with LPCs in mice (Tirnitz-Parker et al., 2010; Bird et al., 2013; Jakubowski et al., 2005) but there have also been suggestions that Fn14 is expressed by a subpopulation of myofibroblasts (Tirnitz-Parker et al., 2010). TWEAK, the ligand for Fn14 is highly expressed in leukocytes and has been detected in tissues during acute injury and inflammation (Serafini et al., 2008; van Kuijk et al., 2010). In the liver, TWEAK transcript levels did not alter significantly after injury with the CDE diet, and the highest TWEAK mRNA levels were seen in NK cells and macrophages (Tirnitz-Parker et al., 2010). Observations from human studies have shown that Fn14 was significantly upregulated in patients with alcoholic hepatitis compared to normal liver and expression was detected in intermediate hepatocytes, progenitor cells (Affò et al., 2012) and duct like structures (Jakubowski et al., 2005).

Despite these initial reports, a detailed analysis of TWEAK and Fn14 expression in human liver disease has not been performed. Therefore, the aim of this chapter was to investigate the localisation and expression levels of TWEAK and Fn14 mRNA and protein in normal and diseased livers.

3.2 Results

3.2.1 TWEAK and Fn14 gene expression are elevated in human liver disease

Real-time qPCR analysis of whole liver extracts detected low levels of Fn14 mRNA in normal liver tissue with significantly higher levels in ALF and chronic end stage liver disease ($p<0.01$). Furthermore, Fn14 mRNA was significantly higher in ALF compared to chronic liver disease ($p<0.05$) (Figure 3.1 A). TWEAK mRNA was also low in normal liver tissue, with significantly higher levels in chronic liver disease ($p<0.01$) but no significant differences in acute liver failure were detected ($p=0.13$) (Figure 3.1 B). TWEAK mRNA was considerably more abundant in liver tissue than Fn14 mRNA (Figure 3.1).

Comparison of chronic liver diseases demonstrated that the levels of Fn14 mRNA were significantly increased in immune-mediated liver diseases (PBC, PSC and AIH) compared to normal livers ($p<0.05$). Fatty liver diseases including NASH and ALD showed no significantly different expression of Fn14 mRNA to normal liver (NASH p=0.18, ALD p=0.08) (Figure 3.2 A). However, levels of TWEAK mRNA were significantly higher in fatty liver diseases ($p<0.05$) and in PBC ($p<0.01$) whereas expression in PSC ($p=0.18$) and AIH ($p=0.13$) livers were similar to normal livers (Figure 3.2 B).

Although the levels of TWEAK and Fn14 mRNA upregulation varied between chronic liver diseases when compared to normal livers, there was a significant positive correlation between Fn14 mRNA and TWEAK mRNA ($p<0.001$) (*Spearman* $\rho=0.53$; Figure 3.3).

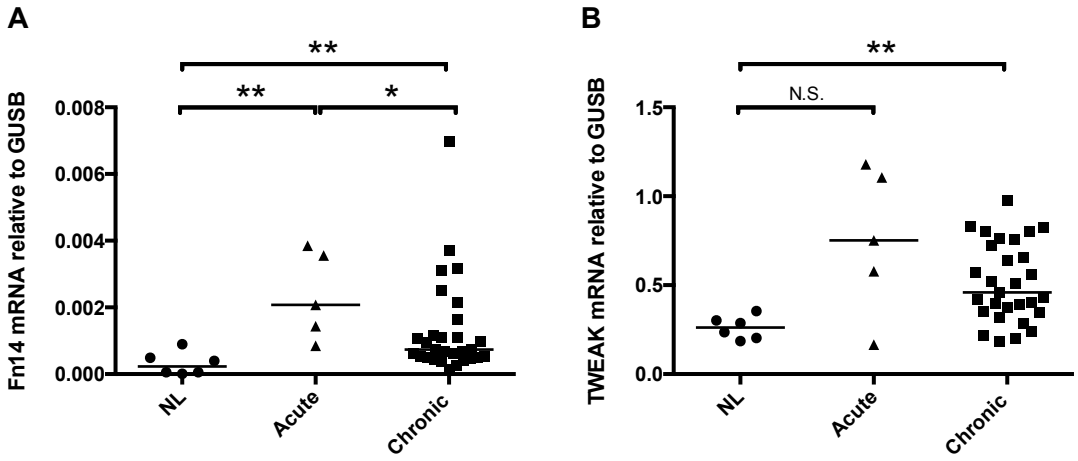

Figure 3.1 Fn14 and TWEAK mRNA is increased in acute and chronic liver disease

Expression of Fn14 **(A)** and TWEAK **(B)** was assessed by qPCR in normal livers (n=6), ALF (n=5) and cirrhotic livers (n=29). Gene expression is shown relative to GUSB using the $2^{-\Delta Ct}$ method (**p<0.05, ** p<0.01, n.s. not significant; Mann-Whitney U test*). The distribution of values was significantly different across the whole population (*p<0.01* (A) and *p<0.05* (B) *Kruskal-Wallis test*).

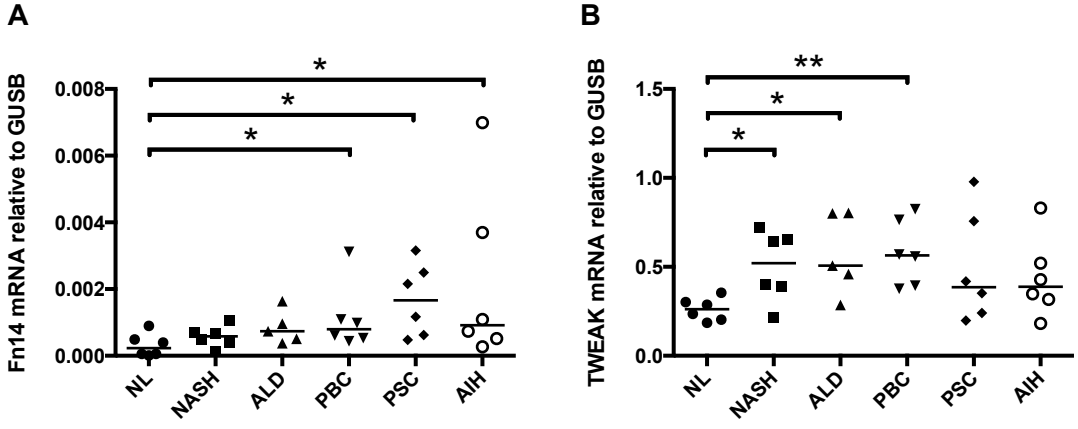

Figure 3.2 Fn14 and TWEAK mRNA in different chronic liver pathologies

Expression of Fn14 **(A)** and TWEAK **(B)** was assessed by qPCR in normal livers (n=6), NASH (n=6), ALD (n=5), PBC (n=6), PSC (n=6) and AIH (n=6). Gene expression is shown relative to *GUSB* using the $2^{-\Delta Ct}$ method (**p<0.05, ** p<0.01; Mann-Whitney U test).* The distribution of values was not significantly different across the whole population (*p=0.052* (A) and *p=0.082* (B) *Kruskal-Wallis test*).

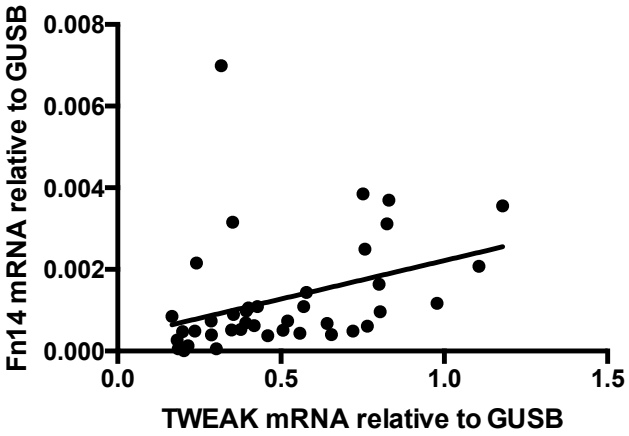

Figure 3.3 Correlation between Fn14 and TWEAK mRNA
Linear regression analysis of Fn14 and TWEAK mRNA in samples from normal livers (n=6), ALF (n=5) NASH (n=6), ALD (n=5), PBC (n=6), PSC (n=6) and AIH (n=6) (ρ=0.53; ****p<0.005; Spearman correlation*).

3.2.2 Fn14 protein levels are elevated in chronic liver diseases

To determine whether the increased levels of Fn14 mRNA resulted in increased protein expression, the levels of Fn14 protein were assessed by western blot using the same patient tissue samples as those used for qPCR. The blots showed two major bands, one at 24 kDa (Figure 3.4 A) and the other at 48 kDa (data not shown). The 24 kDa band is considered to be the main Fn14 protein (Meighan-Mantha et al., 1999) and the 48 kDa band a potential dimer. It has been suggested that the reason why Fn14 migrates at a higher apparent molecular weight is because of the amino acid composition that causes Fn14 to resist denaturation or to bind SDS poorly (Meighan-Mantha et al., 1999).

In contrast to mRNA levels Fn14 protein levels were significantly upregulated in chronic fatty liver diseases compared to normal livers (*$p<0.05$*). Fn14 protein levels in autoimmune liver diseases were also significantly higher compared to normal livers (*$p<0.05$*; Figure 3.4 B).

3.2.3 TWEAK and Fn14 expression correlate with liver fibrosis

Chronic liver disease is commonly associated with significant development of fibrosis. Other research has shown that Fn14 protein expression correlates with peritoneal fibrosis in humans (Sanz et al., 2014). To investigate whether Fn14 or TWEAK correlate with levels of fibrosis in the liver, matched liver sections from NL, NASH, ALD and AIH were stained with sirius red to detect collagens (Figure 3.5 A) and quantified with Image J (Figure 3.5 B). Cirrhotic livers exhibited significantly more collagen compared to normal livers ($p<0.05$; Figure 3.5 B). A positive correlation was detected between the amount of collagen and Fn14 mRNA (*Spearman* $\rho=0.63$*;* $p<0.05$*;* Figure 3.5 C), TWEAK mRNA (*Spearman* $\rho=0.63$*;* $p<0.05$*;* Figure 3.5 D) and Fn14 protein (*Spearman* $\rho=0.66$*;* $p<0.05$*;* Figure 3.5 E).

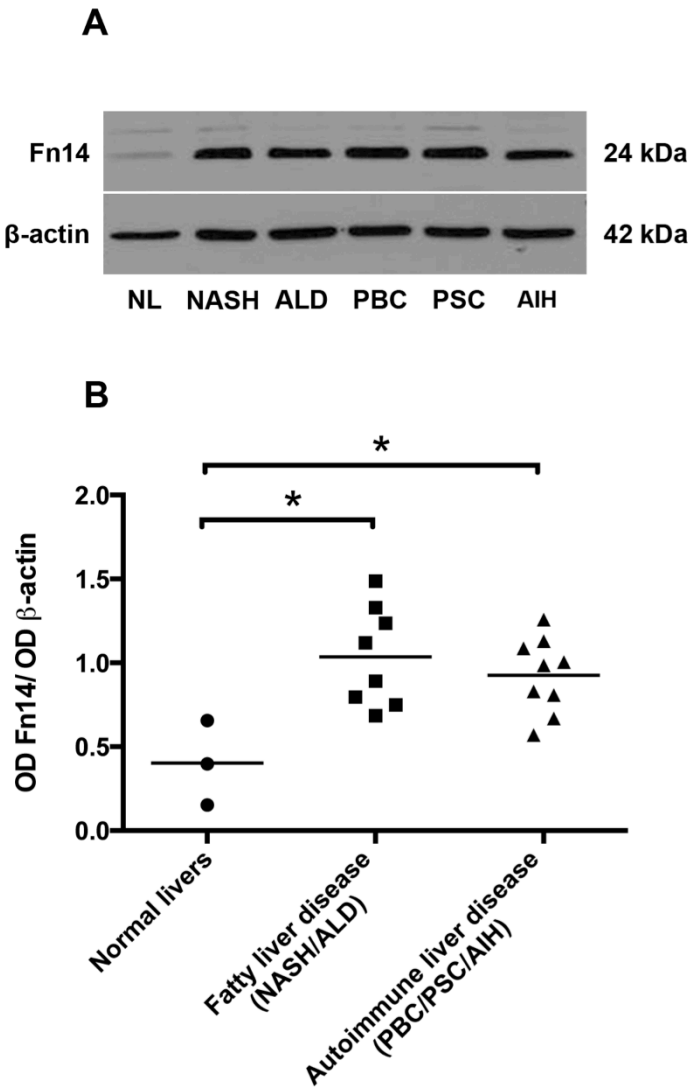

Figure 3.4 Fn14 protein levels are increased in chronic liver disease
Representative western blot image of Fn14 and β-actin levels in normal livers, NASH, ALD, PBC and PSC **(A)** and densitometry analysis of Fn14 protein expressed in normal and cirrhotic livers normalised on β-actin expression **(B)** (NL n=3, NASH n=3, ALD n=5, PBC n=3, PSC n=3, AIH n=3). (**p<0.05; Mann-Whitney U test)* The distribution of values was significantly different across the whole population (*p<0.05; Kruskal-Wallis test*).

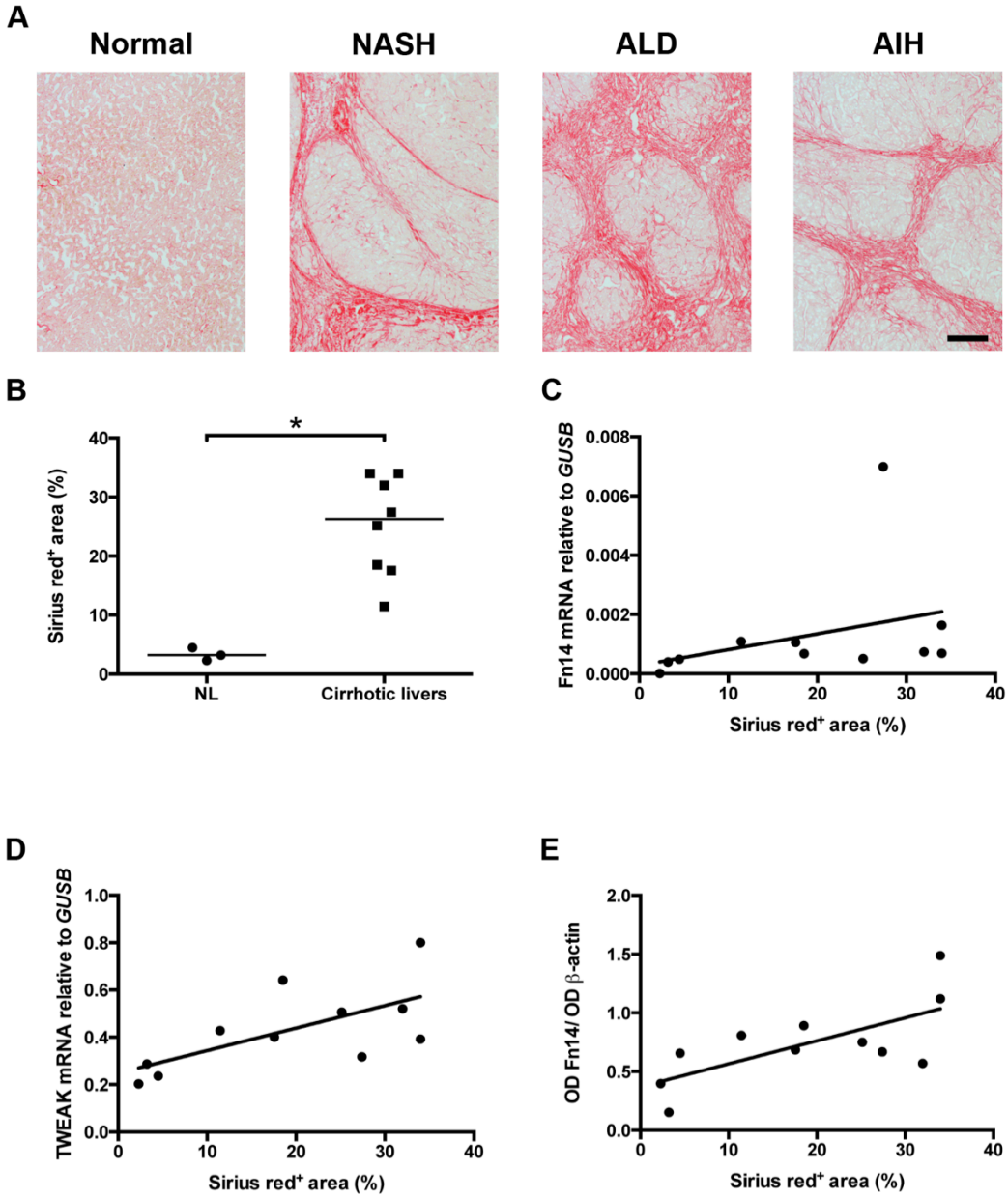

Figure 3.5 A correlation exists between the extent of fibrosis and TWEAK or Fn14 in human liver samples

Normal and cirrhotic livers (NL n=3, NASH n=3, ALD n=2, AIH n=3) were stained using sirius red. Panel A shows images of Normal, NASH, ALD and AIH livers **(A)** Staining was digitally quantified to show amount of sirius red stain expressed as the percentage area of five randomly selected areas per sample (**p<0.05; Mann-Whitney U test)* **(B)**. Extent of fibrosis was compared to mRNA level using Spearman rho analysis of sirius red and Fn14 mRNA (ρ=0.63*;* p<0.05) **(C)** TWEAK mRNA (ρ=0.63*;* p<0.05) **(D)** and Fn14 protein (ρ=0.66*;* p<0.05) (*Spearman rho correlation*) **(E)**. Scale bar 200 µm

3.2.4 Localisation of TWEAK and Fn14 in human liver tissue

3.2.4.1 Fn14 expression by immunohistochemistry

In normal human liver tissue Fn14 expression was low in the portal area (Figure 3.6 A) and no staining was detected in the parenchyma (Figure 3.6 B). Examination of normal tissue at increased magnification localised Fn14 to blood vessels, in particular on smooth muscle cells in the arterial wall, with low-level staining on bile ducts (Figure 3.6 C).

Histological samples from patients with ALF (Figure 3.6 D-F) demonstrated increased Fn14 staining compared to normal livers, which corresponded with the Fn14 qPCR data (Figure 3.1 A). In the portal area of ALF samples, Fn14 was present in bile ducts and blood vessels and in structures that appeared to be ductular reactive cells (DRCs) (Figure 3.6 D). In the parenchyma, cells at the fibrogenic intercept stained positive for Fn14 (Figure 3.6 E). Histological analysis of samples from patients with chronic liver disease (Figure 3.6 G-L and Figure 3.7) also showed increased Fn14 expression compared to normal livers. This was consistent with the results of the western blot (Figure 3.4). In the portal area of samples from patients with NASH (Figure 3.6 G) and ALD (Figure 3.6 J), Fn14 staining was again present in bile ducts and blood vessels. Arteries were consistently positive whereas veins showed variable staining intensities. In addition, neovessel-like structures in the portal area also stained positive for Fn14 (Figure 3.6 J). Besides staining in the portal area, Fn14 was localised to cells in the fibrous septum of NASH and ALD samples (Figure 3.6 H,K). Higher magnification of the sections demonstrated that some cells that stained positive for Fn14 in the fibrotic scar had a spindle shaped appearance (Figure 3.6 I,L). With this technique it was not possible to determine the identity of this cell type. Staining with an isotype matched control was negative in all areas (Figure 3.6 M,N).

Samples from patients with end stage PSC and PBC demonstrated strong Fn14 staining in DRC-like structures in the portal area (Figure 3.7 D,G). In comparison to the Fn14-positive DRCs in ALF, those DRCs were present at the peripheral zone of the portal area and had often a more elongated and thin structure with no recognisable lumen. Similar structures were also detected in the parenchyma of PSC and PBC samples (Figure 3.7 E,H). In AIH, Fn14 expression was present on cells that appeared to be DRCs (Figure 3.7 J) but there were considerably fewer compared to PSC and PBC. Fn14 staining in the fibrotic scar of AIH (Figure 3.7 K,L) was similar to the staining seen in ALD and NASH.

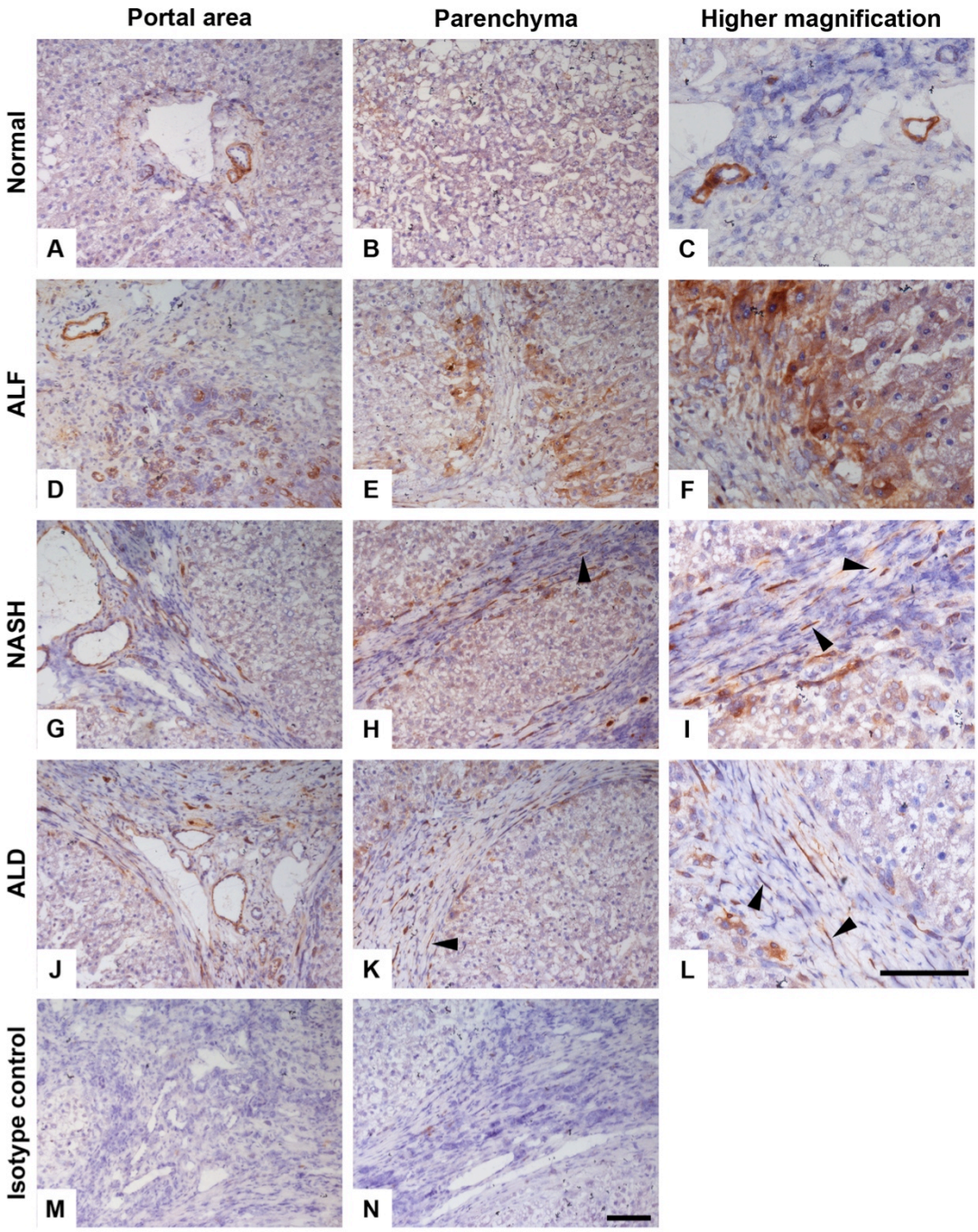

Figure 3.6 Expression of Fn14 in normal livers, ALF and steatotic liver disease

Immunohistochemical staining for Fn14 (brown) in human liver samples from normal donors (**A-C**), patients with ALF (**D-F**), NASH (**G-I**) and ALD (**J-L**). Staining of NASH liver with an isotype-matched control antibody is shown (**M** and **N**). Arrowheads indicate spindle shaped cells in the fibrotic scar. Both scale bars 100 μm

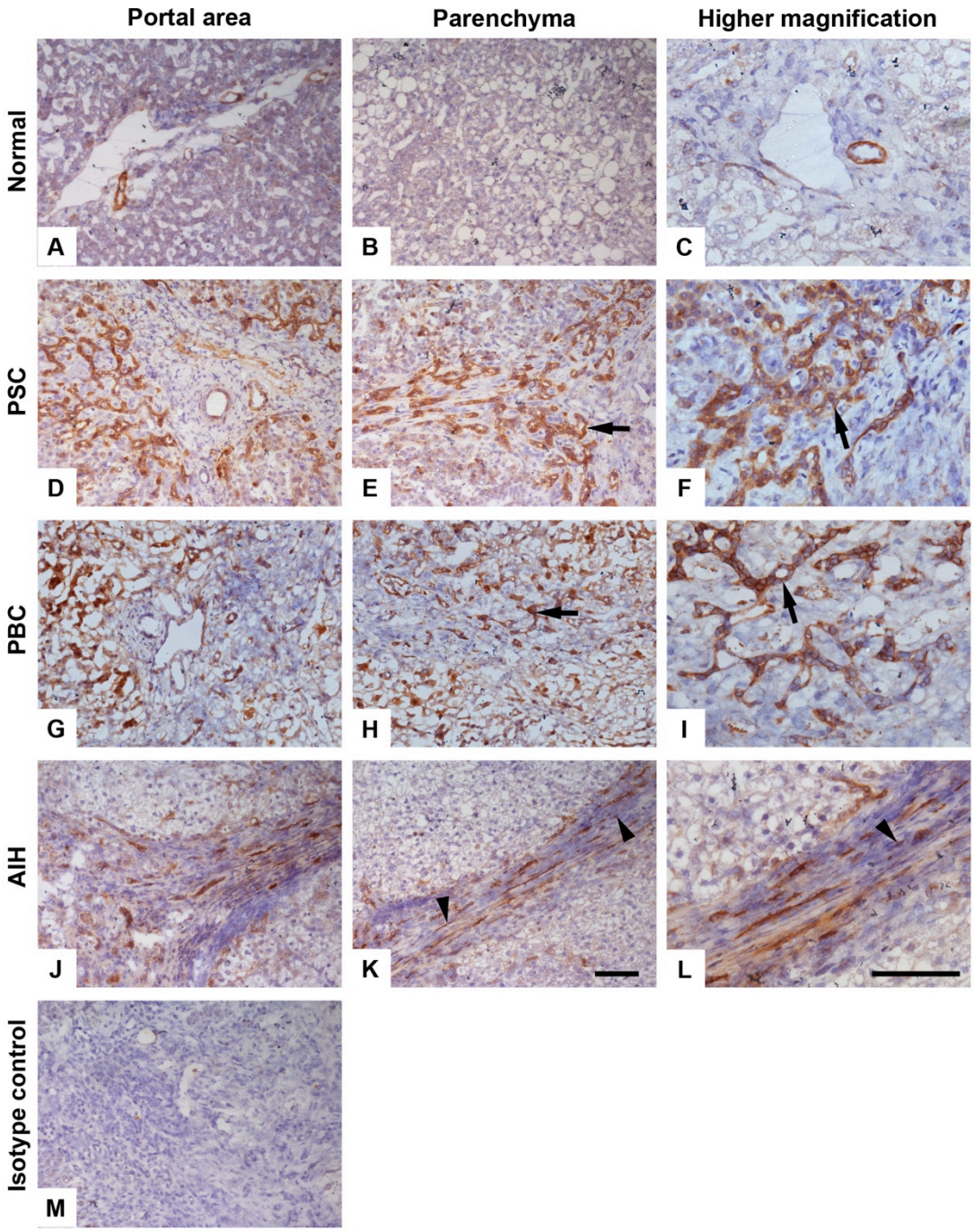

Figure 3.7 Fn14 expression in autoimmune liver diseases
Representative images of Fn14 staining (brown) in liver samples from normal liver **(A-C)** and from patients with PSC **(D-F)**, PBC **(G-I)** and AIH **(J-L)**. Staining of PSC liver with an isotype-matched control antibody is shown **(M)**. Arrows mark ductular reactive cells. Arrowheads indicate spindle shaped cells in the fibrotic scar. Both scale bars 100 μm

3.2.4.2 Cellular localisation of Fn14 expression measured by immunofluorescence

Immunohistochemical staining of normal and cirrhotic livers demonstrated Fn14 expression in several structures including blood vessels and spindle shaped cells in the fibrotic scar. In the blood vessels the Fn14 staining appeared to be present in smooth muscle cells (SMCs) (Figure 3.6 C) and the spindle shaped cells were reminiscent of LMFs (Figure 3.6 I,L). SMCs and LMFs express a number of common phenotypic indicators and one of the main markers is α-SMA. Dual colour confocal microscopy was therefore used to identify whether α-SMA-positive cells do express Fn14. Indeed, Fn14 did colocalise with α-SMA in the walls of blood vessels in normal and cirrhotic livers (Figure 3.8) and also within neovessels in cirrhotic livers (Figure 3.8 F,I) showing that Fn14 was expressed by SMCs. Colocalisation of Fn14 and α-SMA was also detected in the fibrous septa of samples from patients with NASH and ALD (Figure 3.9) suggesting that Fn14 was expressed by LMFs. Not all α-SMA-positive LMFs were also Fn14-positive however, indicating that a subpopulation of LMFs express Fn14. Furthermore, Fn14 expression was also detected in α-SMA negative cells (Figure 3.8 D-I). The endothelial lining of blood vessels as well as the bile ducts also appeared to stain positive for Fn14 (Figure 3.8 F). Colocalisation studies with Fn14 and CD31, a marker for endothelial cells has shown that the endothelial lining of blood vessels also expressed Fn14 (unpublished data by Mamoona Munir). Samples from patients with PSC and PBC showed a different Fn14 staining pattern compared to NASH, ALD and AIH. The morphology of the cells that stained Fn14 positive in PSC and PBC had a DRC-like appearance. To investigate this further, dual colour immunofluorescent staining was carried out using liver samples from PSC patients and antibodies against Fn14 and CK19, a biliary epithelial cell marker (Figure 3.10).

CK19 has been demonstrated to stain DRCs (Suda et al., 2014) but also mature bile ducts. Immunofluorescent staining showed colocalisation of Fn14 with CK19-positive cells that have the morphology of DRCs. Staining with an isotype-matched control was negative.

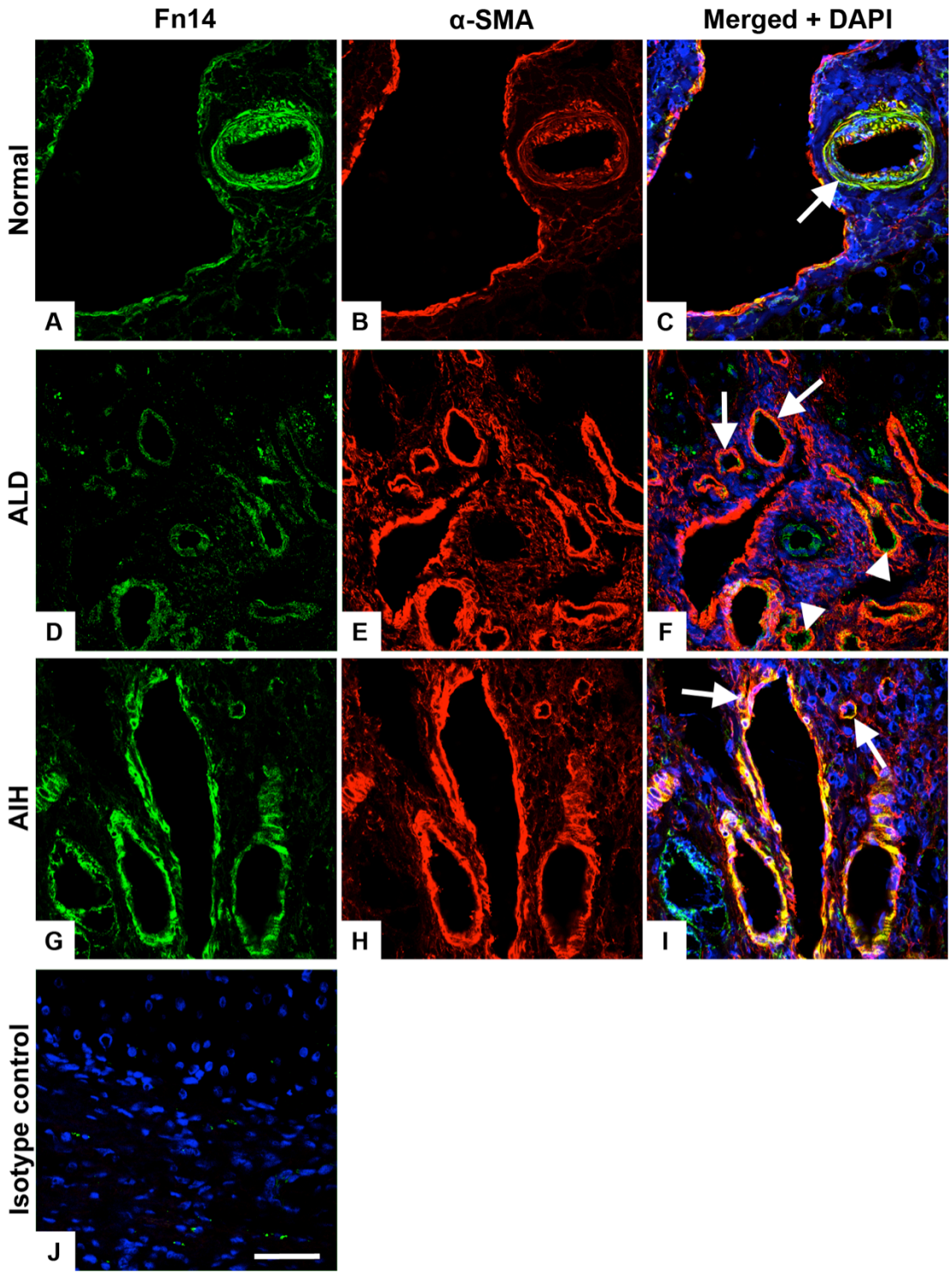

Figure 3.8 Colocalisation of Fn14 with α-SMA in the portal area
Immunofluorescent staining of Fn14 (green) and α-SMA (red) in portal areas of normal liver tissue **(A-C)** ALD **(D-F)** and AIH liver samples **(G-I)**. Isotype-matched control is shown **(G)**. Colocalisation of Fn14 and α-SMA is indicated in yellow and by arrows. Arrowheads indicate endothelial lining of blood vessels. DAPI (blue) was used as a nuclear counterstain. Scale bar 50 μm

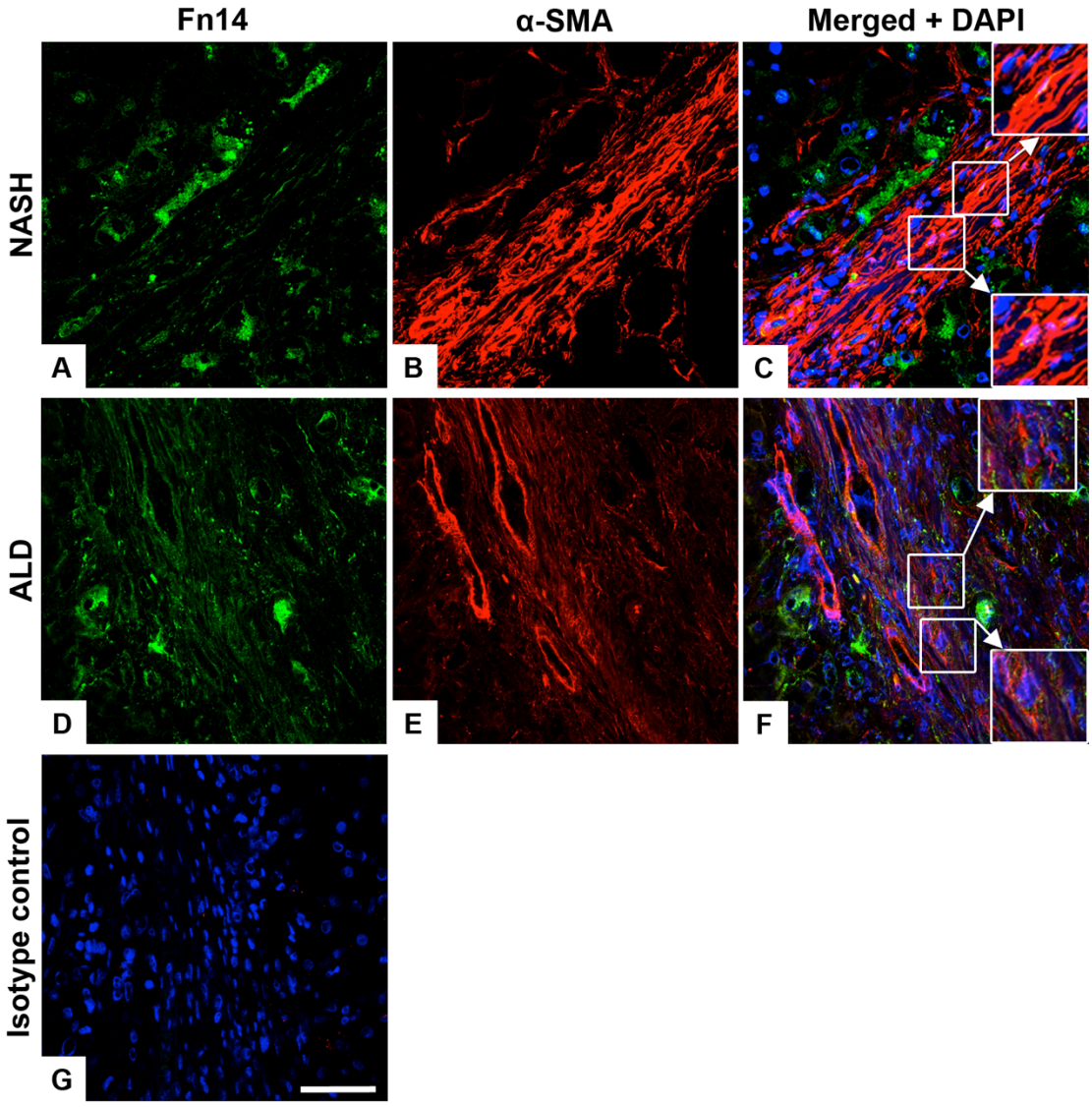

Figure 3.9 Colocalisation of Fn14 with α-SMA in the fibrous septum
Immunofluorescent staining of Fn14 (green) and α-SMA (red) in tissue samples from patients with NASH **(A-C)** and ALD **(D-F)**. Isotype-matched control is shown **(G)**. Colocalisation of Fn14 and α-SMA is indicated by pseudocolour yellow and shown in insert: digitally enlarged image. DAPI (blue) was used as a nuclear counterstain. Scale bar 50 μm

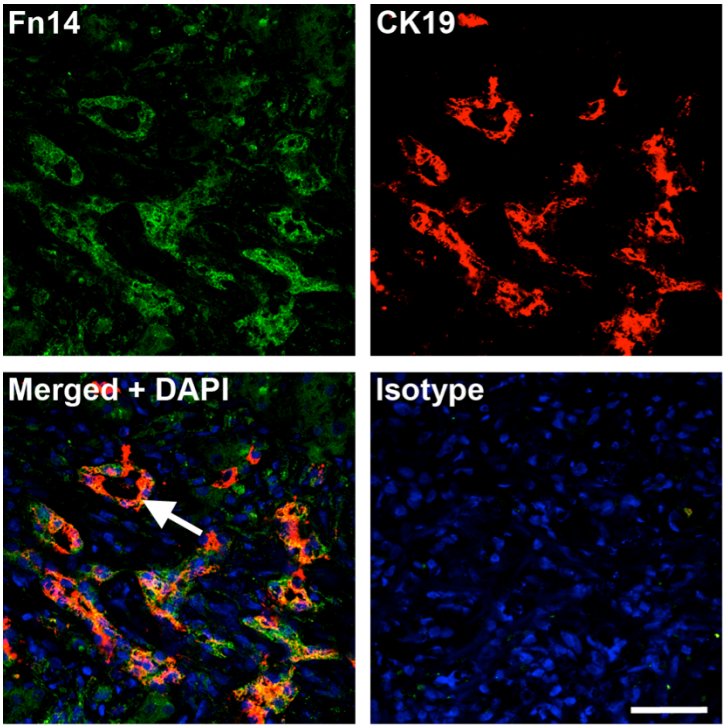

Figure 3.10 Expression of Fn14 by CK19+ epithelial cells
Immunofluorescent staining of Fn14 (green) and CK19 (red) in samples from patients with PSC. Colocalisation of Fn14 and CK19 is indicated in yellow and by arrow. Scale bar 50 µm

3.2.4.3 TWEAK expression by IHC

To investigate where TWEAK localises in the liver, immunohistochemical staining was performed with the same liver samples used for Fn14 staining. Similar to Fn14 staining, TWEAK staining in normal livers was weak (Figure 3.11 A-C). Some staining was detected in the portal area (Figure 3.11 A) whereas the parenchyma showed no immunoreactivity (Figure 3.11 B). Considerably higher levels of TWEAK were detected in ALF and various chronic liver diseases compared to normal controls (Figure 3.11 and Figure 3.12).

TWEAK expression in ALF was abundant in the portal area around ductules possibly in infiltrating leukocytes (Figure 3.11 D). The ductules did not stain positively for TWEAK but they were positive for Fn14 (Figure 3.6 D). TWEAK staining was also

detected in the fibrotic septa (Figure 3.11 E). Higher magnification demonstrated that TWEAK was present in cells with a spindle shaped appearance but also in some cells at the periphery of the scar (Figure 3.11 F). In comparison with Fn14 staining TWEAK was more focused within the fibrotic area (Figure 3.11 E) whereas Fn14 staining was mainly present at the periphery in liver tissue from ALF patients (Figure 3.6 E).

In samples from patients with NASH and ALD, TWEAK staining was also present in the portal area (Figure 3.11 G,J) but to a lesser extent than in ALF (Figure 3.11 D). In the fibrotic septum TWEAK was detected in cells with a spindle shaped morphology (Figure 3.11 H,K), similar to the Fn14 staining seen in NASH and ALD samples (Figure 3.6 H,K). Furthermore, TWEAK staining was observed in the sinusoids (Figure 3.11 K). The major cell populations within the sinusoids are HSCs, Kupffer cells and endothelial cells. However, it was not possible with this technique to differentiate which cell type(s) were expressing TWEAK.

TWEAK staining in immune-mediated liver diseases (Figure 3.12 D-L) was similar to that in fatty liver diseases (Figure 3.11 G-L) and was located in both the portal region and in the fibrotic septum of PSC (Figure 3.12 D,E), PBC (Figure 3.12 G,H) and AIH (Figure 3.12 J,K). In the portal area, infiltrating leukocytes appeared to stain positive for TWEAK. In some instances dense accumulation of TWEAK was also detected in the portal areas of PSC (Figure 3.12 D) and PBC (Figure 3.12 G). TWEAK expression was also present in the sinusoids of immune-mediated liver diseases (Figure 3.12 E,H,K). In addition, higher magnification of TWEAK staining (Figure 3.12 F,I,L) revealed expression in cells with a spindle shaped morphology in the fibrotic septum.

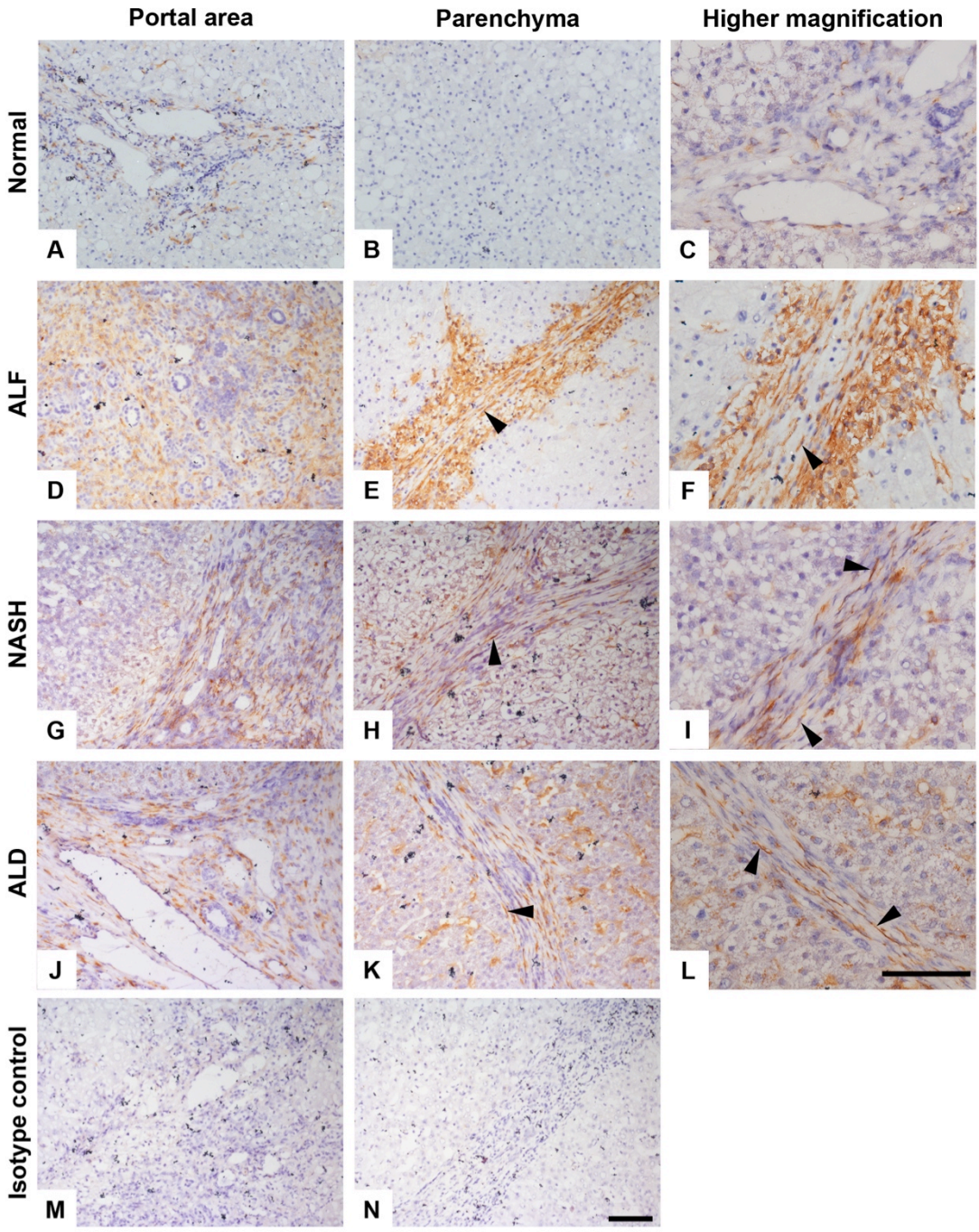

Figure 3.11 TWEAK expression in normal livers, ALF and steatotic liver disease

Representative images of tissue samples from normal donors **(A-C),** patients with ALF **(D-F)**, NASH **(G-I)** and ALD **(J-L)** were stained by immunohistochemistry for TWEAK (brown). Staining with an isotype-matched control antibody is shown **(M** and **N)**. Arrowheads indicate spindle shaped cells in the fibrotic scar. Both scale bars 100 μm

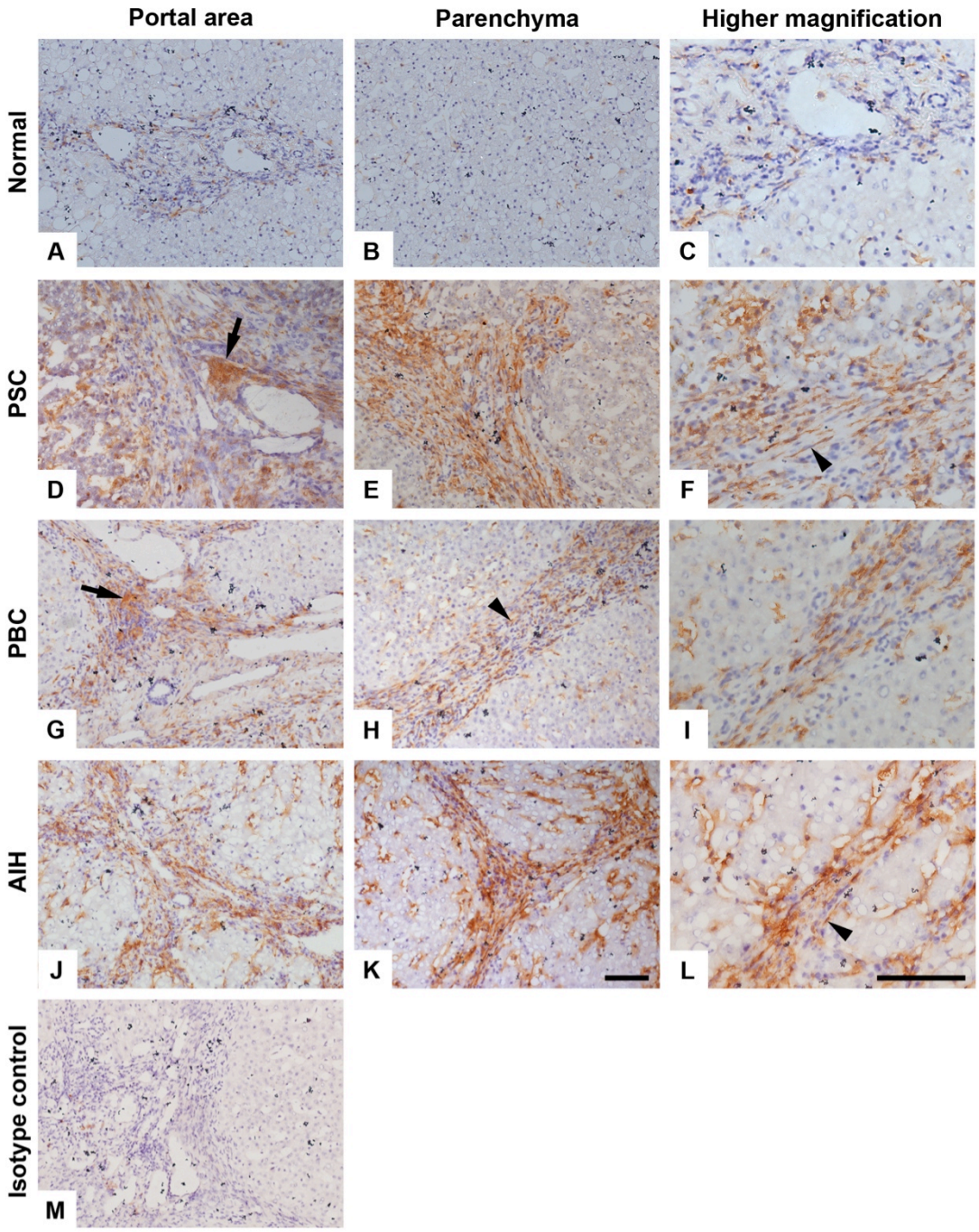

Figure 3.12 TWEAK expression in autoimmune liver disease

Immunohistochemical staining with TWEAK mAb (brown) in liver tissue from normal donor liver **(A-C)** and from patients with PSC **(D-F)**, PBC **(G-I)** and AIH **(J-L)**. Staining with an isotype-matched control antibody of PSC liver is shown **(M)**. Arrows mark dense TWEAK staining. Arrowheads indicate spindle shaped cells in the fibrotic scar. Both scale bars 100 μm

3.2.4.4 TWEAK expression by immunofluorescence

To confirm the identity of the spindle shaped cells staining positive for TWEAK, dual colour immunofluorescent staining was performed in samples of ALF (Figure 3.13) using vimentin as a marker for HSCs/LMFs. Figure 3.13 shows colocalisation of Vimentin and TWEAK in the fibrous septum indicating that HSCs/LMFs express TWEAK.

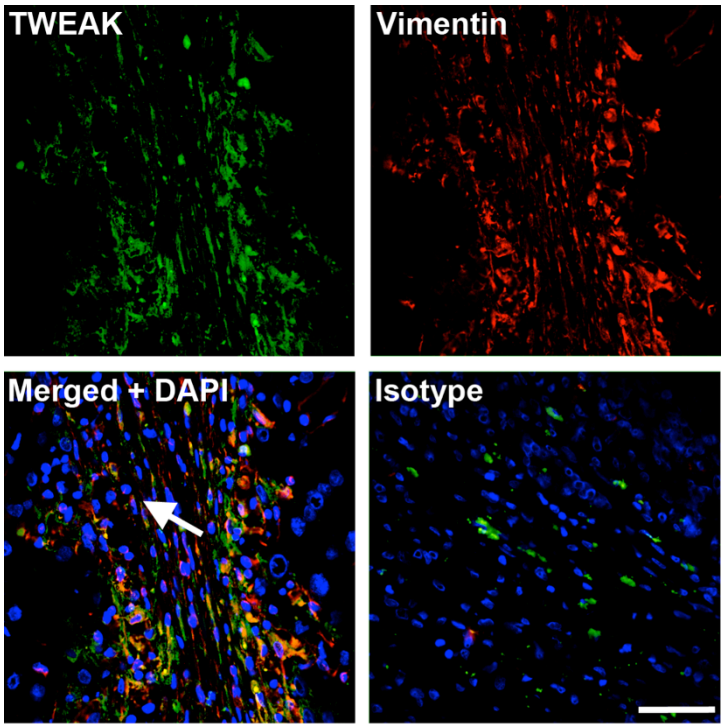

Figure 3.13 Colocalisation of TWEAK with LMFs
ALF samples were stained using dual colour immunofluorescence with TWEAK (green) and Vimentin (red). Colocalisation is seen as yellow. Arrow indicates myofibroblasts positive for TWEAK stain. DAPI (blue) was used as a nuclear counterstain. Scale bar 50 μm

3.3 Discussion

To date few research studies have been published concerning TWEAK and Fn14 expression in the liver with most of them being in mouse models (Bird et al., 2013; Jakubowski et al., 2005; Tirnitz-Parker et al., 2010). To undertake a more systematic approach this chapter characterises the expression of TWEAK and Fn14 in normal human livers and livers from patients with ALF and chronic liver disease. Fn14 mRNA expression in mice has been shown to be low in healthy livers and upregulated during liver disease (Tirnitz-Parker et al., 2010; Feng et al., 2000). The human data presented in this chapter showed a similar pattern of expression; low levels of Fn14 mRNA in normal livers and a significant upregulation in acute and chronic liver injury, which was also reflected by immunohistochemistry and western blot. Of note, the normal livers that have been used for this analysis have all come from donors and the livers often had a steatotic appearance. In addition, the tissue from chronic liver patients was derived from explants from patients undergoing transplantation. In these patients, the liver disease might have reached an end stage and the histological characteristics of specific types of liver diseases might have faded away. It is also worth mentioning that livers with chronic viral hepatitis were not included in this study. Globally, it is the most common type of chronic liver disease (Mokdad et al., 2014) and in future studies they should be included in the investigation to have a complete representation of chronic liver disease.

In my experiments I have analysed Fn14 expression in subgroups of patients with chronic liver disease including fatty liver diseases, NASH and ALD and immune-mediated liver diseases; PBC, PSC and AIH. Fn14 mRNA was similar in fatty liver diseases compared to normal livers whereas immune-mediated liver diseases showed a

significant difference compared to normal. Other research has also shown similar expression of Fn14 mRNA in NASH and normal livers (Affò et al., 2012). Conversely, semi-quantitative analysis of Fn14 protein levels by western blot demonstrated that Fn14 protein levels were significantly higher in fatty liver diseases and also in autoimmune liver diseases compared to normal livers. Fn14 has a rapid turnover as it is constitutively synthesized and degraded, which requires continuous *de novo* receptor synthesis (Gurunathan et al., 2014), and therefore fatty liver diseases might have high Fn14 protein levels despite having low Fn14 mRNA due to a defect in Fn14 protein degradation. The Fn14 receptor might be somehow stabilised and is therefore protected from lysosome degradation. This would allow the cells to maintain high Fn14 proteins levels without requiring mRNA synthesis.

In healthy livers, Fn14 expression was localised in blood vessels and bile ducts. In ALF on the other hand, Fn14 staining was detected in blood vessels and bile ducts but also in DRCs and in cells at the periphery of the fibrotic septum. This is in accordance with a study by Affò *et al.*, who showed Fn14 expression in parenchymal cells around the fibrogenic septum in alcoholic hepatitis (Affò et al., 2012). Using serial liver sections, Affò *et al.* suggested that Fn14 was expressed by intermediate hepatocytes and a subpopulation of DRCs.

Our data has shown that Fn14-positive DRCs were also detected in samples from patients with end-stage PSC and PBC. DRCs are a heterogeneous cell population that also contains LPCs (Gouw et al., 2011). In mice, Fn14 has been identified on LPCs and investigations have shown that TWEAK acts as a mitogen for LPCs (Tirnitz-Parker et al., 2010; Jakubowski et al., 2005). Overexpression of TWEAK in mice led to increased LPC proliferation (Jakubowski et al., 2005) whereas inducing LPC

proliferation with the CDE diet in Fn14 KO mice reduced the number of LPCs compared to their WT controls (Tirnitz-Parker et al., 2010).

Although Fn14 staining was very prominent on DRCs in biliary liver diseases, examination of other chronic liver diseases including NASH, ALD and AIH demonstrated Fn14 expression in LMFs in the fibrotic scar. Very little is known about the expression of Fn14 in liver fibrosis but a study by Tirnitz-Parker *et al.* has shown that Fn14 KO mice that were fed the CDE diet had less liver fibrosis than their WT controls (Tirnitz-Parker et al., 2010). Studies in other organs have also shown that the TWEAK/Fn14 pathway affects fibrosis. Overexpression of TWEAK in mouse models lead to cardiac fibrosis and kidney fibrosis (Jain et al., 2009; Hotta et al., 2011) whereas deletion of Fn14 protected against cardiac fibrosis (Novoyatleva et al., 2013). This suggests that the Fn14-positive LMFs might be involved in fibrogenesis upon stimulation with TWEAK.

Few studies have been conducted that investigate the presence of TWEAK in the liver. A study by Kawakita *et al.* has shown TWEAK staining in human livers with HCC (Kawakita et al., 2004) but to our knowledge nobody has yet looked extensively at TWEAK expression in a range of human liver diseases. In normal human livers, TWEAK staining was weak which was also reflected in low levels of TWEAK transcripts. In contrast, TWEAK transcript levels were significantly higher in fatty liver diseases and PBC whereas samples from patients with ALF, PSC and AIH demonstrated no significant differences of TWEAK mRNA levels compared to normal livers.

Despite varying levels of TWEAK transcripts, acute and chronic liver diseases had enhanced TWEAK protein expression that was localised to infiltrating leukocytes in

the portal area. This was consistent with published work by Tirnitz-Parker *et al.* who demonstrated the presence of TWEAK mRNA in activated monocytes, macrophages and NK cells in mouse livers (Tirnitz-Parker et al., 2010). My data also showed that TWEAK was present in the sinusoids of cirrhotic livers but it was not clear whether TWEAK was expressed by HSCs, Kupffer cells or endothelial cells in the sinusoids. In addition, TWEAK was localised to vimentin-positive HSCs/LMFs in the fibrotic septum of diseased liver tissue similarly to the Fn14 staining. Whether TWEAK-positive HSCs/LMFs also express Fn14 at the same time or whether subpopulations of HSCs/LMFs express either Fn14 or TWEAK remains to be determined.

LMFs are considered to be the main contributor of ECM in liver fibrosis. *In vitro* data has shown that TWEAK regulates fibroblast activation and collagen deposition in other settings (Novoyatleva et al., 2013; Dohi and Burkly, 2012). In accordance with that, my investigations demonstrated a positive correlation between TWEAK and Fn14 expression and the amount of collagen in chronic liver diseases. However, some samples seemed to be potential outliers but the investigated patients did not have any signs of infections or took unusual drugs compared to the other patients that might have affected Fn14 or TWEAK expression. Nevertheless, due to various other factors that could have affected expression levels it would be useful to increase the number of samples. Of note, a positive correlation between Fn14 mRNA and the numbers of LPCs was also detected in mice treated with the CDE diet (Tirnitz-Parker et al., 2010).

Fn14 can be expressed by both LMFs and DRCs, which indicates a possible co-regulation of ductular reaction and fibrogenesis through the TWEAK/Fn14 pathway.

Evidence has shown that ductular reactions are directly proportional to levels of fibrosis (Williams et al., 2014) and studies in mice indicated a potential link between TWEAK-mediated LPC proliferation and fibrogenesis (Tirnitz-Parker et al., 2010; Kuramitsu et al., 2013). Fn14-deficient mice subjected to the CDE diet not only showed reduced LPC proliferation but also exhibited less collagen deposition and reduced transcript levels of TIMP 1 and 2 (Tirnitz-Parker et al., 2010). Another study by Kuramitsu *et al.* demonstrated that administration of recombinant TWEAK in fibrotic mice that were undergoing PH induced LPC proliferation but also increased levels of fibrosis (Kuramitsu et al., 2013). Despite this the mechanism by which TWEAK might influence fibrosis has not been investigated, and it is not known whether the effect occurs directly or indirectly via the ductular reaction. Nevertheless, liver tissue taken from patients with NASH, ALD and AIH that exhibited very little or no ductular reaction demonstrated expression of TWEAK and Fn14 by LMFs in the fibrotic scar indicating that the TWEAK/Fn14 pathway may act on fibrogenesis directly.

In conclusion, this chapter demonstrates an upregulation of TWEAK and Fn14 in acute and chronic liver diseases in humans. Expression of TWEAK and Fn14 is directly linked to the levels of collagen deposition in end-stage liver diseases and Fn14 and TWEAK are expressed by LMFs in the fibrotic septum. The abundance of TWEAK and Fn14 during liver disease raises the possibility of the TWEAK/Fn14 pathway as a potential target for the modulation of liver disease. The next chapter will therefore investigate the regulation and function of TWEAK and Fn14 in HSCs and LMFs *in vitro*.

Chapter 4

The expression and function of TWEAK and Fn14 in hepatic stellate cells *in vitro*

4.1 Introduction

Liver fibrosis is associated with excess accumulation of ECM that can progress to cirrhosis, which is characterised by the lack of normal liver architecture and the replacement of functional parenchyma with scar tissue (Schuppan and Kim, 2013). Research by Mederacke *et al.* using fate tracing confirmed that HSCs are the main progenitors of LMFs in fibrosis of toxic, cholestatic and fatty liver disease *in vivo* (Mederacke et al., 2013). Following liver injury HSCs activate and transdifferentiate into myofibroblast-like cells, which then migrate, proliferate, secrete ECM proteins and pro-inflammatory and pro-fibrogenic cytokines. Therefore, HSCs are prime targets for anti-fibrotic therapies.

The interaction between TWEAK and Fn14 is known to be important in fibrosis in several organs (Burkly et al., 2011). Studies show that overexpression of TWEAK in mouse models lead to cardiac fibrosis and kidney fibrosis (Jain et al., 2009; Hotta et al., 2011). *In vitro* data has shown that TWEAK acts directly on myofibroblasts to induce activation and collagen production (Dohi and Burkly, 2012; Novoyatleva et al., 2013). We therefore hypothesised that TWEAK acts on HSCs and LMFs to promote fibrosis. This chapter therefore investigates the expression and function of TWEAK and Fn14 *in vitro*, focusing on the regulation of Fn14 during HSC activation and the effect of TWEAK stimulation on HSCs.

4.2 Results

4.2.1 Characterisation of HSCs and LMFs *in vitro*

To investigate Fn14 expression *in vitro*, HSCs were isolated either from the non-affected area of human liver samples removed for the treatment of malignant disease or from normal donor tissue surplus to surgical requirements (Figure 4.1). Shortly after isolation, HSCs were stained with Oil Red O to confirm the characteristic lipid vacuoles in the HSC cytoplasm. After 4 days *in vitro*, HSCs were more activated, started to lose the lipid vacuoles and acquired a spindle shaped morphology. Most of the experiments were carried out with HSCs that had been in culture for more than 30 days (4^{th} passage) and had fully transformed into activated HSCs (Figure 4.1 A). Immunohistochemical staining of activated HSC cultures showed that they expressed the activated HSC/LMF markers α-SMA, vimentin and CD90. The markers CD31, CK19, CD68 and hepatocyte marker were used to exclude contamination with endothelial cells, cholangiocytes, Kupffer cells/macrophages and hepatocytes, respectively (Figure 4.1 B). In addition, LMFs from end-stage liver diseases were isolated and phenotyped using HSC/LMF markers (Figure 4.2 A) and negative markers were used to assess contamination (Figure 4.2 B). The purity of the cell cultures was above 95%.

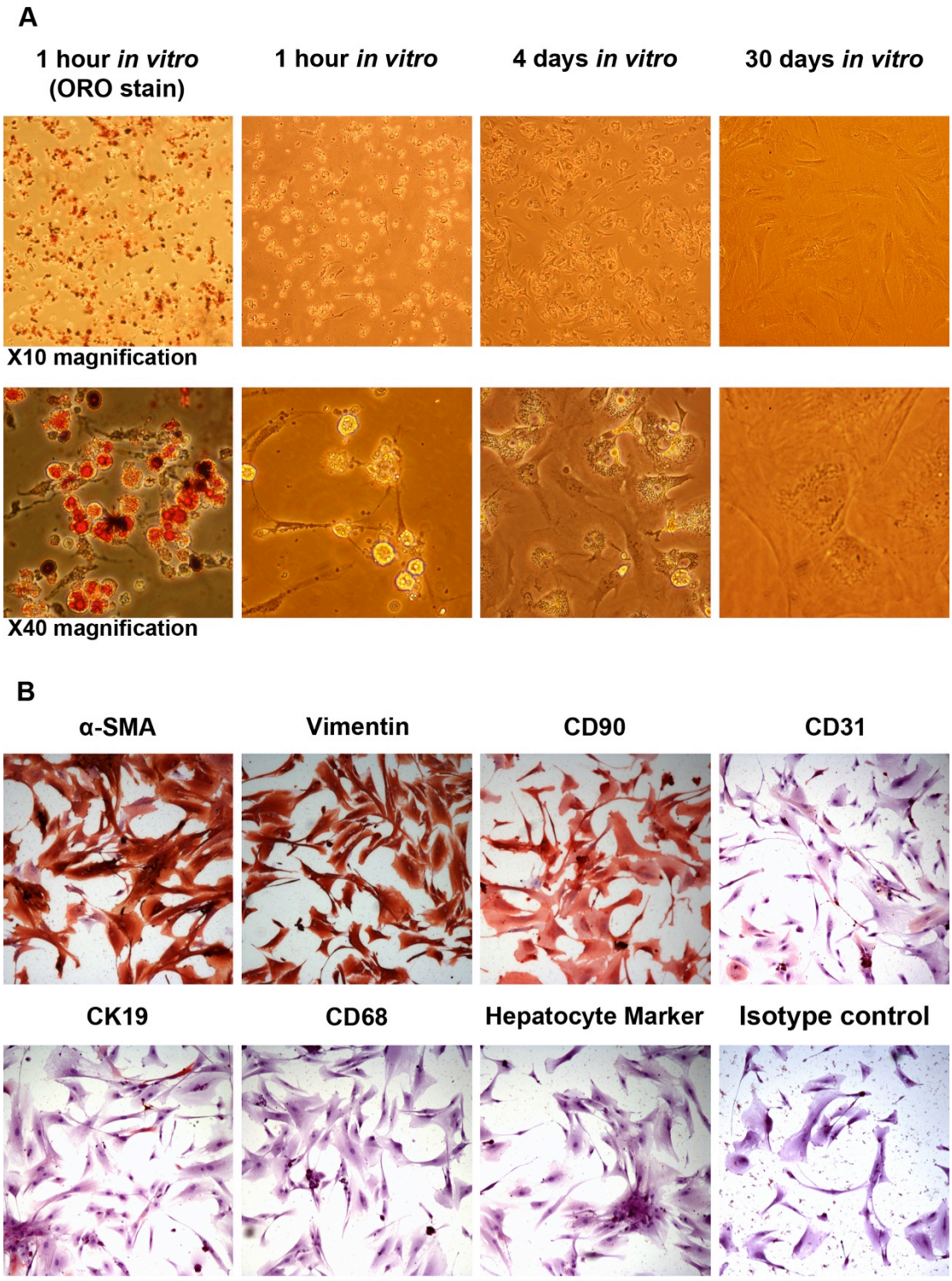

Figure 4.1 Phenotypic characterisation of primary human HSCs
Morphology of HSCs *in vitro* during HSC transformation. Oil Red O (ORO) staining demonstrated the fat-storing abilities of HSCs. Magnification X10 and X40 (**A**) Immunohistochemistry staining of activated HSCs *in vitro* for HSC/LMF markers, α-SMA, vimentin, CD90 and negative markers, CD31, CK19, CD68 and hepatocyte marker. Staining with an isotype-matched control is shown. Magnification X10 (**B**)

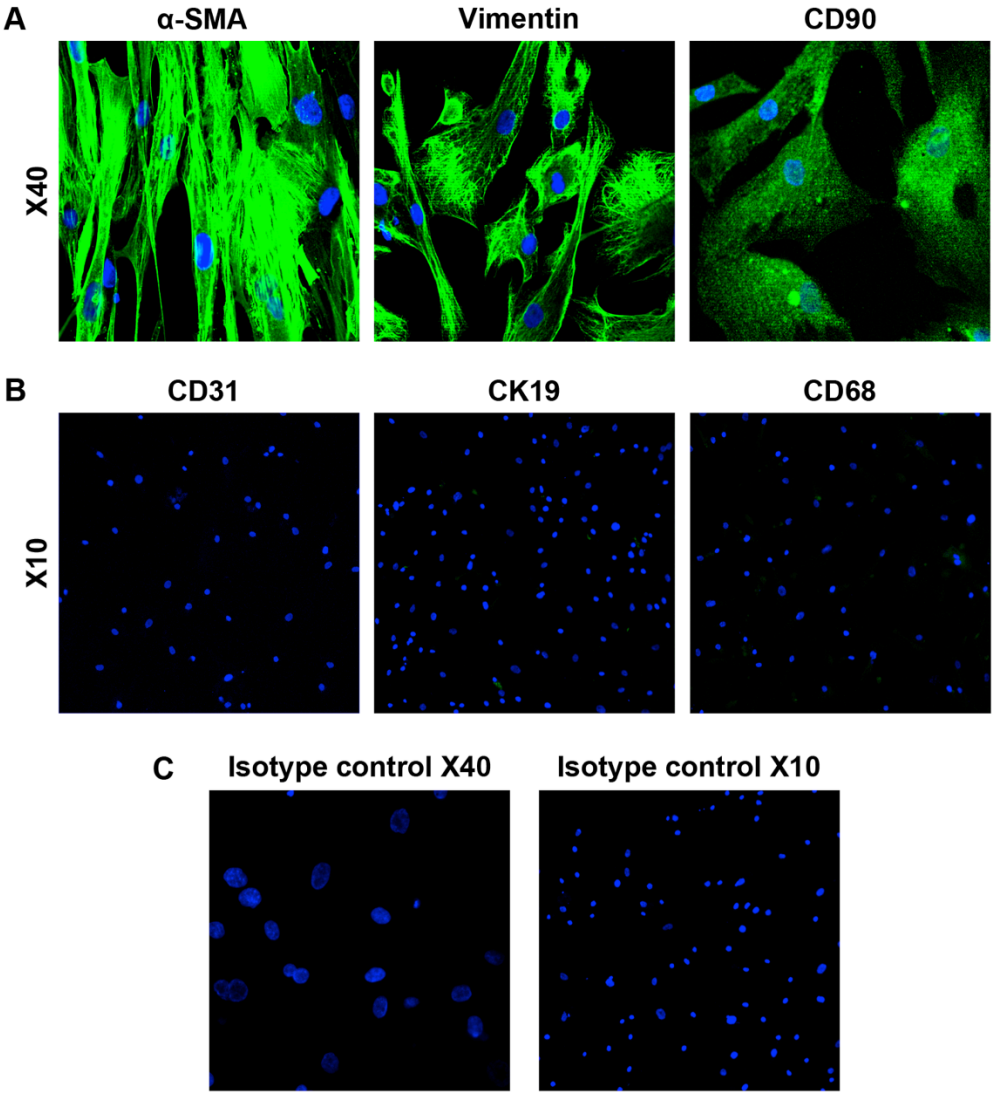

Figure 4.2 Phenotypic characterisation of LMFs isolated from human chronic liver diseases

Immunofluorescent staining of LMFs *in vitro* for HSC/LMF markers, α-SMA, vimentin, CD90. Magnification X40 (**A**) Negative markers, CD31, CK19 and CD68 were used to assess contamination. Magnification X10 (**B**) Staining with an isotype-matched control is shown at X40 and X10 magnification (**C**).

4.2.2 Expression of Fn14 in liver derived cells *in vitro* is highest in HSCs and LMFs

Immunohistochemical staining in diseased liver tissue demonstrated that several different cell types expressed Fn14 (Figure 3.6, Figure 3.7). Therefore, Fn14 transcript levels were quantified in different primary liver derived cell types *in vitro* including HSCs, LMFs, hepatocytes, cholangiocytes and IHECs using qPCR (Figure 4.3). All investigated cell types expressed Fn14 mRNA but the transcript levels were higher in HSCs and LMFs compared to hepatocytes, cholangiocytes and IHECs.

To further investigate Fn14 expression *in vitro*, protein levels were assessed in HSCs, LMFs and IHECs by flow cytometry (Figure 4.4). A greater proportion of HSCs expressed Fn14 (74.4%) than LMFs (58.5%) and IHECs (35.6%) (Figure 4.4 B). The extent of Fn14 expression per cell, as indicated by MFI, was similar in HSCs and LMFs but lower in IHECs (Figure 4.4 C). Fn14 expression in HSCs and LMFs was confirmed by dual colour immunofluorescent staining of Fn14 and α-SMA (Figure 4.5). The staining pattern suggested that Fn14 was mainly present intracellularly in vacuoles rather than on the surface of the cell.

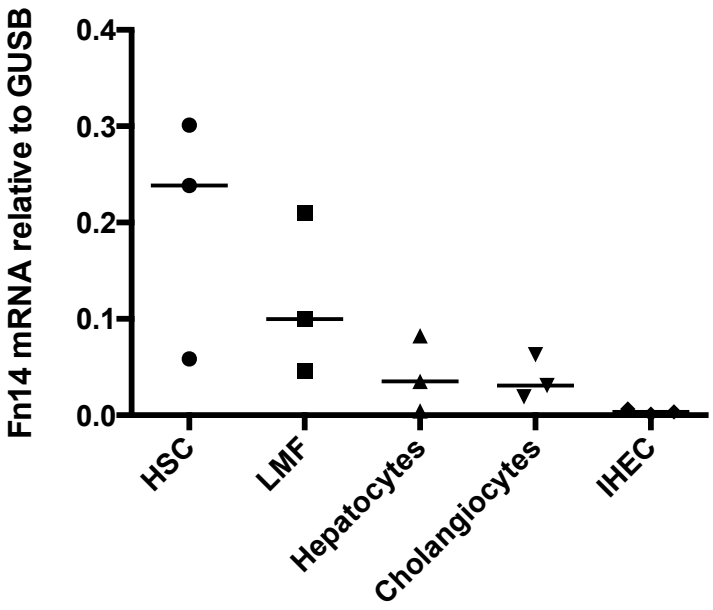

Figure 4.3 Expression of Fn14 mRNA in different primary liver-derived cells

Expression of Fn14 was assessed by qPCR in HSCs, LMFs, hepatocytes (a kind gift from Mr Ricky Bhogal), cholangiocytes and IHECs. Gene expression is shown relative to *GUSB* using the $2^{-\Delta Ct}$ method (n=3 from different isolates).

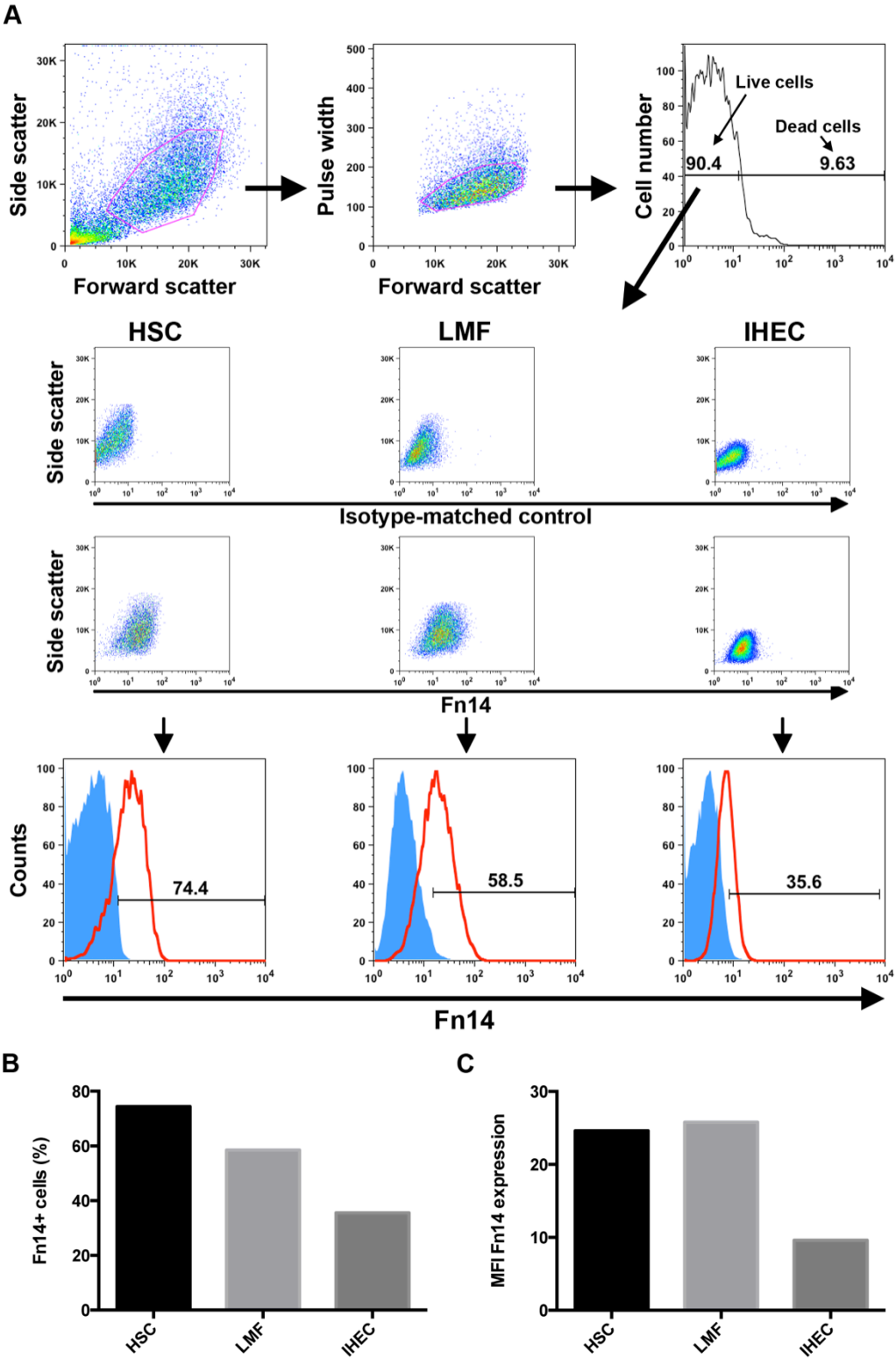

Figure 4.4 Fn14 protein levels in different liver-derived cells
Total Fn14 protein expression was assessed with flow cytometry. Representative flow cytometry scatter plots, histogram of live/dead cells, scatter plots and histograms for HSCs, LMFs and IHECs stained for Fn14 (red in histogram) and an isotype control (blue in histogram) **(A)** Data represents percentage positive cells **(B)** and median fluorescent intensity (MFI) of cells expressing Fn14 (both surface and intracellularly) **(C)**. (n=1 per cell type)

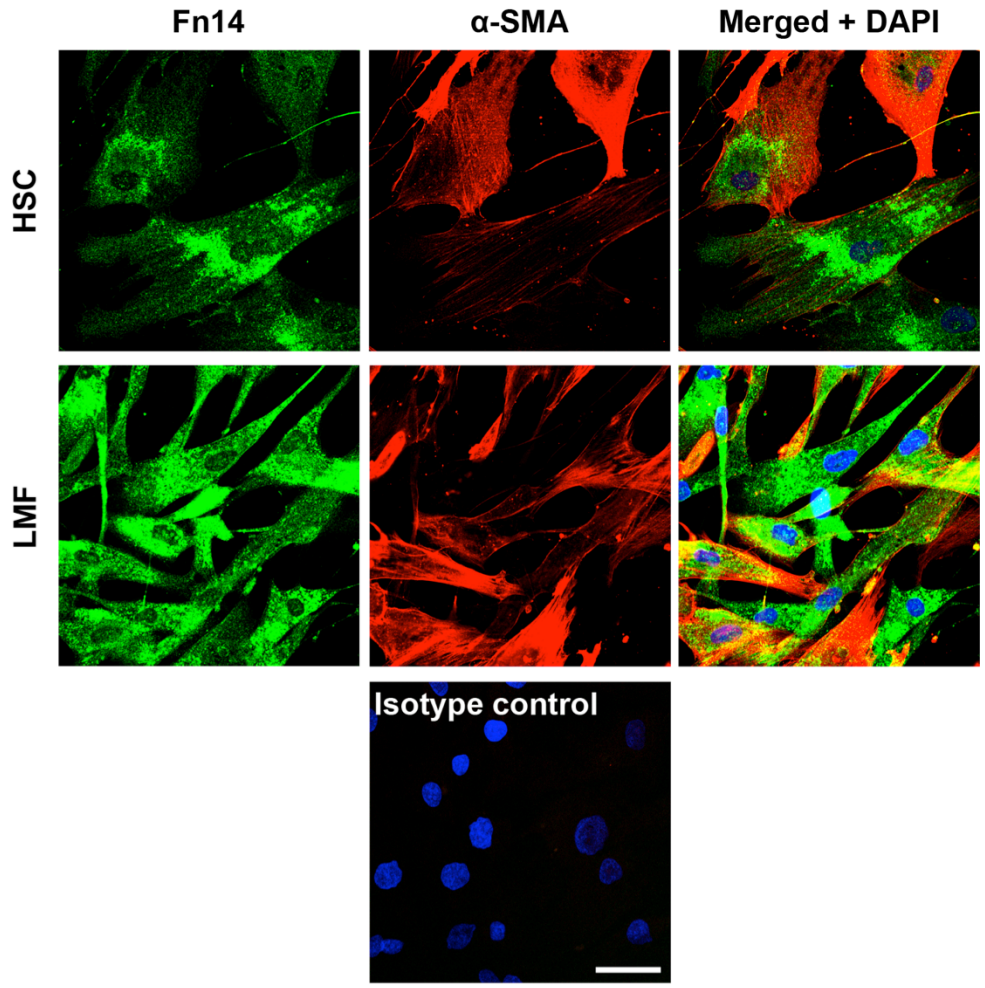

Figure 4.5 Immunofluorescent staining of Fn14 in HSCs and LMFs
Immunofluorescent staining of Fn14 (green) and α-SMA (red) in methanol-fixed HSCs and LMFs. Isotype matched control is shown. Co-expression of Fn14 and α-SMA is indicated in yellow. DAPI (blue) was used as a nuclear counterstain. Scale bar 50 μm

4.2.3 Regulation of Fn14 in HSCs *in vitro*

Expression of Fn14 in normal livers is low but becomes upregulated during injury (Figure 3.6). Therefore we investigated the extent of Fn14 expression during HSC transformation (Figure 4.6). Fn14 expression was detected as early as day 3 after isolation when HSCs were not yet expressing the activation marker, α-SMA. The staining was localised around the nucleus indicative of new Fn14 protein synthesis. Over a period of 14 days, HSCs became more active and started to express α-SMA. During HSC activation, Fn14 expression was increased and became distributed throughout the HSC cytoplasm at days 9 and 14 (Figure 4.6).

During fibrogenesis, many cytokines are released that could potentially affect Fn14 expression in HSCs. Fn14 expression in other cell types was increased with a range of cytokines including bFGF and TNF-α depending on the cell type (Winkles, 2008). To investigate Fn14 expression further, HSCs were treated with bFGF, TGF-β1, TNF-α or IFN-γ for 24 hours *in vitro* and Fn14 mRNA levels were measured by qPCR. Exposure to bFGF and TGF-β1 upregulated Fn14 mRNA whereas TNF-α had no effect on Fn14 expression. IFN-γ seemed to decreased Fn14 mRNA levels (Figure 4.7).

To gain insight into Fn14 localisation, HSCs were treated with either bFGF, TGF-β1 or left untreated and then fluorescently stained for Fn14 and α-SMA (Figure 4.8). Analysis of the Fn14 staining pattern in HSCs revealed that Fn14 was mainly located inside the cell (Figure 4.8 A). A representative histogram is shown of Fn14 and α-SMA intensity throughout a cell following bFGF stimulation (Figure 4.8 B). α-SMA is an isoform of actin and is therefore located intracellularly with close proximity to the cell surface. Fn14 expression was localised throughout the cell and close to the surface but

no obvious differences in Fn14 localisation were detected with bFGF or TGF-β1 stimulation compared to untreated controls. Z-stacks of HSCs also indicated that Fn14 was mainly located intracellularly (Figure 4.8 C).

Immunofluorescent staining to determine Fn14 localisation did not clarify whether Fn14 was only located intracellularly or whether some cells also expressed it on the cell surface. Therefore, flow cytometry was used to investigate the localisation of Fn14 further (Figure 4.9). Approximately 90% of HSCs contained intracellular stores of Fn14 and this did not change significantly following treatment with either bFGF, TGF-β1, TNF-α or IFN-γ (Figure 4.9 B). The total expression of Fn14 per cell, as indicated by the MFI, did also not change significantly with any cytokine stimulation compared to untreated HSCs (Figure 4.9 C). On average 35% of HSCs expressed Fn14 on the cell surface (Figure 4.9 E). This was significantly increased with TGF-β1 stimulation (56% +/- 6.8%; $p < 0.05$). Stimulation with bFGF also enhanced the number cells expressing Fn14 on the surface (57% +/- 9.3%) but this did not reach significance. TNF-α (47% +/-2.5%) or IFN-γ (37% +/- 7.9%) had little effect on Fn14 cell surface expression in HSCs (Figure 4.9 E). The total surface expression levels of Fn14 cell did not change significantly per cell with either treatment compared to the untreated control (Figure 4.9 F).

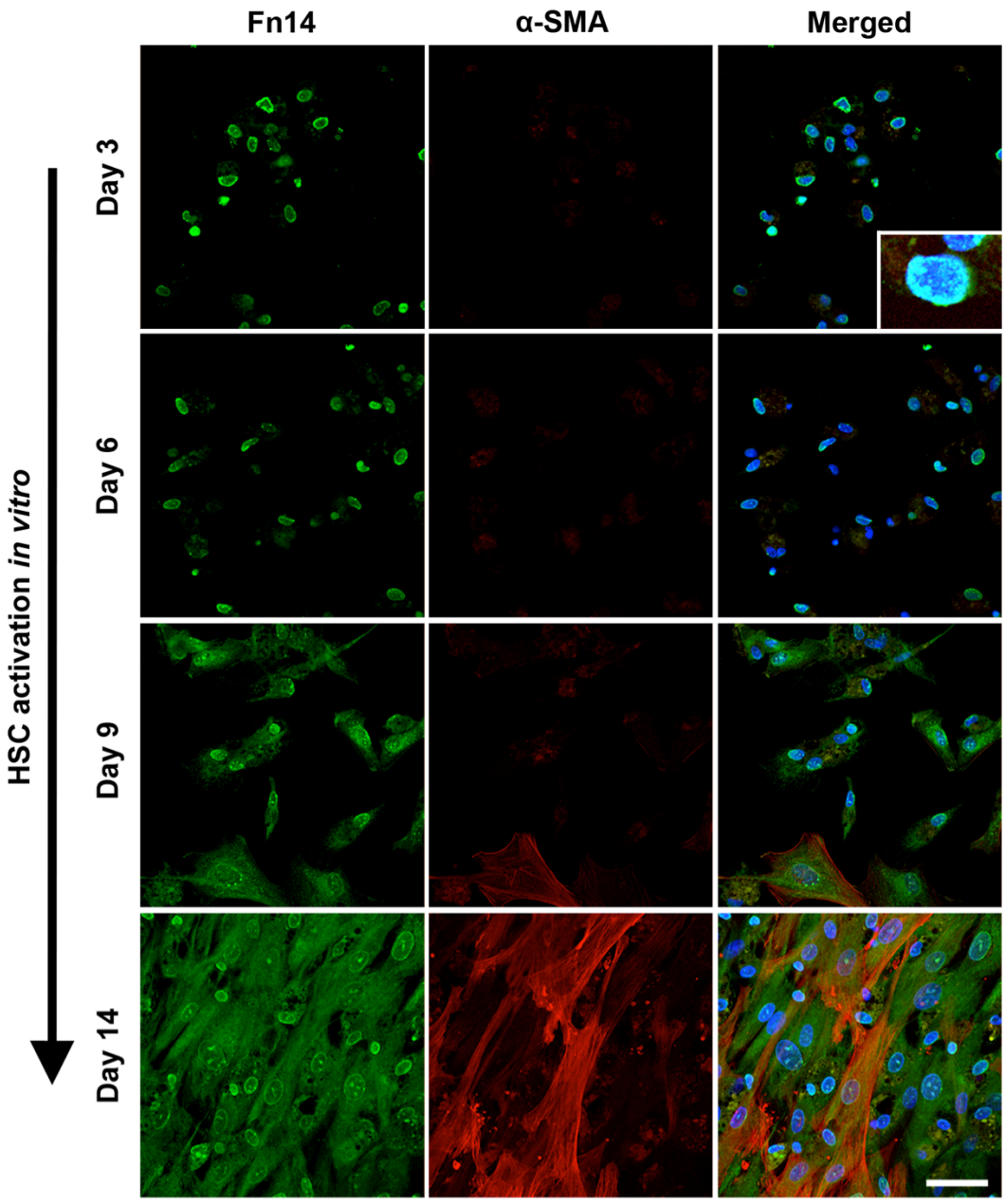

Figure 4.6 Expression of Fn14 during HSC transformation
Immunofluorescent staining of Fn14 (green) and α-SMA (red) in HSCs during the activation period *in vitro*. Insert: image digitally enlarged. DAPI (blue) was used as a nuclear counterstain. Scale bar 50 μm

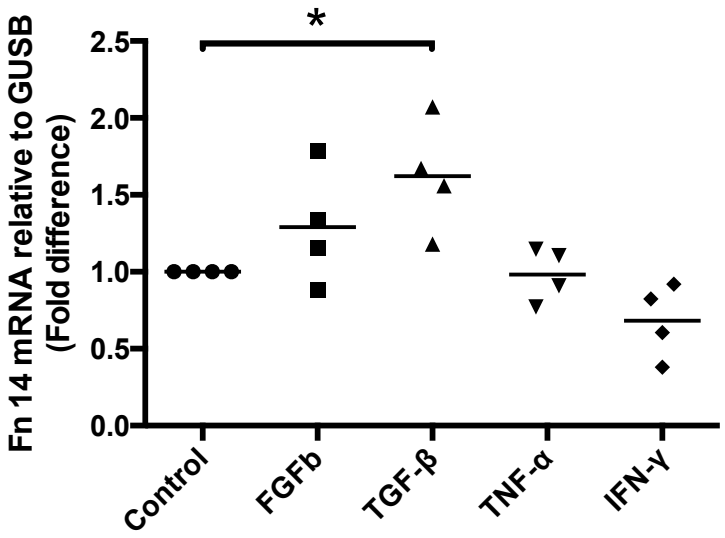

Figure 4.7 Effect of cytokines on Fn14 mRNA in HSCs
Expression of Fn14 was assessed by qPCR in untreated HSCs or HSCs treated with bFGF (10 ng/mL), TGF-β1 (10 ng/mL), TNF-α (10 ng/mL) or IFN-γ (100 ng/mL) for 24 hours *in vitro*. Gene expression is shown as fold change relative to *GUSB*. (n=4 different isolates) (**p<0.05, Kruskal-Wallis test*).

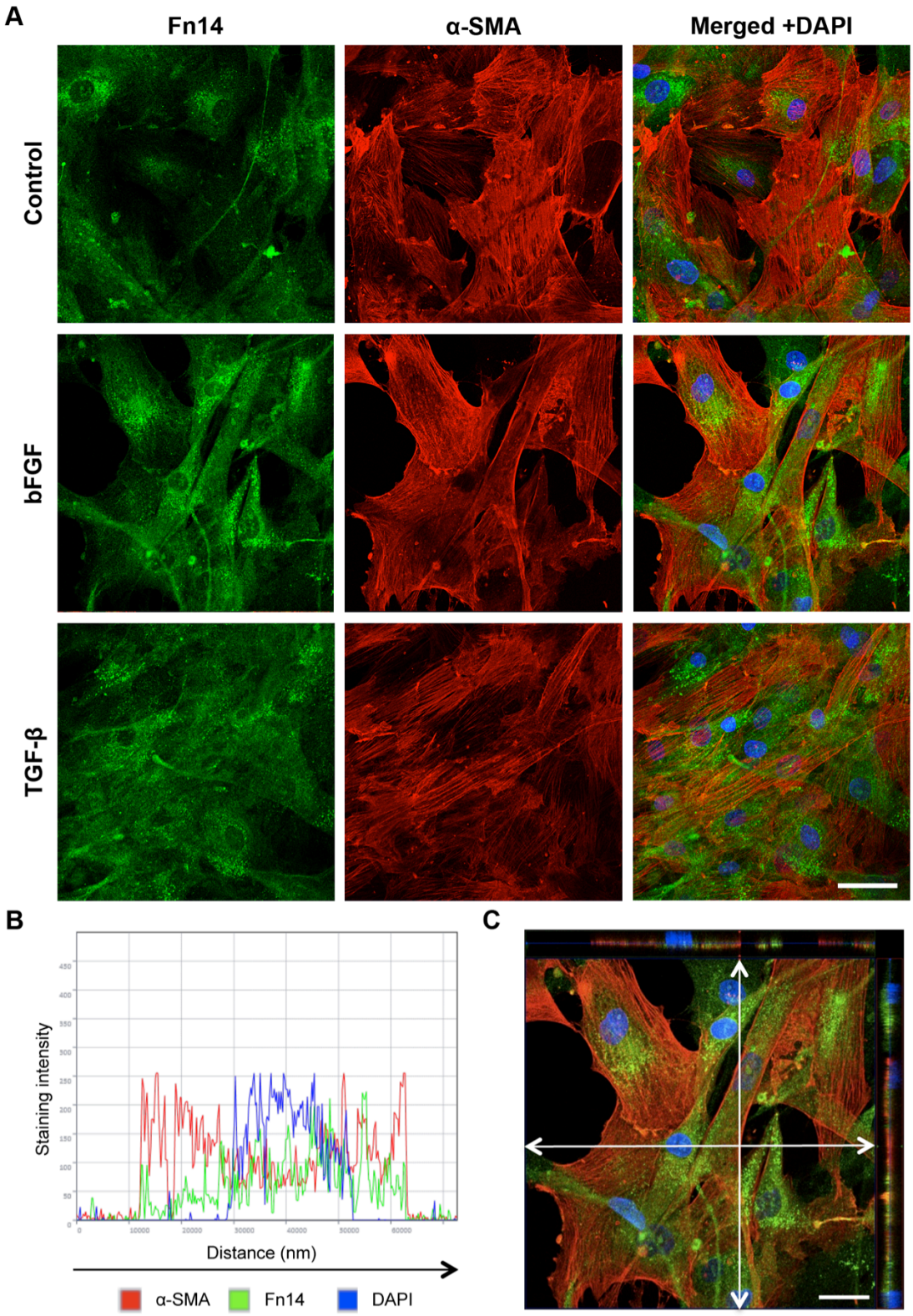

Figure 4.8 Localisation of Fn14 in HSCs

Immunofluorescent staining for Fn14 (green) and α-SMA (red) in untreated, bFGF (10 ng/mL) or TGF-β1 (10 ng/mL) treated primary HSCs for 24 hours *in vitro* (**A**). Representative histogram of Fn14, α-SMA and DAPI staining intensity through a cross sections of a bFGF-treated HSCs (**B**). Confocal Z-stack of bFGF-treated HSCs (**C**). Bar, 50 μm.

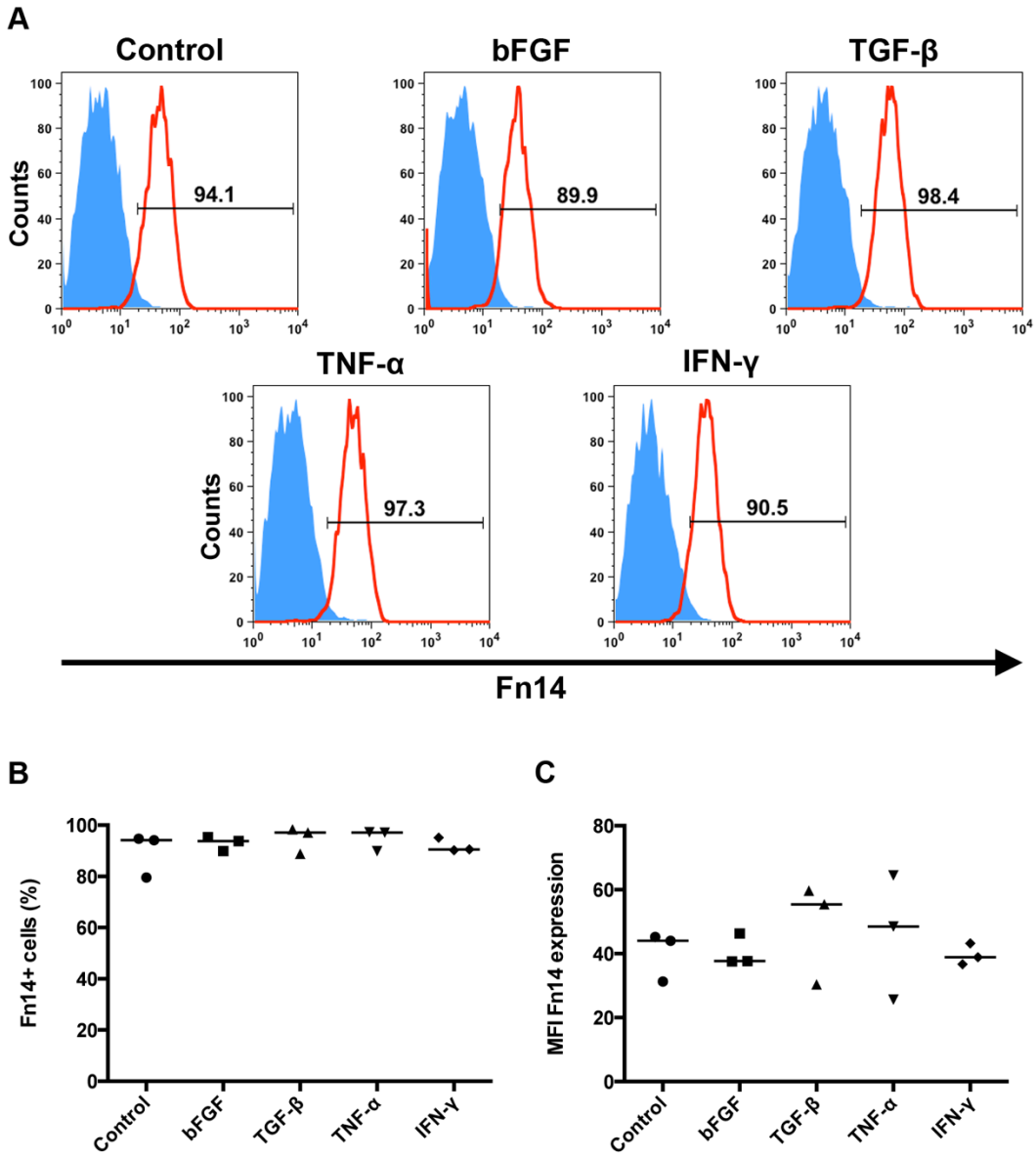

Figure 4.9 Effect of cytokines on intracellular and cell surface Fn14 expression

Flow cytometry analysis of intracellular **(A-C)** and cell surface **(D-F**; see next page) Fn14 expression in unstimulated and bFGF (10 ng/mL), TGF-β1 (10 ng/mL), TNF-α (10 ng/mL) or IFN-γ (100 ng/mL) stimulated HSCs for 24 hours *in vitro*. Representative histograms of Fn14 staining (red) and isotype control (blue) **(A)** percentage positive cells **(B)** and median fluorescent intensity (MFI) **(C)** of intracellular Fn14 expression. Representative histograms **(D)** of percentage positive cells **(E)** and MFI **(F)** of cell surface Fn14 expression. (n=3 different isolates) (*$p<0.05$, *Kruskal-Wallis test*)

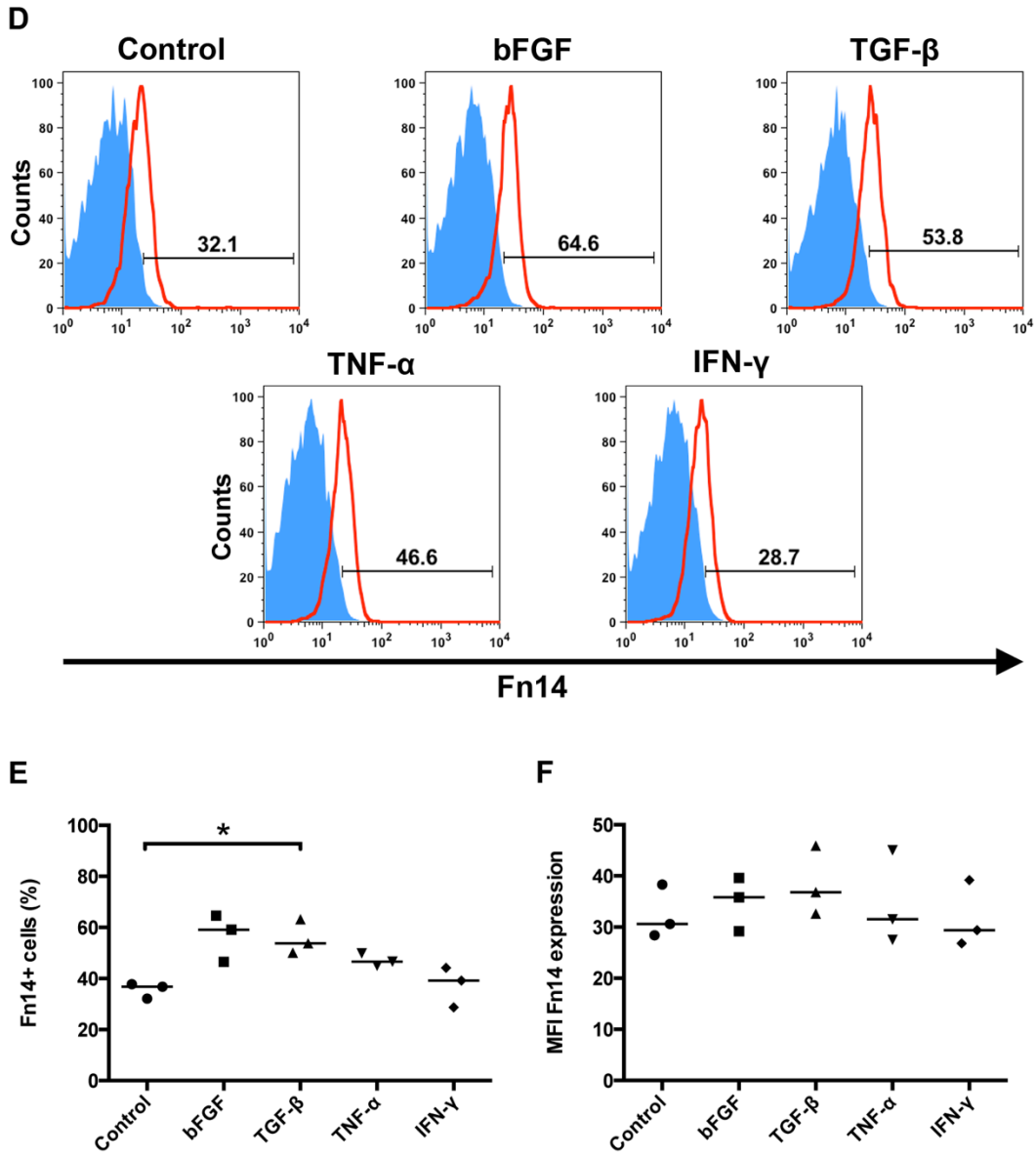

Figure 4.9 Continued

4.2.4 The effect of recombinant TWEAK on HSCs

After demonstrating that HSCs express Fn14 we investigated how its ligand TWEAK affects HSC proliferation. Activated HSCs were therefore treated with different concentrations of recombinant TWEAK and the nuclei were counted before and after TWEAK stimulation (Figure 4.10 A). Enhanced proliferation was detected in TWEAK-treated HSCs compared to untreated controls. The highest proliferative response was detected when HSCs were treated with 100 ng/mL TWEAK, which

induced proliferation to a similar extent as PDGF-BB dosing after 48 hours using the CyQuant assay (Figure 4.10 B).

In contrast, HSC activation was reduced following TWEAK treatment. A significant reduction of *ACTA2* (α-SMA) was detected when HSCs were treated with 100 or 500 ng/mL TWEAK compared to untreated HSCs ($p<0.05$; Figure 4.11 A). Interestingly, *COL1A1* (Collagen1a1) did not change in HSCs after stimulation with different TWEAK concentrations *in vitro* (Figure 4.11 B).

Next to production of ECM, HSCs are involved in leukocyte recruitment by secreting large amounts of chemokines including CCL2, CCL3, CCL5, CXCL8, CXCL9, and CXCL10 (Holt et al., 2009). CCL5 not only facilitates recruitment of immune cells it also directly affects HSC proliferation (Liaskou et al., 2013; Schwabe et al., 2003). TWEAK is a pro-inflammatory cytokine and in order to get an insight on the effect of TWEAK on chemokine production, CCL5 levels in culture supernatant from TWEAK-stimulated HSCs were determined (Figure 4.12). As shown in Figure 4.12 the levels of CCL5 were slightly but not significantly increased in HSCs upon TWEAK stimulation compared to unstimulated HSCs. Levels of CCL5 mRNA were not measured.

TWEAK treatment of Fn14-positive cells activates predominantly the NF-κB pathway (Winkles, 2008). Furthermore, TWEAK's sibling TNF-α plays a key role in HSC homeostasis by regulating anti-apoptotic signals through the NF-κB pathways (Cong et al., 2012). Therefore, I investigated whether TWEAK can also affect NF-κB signalling in HSCs. Indeed, TWEAK induced phosphorylation and translocation of NF-κB into the nucleus as early as 5 min (Figure 4.13). Activation of the canonical NF-κB pathways was then sustained for at least 24 hours.

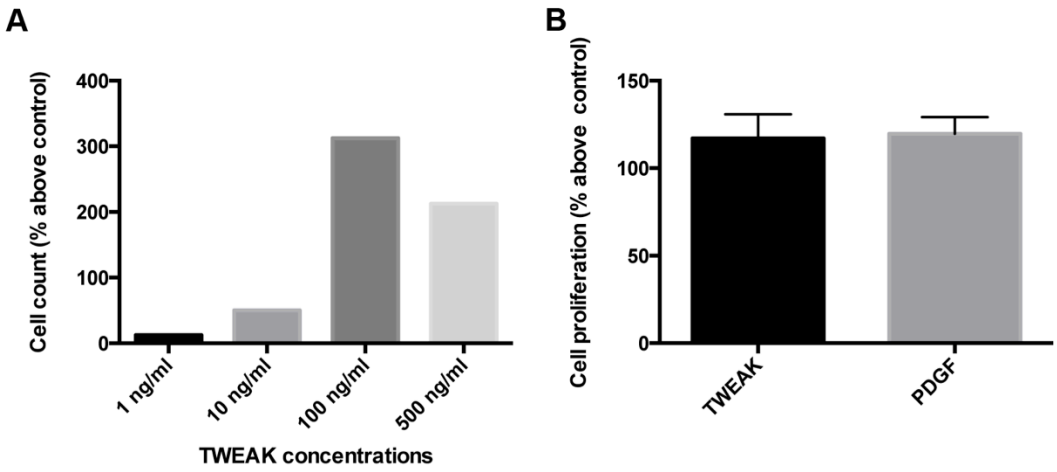

Figure 4.10 HSC proliferative response upon TWEAK stimulation
Activated HSCs were stimulated with different concentrations of recombinant TWEAK and nuclei were counted and normalised to cell number at the start of the experiment (n=1) **(A)**. HSCs were stimulated with TWEAK (100 ng/ml) or PDGF-BB (10 ng/ml) for 48 hrs *in vitro* and DNA levels were measured with the CyQuant kit to determine cell proliferation. (n=3 different isolates)

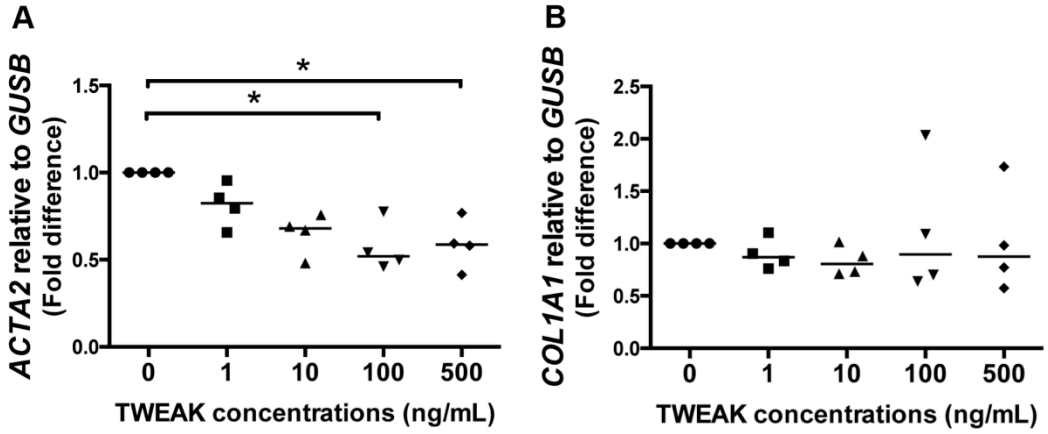

Figure 4.11 Expression levels of *ACTA2* and *COL1A1* in HSCs upon TWEAK stimulation
Activated HSCs were stimulated with different concentrations of recombinant TWEAK for 24 hours and expression of *ACTA2* and *COL1A1* were measured by qPCR. Gene expression is shown relative to *GUSB* using the $2^{-\Delta Ct}$ method. (n=4 from different isolates) (**p<0.05 Mann-Whitney U test*)

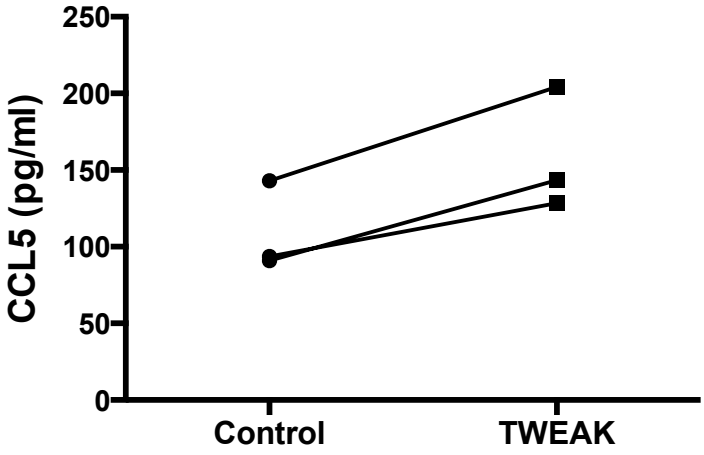

Figure 4.12 Effect of TWEAK on CCL5 production in HSCs
Activated HSCs were treated with TWEAK (100 ng/ml) for 24 hours. The concentrations of CCL5 released in the supernatant were measured by Luminex. (n=3 different isolates) No significant difference was detected. *(Mann-Whitney U test)*

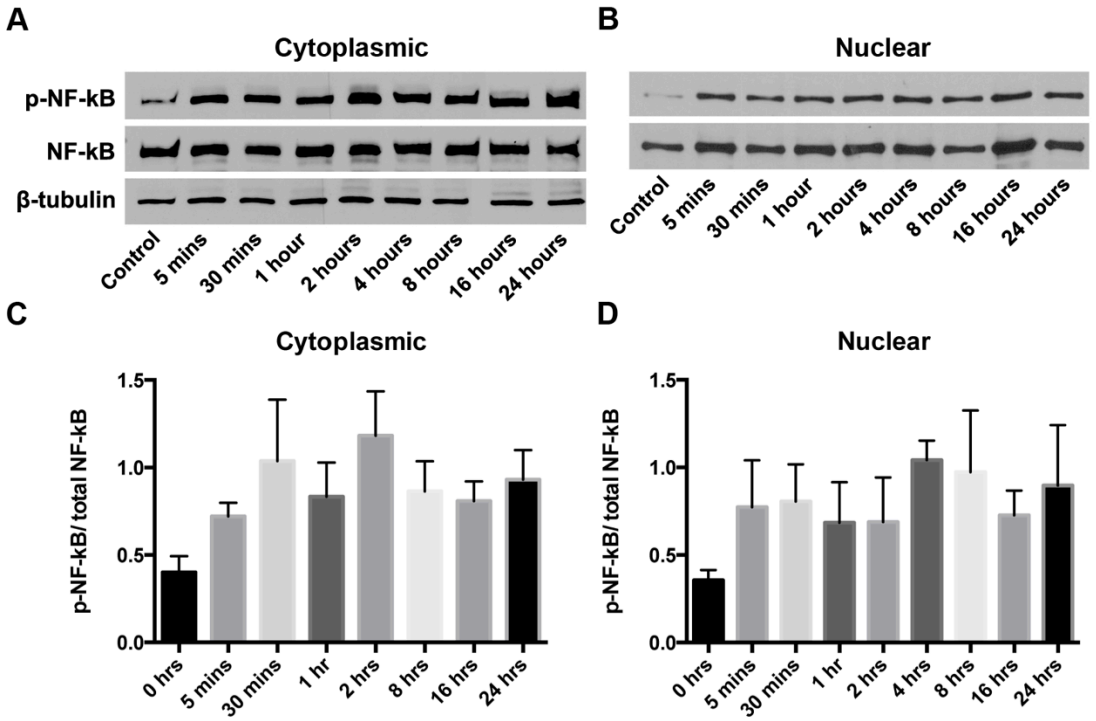

Figure 4.13 Effect of TWEAK on NF-κB activation in HSCs
HSCs were treated with 100 ng/ml TWEAK for the indicated period. Representative blots of cytoplasmic **(A)** and nuclear **(B)** phosphorylated (p) and total NF-κB (p65) and β-tubulin are shown. Quantification of p-NF-κB in relation to total NF-κB in the cytoplasm **(C)** and nucleus **(D)** (n=3 from different isolates)

4.2.5 TWEAK is expressed by HSCs

To date TWEAK expression has been associated with macrophages and NK cells in the liver (Tirnitz-Parker et al., 2010). However, immunofluorescent staining in section 3.2.4.4 has shown that TWEAK is also present in α-SMA-positive cells (Figure 3.13). To further investigate TWEAK expression, the supernatant of HSCs was collected and TWEAK levels were measured by ELISA (Figure 4.14). The data shows that TWEAK expressed by HSCs can be released into the culture media, albeit to a lesser extent than macrophages (a well described source of TWEAK protein) (Figure 4.14 A). Measuring TWEAK levels in HSC culture media following stimulation with TGF-β1 (Figure 4.14 B) TNF-α, IFN-γ, IL-1β (Figure 4.14 D-G) or IL-13 (Figure 4.14 H) did not demonstrate a conclusive up or downregulation of TWEAK expression in HSCs. Increased TWEAK levels were consistently detected in the supernatant from HSCs stimulated with PDGF-BB but this could be due to increased proliferation of HSCs (Figure 4.14 C). Detection of endogenous TWEAK in HSC supernatant led us to investigate how it might affect HSC behaviour. Incubation with varying concentrations of a TWEAK monoclonal function-blocking antibody for 24 hours decreased HSC migration compared to the isotype control (Figure 4.15).

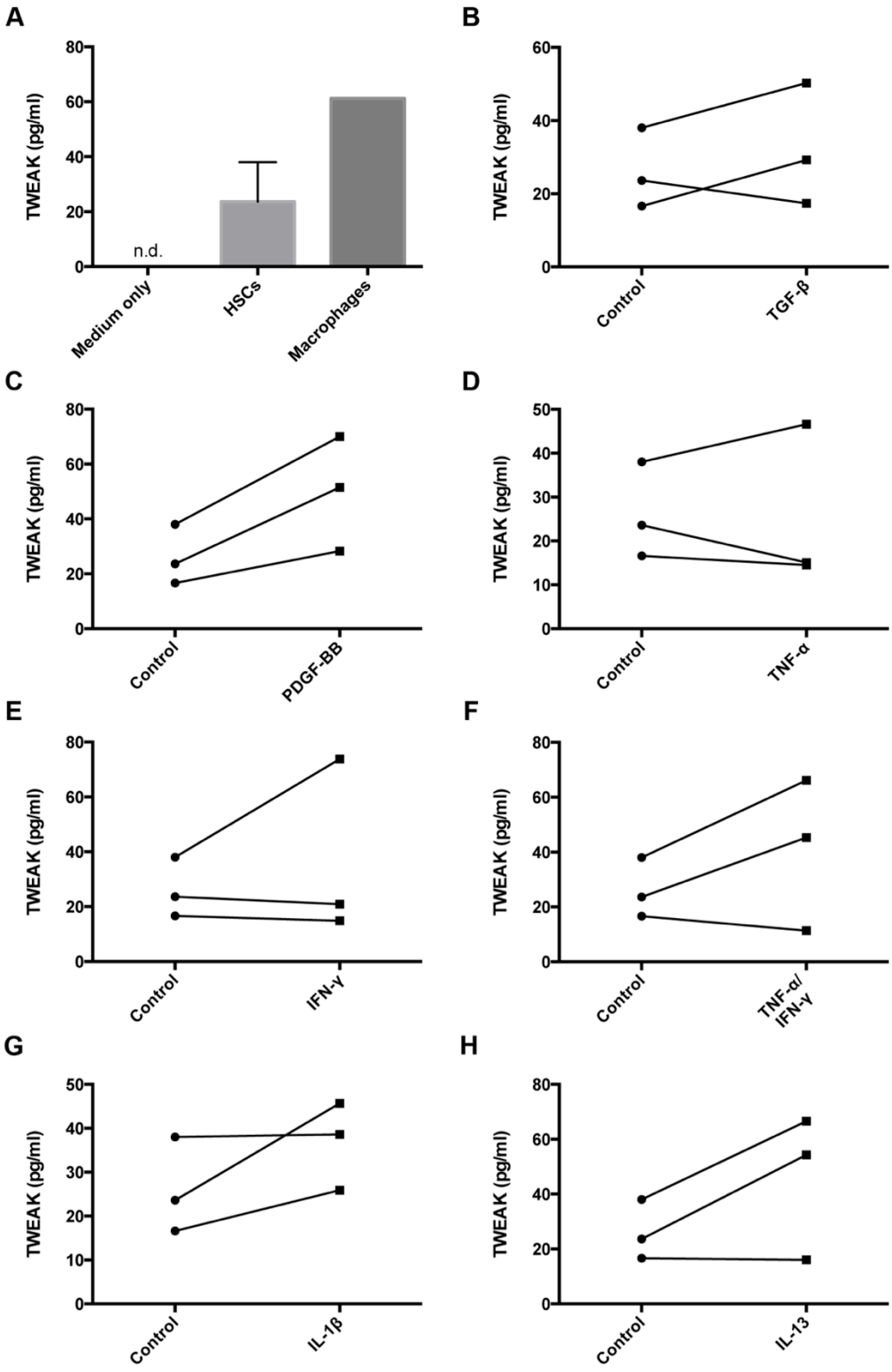

Figure 4.14 Effect of cytokines on TWEAK expression in HSCs
The concentration of TWEAK released in the supernatant was measured by ELISA in HSCs (n=3) and monocyte-derived macrophages (n=1). TWEAK levels in HSC growth medium alone were not detectable (n.d.) (**A**). TWEAK was also measured in supernatant of HSCs treated with TGF-β1 (**B**), PDGF-BB (**C**), TNF-α (**D**) or IFN-γ (**E**), or a combination of TNF-α and IFN-γ (**F**), IL-1β (**G**) or IL-13 (**F**) (all 10 ng/ml) for 24 hours. (n=3 different isolates) No significant difference was detected. *(Mann-Whitney U test)*

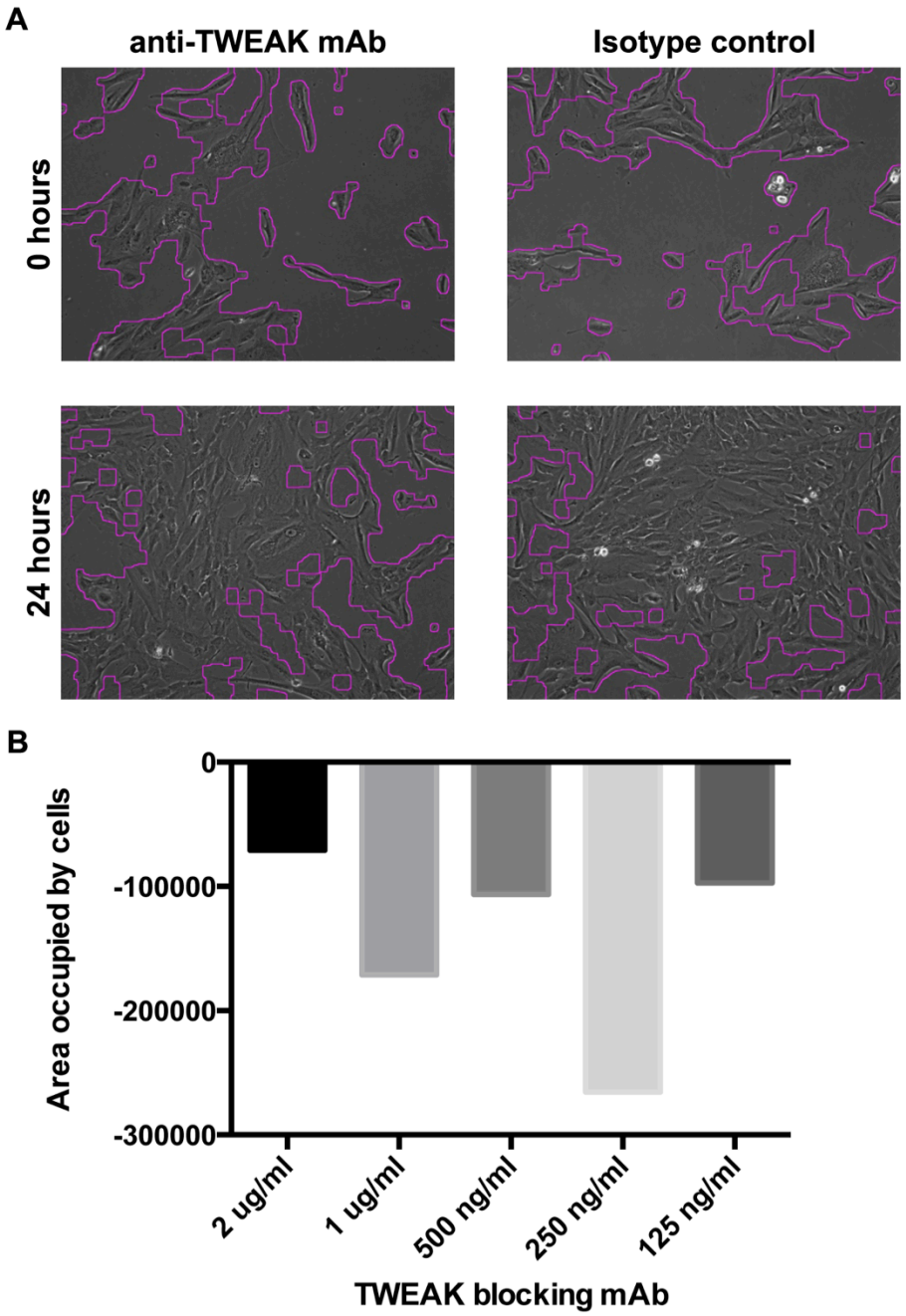

Figure 4.15 Inhibiting endogenous TWEAK with mAb in HSCs
Activated HSCs were treated with the indicated concentrations of monoclonal TWEAK function-blocking antibodies or a matched isotype control antibody for 24 hours. Representative images are shown (cells outlined in pink) **(A)**. Data are expressed as area occupied by cells compared to isotype-matched control (negative values indicate reduced area covered by cells) **(B)**. (n=1)

4.3 Discussion

In chapter 3 I have shown that TWEAK and Fn14 expression is only upregulated during liver disease, suggesting a regulatory role in the pathway of tissue injury and regeneration. Histopathological examination of different liver diseases in chapter 3 demonstrated that Fn14 was expressed by a variety of cell types. This chapter supports this observation through qPCR analysis of Fn14 transcript levels in primary LMFs, HSCs, hepatocytes, cholangiocytes and IHECs *in vitro*. Furthermore this chapter demonstrates the regulation of Fn14 during HSC activation, and that TWEAK was capable of inducing HSC proliferation possibly via NF-κB signalling which could promote the development of liver fibrosis.

Liver injury causes quiescent HSCs to become activated and to proliferate. Fn14 expression in HSCs was detected prior to the expression of the activation marker α-SMA suggesting that Fn14 is regulated by transcription factors that play a role in early transformation and that Fn14 expression might be turned on during early fibrosis. Enhanced Fn14 expression during cell transformation has also been demonstrated in the corneal stroma where quiescent keratocytes start expressing Fn14 after they had activated during injury (Ebihara et al., 2009). As Fn14 is expressed before α-SMA it could be hypothesised that Fn14 is involved in the regulation of α-SMA. However, isolations of HSCs from Fn14 KO mice did not seem to suggest that it does as the cells did express α-SMA (data not shown). Furthermore, as shown in chapter 5, α-SMA expression in Fn14 KO was not significantly different compared to WT mice.

As Fn14 expression seemed to be dependent on phenotypic transdifferentiation of HSCs during liver injury we investigated factors that can induce Fn14 expression

further. Flow cytometry demonstrated that most unstimulated HSCs had intracellular stores of Fn14 and a population of HSCs also expressed Fn14 on the cell surface. Therefore, HSCs were treated with cytokines known to induce Fn14 expression in other cell types (Winkles, 2008) and that have been detected in fibrotic liver tissue (Reeves and Friedman, 2002). FGF is a well-known cytokine to induce Fn14 expression (Winkles, 2008). It is upregulated during liver fibrosis and is a HSC mitogen (Reeves and Friedman, 2002). Stimulation of HSCs with bFGF led to a slight increase of Fn14 mRNA and Fn14 cell surface expression but this did not reach significance. Stimulation of another pro-fibrogenic factor, TGF-β1 significantly enhanced Fn14 mRNA levels in HSCs. In addition, TGF-β1 enhanced the number of HSCs expressing Fn14 on the cell surface making them potentially more susceptible to stimulation with TWEAK and might increase the probability of ligand-independent signalling by the receptor (Brown et al., 2013). The pro-inflammatory cytokine, TNF-α had little effect on Fn14 mRNA levels and cell surface expression. TNF-α has also been associated with HSC activation but compared to TGF-β1, TNF-α reduces synthesis of type I and III collagen in HSCs (Reeves and Friedman, 2002). IFN-γ, another pro-inflammatory cytokine, has been associated with inhibiting HSC activation and proliferation (Reeves and Friedman, 2002). It slightly decreased Fn14 mRNA levels and did not affect cell surface expression in HSCs. This suggests that pro-fibrogenic cytokines rather than pro-inflammatory factors induce Fn14 expression and promote cell surface expression in HSCs. Similarly, PDGF-BB, the most potent mitogen for HSCs, also requires activation dependent expression of its receptor which can be induced by pro-fibrogenic cytokines such as TGF-β1 (Bonner, 2004).

Since a population of HSCs expresses Fn14 on the cell surface we wanted to investigate the role of TWEAK on HSCs. During fibrogenesis HSCs differentiate,

produce ECM and proliferate. My data has shown for the first time that HSCs show enhanced proliferative capacity in the presence of TWEAK. In contrast, *ACTA2* was significantly downregulated in HSCs upon TWEAK stimulation suggesting that TWEAK is involved in enhancing HSC proliferation and decreasing HSC differentiation. It has been demonstrated in a number of other cell types that TWEAK can regulate proliferation and differentiation. In hepatoblasts, skeletal myoblasts and osteoblasts TWEAK promoted proliferation but inhibited differentiation (Ando et al., 2006; Dogra et al., 2006; Girgenrath et al., 2006). In addition, TWEAK inhibited transformation of keratocytes into myofibroblasts *in vitro* (Ebihara et al., 2009). Furthermore, my data also demonstrated that TWEAK stimulation did not have an effect on collagen synthesis in HSCs. In contrast, other studies have demonstrated that TWEAK induces collagen expression in cardiac fibroblasts via Fn14 (Chen et al., 2012; Novoyatleva et al., 2013). Although TWEAK appeared to inhibit activation of HSCs and did not alter *COL1A1* expression, Fn14 KO mice had reduced liver fibrosis compared to their WT controls when fed the CDE diet (Tirnitz-Parker et al., 2010). TWEAK might therefore be important in expanding the HSC population and other factors such as TGF-β1 serve to enhance ECM deposition of HSCs. In addition TWEAK might increase expression of protein but not mRNA levels of collagen I or it might alter expression of other ECM proteins such as collagen III, fibronectin and tenascin. These proteins could be measured with western blot or ELISA. In addition, collagen levels could be measured with the hydroxyproline assay.

Liver fibrosis is closely associated with inflammation and HSCs have been shown to express pro-inflammatory chemokines such as CCL2 and CCL5 and chemokine

receptors such as CCR5 (Pellicoro et al., 2014). CCL5 facilitates leukocyte recruitment (Liaskou et al., 2013) and directly targets HSCs to promote proliferation and migration (Schwabe et al., 2003) thereby perpetuating the fibrotic response. Here, it appears to be a trend that TWEAK increases CCL5 expression in HSCs. Therefore TWEAK might not only act directly on HSCs but also increases expression of other factors that amplify fibrogenesis.

TWEAK induced intracellular signalling pathways in HSCs are unknown. To explore the mechanism by which TWEAK stimulates HSCs, we investigated the NF-κB pathway. TWEAK led to a quick activation of the canonical NF-κB pathway in HSCs, which was as early as 5 minutes and was maintained for 24 hours. Activation of the canonical NF-κB pathway in HSCs has been associated with HSC survival (Cui et al., 2010; Wang et al., 2014) suggesting that NF-κB may promote the persistence of activated HSCs via TWEAK.

TWEAK expression in the liver has so far been demonstrated by infiltrating leukocytes (Tirnitz-Parker et al., 2010). During human liver disease TWEAK expression was upregulated (Figure 3.1) and detected in LMFs amongst other cell types (Figure 3.13). Consistent with these results, activated HSCs secreted TWEAK into their medium, suggesting the presence of an autocrine loop. Therefore, HSCs were treated with a blocking antibody known to inhibit TWEAK signalling (Dohi et al., 2014). Indeed, blocking endogenous TWEAK demonstrated a decrease in HSC migration suggesting that endogenous TWEAK maintains HSCs in a migratory state. However, this experiment has only been carried out once and needs to be repeated several times. In addition, it would be useful to investigate whether the blocking antibody inhibits cell signalling. As shown by Yadava *et al.* administration of the same

blocking antibody in a mouse model of skeletal muscle wasting led to decreased levels of *Nfkb2* and *RelB* (Yadava et al., 2015). Using this approach might then also show a dose response with different concentrations of TWEAK blocking antibody.

In conclusion, our data supports a role of TWEAK and Fn14 interaction in promoting fibrogenic responses in the liver. During HSC activation Fn14 expression increases and both HSCs and LMFs express Fn14. TWEAK dependent Fn14 signalling induced HSC proliferation and TWEAK blocking mAb reduced migration, suggesting that TWEAK could act via both autocrine and paracrine mechanisms driven by HSC production of TWEAK. Therefore, the next chapter will investigate the role of TWEAK and Fn14 during fibrogenesis *in vivo*.

Chapter 5

The role of TWEAK and Fn14 in liver fibrosis *in vivo*

5.1 Introduction

TWEAK and Fn14 KO mice have been used in a variety of experimental models to assess the contribution of TWEAK and Fn14 in physiological and pathological settings (Karaca et al., 2014; Girgenrath et al., 2006; Jain et al., 2009). Liver regeneration has been investigated in Fn14 KO mice treated with the CDE diet, and when compared to WT mice the Fn14 KO mice had fewer LPCs and less collagen deposition (Tirnitz-Parker et al., 2010). Evidence has shown that a correlation exists between ductular expansion and the severity of fibrosis (Williams et al., 2014). Whether TWEAK signalling can promote liver fibrogenesis through direct interactions with HSCs has been investigated in chapter 4 and these *in vitro* studies showed that HSCs expressed both Fn14 and TWEAK and that they may be involved in the development of liver fibrosis through proliferation of human HSCs.

This chapter examines the role of TWEAK and Fn14 in fibrogenesis following acute and chronic liver injury *in vivo*. In order to do so, TWEAK and Fn14 KO mice along with their matching WT littermate controls were dosed with the hepatotoxin CCl_4. CCl_4-induced injury has been used extensively to investigate liver injury in rodents. CCl_4 induces centrilobular necrosis between 24 and 48 hours after administration and liver regeneration becomes evident after 48 and 72 hours as a results of HSC activation and infiltration of inflammatory cells (Ikejima et al., 2001; Karlmark et al., 2010). Liver injury causes increased intestinal permeability and bacterial translocation (Fouts et al., 2012) and gut microbiota can contribute to fibrogenesis by either directly causing HSC activation through the LPS/TLR pathway or via recognition of bacterial products by Kupffer cells (Seki et al., 2007; Rivera et al., 2007).

Therefore, in this study each KO strain was compared to WT littermate controls to avoid differential results caused by a different gut microbiota. The extent of liver fibrosis was investigated by expression levels of fibrogenic mediators, accumulation of α-SMA-positive HSCs/LMFs and increased deposition of ECM.

5.2 Results

5.2.1 Regulation of TWEAK and Fn14 in acute liver injury

To investigate the regulation of TWEAK and Fn14 *in vivo*, WT mice were treated once with CCl_4 orally to induce acute toxic hepatic damage and then sacrificed after 24, 48, 72 or 96 hours. Each mouse was weighed before the CCl_4 dose (Figure 5.1 A) and serum ALT activity was measured at sacrifice (Figure 5.1 B). CCl_4-treatment resulted in centrilobular necrosis and inflammation (Figure 5.1 C) with most damage occurring at 24 and 48 hours that was reflected by significantly elevated serum ALT activity ($p<0.01$, Figure 5.1 B). Mice treated with mineral oil had normal ALT activity (Figure 5.1 B) and tissue architecture (Figure 5.1 C).

Analysis of murine livers revealed a median of 58-, 44-, 33- and 6-fold increase in Fn14 mRNA at 24, 48, 72 and 96 hours post CCl_4 challenge, respectively compared to mineral oil treated controls (Figure 5.2 A). In contrast, levels of TWEAK mRNA did not differ significantly between experimental groups although a slight increase after 48, 72 and 96 hours was noticed in some animals (Figure 5.2 B). Highest levels of TWEAK were observed at 72 hours but they did not reach statistical significance ($p=0.055$). The HSC activation marker α-SMA (*Acta2*) significantly increased at all timepoints after CCl_4 injury with the maximal level again being seen at 72 hours (Figure 5.2 C). Collagen 1α1 (*Col1a1*, a major component of collagen 1) was significantly upregulated after 48 hours and continued to increase until 96 hours (Figure 5.2 D). Of note, the pattern for upregulation of Fn14 was also present in chronic liver injury. In a 4 week CCl_4-induced liver injury model, Fn14 mRNA was upregulated 3.18 fold, ($p<0.01$; Figure 5.3 A) whereas TWEAK mRNA was not elevated above baseline ($p=0.412$; Figure 5.3 B) as seen in the acute injury model.

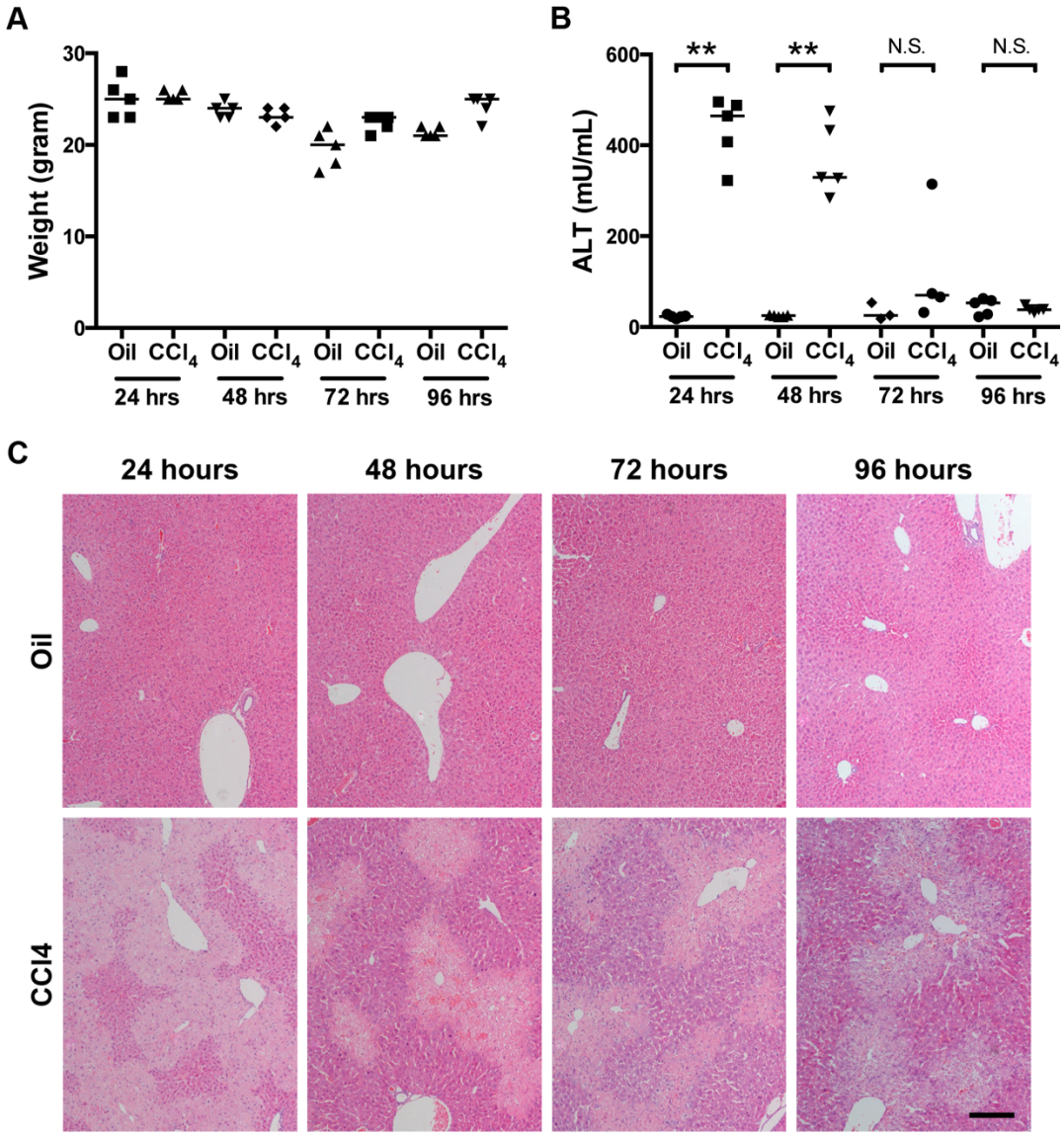

Figure 5.1 General characteristics of wild type mice with acute liver injury

To induce acute liver injury Balb/c WT mice received one oral dose of CCl_4 or mineral oil and were sacrificed at the time points indicated. Each mouse was weighed before the experiment and the volume of CCl_4 was adjusted accordingly (1 mL/kg body weight) **(A)**. Serum ALT activity was assessed as a measure of acute liver injury **(B)**. Representative images of haematoxylin-eosin staining of paraffin-embedded liver tissue sections is shown **(C)** (n=4-5 animals each per group). (***p<0.01* or *n.s. non significant Mann-Whitney U test*). Bar, 200 µm

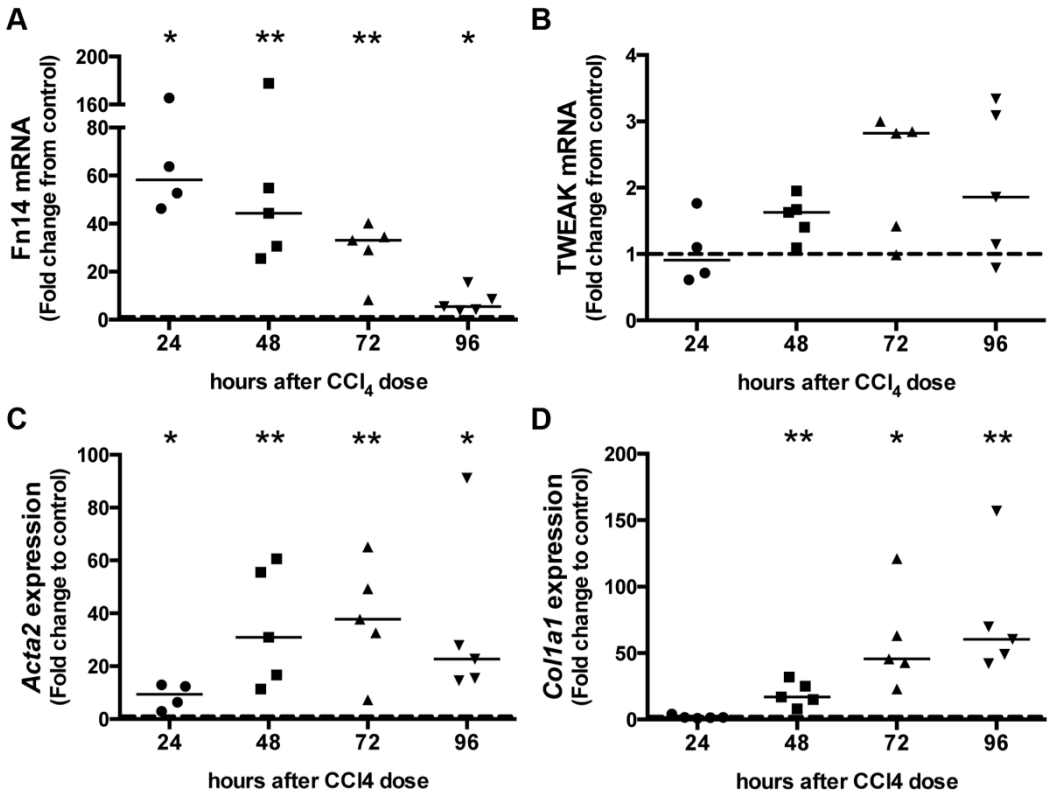

Figure 5.2 Fn14 but not TWEAK mRNA significantly increases following acute CCl_4 injury

Murine Fn14 mRNA, TWEAK mRNA, *Acta2* and *Col1a1* were analysed in liver tissue from WT animals by qPCR following acute CCl_4-induced liver injury, or mineral oil control, at the time points indicated. Data are expressed as fold change compared to mineral oil control. The dashed line indicates mRNA levels of mineral oil treated WT mice (n=4-5 animals per group). (**p<0.05* or ***p<0.01 Mann-Whitney U test*)

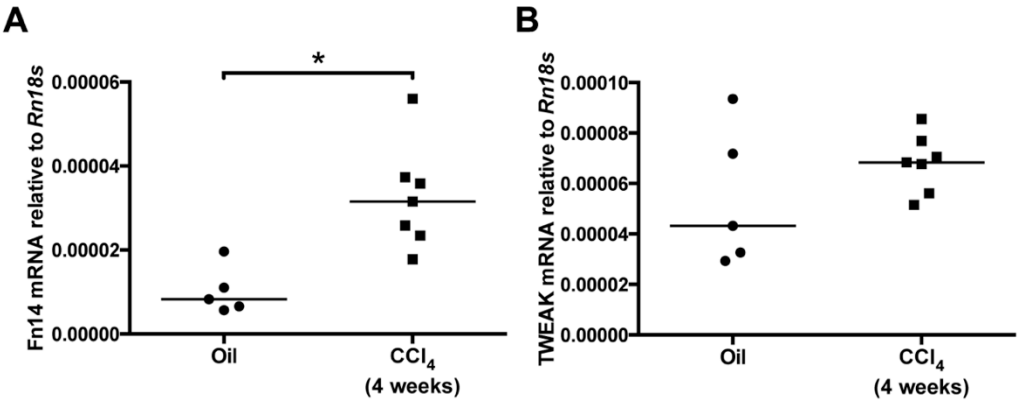

Figure 5.3 Chronic CCl_4-induced liver injury leads to significant upregulation of Fn14 but not TWEAK mRNA

Fn14 and TWEAK mRNA were analysed in liver tissue from WT animals following chronic CCl_4-induced liver injury. Control animals were exposed to mineral oil alone. Gene expression is shown relative to *Rn18s* using the $2^{-\Delta Ct}$ method (n=5-7 animals per group). (**p<0.05 Mann-Whitney U test*)

5.2.2 Acute liver injury in TWEAK and Fn14 KO mice

To further assess the potential functional role of TWEAK and Fn14 in hepatic injury and fibrogenesis *in vivo*, TWEAK KO and Fn14 KO mice along with their matched WT controls were subjected to a single dose of CCl_4 and subsequently sacrificed after 72 hours. Prior to CCl_4 administration, TWEAK KO, Fn14 KO and WT mice exhibited no differences in weight (Figure 5.4 A,B) or liver architecture (Figure 5.4 C).

Following CCl_4 administration, TWEAK KO mice had similar levels of liver injury compared to their WT controls as histological examination demonstrated foci of centrilobular necrosis and inflammation in both KO and WT mice treated with CCl_4 (Figure 5.5 A-D). No significant differences were detected in Sirius red staining between experimental groups (Figure 5.5 E-H). Assessing transcript levels in acutely injured TWEAK KO mice demonstrated significantly lower levels of *Col1a1*, *Tgfb1*, *Mmp2* and *Timp1* upregulation in response to injury compared to injured WT controls (Figure 5.6 B-D,F). However, levels of *Acta2* (p=0.313) and *Mmp9* (p=0.138) in injured TWEAK KO mice, although higher than uninjured animals, were not significantly different than injured WT animals (Figure 5.6 A,E).

Analysis of H&E stained tissue showed that Fn14 KO mice also had similar levels of liver injury compared to their WT controls after CCl_4 administration (Figure 5.7 A-D). In addition, no obvious differences were detected in sections stained with Sirius red (Figure 5.7 E-H). Examination of fibrogenic mediators demonstrated that *Acta2*, *Col1a1, Tgfb1, Mmp9* and *Timp1* all significantly increased in Fn14 WT mice treated with CCl_4 compared to mineral oil (Figure 5.8 A-C,E,F). *Mmp2* levels remained similar between injured and mineral oil-treated Fn14 WT mice (Figure 5.8 D).

Fn14 KO mice treated with CCl_4 also demonstrated significantly higher levels of *Col1a1* and *Timp1* compared to mineral oil treated controls (Figure 5.8 B,F). *Acta2*, *Tgfb1, Mmp2* and *Mmp9* in Fn14 KO did not show a difference between CCl_4 or mineral oil administration (Figure 5.8 A,C-E).

Surprisingly, injured Fn14 KO mice demonstrated no significant difference of fibrogenic mediators compared to injured Fn14 WT mice though there were a trend to reductions in the expression of *Acta2*, *Mmp9* and *Timp1* in the Fn14 KO mice (Figure 5.8). Further examination of collagen protein levels using the hydroxyproline assay also demonstrated no significant difference between Fn14 WT or KO mice treated with CCl_4 (p=0.073; Figure 5.9).

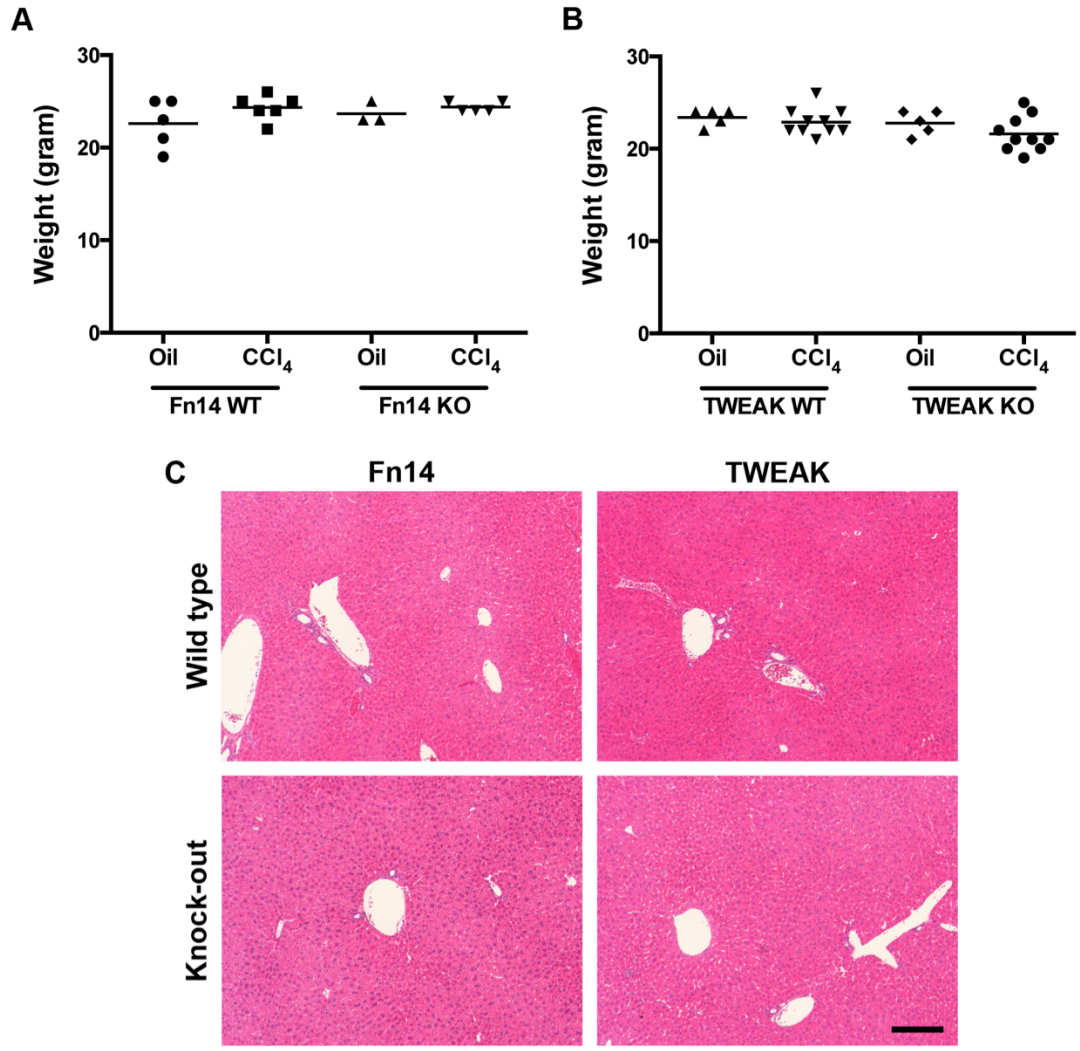

Figure 5.4 TWEAK and Fn14 WT and KO mice display no differences in weight or liver tissue architecture at baseline

Weight **(A)** and liver histology **(B)** was assessed in Balb/c Fn14 and TWEAK WT and KO mice. Representative images of haematoxylin-eosin staining of paraffin-embedded liver tissue sections are shown (n=3-10 animals each per group). Bar, 200 μm

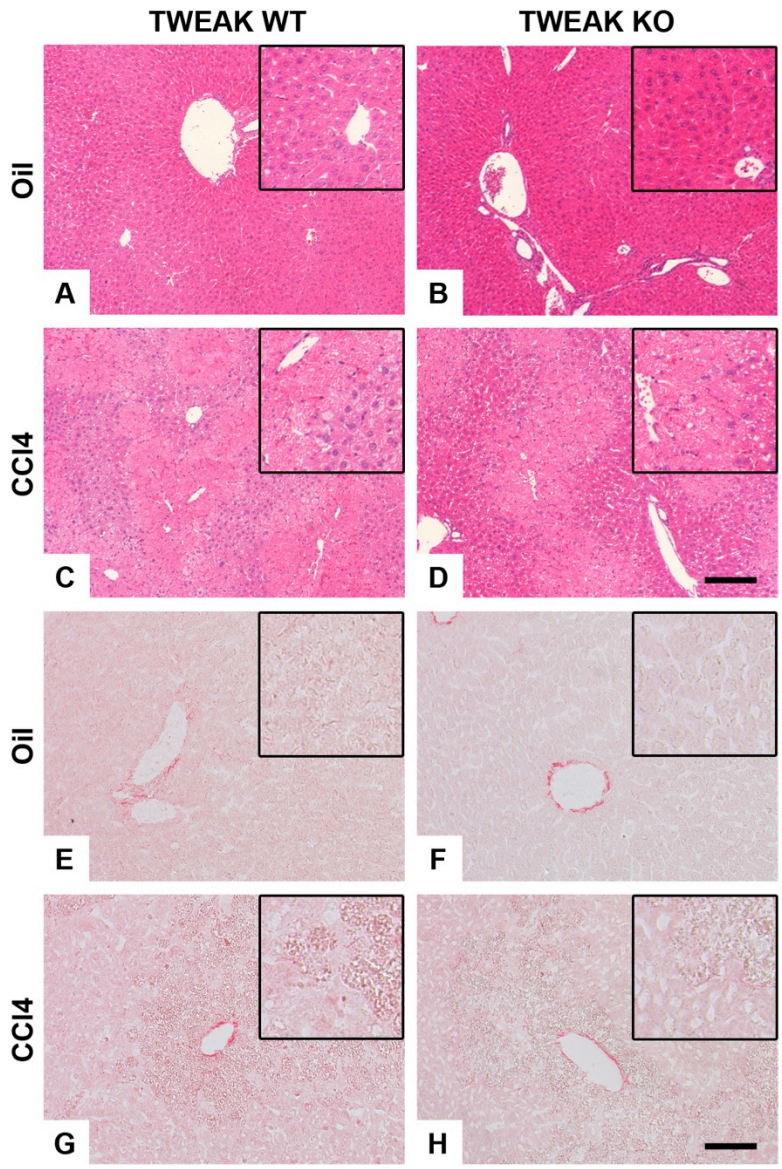

Figure 5.5 No apparent differences in liver histology between TWEAK WT and KO mice after acute liver injury

TWEAK WT and KO mice were injected with a single dose of CCl_4 or mineral oil and sacrificed 72 hours afterwards. Representative images of haematoxylin-eosin staining, Bar 200 μm **(A-D)**. Representative staining using Sirius red. Bar, 100 μm **(E-H)**. Inserts: image digitally enlarged.

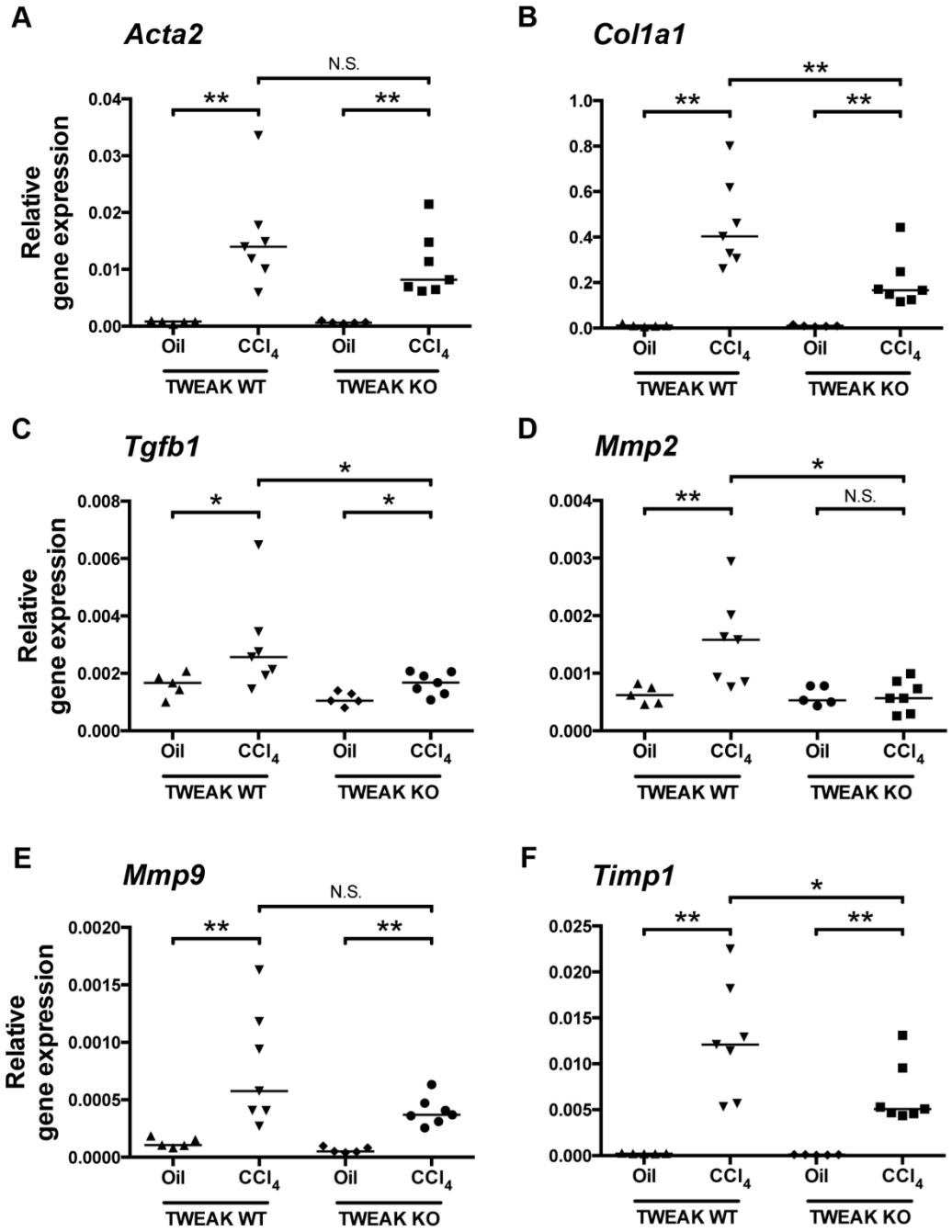

Figure 5.6 TWEAK is critical for liver fibrogenesis following acute hepatic injury *in vivo*

TWEAK KO and corresponding WT mice were injected with a single dose of CCl_4 or mineral oil and sacrificed 72 hours afterwards. Expression levels of fibrogenic mediators were analysed by qPCR (n=5-7 animals per group). Gene expression is shown relative to *Gapdh* using the $2^{-\Delta Ct}$ method. (**p<0.05, **p<0.01* or *n.s. non significant, Mann-Whitney U test*)

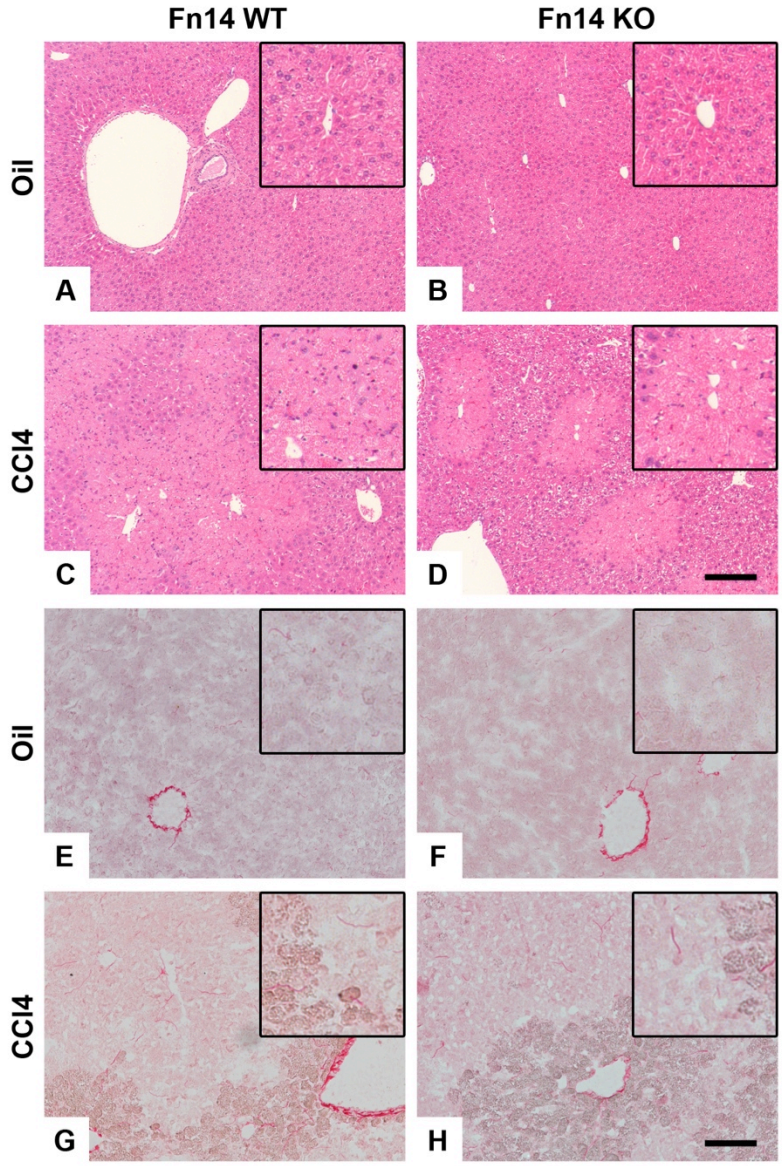

Figure 5.7 Fn14 KO had similar levels of liver injury compared to Fn14 WT mice

Fn14 WT and KO mice were injected with a single dose of CCl_4 or mineral oil and sacrificed 72 hours afterwards. Representative images of haematoxylin-eosin staining, Bar 200 μm **(A-D)**. Representative staining of Sirius red. Bar, 100 μm **(E-H)**. Insert: image digitally enlarged.

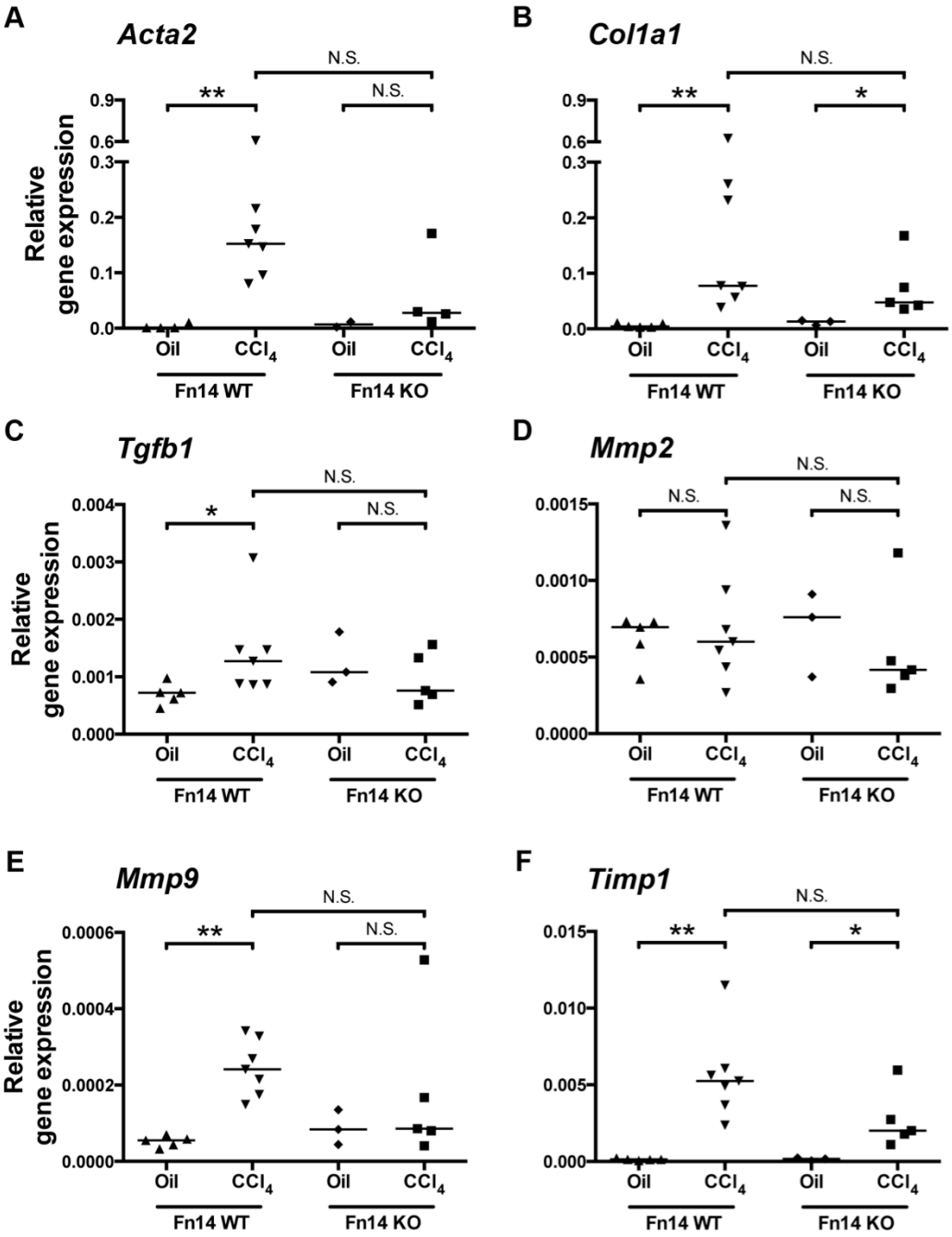

Figure 5.8 Fn14 deletion does not affect levels of fibrogenic mediators after acute liver injury significantly

Fn14 KO and corresponding WT mice were injected with a single dose of CCl_4 or mineral oil and sacrificed 72 hours afterwards. Expression levels of fibrogenic mediators were analysed by qPCR (n=4-7 animals per group). Gene expression is shown relative to *Gapdh* using the $2^{-\Delta Ct}$ method. (**p<0.05, **p<0.01* or *n.s. non significant, Mann-Whitney U test*)

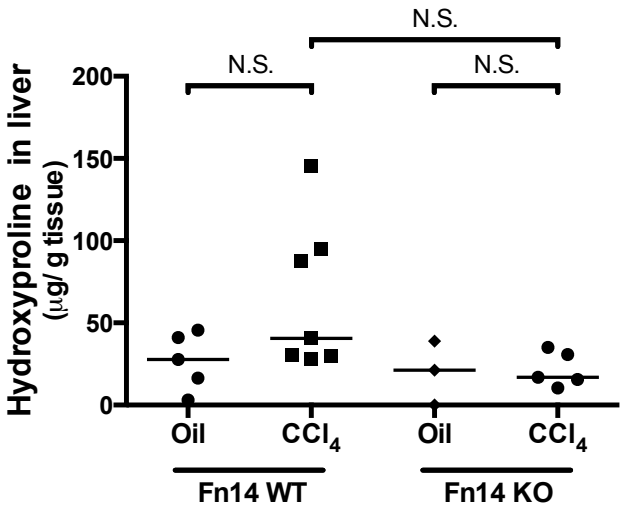

Figure 5.9 Hydroxyproline content does not change in Fn14 WT and KO mice following acute CCl_4-induced liver injury
Fn14 KO and corresponding WT mice were injected with a single dose of CCl_4 or mineral oil and sacrificed 72 hours afterwards. Liver fibrosis was assessed by the hydoxyproline content of the liver (n=3-7 animals per group). Statistical significance is represented as *n.s. non significant (Mann-Whitney U test)*

5.2.3 Chronic liver fibrosis in TWEAK KO mice

To examine the effect of TWEAK on chronic liver fibrosis, TWEAK KO and TWEAK WT mice were treated weekly with CCl_4 for 4 weeks. The weight of TWEAK KO mice did not differ compared to TWEAK WT mice throughout the period of CCl_4 treatment (Figure 5.10 A). Liver injury was similar in TWEAK KO mice compared to TWEAK WT mice as indicated by ALT activity (p=0.944; Figure 5.10 B). Histological examination demonstrated foci of centrilobular necrosis and inflammation in both TWEAK KO and WT mice (Figure 5.10 C). Necrosis was detected between the central veins and the hepatocytes around the portal tracts were unaffected. Fewer foci of mineralisation related to dead cells were present in TWEAK KO mice compared to TWEAK WT mice (Figure 5.10 D).

Following chronic CCl_4 treatment TWEAK KO mice had a diminished induction of *Mmp2* expression compared to injured WT controls ($p<0.01$; Figure 5.11 D). The expression of *Acta2, Col1a1, Tgfb1, Mmp9* and *Timp1* remained unchanged between CCl_4-treated TWEAK KO and WT mice (Figure 5.11 A-C,E,F). Nevertheless, TWEAK KO mice exhibited fewer α-SMA-positive HSCs/LMFs and reduced areas of Sirius red staining in the liver compared to WT control animals (Figure 5.12 A,C). This was confirmed by image analysis which revealed significantly fewer HSCs/LMFs (α-SMA staining; $p<0.005$) and collagen deposition (Sirius red staining; $p<0.005$) compared to TWEAK WT mice (Figure 5.12 B,D).

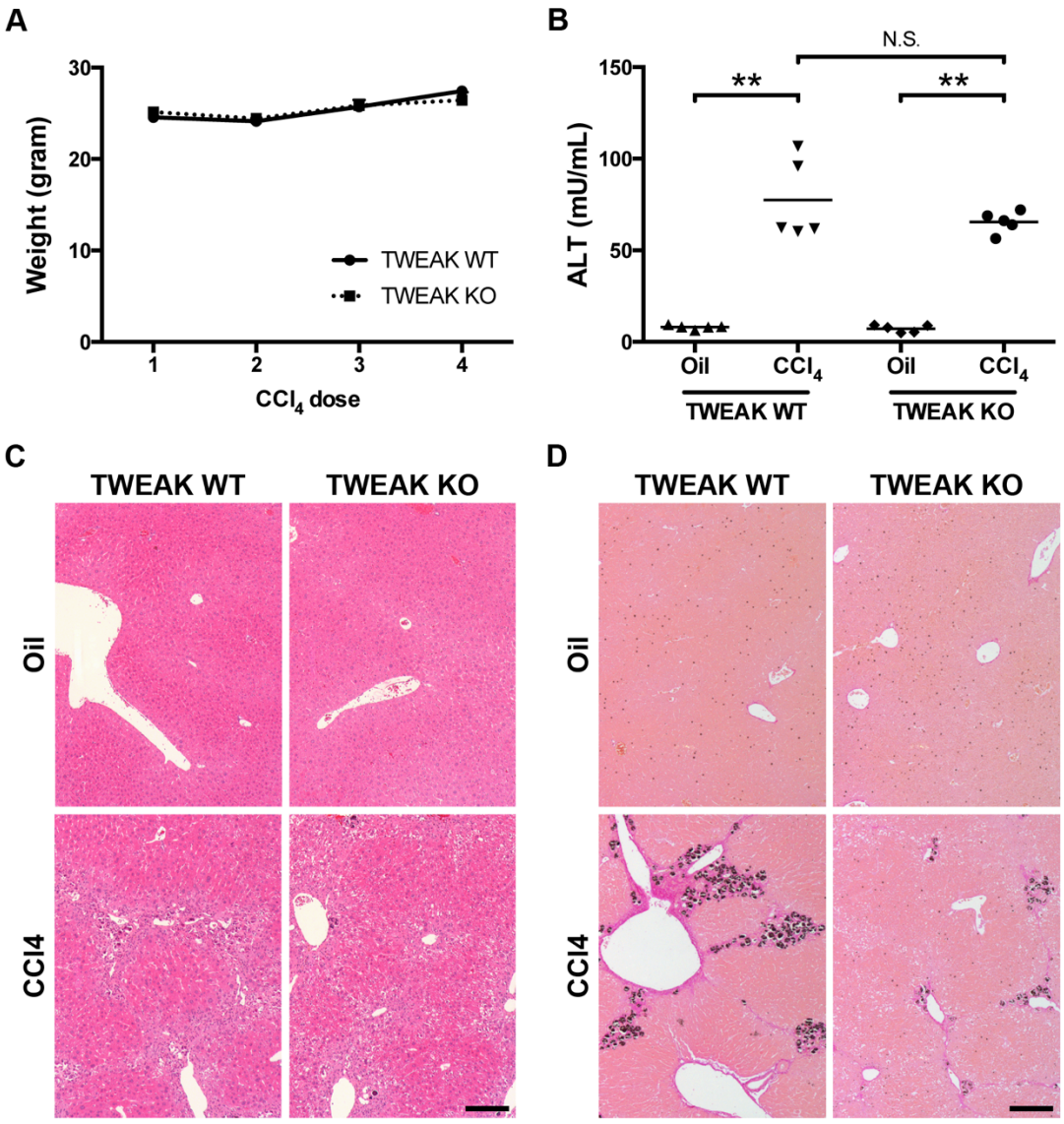

Figure 5.10 Chronic liver injury is similar in TWEAK KO and WT mice
To induce chronic liver injury TWEAK KO and WT mice received one oral dose of CCl_4 or mineral oil per week (4 doses in total) and were sacrificed 72 hours after the final dose. Each mouse was weight before every dose and the volume of CCl_4 was adjusted accordingly (1 mL/kg body weight) **(A)**. Serum ALT activity was assessed as a measure of acute liver injury **(B)** and representative images of haematoxylin-eosin staining **(C)** and von Kossa (used to detect mineralisation) staining **(D)** of paraffin-embedded liver tissue sections are shown (n=5-7 animals each per group). (***$p<0.01$* or *n.s. non significant Mann-Whitney U test*) Bar, 200 µm

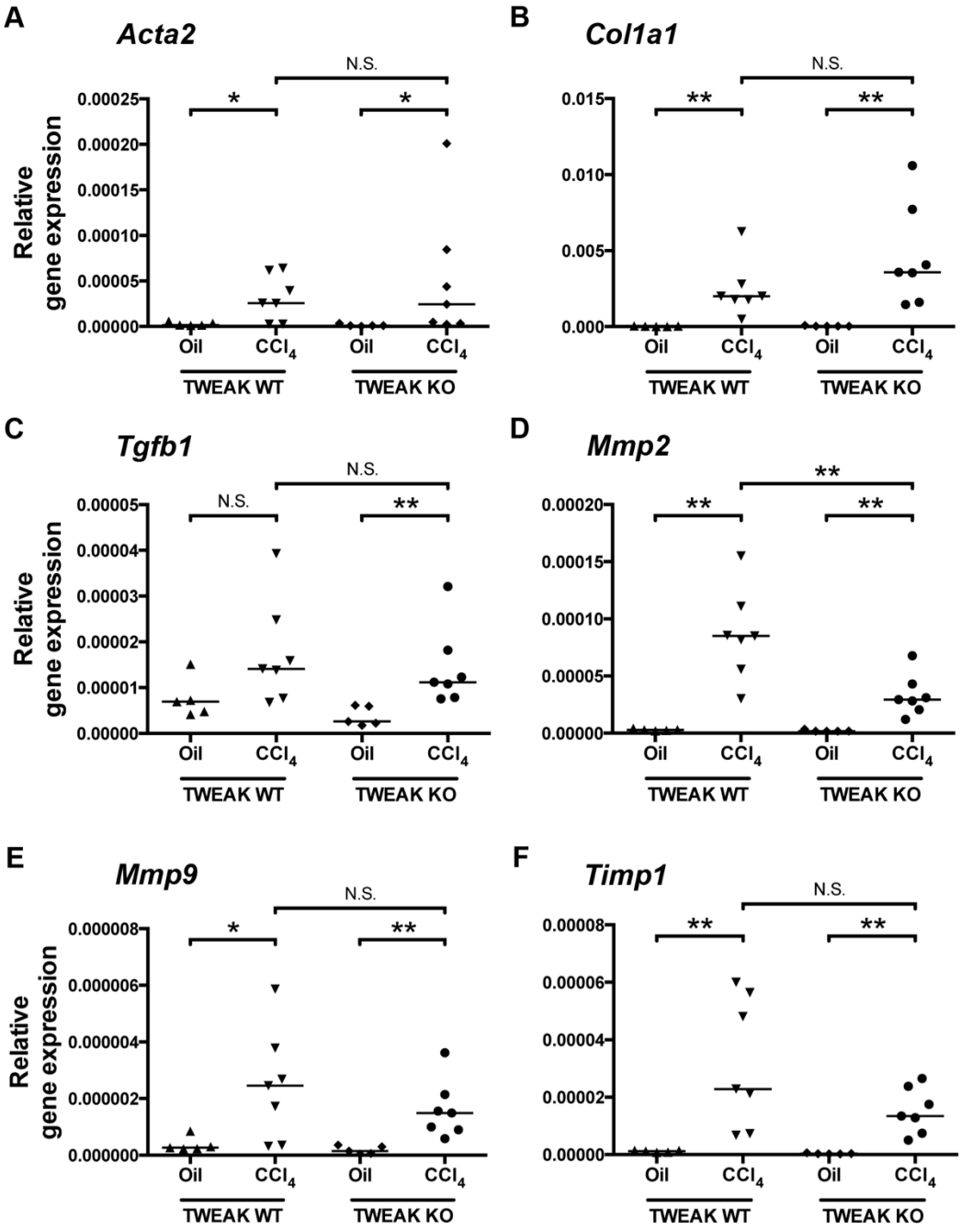

Figure 5.11 TWEAK KO mice have less *Mmp2* after chronic CCl_4 treatment than TWEAK WT mice

TWEAK KO and WT mice were dosed with CCl_4 once a week for four weeks then sacrificed three days after the final dose. Mice treated with mineral oil were used as a control. Levels of fibrosis-associated transcripts were analysed by qPCR **(A-F)**. Gene expression is shown relative to *Rn18s* using the $2^{-\Delta Ct}$ method (n=5-7 animals each per group) (**p<0.05*, ***p<0.01* or *n.s. non significant*, *Mann-Whitney U test*).

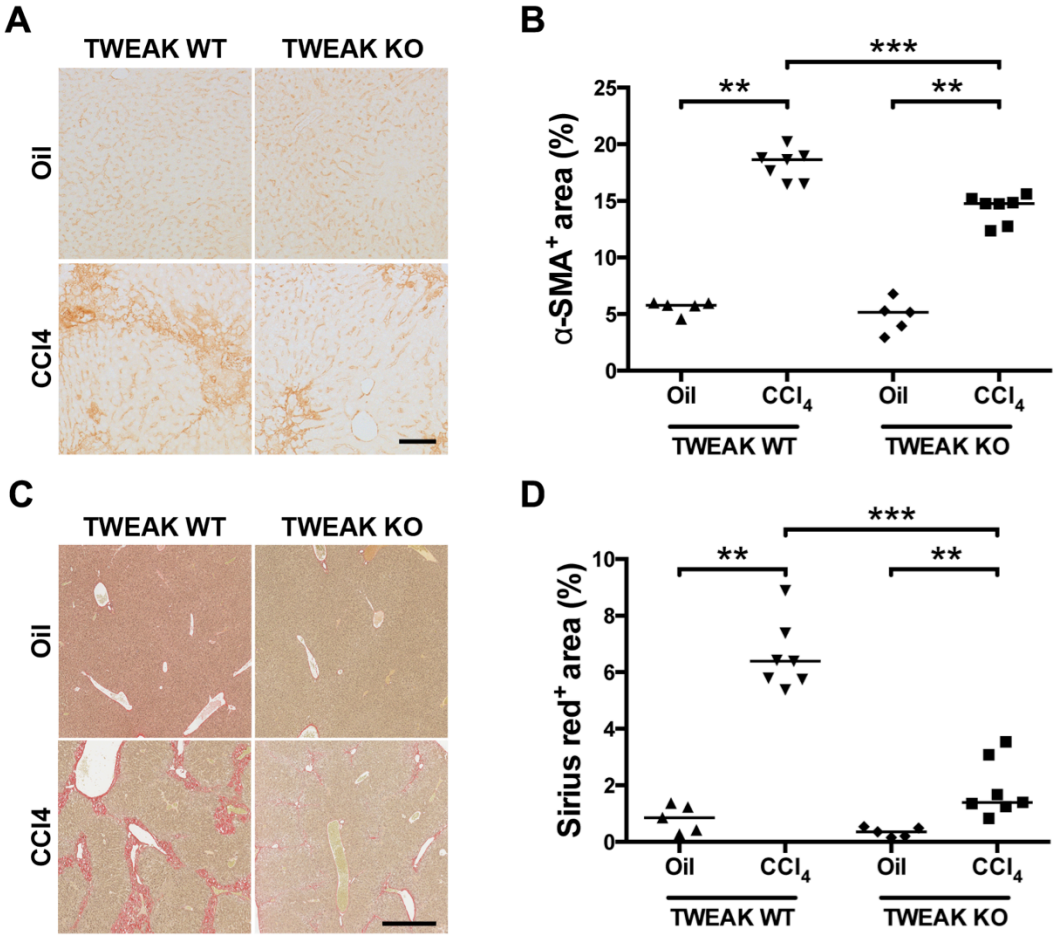

Figure 5.12 TWEAK KO mice present with reduced fibrosis upon chronic CCl_4 treatment

TWEAK KO and WT mice were dosed with CCl_4 once a week for four weeks then sacrificed three days after the final dose. Mice treated with mineral oil were used as a control. Representative images of α-SMA staining (Scale bar 100 μm) **(A)** and digital quantification of α-SMA expressed as the percentage area of ten randomly selected areas per sample **(B)**. Representative images of Sirius red (Scale bar 600 μm) **(C)** with digital quantification of sirius red positive areas of one whole liver section **(D)** (n=5-7 animals each per group). (***p<0.01* or ****p<0.005*, *Mann-Whitney U test*).

5.2.4 Chronic liver fibrosis in Fn14 KO mice

As Fn14 is the most commonly described receptor for TWEAK we also investigated the effect of Fn14 KO in the CCl_4 model of chronic fibrosis. Fn14 KO and WT mice had similar weights throughout the experimental period (Figure 5.13 A). In addition, ALT activity was the same in Fn14 KO mice compared to Fn14 WT mice (p=0.286; Figure 5.13 B). Histological examination demonstrated foci of centrilobular necrosis and inflammation in Fn14 KO and WT mice (Figure 5.13 C), similar to that observed for TWEAK KO and WT mice. Most fibrogenic mediators were significantly upregulated in Fn14 KO and WT mice treated with CCl_4 compared to mineral oil (Figure 5.14). *Acta2* was the only factor that was not significantly higher in injured Fn14 WT compared to mineral oil (p=0.073; Figure 5.14 A). Importantly, levels of all fibrogenic mediators did not differ significantly in Fn14 KO mice compared to Fn14 WT mice (Figure 5.14).

Assessing levels of α-SMA and Sirius red staining showed a significant increase in injured Fn14 WT mice compared to mineral oil (Figure 5.15). Fn14 KO mice treated with CCl_4 also demonstrated more staining of α-SMA and Sirius red compared to Fn14 KO mice treated with mineral oil. However, Fn14 KO mice compared to Fn14 WT mice demonstrated no significant reduction of α-SMA protein levels (p=0.412) or Sirius red staining (p=0.738) after chronic CCl_4 treatment (Figure 5.15).

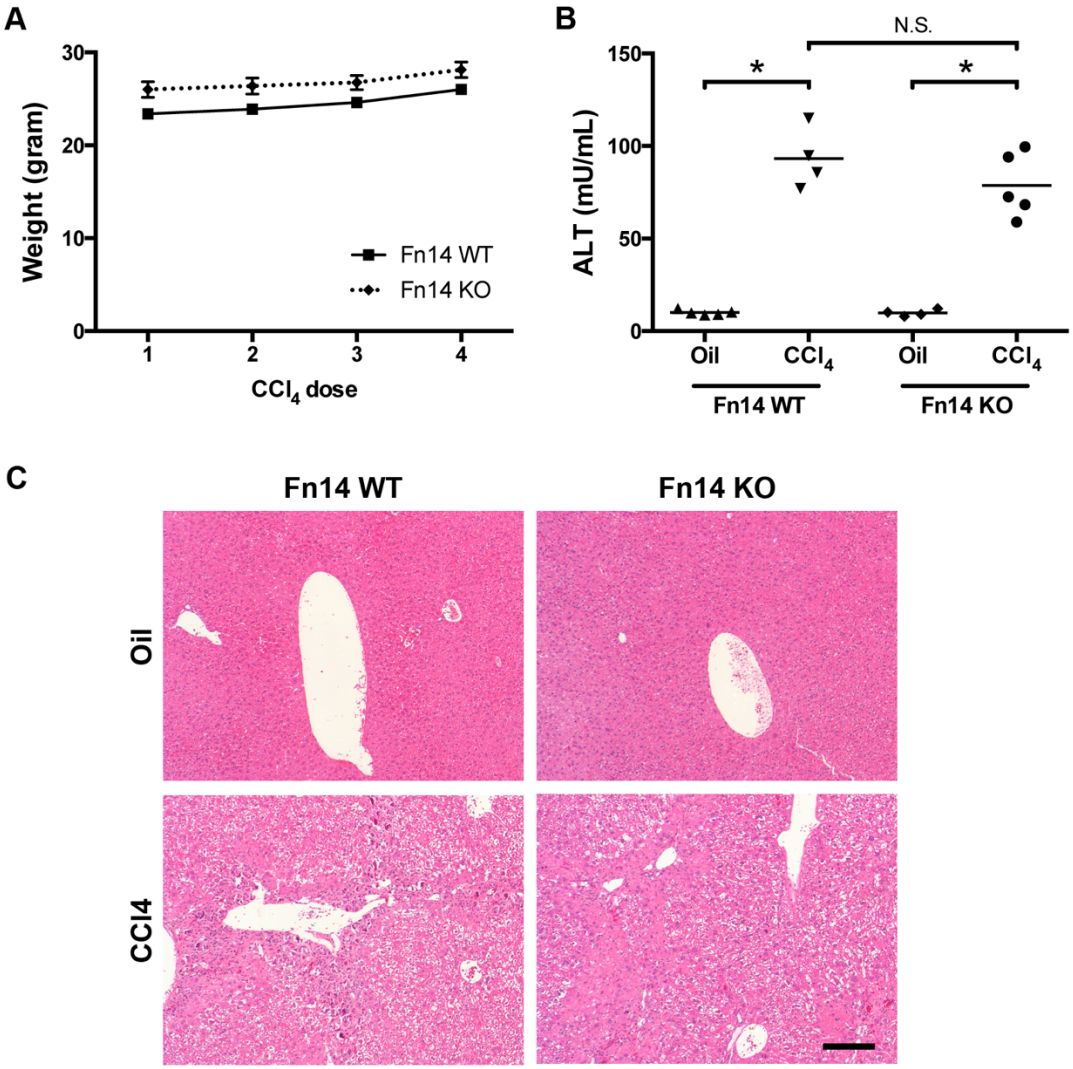

Figure 5.13 Fn14 KO and WT mice exhibit similar levels of chronic liver injury induced by CCl_4

Chronic liver injury was induced in Balb/c Fn14 KO and WT mice with one oral dose of CCl_4 or mineral oil per week (4 doses in total) and mice were sacrificed 72 hours after the final dose. Each mouse was weight before every dose and the volume of CCl_4 was adjusted accordingly (1 mL/kg body weight) **(A)**. Serum ALT activity was assessed as a measure of liver injury **(B)**. Representative images of haematoxylin-eosin staining of paraffin-embedded liver tissue sections **(C)** (n=4-7 animals each per group). (**p<0.05* or *n.s. non significant*, *Mann-Whitney U test*) Bar, 200 µm

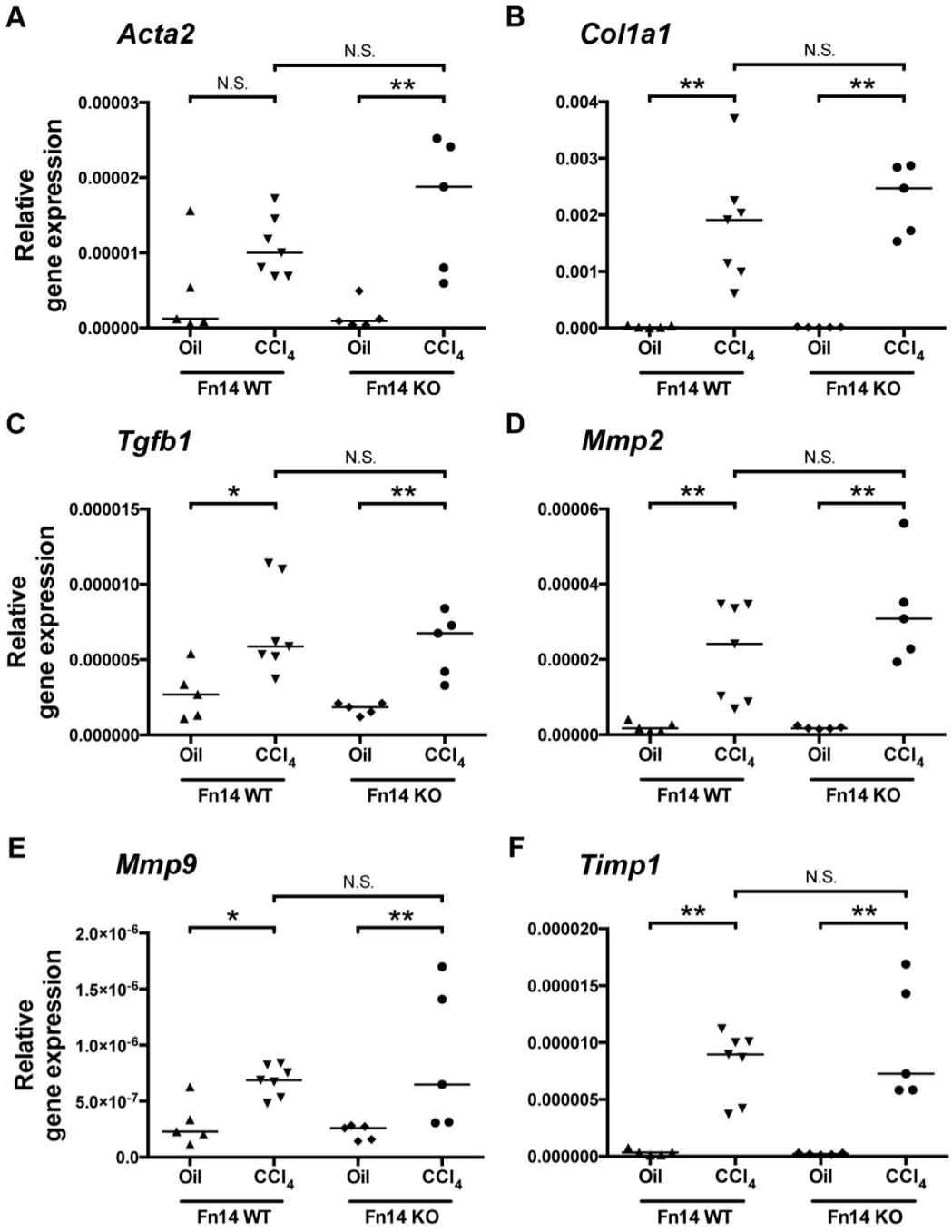

Figure 5.14 Fn14 KO mice did not demonstrate a reduction in fibrogenic marker following chronic liver injury

Fn14 KO and WT mice were dosed with CCl_4 once a week for four weeks then sacrificed three days after the final dose. Mice treated with mineral oil were used as a control. Levels of fibrosis-associated transcripts were analysed by qPCR **(A-F)**. Gene expression is shown relative to *Rn18s* using the $2^{-\Delta Ct}$ method (n=5-7 animals each per group). (**p<0.05*, ***p<0.01* or *n.s. non significant*, *Mann-Whitney U test*).

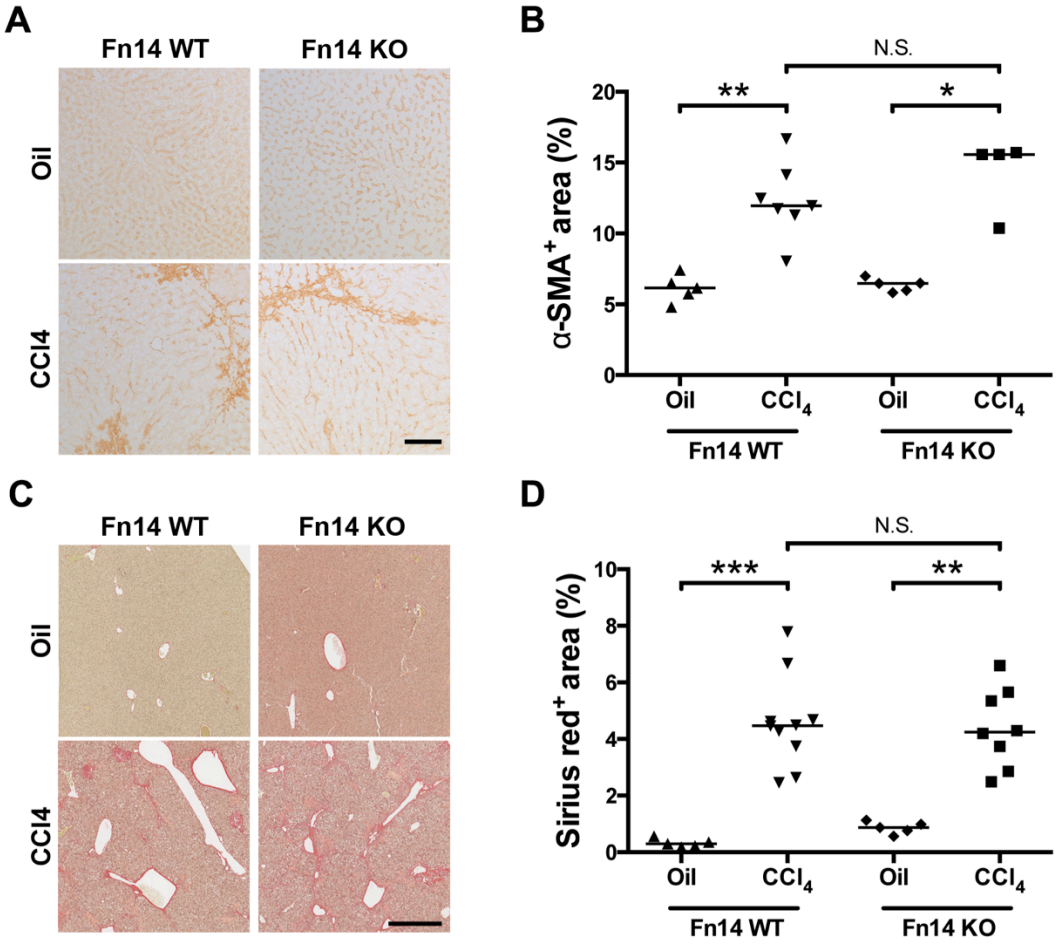

Figure 5.15 Genetic deletion of Fn14 does not ameliorate chronic CCl_4-induced liver fibrosis

Fn14 KO and WT mice were dosed with CCl_4 once a week for four weeks then sacrificed three days after the final dose. Mice treated with mineral oil were used as a control. Representative images of α-SMA stained liver tissue sections (Scale bar 100 μm) **(A)** and digital quantification of α-SMA expressed as the percentage area of ten randomly selected areas per sample **(B)**. Representative images of Sirius red (Scale bar 600 μm) **(C)** with digital quantification of Sirius red positive area of one whole liver section **(D)** (n=5-7 animals each per group). (**p<0.05, **p<0.01, ***p<0.005* or *n.s. non significant*, *Mann-Whitney U test*).

5.3 Discussion

Fibrosis is a common pathological process in most liver diseases. Insights into the role of TWEAK and Fn14 in liver fibrosis have arisen from experimental models of ductular reaction and liver regeneration (Kuramitsu et al., 2013; Tirnitz-Parker et al., 2010). However, the effect of TWEAK and Fn14 has never been directly investigated in a liver injury model primarily associated with fibrosis. This chapter provides a novel approach by treating TWEAK and Fn14 KO mice with the fibrogenic stimulus CCl_4 in both acute and chronic settings. Fibrogenesis involves upregulation of pro-fibrogenic factors such as TGF-β and accumulation of myofibroblasts and ECM. In addition, chronic fibrosis is maintained by increased synthesis of TIMP-1 and decreased production of fibrolytic MMPs (Popov and Schuppan, 2009). Here, I demonstrate the role of TWEAK as a novel stimulator of liver fibrogenesis *in vivo* as evidenced by reduced fibrosis in TWEAK KO animals subjected to acute and chronic CCl_4 injury models. Furthermore, our data suggests that the fibrogenic effect of TWEAK may not exclusively be regulated through Fn14 as Fn14 KO mice had similar levels of fibrosis compared to their WT controls.

Acute CCl_4-liver injury caused a considerable degree of hepatocellular necrosis that was accompanied by early fibrotic changes demonstrated by increased *Acta2* and *Col1a1* expression. Fn14 mRNA peaked as early as 24 hours and was maintained at high levels until 96 hours whereas *Acta2* was elevated the most at 48 and 72 hours after CCl_4 administration. A similar pattern was described in chapter 4, where Fn14 was expressed before α-SMA during HSC activation *in vitro*. Significantly higher levels of Fn14 mRNA were also observed in a chronic model of CCl_4-liver injury. However, this was not in accordance with a study by Affò *et al.* who demonstrated no significant

increase in Fn14 mRNA after chronic CCl_4 injury (Affò et al., 2012). In the study by Affò *et al.* CCl_4 was administered via intraperitoneal injections twice weekly whereas in our study the mice received CCl_4 via oral gavage once a week. Administration of CCl_4 directly into the stomach of mice rather than the abdomen might have caused greater intestinal permeability and hence allowed more translocation of gut microbiota to the liver. This might have led to more HSC activation and therefore more Fn14 expressing cells (Seki et al., 2007; Rivera et al., 2007) or factors from the gut microbiota such as the bacterial component CpG-DNA might have caused have caused an upregulation of Fn14 (Dohi et al., 2009). Furthermore, my data demonstrated that TWEAK mRNA did not change significantly throughout acute or chronic CCl_4 injury. These results were similar to previously published data in mice on the CDE-diet (Tirnitz-Parker et al., 2010).

As Fn14 mRNA was significantly upregulated following acute and chronic toxic liver damage it was surprising that Fn14 KO mice displayed no difference in fibrogenic mediators compared to their Fn14 WT controls after 72 hours or 4 weeks of CCl_4-induced injury. Previously, Fn14 KO mice on the CDE-diet showed a reduction in collagen deposition after 14 days compared to WT mice which correlated with the LPC response (Tirnitz-Parker et al., 2010). Therefore, lower collagen levels might be linked to fewer ductular reactions in Fn14 KO mice. However, it also needs to be considered that the same study demonstrated no significant difference in fibrosis and ductular reaction after 21 days on the CDE-diet between Fn14 KO and WT mice (Tirnitz-Parker et al., 2010). This demonstrates that both fibrogenesis and ductular expansion are possible in the absence of Fn14, which is in accordance with my data. Furthermore my data demonstrated a significant upregulation of some fibrogenic

mediators including *Acta2*, *Tgfb1* and *Mmp9* in Fn14 WT mice after acute CCl_4-injury compared to mineral oil control, which was not observed in Fn14 KO mice. This suggests that Fn14 might have a weak influence on fibrogenesis after acute injury. Furthermore, it might be possible that Fn14 signalling has more influence at a different time point for example at 24 hours post-CCl_4 injury as it is expressed at considerably higher levels. Also quantification of α-SMA, TGF-β1 and MMP-9 protein levels would be useful as a significant difference might be observed at the protein expression but not mRNA levels.

Although genetic interruption of Fn14 did not affect fibrosis my data showed that TWEAK KO mice developed significantly less fibrosis following both acute and chronic CCl_4 injury. This was demonstrated by significant reduction in fibrogenic mediators after acute injury and less collagen deposition and myofibroblast accumulation after chronic injury suggesting that TWEAK might also signal through alternative receptor(s) other than Fn14. CD163 a scavenger receptor that is restricted to the monocyte/macrophage lineage has been reported to interact with TWEAK (Bover et al., 2007). It is upregulated during inflammatory conditions to enhance hemoglobin clearance and heme degradation (Gordon, 2001). Furthermore, CD163 may be involved in the host defense by modulating the release of cytokines by macrophages (Fabriek et al., 2005). In the liver, CD163 expression has been described as a marker of fibrosis (Kazankov et al., 2014) that can be upregulated on monocytes by LMFs *in vitro* (Zhang et al., 2014). The interaction between TWEAK and CD163 leads to internalization of CD163-TWEAK complexes by macrophages (Moreno et al., 2009) thus possibly preventing CD163 from inducing removal and metabolism of the oxidant hemoglobin (Kristiansen et al., 2001) and the release of anti-inflammatory

metabolites (Otterbein et al., 2003). Furthermore, measuring sTWEAK and CD163 in serum of patients with type 1 diabetes mellitus or peripheral arterial disease has shown a close correlation between high CD163 and low TWEAK levels indicating a possible co-regulation of those two molecules (Llaurado et al., 2012; Urbonaviciene et al., 2011). Therefore the presence of TWEAK might block interaction with CD163 and its ligands in the liver leading to a pro-inflammatory and pro-fibrotic environment. However, it needs to be considered that the interaction between TWEAK and CD163 is still poorly understood and not confirmed (Fick et al., 2012).

In conclusion, our findings suggest that TWEAK can regulate the fibrogenic response in a manner that may be at least in part independent of Fn14 in an acute and chronic model of CCl_4 liver injury. Although Fn14 is significantly upregulated during liver injury, it had little effect on fibrogenesis. Therefore, targeting TWEAK in preference to Fn14 could be an effective way in altering fibrogenesis during liver injury. As TWEAK seems to be an important mediator in liver disease, the next chapter will evaluate the expression of sTWEAK in chronic liver disease and its potential prognostic impact.

Chapter 6

Soluble TWEAK levels in serum samples from patients with PSC

6.1 Introduction

In the previous chapters I have examined the expression and role of TWEAK and Fn14 in association with fibrosis in acute and chronic liver disease. Now I move on to consider sTWEAK serum levels as a clinical marker of chronic liver disease with a focus on PSC. Other chronic liver diseases would also be of interest for this study and should be investigated in the future however serum samples from patients with PSC were readily available. PSC is a chronic, progressive liver disease characterised by ongoing inflammation, fibrosis of the intrahepatic and/or extrahepatic bile ducts and stricture formation of the biliary tree. The prevalence of PSC in Northern Europe and North America is approximately 6 to 16 cases per 100,000 people (Eaton et al., 2013). The pathogenesis of PSC is unknown but research so far suggests that PSC is an immune-mediated disease and that it can occur in individuals with a genetic predisposition. The majority (60-80%) of patients with PSC in northern Europe have IBD (Hirschfield et al., 2013). PSC is initially asymptomatic but after patients develop symptoms, over 50% will require liver transplantation caused by biliary cirrhosis, biliary obstruction and hepatobiliary malignant disease (Hirschfield et al., 2013). It is the fifth leading cause for liver transplantation in the USA and the leading cause in some Scandinavian countries (Bjøro et al., 2006).

As not all patients can be transplanted due to shortage of donor livers, prioritisation of patients is critical. In 2008, the UK Liver Transplant Units developed the United Kingdom model for End-stage Liver Disease (UKELD) score as a method for selecting patients with cirrhosis requiring liver transplantation (Barber et al., 2007; Neuberger et al., 2008). The UKELD score is based on four readily available laboratory tests: serum total bilirubin, INR of the prothrombin time, serum creatinine

and serum sodium levels. A minimum UKELD score of 49 is used to put patients on the transplant list. A UKELD score greater than 49 predicts a 1-year mortality of 9% or more without liver transplantation (Neuberger et al., 2008). However, the components used to calculate the UKELD score can be influenced by factors other than the underlying severity of liver disease. Creatinine for example might be influenced by reduced production by the liver, increased tubular secretion or muscle wasting as it is proportional to muscle mass (Sherman et al., 2003; Cholongitas et al., 2007). Furthermore, serum bilirubin levels are often normal in patients with PSC and are only increased when patients have significant biliary obstruction (Eaton et al., 2013). The UKELD scoring system might therefore exclude some PSC patients for liver transplantation despite severe liver disease compared to other chronic liver conditions. In some cases the only biochemical abnormality detectable is elevated levels of serum alkaline phosphatase (ALP) in patients with PSC. High ALP levels are most commonly detected in PSC patients but values can vary throughout the disease in a single individual, and a small number of patients may have normal levels (Stanich et al., 2011). Currently, alternative prognostic tools in PSC are lacking and the identification of patients with a poorer long-term outlook is of critical interest to practicing clinicians, particularly to highlight those in need of novel therapy.

Soluble TWEAK levels can then be measured in blood or urine samples and high levels of sTWEAK have been related to autoimmune diseases such as rheumatoid arthritis and lupus nephritis (Park et al., 2008; Schwartz et al., 2009). Soluble TWEAK levels were also predictive of disease progression in patients with systemic lupus erythematosus and advanced non-ischemic heart failure (Schwartz et al., 2009; Richter et al., 2010).

In this thesis, I have so far demonstrated that TWEAK and Fn14 expression are elevated in liver tissue of patients with chronic liver diseases including PSC, and I have also shown that hepatic expression levels of TWEAK and Fn14 correlated with fibrosis. Thus, we hypothesised that serum levels of sTWEAK may also be altered during liver disease. Therefore, this chapter investigates the expression of sTWEAK in patients with PSC and its prognostic abilities of disease outcome.

6.2 Results

6.2.1 Soluble TWEAK levels are low in patients with PSC

To investigate sTWEAK levels in a chronic liver disease setting, serum samples were acquired from 64 patients with PSC, 24 patients with IBD with no evidence of concurrent PSC and from 22 healthy individuals. A summary of the general characteristics is shown in Table 6.1. Patients with PSC had a median age of 36 years, IBD patients had a median age of 35 years and healthy controls of 34 years at the time of the blood sample. Most PSC patients were diagnosed with IBD (n=51, 79.6%). Immunosuppressive medication was taken by 25 (39.1%) PSC patients and 9 (37.5%) IBD patients.

Soluble TWEAK serum levels as measured by a commercially available ELISA were significantly lower in PSC patients compared to healthy controls ($p<0.01$) and IBD patients ($p<0.0001$; Figure 6.1 A). The median levels of sTWEAK in patients with PSC were 275 pg/mL (Interquartile range; IQR 111-410), in the healthy control group 942 pg/mL (IQR 885-1044) and in patients with IBD 1130 pg/mL (IQR 959-1429). Stratifying by disease severity, PSC patients with cirrhosis demonstrated significantly lower sTWEAK levels than those with pre-cirrhosis [189 pg/mL (IQR 67-299) *versus* 632 pg/mL (IQR 391-862), respectively; $p< 0.001$; Figure 6.1 B].

Soluble TWEAK levels in patients with PSC were then compared to demographic and clinical data (Table 6.2 and Table 6.3). A significant positive correlation between sTWEAK and albumin was detected (*Spearman* $\rho=0.252$ $p<0.05$; Table 6.2). The median of albumin concentration in the investigated PSC patients was 42 g/L (IQR 37-45), which is still in the normal range. No other tested variables such as age, colitis or immunosuppression demonstrated an association with sTWEAK levels (Table 6.2 and Table 6.3).

	Controls	IBD	PSC
Number of patients	22	24	64
Gender, male (%)	12 (54.5)	12 (50.0)	40 (62.5)
Age, years	34 (28-37)	35 (25-55)	36 (26-57)
Immunosuppression:			
Steroids (%)	N/A	5 (20.8)	3 (4.7)
Azathioprine (%)	N/A	4 (16.7)	5 (7.8)
Steroids+Azathioprine (%)	N/A	0 (0.0)	7 (10.9)
Steroids+MMF (%)	N/A	0 (0.0)	10 (15.6)
None (%)	N/A	14 (58.3)	39 (60.9)

Table 6.1 Characteristics of healthy individuals and patients with IBD and PSC

Abbreviation: MMF=Mycophenolate mofetil

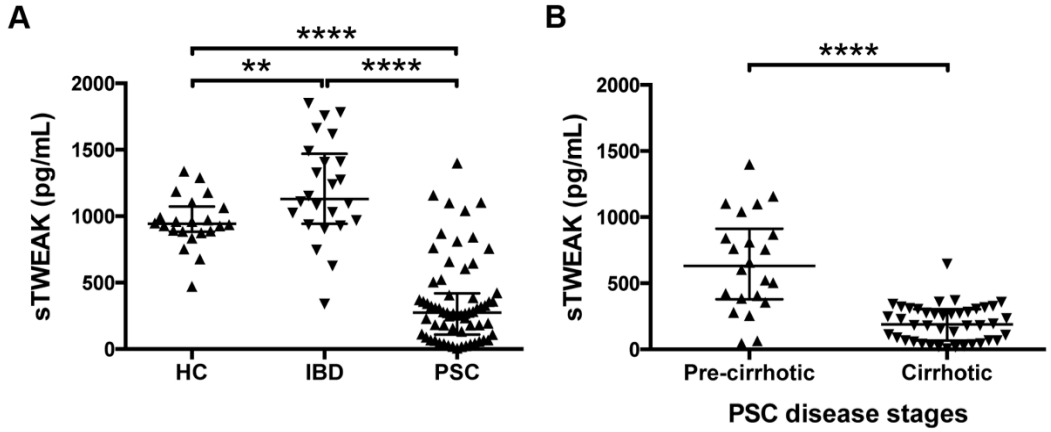

Figure 6.1 Soluble TWEAK levels in serum samples from healthy controls, IBD and PSC patients

Soluble TWEAK levels were measured by ELISA of serum samples from healthy controls (HC, n=22) and patients with IBD (n=24) or with PSC (n=64) **(A)**. sTWEAK levels stratified by PSC disease stages of pre-cirrhotic (n=22) and cirrhotic (n=42) **(B)**. (*** p<0.01, **** p<0.0001; Mann-Whitney U test*). The distribution of values was significantly different across the whole population (*p<0.0001* (A only) *Kruskal-Wallis test*).

Covariate	RHO	*p* value
Age, years	-0.124	0.329
Laboratory findings*:		
AST (iU/L)	-0.107	0.403
ALP (ratio to ULN)	-0.243	0.053
ALT (iU/L)	-0.021	0.885
Albumin (g/L)	**0.252**	**0.045**
Bilirubin (µmol/L)	-0.241	0.055
Platelet count (x10^9/L)	0.058	0.653
Na+(mmol/L)	-0.106	0.406
Creatinine (µmol/L)	0.193	0.126
IgG (g/L)	0.018	0.895
UKELD	-0.119	0.359

Table 6.2 Continuous variables correlating with sTWEAK levels

Abbreviations: UKELD=United Kingdom model for end-stage liver disease. Numbers in bold represent significant *p* values at the $p<0.05$ level (*Spearman correlation*). *At time of taking sample

Characteristics	Median sTWEAK concentration, ng/mL (IQR)		
	Yes	**No**	***p* value**
Gender, male	278 (83-362)	267 (162-540)	0.549
Colitis	304 (110-564)	253 (133-280)	0.239
Active colitis	248 (83-409)	278 (127-410)	0.715
Laboratory findings*:			
INR above normal, ≥1.2	248 (67-314)	290 (129-493)	0.121
UKELD ≥ 49	268 (138-319)	277 (98-625)	0.372
Medication:			
UDCA	268 (110-464)	280 (133-358)	0.987
Immunosuppression	358 (234-522)	248 (98-331)	0.067
Antibiotics**	260 (129-309)	278 (114-518)	0.356

Table 6.3 Factors associated with sTWEAK levels

Abbreviations: IQR= interquartile range, INR=international normalised ratio, UKELD=United Kingdom model for end-stage liver disease, UDCA= Ursodeoxycholic acid. *At time of taking sample ** if taken in the past 3 month (*Mann-Whitney U test*)

6.2.2 Low sTWEAK levels are a predictor of adverse prognosis in patients with PSC

As sTWEAK levels were closely related to a more advanced disease stage in our patient cohort, the predictive value of sTWEAK levels for transplant-free survival was investigated. First, AUROC curve analysis was performed to identify optimal serum sTWEAK levels for potential prediction of outcome (Figure 6.2). The AUROC curve analysis revealed an optimal cut-off level of 330 pg/mL with a sensitivity of 86% and specificity of 56%. The area under the curve was 0.754 (p=0.001). By using the optimal cut-off threshold PSC patients were separated into two groups (low sTWEAK, ≤330 pg/mL; high sTWEAK, >330 pg/mL; Table 6.4). No significant differences were detected between the low and high sTWEAK groups and most clinical factors. However, as expected significantly more patients with cirrhosis were in the low sTWEAK group compared to the high sTWEAK group (90 vs. 26%, respectively, p<0.001). In addition, patients in the low sTWEAK group had significantly higher ALP ratios compared to patients in the high soluble TWEAK group [2.1 (IQR 1.1-3.6) vs. 1.0 (IQR 0.7-2.3) ALP ratio to upper limit of normal (ULN), respectively, p<0.05]. Bilirubin levels were also significantly higher in the low sTWEAK group [28 (IQR 14-53) vs. 12 (IQR 9-34) µmol/L, respectively, p<0.05]. The group with high sTWEAK levels had significantly more patients on immunosuppression compared to the low sTWEAK group (57% vs. 29%, respectively, p<0.05).

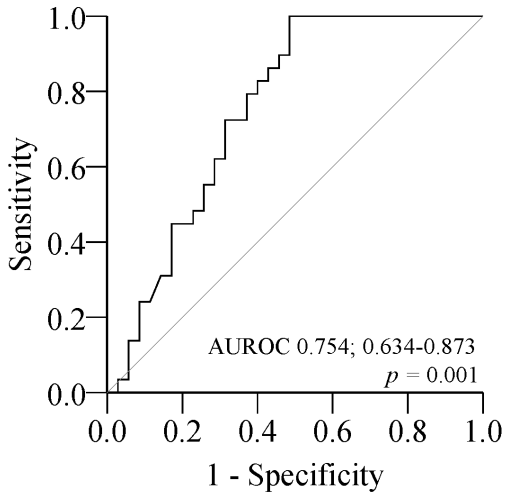

Figure 6.2 Accuracy of sTWEAK at predicting transplant-free survival of PSC patients

Area under the receiver operator characteristic (AUROC) curve analysis was performed to determine the optimal cut-off level of sTWEAK (330 ng/mL) as a predictor of liver transplant/death in PSC patients (n=64).

	≤330 pg/mL	>330 pg/mL	*p* value
Number of patients (%)	41 (64)	23 (36)	N/A
Gender, male (%)	27 (66)	13 (57)	0.592
Age, years	36 (27-57)	40 (24-57)	0.370
Cirrhosis (%)	**37 (90)**	**6 (26)**	**< 0.001**
No. with colitis (%)	31 (76)	20 (87)	0.346
Colitis, active (%)	8 (20)	4 (17)	1.000
Laboratory findings*:			
AST (iU/L)	74 (56-110)	80 (34-112)	0.580
ALP (ratio to ULN)	**2.1 (1.1-3.6)**	**1.0 (0.7-2.3)**	**0.030**
ALT (iU/L)	70 (44-113)	103 (35-156)	0.780
Albumin (g/L)	41 (37-44)	43 (40-45)	0.220
Bilirubin (µmol/L)	**28 (14-53)**	**12 (9-34)**	**0.030**
Platelet count (x10^9/L)	187 (110-298)	245 (168-310)	0.380
INR above normal, ≥1.2 (%)	19 (46)	4 (17)	0.055
Na+(mmol/L)	141 (139-144)	141 (140-142)	0.522
Creatinine (µmol/L)	68 (59-77)	71 (66-84)	0.145
IgG (g/L)	17 (13-20)	14 (13-20)	0.710
UKELD (continuous)	48 (46-52)	46 (44-51)	0.160
UKELD ≥ 49 (%)	19 (46)	6 (26)	0.275
Medication:			
UDCA (%)	33 (81)	18 (78)	1.000
Immunosuppression (%)	**12 (29)**	**13 (57)**	**0.038**
Antibiotics (%)**	9 (22)	1 (4)	0.081

Table 6.4 Characteristics of PSC patients in relation to low and high sTWEAK levels

PSC patients were divided into two groups on the basis of high sTWEAK (>330 pg/mL) and low sTWEAK (≤330 pg/mL) levels in serum samples. Data is expressed as median (interquartile range). Numbers in bold represent significant *p* values at the $p<0.05$ level. Abbreviations: INR=international normalised ratio, UKELD=United Kingdom model for end-stage liver disease, UDCA= Ursodeoxycholic acid. *At time of taking sample ** if taken in the past 3 month (for continuous variables *Mann-Whitney U test* otherwise *Fisher's exact test*)

During the follow up period of 29 (IQR 8-41) months, 29 (45.3%) patients reached the endpoint. Of those patients 18 (28.1%) were transplanted, 7 (10.9%) died and 4 (6.3%) patients died despite transplantation. Kaplan-Meier survival analysis demonstrated a significant difference in transplant-free survival within a 3-year follow-up interval between the low sTWEAK and high sTWEAK groups (log rank test $p<0.01$, Figure 6.3). Within the low sTWEAK group, 25 out of 41 patients (61%) reached an endpoint whereas only 4 out of 23 patients (17%) of the high sTWEAK group reached an endpoint within the follow up period. On univariate Cox analysis, low sTWEAK levels were a significant predictor of death or transplantation (HR: 4.013, 95% CI 1.395-11.545; $p<0.01$) (Table 6.5). Besides low sTWEAK levels, additional predictors of poor outcome were cirrhosis (HR: 20.830, 95% CI 2.820 – 142.860; $p<0.001$), elevated baseline ALP (HR: 1.136, 95% CI 1.029-1.254; $p=0.011$), hypoalbuminaemia (HR: 1.164, 95% CI 1.092-1.241; $p<0.001$), elevated bilirubin (HR: 1.004, 95% CI 1.002-1.006; $p<0.01$), INR>1.2 (HR: 3.497, 95% CI 1.572-7.819; $p<0.01$), low sodium levels (HR: 1.176, 95% CI 1.054-1.314; $p<0.01$) and immunosuppression (HR: 3.501, 95% CI 1.415-8.662; $p<0.01$). In addition, the UKELD score as continuous variable (HR: 1.172, 95% CI 1.105-1.243; $p<0.001$) and as dichotomous variable (HR: 7.576, 95% CI 3.300-17.241; $p<0.001$) with the clinical cut-off point of 49 was predictive of transplantation/death.

Subsequent multivariate analysis by Cox proportional hazards regression demonstrated that sTWEAK levels below 330 pg/mL remained to be an independent predictor of death or transplantation after adjustment for other significant variables (adjusted HR: 3.628, 95% CI 1.033-12.746; $p=0.044$) (Table 6.6 A). The strong predictive value of sTWEAK was also retained when the UKELD score was included in the multivariate analysis as continuous variable (adjusted HR: 4.124, 95% CI

1.224-13.890, p=0.022, Table 6.6 B) or dichotomous variable with the cut-off point of 49 (adjusted HR: 3.944, 95% CI 1.160-13.407, p=0.028, Table 6.6 C). Other factors such as elevated baseline ALP levels were also predictive of transplantation/death when the UKELD score was included in the multivariate analysis as continuous or dichotomous variable but not when the UKELD score was excluded (Table 6.6). In addition, hypoalbuminaemia was a significant predictor of transplantation/death when the UKELD score was excluded or applied as dichotomous variable but not as continuous variable. Furthermore, low sodium levels were predictive of transplantation/death when UKELD was excluded (Table 6.6 A). As low sodium levels are part of the UKELD formula they were not included in analysis containing UKELD.

Finally, including cirrhosis in the multivariate analysis demonstrated that it is a strong predictor of transplant-free survival (adjusted HR: 16.950, 95% CI 2.290-125.000; p<0.01) in addition to immunosuppression (adjusted HR: 3.770, 95% CI 1.420-10.055; p<0.01) (Table 6.6 D). In contrast, sTWEAK levels were no longer significant.

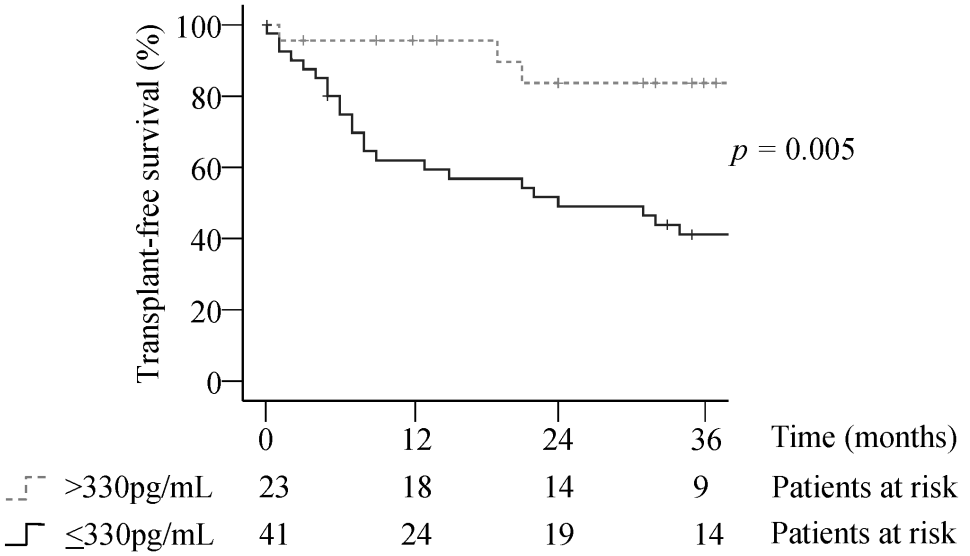

Figure 6.3 Lower sTWEAK levels are associated with poorer transplant-free survival in PSC patients

Kaplan-Meier survivorship estimates for patients with PSC (n=64) having high (>330 pg/mL) and low (≤330 pg/mL) sTWEAK.

	HR (95% CI)	*p* value
Gender, male	1.298 (0.601-2.802)	0.506
Age, years	1.021 (0.998-1.044)	0.168
Colitis	1.926 (0.375-2.288)	0.868
Active colitis	0.922 (0.350-2.430)	0.870
Cirrhosis	**20.830 (2.820 – 142.860)**	**<0.001**
Laboratory findings*:		
AST (iU/L)	1.000 (0.999-1.002)	0.771
ALP (ratio to ULN)	**1.136 (1.029-1.254)**	**0.011**
ALT (iU/L)	1.000 (0.997-1.003)	0.833
Low albumin (g/L)	**1.164 (1.092-1.241)**	**<0.001**
Bilirubin (µmol/L)	**1.004 (1.002-1.006)**	**<0.001**
Low platelets (x10^9/L)	1.001 (0.998-1.004)	0.557
INR above normal/1.2	**3.497 (1.572-7.813)**	**0.002**
Low Na+ (mmol/L)	**1.176 (1.054-1.314)**	**0.004**
Creatinine (µmol/L)	0.989 (0.963-1.015)	0.408
IgG (g/L)	1.011 (0.964-1.060)	0.661
UKELD (continuous)	**1.172 (1.105-1.243)**	**<0.001**
UKELD ≥ 49**	**7.576 (3.300-17.241)**	**<0.001**
Medication:		
UDCA	0.895 (0.339-2.367)	0.824
Immunosuppression	**3.501 (1.415-8.662)**	**0.007**
sTWEAK***	**4.013 (1.395-11.545)**	**0.010**

Table 6.5 Univariate analysis of clinical parameters for the prediction of transplant-free survival in patients with PSC

Numbers in bold represent significant *p* values at the $p<0.05$ level or below. Abbreviations: CI= confidence interval, INR=international normalised ratio, UKELD=United Kingdom model for end-stage liver disease, UDCA= Ursodeoxycholic acid. *At time of taking sample ** clinically used cut-off point *** cut-off at ≤330 pg/mL

	HR (95% CI)	*p* value
A) UKELD excluded		
ALP (ratio to ULN)	n.s.	n.s
Low albumin (g/L)	**1.131 (1.056-1.211)**	**<0.001**
Bilirubin (µmol/L)	n.s.	n.s.
INR above normal/1.2	**3.067 (1.323-7.143)**	**0.009**
Low Na+ (mmol/L)	n.s.	n.s.
Immunosuppression	n.s.	n.s.
sTWEAK*	**3.628 (1.033-12.746)**	**0.044**
B) UKELD included as continuous variable		
ALP (ratio to ULN)	**1.130 (1.007-1.268)**	**0.037**
Low albumin (g/L)	n.s.	n.s.
UKELD	**1.102 (1.003-1.210)**	**0.043**
Immunosuppression	n.s.	n.s.
sTWEAK*	**4.124 (1.224-13.890)**	**0.022**
C) UKELD included as a dichotomous variable		
ALP (ratio to ULN)	**1.134 (1.006-1.279)**	**0.039**
Low albumin (g/L)	**1.106 (1.020-1.199)**	**0.014**
UKELD ≥ 49**	**3.658 (1.342-9.968)**	**0.011**
Immunosuppression	n.s.	n.s.
sTWEAK*	**3.944 (1.160-13.407)**	**0.028**
D) Cirrhosis included		
ALP (ratio to ULN)	n.s.	n.s
Cirrhosis	**16.950 (2.290-125.000)**	**< 0.01**
Immunosuppression	**3.770 (1.420-10.055)**	**< 0.01**
sTWEAK*	n.s.	n.s

Table 6.6 Multivariate analysis of clinical parameters for the prediction of transplant-free survival in patients with PSC

Multivariate analysis using backward stepwise elimination. Numbers in bold represent significant *p* values at the $p<0.05$ level or below. Abbreviations: n.s= not significant CI= confidence interval, INR=international normalised ratio, UKELD=United Kingdom model for end-stage liver disease. * cut-off at ≤330 pg/mL **clinically used cut-off point

6.3 Discussion

This chapter demonstrates that sTWEAK serum levels are altered in patients with PSC and that sTWEAK levels below 330 pg/mL are an independent predictor of transplantation or death. This is the first time that sTWEAK levels have been studied in a cohort of PSC patients.

PSC is characterised by chronic inflammation of the biliary epithelium (Eaton et al., 2013) and significantly higher levels of the pro-inflammatory cytokine TNF-α were detected in the serum of PSC patients (Neuman et al., 2002). In addition, my data in chapter 3 has shown that hepatic expression of TWEAK was more abundant in PSC liver tissue compared to normal donor tissue. Furthermore, I demonstrated in chapter 4 that TWEAK stimulation of activated HSCs *in vitro* enhanced proliferation suggesting a potential pathological role in chronic liver disease. In support of this, I demonstrated a significant reduction of liver fibrosis in TWEAK KO mice in chapter 5. Therefore, it was surprising that not only was sTWEAK significantly reduced in PSC patients compared to healthy controls but was present at even lower levels in PSC patients with cirrhosis than in those without cirrhosis − the opposite of what we had expected. However, this could be potentially very useful in monitoring the progression of cirrhosis, as it is a fast and not very invasive procedure to measure soluble TWEAK levels in serum samples. This would be especially useful as more markers, which could indicate the progression of liver cirrhosis would be required in clinical practice (Lefton et al., 2009).

In agreement with my findings in PSC patients, reduced sTWEAK levels have also been detected in other diseases associated with increased inflammation including chronic heart failure, chronic kidney disease and type 1 diabetes (Chorianopoulos et

al., 2009; Yilmaz et al., 2009; Llaurado et al., 2012). Nevertheless, sTWEAK levels are not consistently decreased in all chronic inflammatory diseases. Research by Park *et al.* has demonstrated significantly higher levels in patients with rheumatoid arthritis (Park et al., 2008), which is consistent with my data from the IBD patients who also had higher levels of sTWEAK than healthy controls.

Why serum sTWEAK levels were reduced in patients with PSC in spite of increased expression in the liver is not known. A possible explanation for lower sTWEAK levels in PSC is that increased Fn14 expression in the liver contributes to enhanced uptake of sTWEAK leading to lower serum sTWEAK concentration. This may lead to increased signalling through Fn14 in the tissue microenvironment thus also inducing more ductular reaction and fibrosis and therefore a more severe liver disease. Correlations between TWEAK or Fn14 expression with the severity of disease have been investigated previously (Affò et al., 2012; Li et al., 2013). A study by Affò *et al.* demonstrated that alcoholic hepatitis patients with higher hepatic Fn14 mRNA expression (and thus possibly lower sTWEAK) had a worse 90-day survival rate than patients with lower Fn14 mRNA levels (Affò et al., 2012). They confirmed that patients with alcoholic hepatitis had lower sTWEAK levels but did not show whether this was predictive of disease outcome. In addition, high hepatic expression levels of Fn14 were also suggested to be a predictor of poorer surgical outcome in patients with HCC (Li et al., 2013). This suggests that whilst sTWEAK levels vary dependent on disease type and severity they may have promise as predictors of survival in several chronic inflammatory diseases. Inclusion of an assessment of hepatic Fn14 expression may add to the predictive power of TWEAK assessment. However, investigating

hepatic Fn14 expression may not be a practical option clinically, as it would require a more invasive biopsy in order to serve as a predictor of disease outcome.

Another explanation for lower sTWEAK levels could be that through some unknown mechanism, sTWEAK levels are reduced in chronic diseases like PSC in an attempt to prevent further tissue damage. A potential way through which sTWEAK is reduced is through CD163, a TWEAK scavenger receptor. CD163-positive inflammatory macrophages and monocytes can bind and internalise sTWEAK leading to low sTWEAK concentrations (Bover et al., 2007; Moreno et al., 2009). Research has shown that patients with liver cirrhosis have significantly higher serum soluble CD163 levels than healthy controls (Holland-Fischer et al., 2011). In addition, high soluble CD163 and low sTWEAK concentrations have been correlated with type 1 diabetes mellitus diagnosis and cardiovascular mortality in peripheral arterial disease (Llaurado et al., 2012; Urbonaviciene et al., 2011). Thus it is possible that low levels of sTWEAK in PSC serum result from increased scavenging by CD163.

Finally, sTWEAK levels might be decreased because membrane-bound TWEAK is not shed from the cell surface of leukocytes in the blood. When measuring sTWEAK in serum samples the cells are removed and therefore membrane-bound TWEAK would be excluded in the measurement. TWEAK is processed by the serine endoprotease, furin inside the cells (Brown et al., 2010). Therefore, decreased furin expression or function might lead to decreased shedding of TWEAK but this would need to be further investigated. Nevertheless, it has been demonstrated that TWEAK can be expressed on the cell surface of monocytes in patients with multiple sclerosis but not in control patients (Desplat-Jégo et al., 2009). However, this did not seem to

affect sTWEAK levels as they were similar between the multiple sclerosis patients and the control group (Desplat-Jégo et al., 2009). Furthermore it is not know yet whether sTWEAK and the membrane-bound form have comparable affinities for the Fn14 or comparable biological activity leading to different biological responses (Brown et al., 2010).

My data has shown that sTWEAK levels in patient serum samples are predictive of transplant-free survival in a multivariate regression model using individual components and even despite including the UKELD score as a variable. PSC patients with low sTWEAK levels were more likely to die or require a transplant. In accordance with this, research by Richter *et al.* also demonstrated that sTWEAK levels in serum samples could be used as a predictive tool of mortality in patients with advanced non-ischemic heart failure (Richter et al., 2010). Using the multivariate regression model my data has demonstrated that serum albumin and INR, when the UKELD score was excluded as a variable, were independently associated with transplant-free survival. Other research has shown that serum albumin improved prediction of waiting list mortality in patients with liver cirrhosis when added to the Model for End-Stage Liver Disease (MELD) used in America (Myers et al., 2013). The prothrombin time expressed as INR is used to assess clotting and is included worldwide in almost all the prognostic models regarding transplantation for liver disease. Considering that patients with liver disease have a more complex coagulopathy and that the method for calibrating the INR calculation is based on serum levels from people with stable anticoagulation, the usefulness of INR seems to be suboptimal (Tripodi et al., 2007). However despite these limitations, INR is still considered a valid measure (Kamath and Kim, 2009).

Including the UKELD score in the multivariate analysis as a continuous or dichotomous variable showed that it is also predictive of patients at risk requiring transplantation. This was expected as the scoring system is currently used to place patients on the transplant list. However using the UKELD score to decide on the urgency of transplantation may not be useful for patients with PSC and other forms of cholestatic liver disease as such patients face unique clinical features that would better reflect the severity of illness for example ascending cholangitis due to biliary strictures (Goldberg et al., 2011). ALP was only significant when UKELD score was applied as continuous or dichotomous variable but not when it was excluded from the calculation. ALP fluctuations are frequent during the clinical course, influenced by a variety of confounding variables (Stanich et al., 2011). Nevertheless, ALP remains to be an important indicator of disease severity and higher ALP correlated with lower sTWEAK levels, which is consistent with the predictive ability of sTWEAK. Furthermore, a larger number of patients in the high sTWEAK group were on immunosuppressant but a benefit of immunosuppressive medication in inhibiting disease progression remains yet to be determined (Hirschfield et al., 2013).

Substituting low albumin levels, low platelet count, high INR, UKELD score, low sodium levels and elevated bilirubin levels for the collective variable termed cirrhosis the multivariate analysis was rerun. In doing so cirrhosis and immunosuppression were the only significant predictors of transplant-free survival. Given the interaction between cirrhosis and sTWEAK it was unsurprising that TWEAK was no longer significant.

Although sTWEAK levels seem to be an independent predictor of transplant-free survival in patients with PSC, it remains to be determined whether the prognostic

values of sTWEAK are disease specific or whether it also applies to other cirrhotic liver diseases such as chronic infections with HCV or HBV and ALD. Further investigating a broad variety of chronic liver diseases could then potentially aid in selecting patients for liver transplantation similarly to how the UKELD score is currently used. In addition, it would be interesting to determine whether sTWEAK levels might increase in certain types of chronic liver diseases compared to others and why that might be. However, so far sTWEAK could serve as a predictive tool in patients with PSC and improve the way patients are allocated on the transplant waiting list. A pragmatic approach could be to adopt sTWEAK measurements as part of the routine diagnostic measurements and possibly include it as a variable of the UKELD scoring system.

In conclusion, lower sTWEAK levels distinguish patients with PSC compared to those with IBD alone and healthy subjects. Moreover, sTWEAK inversely correlates with disease severity and is an excellent predictor of poorer clinical outcome. However, TWEAK has been shown to be involved in liver disease processes and therefore most probably functions as a pathogenic cytokine rather than purely a biomarker in patients with PSC.

Chapter 7

Overview and final remarks

7.1 Overview and general discussion

Fibrosis is normally a highly regulated and protective response to tissue injury. Numerous pathways and molecules contribute to determine whether this process remains homeostatic or whether it is uncontrolled and excessive (Pellicoro et al., 2014).

In vivo studies demonstrated that a limited degree of liver fibrosis can be beneficial as it leads to greater resistance to further acute injury and offers protection to hepatocytes against various toxic stimuli (Bourbonnais et al., 2012). However, in response to chronic liver inflammation the fibrotic response becomes uncontrolled leading to the progressive replacement of functional hepatic tissue, which can potentially progress to cirrhosis and/or hepatocellular carcinoma. The burden of chronic liver disease is increasing in the UK and worldwide (Ellis and Mann, 2012). Therefore it is important to discover safe therapies that can control fibrogenesis. As our understanding of the pathogenesis of liver fibrosis advances an increasing number of factors are being explored as novel treatments. However, effective treatment strategies are difficult to identify, due to the involvement of many fibrotic molecules in the maintenance of normal tissue homeostasis. This hinders the progress of novel strategies for the treatment of liver fibrosis, and so it is necessary to gain a greater understanding of the pathways and molecules involved, in order to develop new anti-fibrotic therapies.

Previous research has demonstrated that two members of the TNF superfamily, TWEAK and its receptor Fn14, are implicated in the pathogenesis of fibrosis. Overexpression of TWEAK in mouse models led to cardiac fibrosis and kidney fibrosis (Jain et al., 2009; Hotta et al., 2011) whereas deletion of Fn14 protected against cardiac fibrosis (Novoyatleva et al., 2013). However, no studies so far directly

address the role of TWEAK and Fn14 in fibrotic liver disease. Therefore this thesis examined the role of TWEAK and Fn14 in human and mouse acute and chronic liver injury and provides evidence that TWEAK is directly involved in the modulation of liver fibrosis (Figure 7.1). Furthermore, the soluble form of TWEAK was detected in serum samples of patients with chronic liver disease and has the potential to predict disease progression in patients with PSC.

7.1.1 TWEAK and Fn14 expression in diseased liver

Initially, I investigated the expression of Fn14 and TWEAK in different types of human liver diseases including acute, fatty and immune-mediated liver diseases and in experimental models of acute and chronic liver injury.

ALF causes a rapid loss of liver function and has been associated with increased but restricted liver fibrosis (Dechêne et al., 2010). My data demonstrated elevated Fn14 mRNA and protein levels in patients with ALF compared to normal livers. I also detected high Fn14 mRNA levels in an experimental model of acute liver injury induced by CCl_4. Consistent with this a study by Affò *et al.* demonstrated high Fn14 mRNA levels in experimental models of acute liver injury (Affò et al., 2012). Furthermore, my data showed that TWEAK mRNA was not significantly elevated in patients with ALF or in mice with CCl_4-induced acute liver injury. Nevertheless, TWEAK protein levels were abundant around the portal area and the fibrous septum in patients with ALF compared to healthy controls. Following acute injury, the TWEAK and Fn14 pathway is considered to facilitate tissue regeneration and repair whereas prolonged TWEAK stimulation in diseased tissue can contribute to pathogenic tissue degeneration (Cheng et al., 2013). Therefore, expression of TWEAK and Fn14 was also investigated in chronic steatotic liver diseases including

ALD and NASH. Patients with ALD and NASH often have perisinusoidal fibrosis as ECM primarily accumulates in the space of Disse. A significant upregulation of Fn14 protein but not mRNA expression was observed in chronic steatotic liver disease, which revealed the co-expression of Fn14 with α-SMA-positive myofibroblasts in the fibrotic scar. I also demonstrated that TWEAK mRNA and protein expression were significantly upregulated in chronic steatotic liver diseases, and was not only associated with infiltrating leukocytes but also with myofibroblasts in the fibrotic septa in NASH and ALD.

A role for the TWEAK and Fn14 pathway in driving several different human autoimmune-mediated diseases including rheumatoid arthritis, multiple sclerosis and systemic lupus erythematosus has been described. The first phase II clinical trials in patients with systemic lupus erythematosus are now in progress using anti-TWEAK blocking therapies (Bertin et al., 2013). The chronic liver diseases PBC and AIH are also autoimmune-mediated liver diseases whereas PSC is idiopathic but considered to be an immune-mediated liver disease (O'Hara et al., 2013). Consistent with this, my data showed elevated Fn14 and TWEAK expression in liver tissue from patients with PSC, PBC and AIH compared to normal controls.

PBC and PSC are additionally characterised as cholangiopathies. They present with chronic inflammation of the bile ducts causing ductular reaction that encompasses proliferation of biliary epithelial cells and expansion of differentiating LPCs that may lead to periductular and biliary fibrosis (Hirschfield et al., 2010; O'Hara et al., 2013). Fn14 expression has previously been described in LPCs and biliary epithelial cells but to my knowledge has not been investigated in PBC or PSC (Tirnitz-Parker et al., 2010; Jakubowski et al., 2005; Affò et al., 2012). My studies

demonstrated that indeed Fn14 was present in CK19-positive ductule-like structures in PBC and PSC samples. Overall, increased expression of TWEAK and Fn14 in acute and chronic liver diseases, and their association with the stromal population, suggested that they are involved in the disease process.

7.1.2 The role of TWEAK and Fn14 in liver fibrosis

As all of the investigated liver diseases above develop a certain degree of fibrosis, I then investigated the expression and function of TWEAK and Fn14 in human HSCs *in vitro*. Fn14 expression was present in quiescent and activated HSCs *in vitro*, which could be translocated to the cell surface with TGF-β stimulation. A similar pattern has been observed in the corneal stroma where quiescent keratocytes upregulate Fn14 expression after TGF-β stimulation (Ebihara et al., 2009). In addition, HSCs constitutively produced TWEAK supporting a concept of a paracrine and/or autocrine loop in which TWEAK produced by HSCs feeds back on them via the Fn14 receptor. The co-expression of TWEAK and Fn14 has also been detected on primary proximal tubular epithelial cells and human blastoma cell lines (Hotta et al., 2011; Pettersen et al., 2013). Importantly, my data showed that TWEAK induced HSC proliferation and NF-κB signalling suggesting an active role of this cytokine in the development of hepatic fibrosis.

The role of TWEAK as a stimulator of liver fibrogenesis *in vivo* was evidenced by reduced fibrosis in TWEAK KO animals subjected to acute and chronic CCl_4 injury. Following acute liver injury, *Col1a1* was significantly lower in TWEAK KO mice compared to TWEAK WT mice. Similarly, TWEAK KO mice subjected to chronic CCl_4 had less collagen deposition compared to their WT control. In contrast, my data

also demonstrated that TWEAK stimulation of human HSCs *in vitro* did not lead to changes in *COL1A1*. However, the microenvironment of HSCs in a fibrotic liver is completely different and exposes the cells to other cell types and molecules not found when culturing HSCs leading them to have a different gene expression profile (De Minicis et al., 2007). This could possibly mean that TWEAK does not have an immediate effect on HSC collagen production but functions via other as yet unknown mechanisms such as inducing secretion of TGF-β or inflammatory cytokines. Indeed, transcription levels of *Tgfb1* were significantly reduced in TWEAK KO mice compared to WT mice after acute injury indicating that TWEAK might be involved in the regulation of *Tgfb1*.

Acta2 transcription was similar in TWEAK KO and WT mice after acute liver injury whereas fewer α-SMA-positive LMFs were present in TWEAK KO mice after chronic injury. In contrast, my *in vitro* experiments demonstrated that TWEAK has an inhibitory effect on HSC activation. Again, depending on the microenvironment TWEAK might affect HSC activation in different ways and other research has demonstrated a dual role for TWEAK where it can stimulate progenitor cells after acute injury but also inhibit differentiation of the same progenitor cells in chronic disease (Burkly et al., 2007).

An important group of proteins that are involved in liver fibrosis are MMPs. Commonly MMPs are considered to be involved in the turnover and degradation of ECM but they also involved in the regulation of inflammation and activation and de-activation of myofibroblasts (Giannandrea and Parks, 2014). One group of MMPs are gelatinases, MMP-2 and MMP-9, that cause the degradation of collagen type IV, an important element of the endothelial basement membrane, facilitating the recruitment

of inflammatory cells and leading to the replacement by collagen type I and III after liver injury (Kurzepa et al., 2014). However, depending on the timing, MMPs can play dual roles both bad and good in liver fibrosis. MMP-2 for example can induce HSC proliferation and migration but is also involved in the regression of fibrosis as it has collagenolytic properties (Hemmann et al., 2007). MMP-9 on the other hand is involved in HSC activation but can also promote HSC apoptosis (Hemmann et al., 2007).

My data demonstrated that *Mmp2*, but not *Mmp9*, was significantly lower in TWEAK KO mice compared to TWEAK WT mice after acute and chronic liver injury. Conversely, recent research has demonstrated that TWEAK decreased or had no effect on MMP-2 production but increased MMP-9 production in different cell types including cardiac fibroblasts and macrophages (Kim et al., 2004; Li et al., 2009; Panguluri et al., 2010; Chen et al., 2012). Therefore, TWEAK might not directly affect MMP-2 production in HSCs or macrophages during liver injury. It may act through a secondary mechanism. MMP activity is very controlled and one way in which this is achieved is by stopping their catalytic activity through TIMPs. TIMP-1 is mainly produced by activated HSCs and is expressed as early as 9 hours after CCl_4 injury (Knittel et al., 2000). It is controlled by TGF-β but also by other pro-inflammatory cytokines such as TNF-α (Hemmann et al., 2007). Blocking TIMP-1 in a mouse model of fibrosis induced fibrolysis (Nie et al., 2001). My experiments demonstrated that *Timp1* was significantly less in TWEAK KO mice than WT mice after acute but not after chronic injury. Again, this might be due to different functions that TWEAK exhibits during acute and chronic injury.

In addition, my data suggests that the fibrogenic effect of TWEAK may not exclusively be regulated through Fn14 as Fn14 KO mice had similar levels of fibrosis

compared to their WT controls after acute and chronic CCl_4 injury. This was also demonstrated in Fn14 KO mice after they were fed the CDE-diet for 21 days where they expressed similar levels of *Col1a1*, *Mmp2*, *Mmp9* and *Timp1* compared to WT mice despite having significantly higher Fn14 mRNA expression (Tirnitz-Parker et al., 2010). Nevertheless, the same experimental model also demonstrated that after only 14 days on the CDE-diet immune infiltration of CD45-positive and F4/80-positive lymphocytes, collagen deposition and LPCs were significantly lower in Fn14 KO mice compared to WT mice (Tirnitz-Parker et al., 2010). This suggest that Fn14 might be involved at earlier time points during the development of liver fibrosis and becomes later on substituted with other mediators that exhibit a stronger effect on fibrosis.

The inflammatory response plays a crucial role during the development of liver fibrosis. Research by Holt *et al.* has demonstrated that activated HSCs are involved in the recruitment of immune cells to the site of injury by secreting large amounts of chemokines (Holt et al., 2009). CCL5 has been identified as an important mediator of fibrosis (Berres et al., 2010) and it directly effects HSCs and the immune environment (Liaskou et al., 2013; Schwabe et al., 2003). My data demonstrated that TWEAK stimulation led to a trend towards an upregulation of CCL5 in HSCs. Other research has demonstrated the ability of TWEAK to induce expression of pro-inflammatory cytokines and chemokines (IL-8, CCL2 and CCL5) in human corneal myofibroblasts, which was further increased with co-stimulation of TGF-β (Ebihara et al., 2009). Similarly, IL-8 production induced by TWEAK was enhanced by TGF-β in gingival fibroblasts (Hosokawa et al., 2006) indicating that TWEAK and TGF-β might work synergistically to enhance the inflammatory response during fibrotic liver disease.

7.1.3 Soluble TWEAK levels as indicator of disease severity

My data and that generated by other groups (Tirnitz-Parker et al., 2010; Kuramitsu et al., 2013; Bird et al., 2013) has demonstrated that TWEAK can affect different aspects of liver disease including fibrogenesis and LPC proliferation. Despite being involved in disease progression, research has also shown that the quantity of sTWEAK in serum or urine samples can be a predictor of disease progression (Chorianopoulos et al., 2009; Bertin et al., 2013). In accordance with that, I demonstrated that sTWEAK levels in patients with PSC could be a predictor of disease outcome. Lower sTWEAK levels were associated with a worse transplant-free survival. However, whether this is exclusively in patients with PSC or whether this can also be applied to other liver diseases remains to be determined.

7.2 Conclusion

In conclusion, this thesis demonstrates that TWEAK and Fn14 can be upregulated in various different liver diseases and that TWEAK can regulate the fibrogenic response at least in parts independent of Fn14 *in vivo*. Furthermore, TWEAK can induce the expansion of activated HSCs through an enhanced proliferative response *in vitro*. Targeting TWEAK could therefore be an effective way in altering fibrogenesis during liver injury. Finally, sTWEAK levels could be a potential new biomarker for patients with PSC.

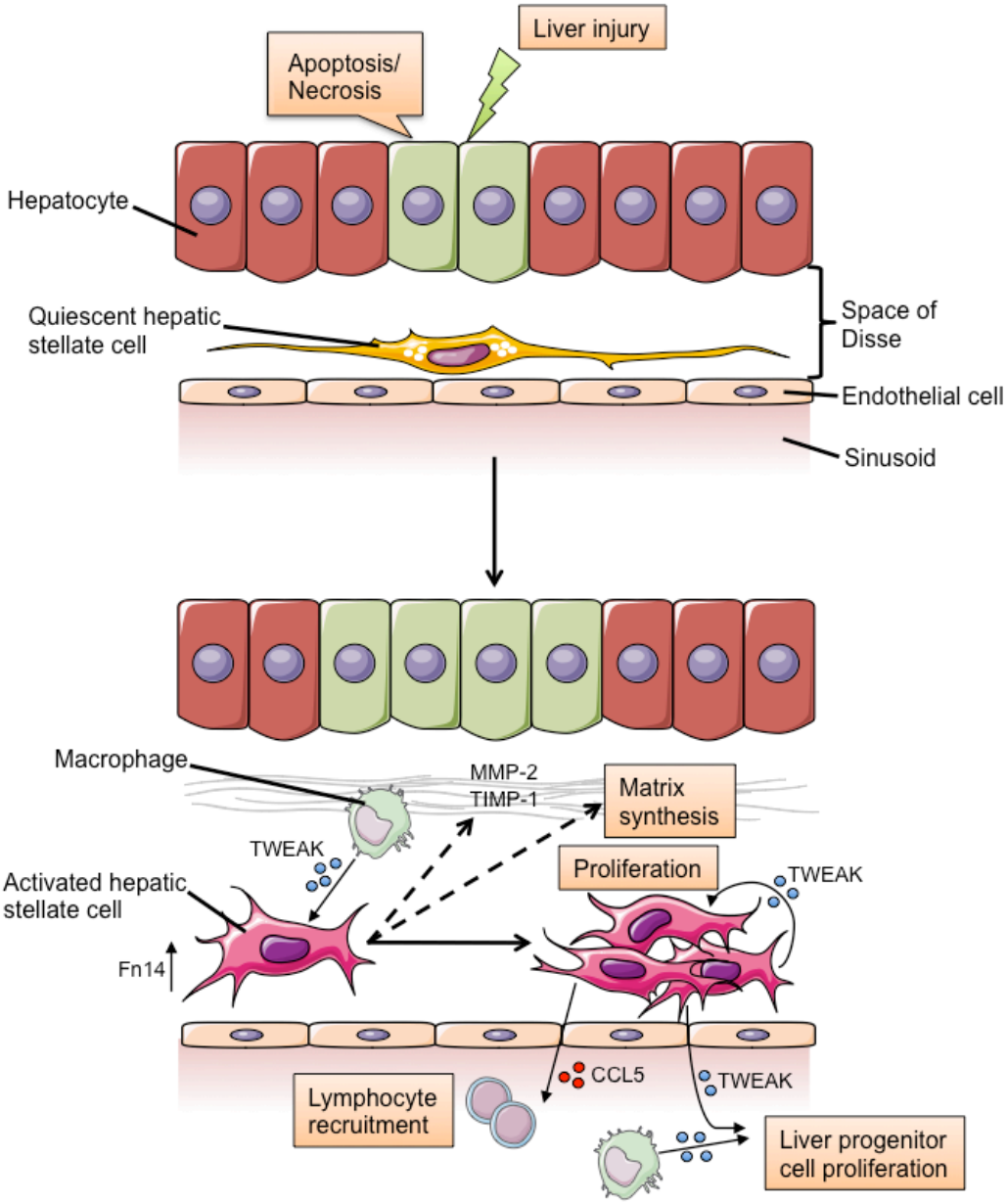

Figure 7.1 Proposed role of TWEAK in the pathogenesis of liver fibrosis
In the normal liver hepatic stellate cells (HSCs) are quiescent and TWEAK expression is low. In response to liver injury quiescent HSCs become activated and lymphocyte infiltrate induces TWEAK expression. TWEAK enhances HSC proliferation and CCL5 production. CCL5 then exacerbates lymphocyte recruitment. In addition, TWEAK is involved in collagen deposition and production of MMP-2 and TIMP-1.

7.3 Limitations and future areas for development

Hepatic TWEAK was expressed by a variety of cell types. I demonstrated that TWEAK is expressed by vimentin-positive stromal cells in the fibrotic septum and by HSCs *in vitro*. In contrast most research has demonstrated that TWEAK is expressed by immune cells. In the liver, TWEAK mRNA has been shown to be highly expressed in NK cells and macrophages but was also detected in CD4-positive T cells, CD8-positive T cells and NKT cells (Tirnitz-Parker et al., 2010). Further work is required to determine lymphocyte populations in the liver that are expressing TWEAK protein. This could be achieved by dual staining of liver tissue or performing flow cytometry with antibodies against TWEAK and markers for leukocyte subpopulations such as CD14 (monocytes/macrophages), CD11c (Dendritic cells), CD56 (NK cells) and CD8 (T cells). More insight into what cell types express TWEAK at which timepoint in acute and chronic liver injury could give vital clues on the understanding of disease pathogenesis.

Fn14 expression has been detected in different liver cells including HSCs, cholangiocytes, and IHECs whereas TWEAK can be expressed by macrophages and HSCs. *In vitro* co-culture experiments could be used to mimic the liver microenvironment more closely and investigate the cellular behaviour of for example cholangiocytes in combination with HSCs or macrophages. TWEAK or Fn14 could then be inhibited by function blocking antibodies or siRNA in order to determine the role of TWEAK and Fn14 on cell behaviour. Furthermore, dual staining of TWEAK and Fn14 in liver sections could be carried out to determine the proximity of TWEAK and Fn14-positive cells.

In functional assays, TWEAK was found to promote HSC proliferation but inhibited activation as indicated by lower *ACTA2* levels. I have not investigated the effect on HSCs when they are stimulated with other cytokines or growth factors in combination with TWEAK. Co-stimulation of TWEAK and TGF-β1 would be a likely combination especially because Fn14 is upregulated with TGF-β1 in HSCs *in vitro*. In addition, it needs to be investigated whether TWEAK does indeed induce proliferation of HSCs through Fn14 signalling using anti-Fn14 blocking antibodies.

Work on this thesis has focused on the role of TWEAK and Fn14 in liver fibrosis. There is strong evidence that TWEAK is also involved in the modulation of the immune system (Burkly et al., 2011). Previous work by other groups has demonstrated a pro-inflammatory effect of TWEAK on myofibroblasts and keratocytes expressing cytokines and chemokines such as IL-8, CCL2 and CCL5 (Chicheportiche et al., 2002; Jin et al., 2004; Ebihara et al., 2009). I have investigated CCL5 expression in HSCs upon TWEAK treatment but this should be further investigated by increasing the number of repeats and looking at other pro- and anti-inflammatory cytokines and chemokines.

So far I have demonstrated that TWEAK activates the NF-κB pathway in HSCs. To get further insights how TWEAK affects HSCs other pathways could be investigated. For example TWEAK has been shown to activate p44/p42 mitogen activated protein kinases (MAPK), c-jun-N-terminal kinase 1 (JNK1), and activator protein-1 (AP-1) and transforming growth factor beta activated kinase-1 (TAK1) in various cell types (Dogra et al., 2007; Polek et al., 2003; Kumar et al., 2009). Furthermore, whether the effect of TWEAK on HSC proliferation and activation is regulated through the NF-

κB pathway could be investigated with agents that inhibit NF-κB pathway (Yamamoto and Gaynor, 2001).

As discussed earlier, *in vivo* studies have shown that TWEAK but not Fn14 seem to be involved in fibrogenesis in a chemical injury model. Further studies are required to investigate the Fn14 KO phenotype in context of other injury models. A biliary model such as bile duct ligation would be of interest. Bile duct ligation causes proliferation of biliary epithelial cells and LPCs with an accompanying portal inflammation and fibrosis (Georgiev et al., 2008). Another model that could be studied is the MCD model, which is nutritional animal model of NASH. The MCD diet causes steatohepatitis and perisinusoidal fibrosis (Takahashi et al., 2012).

Low sTWEAK levels were detected in serum samples from patients with PSC that correlated with disease progression. Other liver diseases should be investigated to determine whether the results are specific for PSC patients. Furthermore, it would be of interest whether soluble levels of CD163 inversely correlate with sTWEAK as it has been shown in other disease (Urbonaviciene et al., 2011; Llaurado et al., 2012; Bertin et al., 2013). Indeed in patients with atherosclerosis the CD163/TWEAK ratio was a better marker than sTWEAK levels alone (Moreno et al., 2009).

List of references

Afford, S.C., Randhawa, S., Eliopoulos, A.G., et al. (1999) CD40 activation induces apoptosis in cultured human hepatocytes via induction of cell surface fas ligand expression and amplifies fas-mediated hepatocyte death during allograft rejection. The Journal of experimental medicine, 189 (2): 441–446

Affò, S., Dominguez, M., Lozano, J.J., et al. (2012) Transcriptome analysis identifies TNF superfamily receptors as potential therapeutic targets in alcoholic hepatitis. Gut, 62 (3): 452–460

Aggarwal, B.B. (2003) Signalling pathways of the TNF superfamily: a double-edged sword. Nature reviews. Immunology, 3 (9): 745–756

Al-Sawaf, O., Fragoulis, A., Rosen, C., et al. (2014) Nrf2 Protects Against TWEAK-mediated Skeletal Muscle Wasting. Scientific Reports, 4

Alabraba, E.B., Lai, V., Boon, L., et al. (2008) Coculture of human liver macrophages and cholangiocytes leads to CD40-dependent apoptosis and cytokine secretion. Hepatology, 47 (2): 552–562

Ando, T., Ichikawa, J., Wako, M., et al. (2006) TWEAK/Fn14 interaction regulates RANTES production, BMP-2-induced differentiation, and RANKL expression in mouse osteoblastic MC3T3-E1 cells. Arthritis research & therapy, 8 (5): R146

Arthur, M.J., Stanley, A., Iredale, J.P., et al. (1992) Secretion of 72 kDa type IV collagenase/gelatinase by cultured human lipocytes. Analysis of gene expression, protein synthesis and proteinase activity. Biochemical Journal, 287 (Pt 3): 701–707

Baek, J.Y., Morris, S.M., Campbell, J., et al. (2010) TGF-beta inactivation and TGF-alpha overexpression cooperate in an in vivo mouse model to induce hepatocellular carcinoma that recapitulates molecular features of human liver cancer. International journal of cancer. Journal international du cancer, 127 (5): 1060–1071

Barber, K.M., Pioli, S.E., Blackwell, J.E., et al. (2007) Development of a UK score for patients with end-stage liver disease. Hepatology, 46 (4): 510A–510A

Barron, L. and Wynn, T.A. (2011) Fibrosis is regulated by Th2 and Th17 responses and by dynamic interactions between fibroblasts and macrophages. American Journal of Physiology-Gastrointestinal and Liver Physiology, 300 (5): G723–8

Bataller, R. and Brenner, D.A. (2005) Liver fibrosis. Journal of Clinical Investigation, 115 (115(2)): 209–218

Bauvois, B. (2012) New facets of matrix metalloproteinases MMP-2 and MMP-9 as cell surface transducers: Outside-in signaling and relationship to tumor progression. Biochimica et biophysica acta, 1825 (1): 29–36

Baxter, F.O., Came, P.J., Abell, K., et al. (2006) IKK beta/2 induces TWEAK and apoptosis in mammary epithelial cells. Development, 133 (17): 3485–3494

Berres, M.-L., Koenen, R.R., Rueland, A., et al. (2010) Antagonism of the chemokine Ccl5 ameliorates experimental liver fibrosis in mice. Journal of Clinical Investigation, 120 (11): 4129–4140

Bertin, D., Stephan, D., Khrestchatisky, M., et al. (2013) Is TWEAK a Biomarker for Autoimmune/Chronic Inflammatory Diseases? Frontiers in immunology, 4: 489

Bird, T.G., Lu, W.-Y., Boulter, L., et al. (2013) Bone marrow injection stimulates hepatic ductular reactions in the absence of injury via macrophage-mediated TWEAK signaling. Proceedings of the National Academy of Sciences of the United States of America, 110 (16): 6542–6547

Bjøro, K., Brandsæter, B., Foss, A., et al. (2006) Liver Transplantation in Primary Sclerosing Cholangitis Berk, P.D. and Chapman, R.W. (eds.). Seminars in Liver Disease, 26 (01): 069–079

Boetticher, N.C., Peine, C.J., Kwo, P., et al. (2008) A Randomized, Double-Blinded, Placebo-Controlled Multicenter Trial of Etanercept in the Treatment of Alcoholic Hepatitis. Gastroenterology, 135 (6): 1953–1960

Bomble, M., Tacke, F., Rink, L., et al. (2010) Analysis of antigen-presenting functionality of cultured rat hepatic stellate cells and transdifferentiated myofibroblasts. Biochemical and Biophysical Research Communications, 396 (2): 342–347

Bonacchi, A., Romagnani, P., Romanelli, R.G., et al. (2001) Signal transduction by the chemokine receptor CXCR3 - Activation of Ras/ERK, Src, and phosphatidylinositol 3-kinase/Akt controls cell migration and proliferation in human vascular pericytes. The Journal of biological chemistry, 276 (13): 9945–9954

Bonner, J.C. (2004) Regulation of PDGF and its receptors in fibrotic diseases. Cytokine & Growth Factor Reviews, 15 (4): 255–273

Borkham-Kamphorst, E., Kovalenko, E., van Roeyen, C.R.C., et al. (2008) Platelet-derived growth factor isoform expression in carbon tetrachloride-induced chronic liver injury. Laboratory investigation; a journal of technical methods and pathology, 88 (10): 1090–1100

Borkham-Kamphorst, E., van Roeyen, C.R.C., Ostendorf, T., et al. (2007) Pro-fibrogenic potential of PDGF-D in liver fibrosis. Journal of Hepatology, 46 (6): 1064–1074

Bossen, C., Ingold, K., Tardivel, A., et al. (2006) Interactions of tumor necrosis factor (TNF) and TNF receptor family members in the mouse and human. The Journal of biological chemistry, 281 (20): 13964–13971

Bourbonnais, E., Raymond, V.-A., Ethier, C., et al. (2012) Liver fibrosis protects mice from acute hepatocellular injury. Gastroenterology, 142 (1): 130–139.e4

Bover, L.C., Cardó-Vila, M., Kuniyasu, A., et al. (2007) A previously unrecognized protein-protein interaction between TWEAK and CD163: potential biological implications. Journal of immunology (Baltimore, Md. : 1950), 178 (12): 8183–8194

Bremer, E. (2013) Targeting of the tumor necrosis factor receptor superfamily for cancer immunotherapy. ISRN oncology, 2013 (4): 371854–25

Brenner, C., Galluzzi, L., Kepp, O., et al. (2013) Decoding cell death signals in liver inflammation. Journal of Hepatology, 59 (3): 583–594

Brenner, D.A., Kisseleva, T., Scholten, D., et al. (2012) Origin of myofibroblasts in liver fibrosis. Fibrogenesis & tissue repair, 5 Suppl 1 (Suppl 1): S17

Brown, S.A.N., Cheng, E., Williams, M.S., et al. (2013) TWEAK-Independent Fn14 Self-Association and NF-κB Activation Is Mediated by the C-Terminal Region of the Fn14 Cytoplasmic Domain LEE, Y.J. (ed.). PloS one, 8 (6): e65248

Brown, S.A.N., Ghosh, A. and Winkles, J.A. (2010) Full-length, membrane-anchored TWEAK can function as a juxtacrine signaling molecule and activate the NF-kappaB pathway. Journal of Biological Chemistry, 285 (23): 17432–17441

Brown, S.A.N., Richards, C.M., Hanscom, H.N., et al. (2003) The Fn14 cytoplasmic tail binds tumour-necrosis-factor-receptor-associated factors 1, 2, 3 and 5 and mediates nuclear factor-κB activation. Biochemical Journal, 371 (2): 395

Burkly, L.C. (2014) TWEAK/Fn14 axis: The current paradigm of tissue injury-inducible function in the midst of complexities. Seminars in Immunology, 26 (3): 229–236

Burkly, L.C., Michaelson, J.S. and Zheng, T.S. (2011) TWEAK/Fn14 pathway: an immunological switch for shaping tissue responses. Immunological reviews, 244 (1): 99–114

Burkly, L.C., Michaelson, J.S., Hahm, K., et al. (2007) TWEAKing tissue remodeling by a multifunctional cytokine: Role of TWEAK/Fn14 pathway in health and disease. Cytokine, 40 (1): 1–16

Callaghan, C.J., Charman, S.C., Muiesan, P., et al. (2013) Outcomes of transplantation of livers from donation after circulatory death donors in the UK: a cohort study. BMJ open, 3 (9): e003287–e003287

Campbell, S., Burkly, L.C., Gao, H.-X., et al. (2006) Proinflammatory effects of TWEAK/Fn14 interactions in glomerular mesangial cells. Journal of immunology (Baltimore, Md. : 1950), 176 (3): 1889–1898

Canbay, A., Feldstein, A.E., Higuchi, H., et al. (2003) Kupffer cell engulfment of apoptotic bodies stimulates death ligand and cytokine expression. Hepatology, 38 (5): 1188–1198

Cassiman, D. and Roskams, T. (2002) Beauty is in the eye of the beholder: emerging concepts and pitfalls in hepatic stellate cell research. Journal of Hepatology, 37 (4): 527–535

Chen, H.-N., Wang, D.-J., Ren, M.-Y., et al. (2012) TWEAK/Fn14 promotes the proliferation and collagen synthesis of rat cardiac fibroblasts via the NF-κB pathway. Molecular biology reports, 39 (8): 8231–8241

Cheng, E., Armstrong, C.L., Galisteo, R., et al. (2013) TWEAK/Fn14 Axis-Targeted Therapeutics: Moving Basic Science Discoveries to the Clinic. Frontiers in immunology, 4: 473

Chicheportiche, Y., Bourdon, P.R., Xu, H., et al. (1997) TWEAK, a new secreted ligand in the tumor necrosis factor family that weakly induces apoptosis. The Journal of biological chemistry, 272 (51): 32401–32410

Chicheportiche, Y., Chicheportiche, R., Sizing, I., et al. (2002) Proinflammatory activity of TWEAK on human dermal fibroblasts and synoviocytes: blocking and enhancing effects of anti-TWEAK monoclonal antibodies. Arthritis research, 4 (2): 126–133

Cholongitas, E., Shusang, V., Marelli, L., et al. (2007) Review article: renal function assessment in cirrhosis - difficulties and alternative measurements. Alimentary Pharmacology & Therapeutics, 26 (7): 969–978

Chorianopoulos, E., Rosenberg, M., Zugck, C., et al. (2009) Decreased soluble TWEAK levels predict an adverse prognosis in patients with chronic stable heart failure. European journal of heart failure, 11 (11): 1050–1056

Chung, R.T., Stravitz, R.T., Fontana, R.J., et al. (2012) Pathogenesis of liver injury in acute liver failure. In September 2012. pp. e1–7

Cong, M., Iwaisako, K., Jiang, C., et al. (2012) Cell signals influencing hepatic fibrosis. International journal of hepatology, 2012 (24): 158547–18

Cook, R.T. (1998) Alcohol abuse, alcoholism, and damage to the immune system--a review. Alcoholism, clinical and experimental research, 22 (9): 1927–1942

Corpechot, C., Gaouar, F., Naggar, El, A., et al. (2014) Baseline values and changes in liver stiffness measured by transient elastography are associated with severity of fibrosis and outcomes of patients with primary sclerosing cholangitis. Gastroenterology, 146 (4): 970–9– quiz e15–6

Croft, M., Benedict, C.A. and Ware, C.F. (2013) Clinical targeting of the TNF and TNFR superfamilies. Nature reviews. Drug discovery, 12 (2): 147–168

Croft, M., Duan, W., Choi, H., et al. (2012) TNF superfamily in inflammatory disease: translating basic insights. Trends in Immunology, 33 (3): 144–152

Cui, D., Zhang, S., Ma, J., et al. (2010) Short interfering RNA targetting NF-kappa B induces apoptosis of hepatic stellate cells and attenuates extracellular matrix production. Digestive and Liver Disease, 42 (11): 813–817

D'Ambrosio, D.N., Walewski, J.L., Clugston, R.D., et al. (2011) Distinct populations of hepatic stellate cells in the mouse liver have different capacities for retinoid and lipid storage. Shoukry, N.H. (ed.). PloS one, 6 (9): e24993

De Ketelaere, A., Vermeulen, L., Vialard, J., et al. (2004) Involvement of GSK-3beta in TWEAK-mediated NF-kappaB activation. FEBS Letters, 566 (1-3): 60–64

De Minicis, S., Seki, E., Uchinami, H., et al. (2007) Gene Expression Profiles During Hepatic Stellate Cell Activation in Culture and In Vivo. Gastroenterology, 132 (5): 1937–1946

Dechêne, A., Sowa, J.-P., Gieseler, R.K., et al. (2010) Acute liver failure is associated with elevated liver stiffness and hepatic stellate cell activation. Hepatology, 52 (3): 1008–1016

DeLeve, L.D., Wang, X. and Guo, Y. (2008) Sinusoidal endothelial cells prevent rat stellate cell activation and promote reversion to quiescence. Hepatology, 48 (3): 920–930

Desplat-Jégo, S., Feuillet, L., Creidy, R., et al. (2009) TWEAK is expressed at the cell surface of monocytes during multiple sclerosis. Journal of leukocyte biology, 85 (1): 132–135

Diehl, A.M. and Chute, J. (2013) Underlying potential: cellular and molecular determinants of adult liver repair. Journal of Clinical Investigation, 123 (5): 1858–1860

Distler, J.H.W., Schett, G., Gay, S., et al. (2008) The controversial role of tumor necrosis factor alpha in fibrotic diseases. Arthritis and rheumatism, 58 (8): 2228–2235

Dogra, C., Changotra, H., Mohan, S., et al. (2006) Tumor necrosis factor-like weak inducer of apoptosis inhibits skeletal myogenesis through sustained activation of nuclear factor-kappaB and degradation of MyoD protein. The Journal of biological chemistry, 281 (15): 10327–10336

Dogra, C., Hall, S.L., Wedhas, N., et al. (2007) Fibroblast growth factor inducible 14 (Fn14) is required for the expression of myogenic regulatory factors and differentiation of myoblasts into myotubes - Evidence for tweak- independent functions of Fn14 during myogenesis. The Journal of biological chemistry, 282 (20): 15000–15010

Dohi, T. and Burkly, L.C. (2012) The TWEAK/Fn14 pathway as an aggravating and perpetuating factor in inflammatory diseases: focus on inflammatory bowel diseases. Journal of leukocyte biology, 92 (2): 265–279

Dohi, T., Borodovsky, A., Wu, P., et al. (2009) TWEAK/Fn14 pathway: a nonredundant role in intestinal damage in mice through a TWEAK/intestinal epithelial cell axis. Gastroenterology, 136 (3): 912–923

Dohi, T., Kawashima, R., Kawamura, Y.I., et al. (2014) Pathological activation of canonical nuclear-factor κB by synergy of tumor necrosis factor α and TNF-like weak inducer of apoptosis in mouse acute colitis. Cytokine, 69 (1): 14–21

Duffield, J.S., Forbes, S.J., Constandinou, C.M., et al. (2005) Selective depletion of macrophages reveals distinct, opposing roles during liver injury and repair. Journal of Clinical Investigation, 115 (1): 56–65

Duncan, A.W., Dorrell, C. and Grompe, M. (2009) Stem Cells and Liver Regeneration. Gastroenterology, 137 (2): 466–481

Eaton, J.E., Talwalkar, J.A., Lazaridis, K.N., et al. (2013) Pathogenesis of primary sclerosing cholangitis and advances in diagnosis and management. Gastroenterology, 145 (3): 521–536

Ebihara, N., Nakayama, M., Tokura, T., et al. (2009) Expression and function of fibroblast growth factor-inducible 14 in human corneal myofibroblasts. Experimental eye research, 89 (2): 256–262

El-Masry, M., Gilbert, C.P. and Saab, S. (2011) Recurrence of non-viral liver disease after orthotopic liver transplantation. Liver International, 31 (3): 291–302

Ellis, E.L. and Mann, D.A. (2012) Clinical evidence for the regression of liver fibrosis. Journal of Hepatology, 56 (5): 1171–1180

Elmetwali, T., Searle, P.F., McNeish, I., et al. (2010) CD40 ligand induced cytotoxicity in carcinoma cells is enhanced by inhibition of metalloproteinase cleavage and delivery via a conditionally-replicating adenovirus. Molecular Cancer, 9 (1)

Fabriek, B.O., Dijkstra, C.D. and van den Berg, T.K. (2005) The macrophage scavenger receptor CD163. Immunobiology, 210 (2-4): 153–160

Fallowfield, J.A., Mizuno, M., Kendall, T.J., et al. (2007) Scar-associated macrophages are a major source of hepatic matrix metalloproteinase-13 and facilitate the resolution of murine hepatic fibrosis. Journal of immunology (Baltimore, Md. : 1950), 178 (8): 5288–5295

Feng, S.-L.Y., Guo, Y., Factor, V.M., et al. (2000) The Fn14 immediate-early response gene is induced during liver regeneration and highly expressed in both human and murine hepatocellular carcinomas. The American Journal of Pathology, 156 (4): 1253–1261

Fernández, M., Semela, D., Bruix, J., et al. (2009) Angiogenesis in liver disease. Journal of Hepatology, 50 (3): 604–620

Fibbi, G., Pucci, M., D'Alessio, S., et al. (2001) Transforming growth factor beta-1 stimulates invasivity of hepatic stellate cells by engagement of the cell-associated fibrinolytic system. Growth factors (Chur, Switzerland), 19 (2): 87–100

Fibbi, G., Pucci, M., Grappone, C., et al. (1999) Functions of the fibrinolytic system in human Ito cells and its control by basic fibroblast and platelet-derived growth factor. Hepatology, 29 (3): 868–878

Fick, A., Lang, I., Schäfer, V., et al. (2012) Studies of binding of tumor necrosis factor (TNF)-like weak inducer of apoptosis (TWEAK) to fibroblast growth factor inducible 14 (Fn14). Journal of Biological Chemistry, 287 (1): 484–495

Fletcher, N.F., Sutaria, R., Jo, J., et al. (2014) Activated macrophages promote hepatitis C virus entry in a tumor necrosis factor-dependent manner. Hepatology, 59 (4): 1320–1330

Forner, A., Llovet, J.M. and Bruix, J. (2012) Hepatocellular carcinoma. Lancet, 379 (9822): 1245–1255

Fouts, D.E., Torralba, M., Nelson, K.E., et al. (2012) Bacterial translocation and changes in the intestinal microbiome in mouse models of liver disease. Journal of Hepatology, 56 (6): 1283–1292

Friedman, S.L. (2008) Hepatic stellate cells: protean, multifunctional, and enigmatic cells of the liver. Physiological Reviews, 88 (1): 125–172

Friedman, S.L., Sheppard, D., Duffield, J.S., et al. (2013) Therapy for fibrotic diseases: nearing the starting line. Science translational medicine, 5 (167): 167sr1–167sr1

Gao, B. and Bataller, R. (2011) Alcoholic liver disease: pathogenesis and new therapeutic targets. Gastroenterology, 141 (5): 1572–1585

Gao, B. and Radaeva, S. (2013) Natural killer and natural killer T cells in liver fibrosis. Biochimica et biophysica acta, 1832 (7): 1061–1069

Gäbele, E., Froh, M., Arteel, G.E., et al. (2009) TNFalpha is required for cholestasis-induced liver fibrosis in the mouse. Biochemical and Biophysical Research Communications, 378 (3): 348–353

Geerts, A. (2001) History, heterogeneity, developmental biology, and functions of quiescent hepatic stellate cells. Seminars in Liver Disease, 21 (3): 311–335

Georgiev, P., Jochum, W., Heinrich, S., et al. (2008) Characterization of time-related changes after experimental bile duct ligation. British Journal of Surgery, 95 (5): 646–656

Giannandrea, M. and Parks, W.C. (2014) Diverse functions of matrix metalloproteinases during fibrosis. Disease models & mechanisms, 7 (2): 193–203

Girgenrath, M., Weng, S., Kostek, C.A., et al. (2006) TWEAK, via its receptor Fn14, is a novel regulator of mesenchymal progenitor cells and skeletal muscle regeneration. The EMBO Journal, 25 (24): 5826–5839

Goldberg, D., French, B., Thomasson, A., et al. (2011) Waitlist survival of patients with primary sclerosing cholangitis in the model for end - stage liver disease era. Liver Transplantation, 17 (11): 1355–1363

Gordon, S. (2001) Homeostasis: a scavenger receptor for haemoglobin. Current Biology, 11 (10): R399–401

Gouw, A.S.H., Clouston, A.D. and Theise, N.D. (2011) Ductular reactions in human liver: diversity at the interface. Hepatology, 54 (5): 1853–1863

Grell, M., DOUNI, E., WAJANT, H., et al. (1995) The Transmembrane Form of Tumor-Necrosis-Factor Is the Prime Activating Ligand of the 80 Kda Tumor-Necrosis-Factor Receptor. Cell, 83 (5): 793–802

Gurunathan, S., Winkles, J.A., Ghosh, S., et al. (2014) Regulation of fibroblast growth factor-inducible 14 (Fn14) expression levels via ligand-independent lysosomal degradation. Journal of Biological Chemistry, 289 (19): 12976–12988

Hahn, E., WICK, G., PENCEV, D., et al. (1980) Distribution of Basement-Membrane Proteins in Normal and Fibrotic Human-Liver - Collagen Type-Iv, Laminin, and Fibronectin. Gut, 21 (1): 63–71

Han, Y.-P., Yan, C., Zhou, L., et al. (2007) A matrix metalloproteinase-9 activation cascade by hepatic stellate cells in trans-differentiation in the three-dimensional extracellular matrix. The Journal of biological chemistry, 282 (17): 12928–12939

Hellerbrand, C., Stefanovic, B., Giordano, F., et al. (1999) The role of TGFβ1 in initiating hepatic stellate cell activation in vivo. Journal of Hepatology, 30 (1): 77–87

Hemmann, S., Graf, J., Roderfeld, M., et al. (2007) Expression of MMPs and TIMPs in liver fibrosis – a systematic review with special emphasis on anti-fibrotic strategies. Journal of Hepatology, 46 (5): 955–975

Hirschfield, G.M. and Gershwin, M.E. (2013) The immunobiology and pathophysiology of primary biliary cirrhosis. Annual review of pathology, 8 (1): 303–330

Hirschfield, G.M., Heathcote, E.J. and Gershwin, M.E. (2010) Pathogenesis of Cholestatic Liver Disease and Therapeutic Approaches. Gastroenterology, 139 (5): 1481–1496

Hirschfield, G.M., Karlsen, T.H., Lindor, K.D., et al. (2013) Primary sclerosing cholangitis. The Lancet, 382 (9904): 1587–1599

Holland-Fischer, P., Grønbaek, H., Sandahl, T.D., et al. (2011) Kupffer cells are activated in cirrhotic portal hypertension and not normalised by TIPS. Gut, 60 (10): 1389–1393

Holt, A.P., Haughton, E.L., Lalor, P.F., et al. (2009) Liver myofibroblasts regulate infiltration and positioning of lymphocytes in human liver. Gastroenterology, 136 (2): 705–714

Hommes, D.W., Erkelens, W., Ponsioen, C., et al. (2008) A double-blind, placebo-controlled, randomized study of infliximab in primary sclerosing cholangitis. Journal of clinical gastroenterology, 42 (5): 522–526

Hong, F., Tuyama, A., Lee, T.F., et al. (2009) Hepatic Stellate Cells Express Functional CXCR4: Role in Stromal Cell-Derived Factor-1 alpha-Mediated Stellate Cell Activation. Hepatology, 49 (6): 2055–2067

Hosokawa, Y., Hosokawa, I., Ozaki, K., et al. (2006) Proinflammatory effects of tumour necrosis factor-like weak inducer of apoptosis (TWEAK) on human gingival fibroblasts. Clinical and experimental immunology, 146 (3): 540–549

Hotta, K., Sho, M., Yamato, I., et al. (2011) Direct targeting of fibroblast growth factor-inducible 14 protein protects against renal ischemia reperfusion injury. Kidney international, 79 (2): 179–188

Ide, M., Kuwamura, M., Kotani, T., et al. (2005) Effects of Gadolinium Chloride (GdCl3) on the Appearance of Macrophage Populations and Fibrogenesis in Thioacetamide-Induced Rat Hepatic Lesions. Journal of Comparative Pathology, 133 (2-3): 92–102

Ikejima, K., Honda, H., Yoshikawa, M., et al. (2001) Leptin augments inflammatory and profibrogenic responses in the murine liver induced by hepatotoxic chemicals. Hepatology, 34 (2): 288–297

Iredale, J.P., Benyon, R.C., Arthur, M.J., et al. (1996) Tissue inhibitor of metalloproteinase-1 messenger RNA expression is enhanced relative to interstitial collagenase messenger RNA in experimental liver injury and fibrosis. Hepatology, 24 (1): 176–184

Iredale, J.P., Benyon, R.C., Pickering, J., et al. (1998) Mechanisms of spontaneous resolution of rat liver fibrosis. Hepatic stellate cell apoptosis and reduced hepatic expression of metalloproteinase inhibitors. Journal of Clinical Investigation, 102 (3): 538–549

Iredale, J.P., Thompson, A. and Henderson, N.C. (2013) Extracellular matrix degradation in liver fibrosis: Biochemistry and regulation. Biochimica et biophysica acta, 1832 (7): 876–883

Jain, M., Jakubowski, A., Cui, L., et al. (2009) A novel role for tumor necrosis factor-like weak inducer of apoptosis (TWEAK) in the development of cardiac dysfunction and failure. Circulation Journal, 119 (15): 2058–2068

Jakubowski, A., Ambrose, C., Parr, M., et al. (2005) TWEAK induces liver progenitor cell proliferation. Journal of Clinical Investigation, 115 (9): 2330–2340

Jeong, W.-I., Park, O. and Gao, B. (2008) Abrogation of the antifibrotic effects of natural killer cells/interferon-gamma contributes to alcohol acceleration of liver fibrosis. Gastroenterology, 134 (1): 248–258

Jeong, W.-I., Park, O., Suh, Y.-G., et al. (2011) Suppression of innate immunity (natural killer cell/interferon-γ) in the advanced stages of liver fibrosis in mice. Hepatology, 53 (4): 1342–1351

Jiang, J.X., Mikami, K., Venugopal, S., et al. (2009) Apoptotic body engulfment by hepatic stellate cells promotes their survival by the JAK/STAT and Akt/NF-κB-dependent pathways. Journal of Hepatology, 51 (1): 139–148

Jin, L., Nakao, A., Nakayama, M., et al. (2004) Induction of RANTES by TWEAK/Fn14 interaction in human keratinocytes. The Journal of investigative dermatology, 122 (5): 1175–1179

Kaimori, A., Potter, J., Kaimori, J.-Y., et al. (2007) Transforming growth factor-beta1 induces an epithelial-to-mesenchymal transition state in mouse hepatocytes in vitro. The Journal of biological chemistry, 282 (30): 22089–22101

Kamath, P.S. and Kim, W.R. (2009) The International Normalized Ratio of Prothrombin Time in the Model for End-Stage Liver Disease Score: A Reliable Measure. Clinics in liver disease, 13 (1): 63–66

Karaca, G., Swiderska-Syn, M., Xie, G., et al. (2014) TWEAK/Fn14 signaling is required for liver regeneration after partial hepatectomy in mice. PloS one, 9 (1): e83987

Karlmark, K.R., Zimmermann, H.W., Roderburg, C., et al. (2010) The fractalkine receptor CX_3CR1 protects against liver fibrosis by controlling differentiation and survival of infiltrating hepatic monocytes. Hepatology, 52 (5): 1769–1782

Kawakita, T., Shiraki, K., Yamanaka, Y., et al. (2004) Functional expression of TWEAK in human hepatocellular carcinoma: possible implication in cell proliferation and tumor angiogenesis. Biochemical and Biophysical Research Communications, 318 (3): 726–733

Kazankov, K., Barrera, F., Møller, H.J., et al. (2014) Soluble CD163, a macrophage activation marker, is independently associated with fibrosis in patients with chronic viral hepatitis B and C. Hepatology, 60 (2): 521–530

Kim, S.H., Kang, Y.J., Kim, W.J., et al. (2004) TWEAK can induce pro-inflammatory cytokines and matrix metalloproteinase-9 in macrophages. Circulation Journal, 68: 396–399

Kisseleva, T., Cong, M., Paik, Y., et al. (2012) Myofibroblasts revert to an inactive phenotype during regression of liver fibrosis. Proceedings of the National Academy of Sciences of the United States of America, 109 (24): 9448–9453

Knight, B., Akhurst, B., Matthews, V.B., et al. (2007) Attenuated liver progenitor (oval) cell and fibrogenic responses to the choline deficient, ethionine supplemented diet in the BALB/c inbred strain of mice. Journal of Hepatology, 46 (1): 134–141

Knittel, T., Mehde, M., Grundmann, A., et al. (2000) Expression of matrix metalloproteinases and their inhibitors during hepatic tissue repair in the rat. Histochemistry and cell biology, 113 (6): 443–453

Kristiansen, M., Graversen, J.H., Jacobsen, C., et al. (2001) Identification of the haemoglobin scavenger receptor. Nature, 409 (6817): 198–201

Kumar, M., Makonchuk, D.Y., Li, H., et al. (2009) TNF-like weak inducer of apoptosis (TWEAK) activates proinflammatory signaling pathways and gene expression through the activation of TGF-beta-activated kinase 1. The Journal of Immunology, 182 (4): 2439–2448

Kuramitsu, K., Sverdlov, D.Y., Liu, S.B., et al. (2013) Failure of fibrotic liver regeneration in mice is linked to a severe fibrogenic response driven by hepatic progenitor cell activation. The American Journal of Pathology, 183 (1): 182–194

Kurzepa, J., Madro, A., Czechowska, G., et al. (2014) Role of MMP-2 and MMP-9 and their natural inhibitors in liver fibrosis, chronic pancreatitis and non-specific inflammatory bowel diseases. Hepatobiliary Pancreat Dis Int, 13 (6): 570–579

Lapierre, P., Béland, K. and Alvarez, F. (2007) Pathogenesis of autoimmune hepatitis: from break of tolerance to immune-mediated hepatocyte apoptosis. Translational research : the journal of laboratory and clinical medicine, 149 (3): 107–113

Lazaridis, K.N., Strazzabosco, M. and Larusso, N.F. (2004) The cholangiopathies: Disorders of biliary epithelia. Gastroenterology, 127 (5): 1565–1577

Lechler, R.I., Sykes, M., Thomson, A.W., et al. (2005) Organ transplantation--how much of the promise has been realized? Nature medicine, 11 (6): 605–613

Lee, U.E. and Friedman, S.L. (2011) Mechanisms of hepatic fibrogenesis. Best practice & research. Clinical gastroenterology, 25 (2): 195–206

Lefton, H.B., Rosa, A. and Cohen, M. (2009) Diagnosis and Epidemiology of Cirrhosis. Medical Clinics of North America, 93 (4): 787–799

Leon, D.A. and McCambridge, J. (2006) Liver cirrhosis mortality rates in Britain from 1950 to 2002: an analysis of routine data. Lancet, 367 (9504): 52–56

Leroux, A., Ferrere, G., Godie, V., et al. (2012) Toxic lipids stored by Kupffer cells correlates with their pro-inflammatory phenotype at an early stage of steatohepatitis. Journal of Hepatology, 57 (1): 141–149

Li, H., Mittal, A., Paul, P.K., et al. (2009) Tumor Necrosis Factor-related Weak Inducer of Apoptosis Augments Matrix Metalloproteinase 9 (MMP-9) Production in Skeletal Muscle through the Activation of Nuclear Factor-kappa B-inducing Kinase and p38 Mitogen-activated Protein Kinase A POTENTIAL ROLE OF MMP-9 IN MYOPATHY. The Journal of biological chemistry, 284 (7): 4439–4450

Li, N., Hu, W.-J., Shi, J., et al. (2013) Roles of fibroblast growth factor-inducible 14 in hepatocellular carcinoma. Asian Pacific journal of cancer prevention : APJCP, 14 (6): 3509–3514

Liaskou, E., Zimmermann, H.W., Li, K.-K., et al. (2013) Monocyte subsets in human liver disease show distinct phenotypic and functional characteristics. Hepatology, 57 (1): 385–398

Livak, K.J. and Schmittgen, T.D. (2001) Analysis of relative gene expression data using real-time quantitative PCR and the 2(-Delta Delta C(T)) Method. Methods (San Diego, Calif.), 25 (4): 402–408

Llaurado, G., Gonzalez-Clemente, J.-M., Maymo-Masip, E., et al. (2012) Serum Levels of TWEAK and Scavenger Receptor CD163 in Type 1 Diabetes Mellitus: Relationship with Cardiovascular Risk Factors. A Case-Control Study Dotta, F. (ed.). PloS one, 7 (8)

Lozano, R., Naghavi, M., Foreman, K., et al. (2012) Global and regional mortality from 235 causes of death for 20 age groups in 1990 and 2010: a systematic analysis for the Global Burden of Disease Study 2010. The Lancet, 380 (9859): 2095–2128

Maecker, H., Varfolomeev, E., Kischkel, F., et al. (2005) TWEAK attenuates the transition from innate to adaptive immunity. Cell, 123 (5): 931–944

Marsters, S.A., Sheridan, J.P., Pitti, R.M., et al. (1998) Identification of a ligand for the death-domain-containing receptor Apo3. Current Biology, 8 (9): 525–528

Mederacke, I., Hsu, C.C., Troeger, J.S., et al. (2013) Fate tracing reveals hepatic stellate cells as dominant contributors to liver fibrosis independent of its aetiology. Nature Communications, 4: 2823

Meighan-Mantha, R.L., Hsu, D.K., Guo, Y., et al. (1999) The mitogen-inducible Fn14 gene encodes a type I transmembrane protein that modulates fibroblast adhesion and migration. The Journal of biological chemistry, 274 (46): 33166–33176

Meng, F., Wang, K., Aoyama, T., et al. (2012) Interleukin-17 signaling in inflammatory, Kupffer cells, and hepatic stellate cells exacerbates liver fibrosis in mice. Gastroenterology, 143 (3): 765–76.e1–3

Mittal, A., Bhatnagar, S., Kumar, A., et al. (2010) The TWEAK-Fn14 system is a critical regulator of denervation-induced skeletal muscle atrophy in mice. The Journal of cell biology, 188 (6): 833–849

Mokdad, A.A., Lopez, A.D., Shahraz, S., et al. (2014) Liver cirrhosis mortality in 187 countries between 1980 and 2010: a systematic analysis. Bmc Medicine, 12 (1)

Moreno, J.A., Muñoz-García, B., Martin-Ventura, J.L., et al. (2009) The CD163-expressing macrophages recognize and internalize TWEAK: potential consequences in atherosclerosis. Atherosclerosis, 207 (1): 103–110

Muhanna, N., Doron, S., Wald, O., et al. (2008) Activation of hepatic stellate cells after phagocytosis of lymphocytes: A novel pathway of fibrogenesis. Hepatology, 48 (3): 963–977

Murray, P.J. and Wynn, T.A. (2011) Protective and pathogenic functions of macrophage subsets. Nature reviews. Immunology, 11 (11): 723–737

Müsch, A. (2014) The unique polarity phenotype of hepatocytes. Experimental Cell Research, 328 (2): 276–283

Myers, R.P., Shaheen, A.A.M., Faris, P., et al. (2013) Revision of MELD to include serum albumin improves prediction of mortality on the liver transplant waiting list. Mandell, M.S. (ed.). PloS one, 8 (1): e51926

Napetschnig, J. and Wu, H. (2013) Molecular Basis of NF-κB Signaling. Annual review of biophysics, 42 (1): 443–468

Naveau, S., Chollet-Martin, S., Dharancy, S., et al. (2004) A double-blind randomized controlled trial of infliximab associated with prednisolone in acute alcoholic hepatitis. Hepatology, 39 (5): 1390–1397

Neuberger, J., Gimson, A., Davies, M., et al. (2008) Selection of patients for liver transplantation and allocation of donated livers in the UK. Gut, 57 (2): 252–257

Neuman, M., Angulo, P., Malkiewicz, I., et al. (2002) Tumor necrosis factor-alpha and transforming growth factor-beta reflect severity of liver damage in primary biliary cirrhosis. Journal of gastroenterology and hepatology, 17 (2): 196–202

Neumann, U.P., Langrehr, J.M. and Neuhaus, P. (2002) Chronic rejection after human liver transplantation. Graft, 5: 102–107

Nie, Q.H., Cheng, Y.Q., Xie, Y.M., et al. (2001) Inhibiting effect of antisense oligonucleotides phosphorthioate on gene expression of TIMP-1 in rat liver fibrosis. World Journal of Gastroenterology, 7 (3): 363–369

Novobrantseva, T.I., Majeau, G.R., Amatucci, A., et al. (2005) Attenuated liver fibrosis in the absence of B cells. Journal of Clinical Investigation, 115 (11): 3072–3082

Novoyatleva, T., Diehl, F., van Amerongen, M.J., et al. (2010) TWEAK is a positive regulator of cardiomyocyte proliferation. Cardiovascular research, 85 (4): 681–690

Novoyatleva, T., Schymura, Y., Janssen, W., et al. (2013) Deletion of Fn14 receptor protects from right heart fibrosis and dysfunction. Basic research in cardiology, 108 (2): 325–13

O'Hara, S.P., Tabibian, J.H., Splinter, P.L., et al. (2013) The dynamic biliary epithelia: molecules, pathways, and disease. Journal of Hepatology, 58 (3): 575–582

Ochoa, B., Syn, W.-K., Delgado, I., et al. (2010) Hedgehog signaling is critical for normal liver regeneration after partial hepatectomy in mice. Hepatology, 51 (5): 1712–1723

Oeckinghaus, A., Hayden, M.S. and Ghosh, S. (2011) Crosstalk in NF-κB signaling pathways. Nature immunology, 12 (8): 695–708

Olsen, A.L., Bloomer, S.A., Chan, E.P., et al. (2011) Hepatic stellate cells require a stiff environment for myofibroblastic differentiation. American Journal of Physiology-Gastrointestinal and Liver Physiology, 301 (1): G110–G118

Onozuka, I., Kakinuma, S., Kamiya, A., et al. (2011) Cholestatic liver fibrosis and toxin-induced fibrosis are exacerbated in matrix metalloproteinase-2 deficient mice. Biochemical and Biophysical Research Communications, 406 (1): 134–140

Osawa, Y., Hoshi, M., Yasuda, I., et al. (2013) Tumor necrosis factor-α promotes cholestasis-induced liver fibrosis in the mouse through tissue inhibitor of metalloproteinase-1 production in hepatic stellate cells. Afford, S. (ed.). PloS one, 8 (6): e65251

Otterbein, L.E., Soares, M.P., Yamashita, K., et al. (2003) Heme oxygenase-1: unleashing the protective properties of heme. Trends in Immunology, 24 (8): 449–455

Panguluri, S.K., Bhatnagar, S., Kumar, A., et al. (2010) Genomic Profiling of Messenger RNAs and MicroRNAs Reveals Potential Mechanisms of TWEAK-Induced Skeletal Muscle Wasting in Mice Nogales-Gadea, G. (ed.). PloS one, 5 (1): e8760

Park, M.-C., Chung, S.J., Jung, S.-J., et al. (2008) Relationship of serum TWEAK level to cytokine level, disease activity, and response to anti-TNF treatment in patients with rheumatoid arthritis. Scandinavian journal of rheumatology, 37 (3): 173–178

Park, O., Jeong, W.-I., Wang, L., et al. (2009) Diverse roles of invariant natural killer T cells in liver injury and fibrosis induced by carbon tetrachloride. Hepatology, 49 (5): 1683–1694

Pellicoro, A., Aucott, R.L., Ramachandran, P., et al. (2012) Elastin accumulation is regulated at the level of degradation by macrophage metalloelastase (MMP-12) during experimental liver fibrosis. Hepatology, 55 (6): 1965–1975

Pellicoro, A., Ramachandran, P., Iredale, J.P., et al. (2014) Liver fibrosis and repair: immune regulation of wound healing in a solid organ. Nature reviews. Immunology, 14 (3): 181–194

Pettersen, I., Baryawno, N., Abel, F., et al. (2013) Expression of TWEAK/Fn14 in neuroblastoma: implications in tumorigenesis. International journal of oncology, 42 (4): 1239–1248

Peverill, W., Powell, L.W. and Skoien, R. (2014) Evolving concepts in the pathogenesis of NASH: beyond steatosis and inflammation. International journal of molecular sciences, 15 (5): 8591–8638

Pinzani, M., Gesualdo, L., Sabbah, G.M., et al. (1989) Effects of platelet-derived growth factor and other polypeptide mitogens on DNA synthesis and growth of cultured rat liver fat-storing cells. Journal of Clinical Investigation, 84 (6): 1786–1793

Pinzani, M., Knauss, T.C., Pierce, G.F., et al. (1991) Mitogenic signals for platelet-derived growth factor isoforms in liver fat-storing cells. The American journal of physiology, 260 (3 Pt 1): C485–91

Pinzani, M., Milani, S., Grappone, C., et al. (1994) Expression of platelet-derived growth factor in a model of acute liver injury. Hepatology, 19 (3): 701–707

Polek, T.C., Talpaz, M., Darnay, B.G., et al. (2003) TWEAK mediates signal transduction and differentiation of RAW264.7 cells in the absence of Fn14/TweakR - Evidence for a second TWEAK receptor. The Journal of biological chemistry, 278 (34): 32317–32323

Popov, Y. and Schuppan, D. (2009) Targeting liver fibrosis: Strategies for development and validation of antifibrotic therapies. Hepatology, 50 (4): 1294–1306

Popov, Y., Sverdlov, D.Y., Bhaskar, K.R., et al. (2010) Macrophage-mediated phagocytosis of apoptotic cholangiocytes contributes to reversal of experimental biliary fibrosis. American Journal of Physiology-Gastrointestinal and Liver Physiology, 298 (3): G323–34

Pradere, J.-P., Kluwe, J., De Minicis, S., et al. (2013) Hepatic macrophages but not dendritic cells contribute to liver fibrosis by promoting the survival of activated hepatic stellate cells in mice. Hepatology, 58 (4): 1461–1473

Puche, J.E., Lee, Y.A., Jiao, J., et al. (2013) A novel murine model to deplete hepatic stellate cells uncovers their role in amplifying liver damage in mice. Hepatology, 57 (1): 339–350

Radbill, B.D., Gupta, R., Ramirez, M.C.M., et al. (2011) Loss of Matrix Metalloproteinase-2 Amplifies Murine Toxin-Induced Liver Fibrosis by Upregulating Collagen I Expression. Digestive Diseases and Sciences, 56 (2): 406–416

Ramachandran, P., Pellicoro, A., Vernon, M.A., et al. (2012) Differential Ly-6C expression identifies the recruited macrophage phenotype, which orchestrates the regression of murine liver fibrosis. Proceedings of the National Academy of Sciences of the United States of America, 109 (46): E3186–95

Reeves, H.L. and Friedman, S.L. (2002) Activation of hepatic stellate cells--a key issue in liver fibrosis. Frontiers in bioscience : a journal and virtual library, 7: d808–26

Reilly, L.A.O., Tai, L., Lee, L., et al. (2009) Membrane-bound Fas ligand only is essential for Fas-induced apoptosis. Nature, 461 (7264): 659–U106

Richter, B., Rychli, K., Hohensinner, P.J., et al. (2010) Differences in the predictive value of tumor necrosis factor-like weak inducer of apoptosis (TWEAK) in advanced ischemic and non-ischemic heart failure. Atherosclerosis, 213 (2): 545–548

Rivera, C.A., Adegboyega, P., van Rooijen, N., et al. (2007) Toll-like receptor-4 signaling and Kupffer cells play pivotal roles in the pathogenesis of non-alcoholic steatohepatitis. Journal of Hepatology, 47 (4): 571–579

Robinson, S.M. and Mann, D.A. (2010) Role of nuclear factor kappaB in liver health and disease. Clinical science (London, England : 1979), 118 (12): 691–705

Roderfeld, M., Weiskirchen, R., Wagner, S., et al. (2006) Inhibition of hepatic fibrogenesis by matrix metalloproteinase-9 mutants in mice. Faseb Journal, 20 (3): 444–454

Roos, C., Wicovsky, A., Müller, N., et al. (2010) Soluble and transmembrane TNF-like weak inducer of apoptosis differentially activate the classical and noncanonical NF-kappa B pathway. The Journal of Immunology, 185 (3): 1593–1605

Safadi, R., Ohta, M., Alvarez, C.E., et al. (2004) Immune stimulation of hepatic fibrogenesis by CD8 cells and attenuation by transgenic interleukin-10 from hepatocytes. Gastroenterology, 127 (3): 870–882

Saitoh, T., Nakayama, M., Nakano, H., et al. (2003) TWEAK induces NF-kappaB2 p100 processing and long lasting NF-kappaB activation. The Journal of biological chemistry, 278 (38): 36005–36012

Sanz, A.B., Aroeira, L.S., Bellon, T., et al. (2014) TWEAK promotes peritoneal inflammation. Ryffel, B. (ed.). PloS one, 9 (3): e90399

Sanz, A.B., Justo, P., Sanchez-Niño, M.D., et al. (2008) The cytokine TWEAK modulates renal tubulointerstitial inflammation. Journal of the American Society of Nephrology : JASN, 19 (4): 695–703

Sato, M., Suzuki, S. and Senoo, H. (2003) Hepatic stellate cells: unique characteristics in cell biology and phenotype. Cell structure and function, 28 (2): 105–112

Schapira, K., Burkly, L.C., Zheng, T.S., et al. (2009) Fn14-Fc fusion protein regulates atherosclerosis in ApoE-/- mice and inhibits macrophage lipid uptake in vitro. Arteriosclerosis, Thrombosis, and Vascular Biology, 29 (12): 2021–2027

Scholten, D., Osterreicher, C.H., Scholten, A., et al. (2010) Genetic labeling does not detect epithelial-to-mesenchymal transition of cholangiocytes in liver fibrosis in mice. Gastroenterology, 139 (3): 987–998

Schuppan, D. and Kim, Y.O. (2013) Evolving therapies for liver fibrosis. Journal of Clinical Investigation, 123 (5): 1887–1901

Schuppan, D., Ruehl, M., Somasundaram, R., et al. (2001) Matrix as a modulator of hepatic fibrogenesis. Seminars in Liver Disease, 21 (3): 351–372

Schuppan, D., Schmid, M., Somasundaram, R., et al. (1998) Collagens in the liver extracellular matrix bind hepatocyte growth factor. Gastroenterology, 114 (1): 139–152

Schwabe, R.F., Bataller, R. and Brenner, D.A. (2003) Human hepatic stellate cells express CCR5 and RANTES to induce proliferation and migration. American Journal of Physiology-Gastrointestinal and Liver Physiology, 285 (5): G949–G958

Schwartz, N., Rubinstein, T. and Burkly, L.C. (2009) Urinary TWEAK as a biomarker of lupus nephritis: a multicenter cohort study. Arthritis research, 11 (5): R143

Seki, E., De Minicis, S., Osterreicher, C.H., et al. (2007) TLR4 enhances TGF-beta signaling and hepatic fibrosis. Nature medicine, 13 (11): 1324–1332

Serafini, B., Magliozzi, R., Rosicarelli, B., et al. (2008) Expression of TWEAK and its receptor Fn14 in the multiple sclerosis brain: implications for inflammatory tissue injury. Journal of neuropathology and experimental neurology, 67 (12): 1137–1148

Sharma, P., Kumar, A., Sharma, B.C., et al. (2009) Infliximab monotherapy for severe alcoholic hepatitis and predictors of survival: an open label trial. Journal of Hepatology, 50 (3): 584–591

Sherman, D.S., Fish, D.N. and Teitelbaum, I. (2003) Assessing renal function in cirrhotic patients: problems and pitfalls. American journal of kidney diseases : the official journal of the National Kidney Foundation, 41 (2): 269–278

Son, A., Oshio, T., Kawamura, Y.I., et al. (2013) TWEAK/Fn14 pathway promotes a T helper 2-type chronic colitis with fibrosis in mice. Mucosal immunology, 6 (6): 1131–1142

Sorokin, L. (2010) The impact of the extracellular matrix on inflammation. Nature reviews. Immunology, 10 (10): 712–723

Spahr, L., Rubbia-Brandt, L., Frossard, J.-L., et al. (2002) Combination of steroids with infliximab or placebo in severe alcoholic hepatitis: a randomized controlled pilot study. Journal of Hepatology, 37 (4): 448–455

Stanich, P.P., Björnsson, E., Gossard, A.A., et al. (2011) Alkaline phosphatase normalization is associated with better prognosis in primary sclerosing cholangitis. Digestive and Liver Disease, 43 (4): 309–313

Suda, H., Yoshii, D., Yamamura, K., et al. (2014) New insight into reactive ductular cells of biliary atresia provided by pathological assessment of SOX9. Pediatric surgery international, 30 (5): 481–492

Suda, T., Hashimoto, H., Tanaka, M., et al. (1997) Membrane Fas ligand kills human peripheral blood T lymphocytes, and soluble Fas ligand blocks the killing. The Journal of experimental medicine, 186 (12): 2045–2050

Sudo, K., Yamada, Y., Moriwaki, H., et al. (2005) Lack of tumor necrosis factor receptor type 1 inhibits liver fibrosis induced by carbon tetrachloride in mice. Cytokine, 29 (5): 236–244

T Georgopoulos, N., Steele, L. P., Thomson, M.J., et al. (2006) A novel mechanism of CD40-induced apoptosis of carcinoma cells involving TRAF3 and JNK/AP-1 activation. Cell Death and Differentiation, 13 (10): 1789–1801

Tacke, F. and Zimmermann, H.W. (2014) Macrophage heterogeneity in liver injury and fibrosis. Journal of Hepatology, 60 (5): 1090–1096

Takahashi, Y., Soejima, Y. and Fukusato, T. (2012) Animal models of nonalcoholic fatty liver disease/nonalcoholic steatohepatitis. World Journal of Gastroenterology, 18 (19): 2300–2308

Tarrats, N., Moles, A., Morales, A., et al. (2011) Critical role of tumor necrosis factor receptor 1, but not 2, in hepatic stellate cell proliferation, extracellular matrix remodeling, and liver fibrogenesis. Hepatology, 54 (1): 319–327

Taub, R. (2004) Liver regeneration: from myth to mechanism. Nature Reviews Molecular Cell Biology, 5 (10): 836–847

Taura, K., Miura, K., Iwaisako, K., et al. (2010) Hepatocytes do not undergo epithelial-mesenchymal transition in liver fibrosis in mice. Hepatology, 51 (3): 1027–1036

Tirnitz-Parker, J.E.E., Viebahn, C.S., Jakubowski, A., et al. (2010) Tumor necrosis factor-like weak inducer of apoptosis is a mitogen for liver progenitor cells. Hepatology, 52 (1): 291–302

Tripodi, A., Chantarangkul, V., Primignani, M., et al. (2007) The international normalized ratio calibrated for cirrhosis (INRliver) normalizes prothrombin time results for model for end - stage liver disease calculation. Hepatology, 46 (2): 520–527

Troeger, J.S., Mederacke, I., Gwak, G.-Y., et al. (2012) Deactivation of hepatic stellate cells during liver fibrosis resolution in mice. Gastroenterology, 143 (4): 1073–83.e22

Ucero, A.C., Benito-Martin, A., Fuentes-Calvo, I., et al. (2013) TNF-related weak inducer of apoptosis (TWEAK) promotes kidney fibrosis and Ras-dependent proliferation of cultured renal fibroblast. Biochimica et biophysica acta, 1832 (10): 1744–1755

Urbonaviciene, G., Martin-Ventura, J.L., Lindholt, J.S., et al. (2011) Impact of soluble TWEAK and CD163/TWEAK ratio on long-term cardiovascular mortality in patients with peripheral arterial disease. Atherosclerosis, 219 (2): 892–899

Van Hul, N.K.M., Abarca Quinones, J., Sempoux, C., et al. (2009) Relation between liver progenitor cell expansion and extracellular matrix deposition in a CDE - induced murine model of chronic liver injury. Hepatology, 49 (5): 1625–1635

van Kuijk, A.W.R., Wijbrandts, C.A., Vinkenoog, M., et al. (2010) TWEAK and its receptor Fn14 in the synovium of patients with rheumatoid arthritis compared to psoriatic arthritis and its response to tumour necrosis factor blockade. Annals of the rheumatic diseases, 69 (1): 301–304

Vollmar, B. and Menger, M.D. (2009) The Hepatic Microcirculation: Mechanistic Contributions and Therapeutic Targets in Liver Injury and Repair. Physiological Reviews, 89 (4): 1269–1339

Wajant, H. (2013) The TWEAK-Fn14 system as a potential drug target. British journal of pharmacology, 170 (4): 748–764

Wang, F., Liu, S., Du, T., et al. (2014) NF-kappa B inhibition alleviates carbon tetrachloride-induced liver fibrosis via suppression of activated hepatic stellate cells. Experimental and Therapeutic Medicine, 8 (1): 95–99

Wang, S., Jiang, W., Chen, X., et al. (2012) Alpha-fetoprotein acts as a novel signal molecule and mediates transcription of Fn14 in human hepatocellular carcinoma. Journal of Hepatology, 57 (2): 322–329

Watanabe, A., Hashmi, A., Gomes, D.A., et al. (2007) Apoptotic hepatocyte DNA inhibits hepatic stellate cell chemotaxis via toll-like receptor 9. Hepatology, 46 (5): 1509–1518

Wells, R.G. (2014) The portal fibroblast: not just a poor man's stellate cell. Gastroenterology, 147 (1): 41–47

Wennerberg, A.E., Nalesnik, M.A. and Coleman, W.B. (1993) Hepatocyte paraffin 1: a monoclonal antibody that reacts with hepatocytes and can be used for differential diagnosis of hepatic tumors. American Journal of Pathology, 143 (4): 1050–1054

Wiley, S.R. and Winkles, J.A. (2003) TWEAK, a member of the TNF superfamily, is a multifunctional cytokine that binds the TweakR/Fn14 receptor. Cytokine & Growth Factor Reviews, 14 (3-4): 241–249

Wiley, S.R., Cassiano, L., Lofton, T., et al. (2001) A novel TNF receptor family member binds TWEAK and is implicated in angiogenesis. Immunity, 15 (5): 837–846

Williams, M.J., Clouston, A.D. and Forbes, S.J. (2014) Links Between Hepatic Fibrosis, Ductular Reaction, and Progenitor Cell Expansion. Gastroenterology, 146 (2): 349–356

Winau, F., Hegasy, G., Weiskirchen, R., et al. (2007) Ito cells are liver-resident antigen-presenting cells for activating T cell responses. Immunity, 26 (1): 117–129

Winkles, J.A. (2008) The TWEAK-Fn14 cytokine-receptor axis: discovery, biology and therapeutic targeting. Nature reviews. Drug discovery, 7 (5): 411–425

Winwood, P.J., Schuppan, D., Iredale, J.P., et al. (1995) Kupffer Cell-Derived 95-Kd Type-Iv Collagenase/Gelatinase-B - Characterization and Expression in Cultured-Cells. Hepatology, 22 (1): 304–315

Wisniacki, N., Amaravadi, L., Galluppi, G.R., et al. (2013) Safety, Tolerability, Pharmacokinetics, and Pharmacodynamics of Anti-TWEAK Monoclonal Antibody in Patients With Rheumatoid Arthritis. Clinical Therapeutics, 35 (8): 1137–1149

Wong, L., Yamasaki, G., Johnson, R.J., et al. (1994) Induction of beta-platelet-derived growth factor receptor in rat hepatic lipocytes during cellular activation in vivo and in culture. Journal of Clinical Investigation, 94 (4): 1563–1569

Wu, F., Guo, L., Jakubowski, A., et al. (2013) TNF-like weak inducer of apoptosis (TWEAK) promotes beta cell neogenesis from pancreatic ductal epithelium in adult mice. Maedler, K. (ed.). PloS one, 8 (8): e72132

Wynn, T.A. and Barron, L. (2010) Macrophages: master regulators of inflammation and fibrosis. Seminars in Liver Disease, 30 (3): 245–257

Xie, G., Wang, X., Wang, L., et al. (2012) Role of Differentiation of Liver Sinusoidal Endothelial Cells in Progression and Regression of Hepatic Fibrosis in Rats. Gastroenterology, 142 (4): 918–U392

Xu, J., Liu, X., Koyama, Y., et al. (2014) The types of hepatic myofibroblasts contributing to liver fibrosis of different etiologies. Frontiers in pharmacology, 5: 167

Xu, R., Zhang, Z. and Wang, F.-S. (2012) Liver fibrosis: mechanisms of immune-mediated liver injury. Cellular and Molecular Immunology, 9 (4): 296–301

Yadava, R.S., Foff, E.P., Yu, Q., et al. (2015) TWEAK/Fn14, a pathway and novel therapeutic target in myotonic dystrophy. Human molecular genetics, 24 (7): 2035–2048

Yamaguchi, H., Matsumoto, S., Ishibashi, M., et al. (2013) β-Glucuronidase is a suitable internal control gene for mRNA quantitation in pathophysiological and non-pathological livers. Experimental and molecular pathology, 95 (2): 131–135

Yamamoto, Y. and Gaynor, R.B. (2001) Therapeutic potential of inhibition of the NF-kappaB pathway in the treatment of inflammation and cancer. Journal of Clinical Investigation, 107 (2): 135–142

Yang, C.Q., Zeisberg, M., Mosterman, B., et al. (2003) Liver fibrosis: Insights into migration of hepatic stellate cells in response to extracellular matrix and growth factors. Gastroenterology, 124 (1): 147–159

Yang, L., Pang, Y. and Moses, H.L. (2010) TGF-beta and immune cells: an important regulatory axis in the tumor microenvironment and progression. Trends in Immunology, 31 (6): 220–227

Yilmaz, M.I., Carrero, J.J., Ortiz, A., et al. (2009) Soluble TWEAK plasma levels as a novel biomarker of endothelial function in patients with chronic kidney disease. Clinical journal of the American Society of Nephrology : CJASN, 4 (11): 1716–1723

Yoshiji, H., Kuriyama, S., Miyamoto, Y., et al. (2000) Tissue inhibitor of metalloproteinases-1 promotes liver fibrosis development in a transgenic mouse model. Hepatology, 32 (6): 1248–1254

Yu, C.D., Wang, F., Jin, C.L., et al. (2003) Role of fibroblast growth factor type 1 and 2 in carbon tetrachloride-induced hepatic injury and fibrogenesis. American Journal of Pathology, 163 (4): 1653–1662

Yu, Q. and Stamenkovic, I. (2000) Cell surface-localized matrix metalloproteinase-9 proteolytically activates TGF-beta and promotes tumor invasion and angiogenesis. Genes & Development, 14 (2): 163–176

Zhan, S.S., Jiang, J.X., Wu, J., et al. (2006) Phagocytosis of apoptotic bodies by hepatic stellate cells induces NADPH oxidase and is associated with liver fibrosis in vivo. Hepatology, 43 (3): 435–443

Zhang, M., Ye, Y., Wang, F., et al. (2014) Liver myofibroblasts up-regulate monocyte CD163 expression via PGE2 during hepatitis B induced liver failure. Journal of translational medicine, 12 (1): 60

Zhang, Y., Ikegami, T., Honda, A., et al. (2006) Involvement of integrin-linked kinase in carbon tetrachloride-induced hepatic fibrosis in rats. Hepatology, 44 (3): 612–622